IMPACT OF SOLAR WATER HEATING ON ESKOM'S PEAK DEMAND

Ketrine Pamela Ijumba

IJMKET001

Thesis submitted to the

University of Cape Town

In partial fulfillment of the requirements for the degree of

Master of Science in Engineering

In the Department of Electrical Engineering

Supervised by

Professor P. Pillay
Hydro Quebec Senior Chair, Department of Electrical and Computer Engineering
Concordia University
and
Part-time Professor, Department of Electrical Engineering
University of Cape Town

Dr A.B. Sebitosi
Senior Research Officer, Department of Electrical Engineering
University of Cape Town

Professor K. Folly
Associate Professor, Department of Electrical Engineering
University of Cape Town

July 2008

PLAGIARISM DECLARATION

Declaration

I know the meaning of plagiarism and declare that all the work in the document, save for that which is properly acknowledged, is my own.

Signature _____

This Thesis is dedicated to the Loving Memory of Dr. Jane Ilahuka

ACKNOWLEDGEMENTS

First and foremost, I would like to give thanks and glory to God, without whom, none of this would be possible.

I am indebted to Dr. Sebitosi, Prof. Pillay and Prof. Folly for all the guidance and support during this project. Your knowledge, input and advice is greatly appreciated. In the same vein, thanks must also go to the past and present members of the Advanced Machines and Energy Research Group at UCT: Lotten, Richard, Ramzi, Heskin, Gomez, Taru and Chris for all your input at those group meetings!

My deepest gratitude goes to the staff at Atlantic Solar, especially Helmut Hertzog and Sean, all the homeowners who participated in the data logging part of the project and Mutenda Tshipala at ESKOM Transmission. This thesis would not have come to fruition without your input.

My studies were funded by ESKOM KSACS. Thanks to Dhevan Pillay, Johan Pfister, Hettie Loots, Danielle Sutherland and Sipokazi Ngxoweni for all their assistance in that regard.

A hearty thank you to ALL my friends for the support they provided during the project. Special thanks go to Mercy and Njenga, for the crash course in Excel and VBA; and to Neema, Muonga, Ruth and Melba, for constantly urging me on. Last but not least, to Vido: thank you, for your seemingly endless patience, assistance and encouragement.

Finally, and most importantly, thanks to my family. Mama and Baba, you've taught me the importance of education. Your unwavering encouragement and advice during my pursuit have been invaluable. Ken and Karen, I couldn't have asked for crazier siblings! You are my number one cheerleaders; your zany ways have kept me going.

SHUKRANI ZANGU POKEENI NA DUA NJEMA NINAWAOMBEA

ABSTRACT

Over the past few years, South Africa has experienced a high growth rate in its economy as well as a rapid expansion in the power consumer base. As a result, the demand for electricity has escalated. The situation has now reached a critical point, with regular countrywide blackouts and load shedding expected to persist for several years.

Currently, the bulk of electricity is generated in coal-based power stations, which are situated in the coal rich Northeastern regions of the country. The big load centers, however, are situated in Gauteng, KwaZulu Natal and the Western Cape. Therefore, power needs to be transmitted over long distances to these areas. As a result, substantial losses are incurred, particularly during times of peak demand, when large amounts of power are being transmitted.

Electricity consumption in South African households accounts for approximately 37% of peak demand, with water heating comprising more or less 40%, which is a significant figure.

Solar energy is widely available in South Africa, and it would offer a logical and timely compliment to the country's coal-based generation. Moreover, the power can be generated where it is needed, thereby relieving demand on the transmission infrastructure. This resource, however, is yet to be fully exploited in South Africa.

One way to utilise solar energy is through the use of solar water-heating. Studies worldwide have shown that solar water heating saves energy and this knowledge is already in the public domain. However, what has not been adequately established is the impact and extent to which solar energy mitigates peak power demand. This is particularly intriguing in the case of South Africa where peak demand occurs in the morning and evening, when solar radiation is at its lowest.

This thesis aims to investigate the impact of solar water heating on power system peak demand and consequently on peak transmission losses.

Simulations were carried out using TRNSYS, and MeteoNorm generated data, in order to determine the impact that solar water heating has on a geyser's daily consumption profile. This information was then used to determine the impact on a household's entire peak demand. Simulations were carried out for households located in the major cities in each province of South Africa. The simulations showed that solar water heating has the potential to reduce household peak demand, especially in the evenings.

The study was initially focused on Cape Town, as this is the worst-case power delivery scenario, due to the length of transmission lines from the main base load stations. The focus then shifted to the impact of a nationwide solar water heating program. These results showed that the impact of a solar water heating system varies in different regions of the country (as expected due to South Africa's many climatic regions). In each case though, solar water heating did have an impact on the evening peak demand.

Consequently, field case studies were carried out over a period of 6 months, in order to validate the simulations. A few solar water heating installations were monitored, in order to observe the reduction in electricity consumption that a solar water heating system brought about. The results varied from household to household, but overall, confirmed the results obtained through the simulations. There was a marked reduction in the electricity consumption of the geyser.

The author made additional contributions by proposing changes in consumer social behaviour that could realise further improvements in the energy performance of a solar water heater. Simulations were carried out to determine the best showering hours, thermostat settings and insulation levels to maximise the benefits of the solar water heating. Results showed that with a thermostat setting of 55°C, some extra insulation and a usage time as close to the optimum as possible, further savings of up to 14.5% could be achieved annually.

Finally, a power system model was developed in order to investigate the impact of the large scale implementation of solar water heating on a transmission system. Using the model and the results obtained from the simulations, a utility impact analysis was carried out in order to determine the effect on transmission losses. The results showed that solar water heating can reduce transmission losses by as much as 5% depending on the level of penetration of the technology.

Drawing from the above results the author concluded that the large-scale implementation of solar water heating can be used as a means to alleviate loading and losses on power systems' transmission lines and thus defer the need for infrastructure upgrade and capital expansion.

TABLE OF CONTENTS

LIST OF TABLES

LIST OF FIGURES

NOMENCLATURE

ACRONYMS

EDHW	**Electric Domestic Hot Water**
SDHW	**Solar Domestic Hot Water**
EHW	**Electric Hot Water**
SHW	**Solar Hot Water**

SYMBOLS

SYMBOL	DEFINITION	UNIT
I	**Current**	**A**
R	**Resistance**	**Ω**
P	**Power**	**W**
V	**Voltage**	**V**
T	**Temperature**	**°C**
η	**Efficiency**	**-**
Q	**Energy**	**J or Wh**
A	**Area**	**m^2**
I_T	**Incident Solar Radiation**	**J/m^2 or Wh/m^2**
m	**Flow rate**	**m^3/s**
C	**Specific Heat**	**J/g.°C**
ρ	**Density**	**m^2**
V	**Volume**	**m^3**
P	**Pressure**	**Pa**
g	**Gravitational Constant**	**m/s^2**
h	**Height**	**m**

CHAPTER I

1. INTRODUCTION

This chapter aims to offer motivation for the research that has been undertaken during the course of this thesis. It will also cover previous work that has been carried out in this field and outline the objectives of the research.

1.1 Background

South Africa is a developing country, with a rapidly growing economy. This progress, amongst other factors, has led to a rising demand for electricity. Demand now outstrips maximum generating capacity, consequently, since November 2005; load shedding has become an increasingly common phenomenon.

Coal is currently the main fuel used for electricity production, as can be seen in Table 1.1. However, the burning of fossil fuels has a detrimental effect on the environment, thus cleaner methods of energy production are desirable [1].

Table 1.1: Eskom Electricity Generation Mix in 2007 [1]

Fuel Type	GWh produced	% Contribution
Coal	215211	92.59
Nuclear	11780	5.07
Pumped Storage	2947	1.27
Hydro	2443	1.05
Gas Turbine	62	0.03

Furthermore, the bulk of South Africa's electricity is generated from a central location, in the coal rich areas of Mpumalanga. This power is then transmitted over long distances across the country and substantial losses are incurred. The problem is aggravated at peak demand, when large amounts of power are being transmitted. It has thus become necessary to find a means of easing the loading on the system, especially during these times of peak demand.

Approximately 37% of peak demand in South Africa can be attributed to residential household electricity consumption, with water heating accounting for about 40% [2].

This research aims to investigate the possible impact and extent of the use of solar water heating as a clean means of reducing peak demand, thereby reducing loading on transmission lines, especially during times of peak demand.

1.2 Motivation for Research

1.2.1 PEAK DEMAND

From a utility perspective, an ideal scenario would be when the electricity demand is the same around the clock. In practice, however, there are hours of low demand, and high demand. Large amounts of electricity cannot be efficiently stored; therefore utilities need to be able to produce electrical power when it is needed.

Peak demand refers to the largest average amount of power required by a utility's customers within a specific time frame, normally averaged over an hour. It is an indication of the amount of power that an electrical utility must be able to produce, within a short time frame, in order to meet the customers' maximum demand [3]. Electricity demand fluctuates both daily and seasonally.

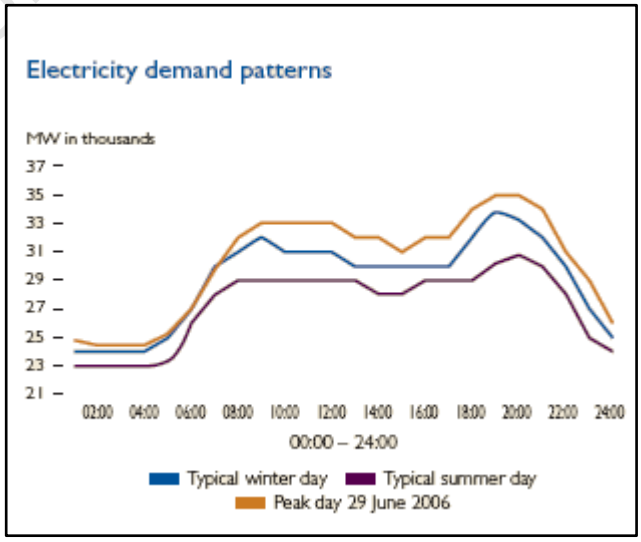

Figure 1.1: Eskom Electricity Demand Patterns 2006 [1]

Figure 1.1, depicts typical demand patterns on the Eskom grid. It can clearly be seen that the Eskom system experiences daily peaks in the morning and evening, and a seasonal peak in winter, when heating loads and longer burning hours for lights add to electricity consumption.

1.2.2 EFFECTS OF PEAK DEMAND ON A POWER SYSTEM AND TRANSMISSION GRID

Power systems are heavily loaded during times of peak demand. This results in increased line losses. Transmission line losses are governed by the following equations [4].

$$Losses = I^2R = (P^2R)/V^2 \quad \textbf{(1.1)}$$

$$R \; \alpha \; T \; \alpha \; I \quad \textbf{(1. 2)}$$

$$R \; \alpha \; Line\ length \quad \textbf{(1.3)}$$

P = System Demand; R = Line Resistance; V = Transmission Voltage; T = Line Temperature; I = Line Current

Equations 1.1 to 1.3 can be summarised by the statement that a small increase in load (I), results in a large increase in losses on the transmission network. This non-linear relationship is clearly illustrated in Figure 1.2.

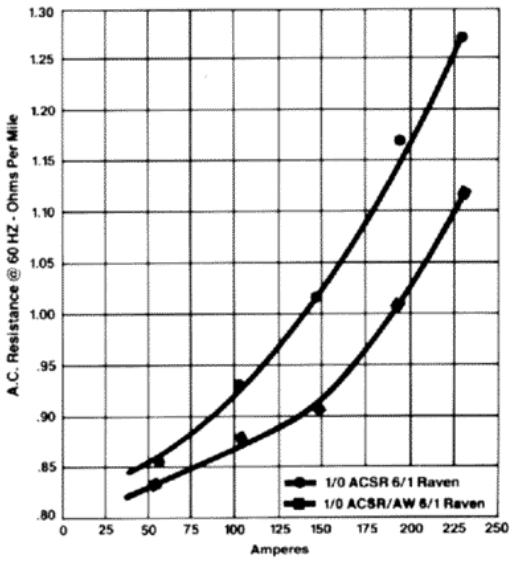

Figure 1.2: A Plot of AC Resistance vs. Current (Load) of an ACSR Conductor [5]

This is particularly pertinent for long transmission lines, as line resistance is directly proportional to line length. The line temperature also increases as the line current rises, which increases the resistance and further escalates system losses.

In 2007, losses on the Eskom grid were 8.4%. The peak demand and line losses on the Eskom grid are on the increase, as can be seen in Figure 1.3 [1].

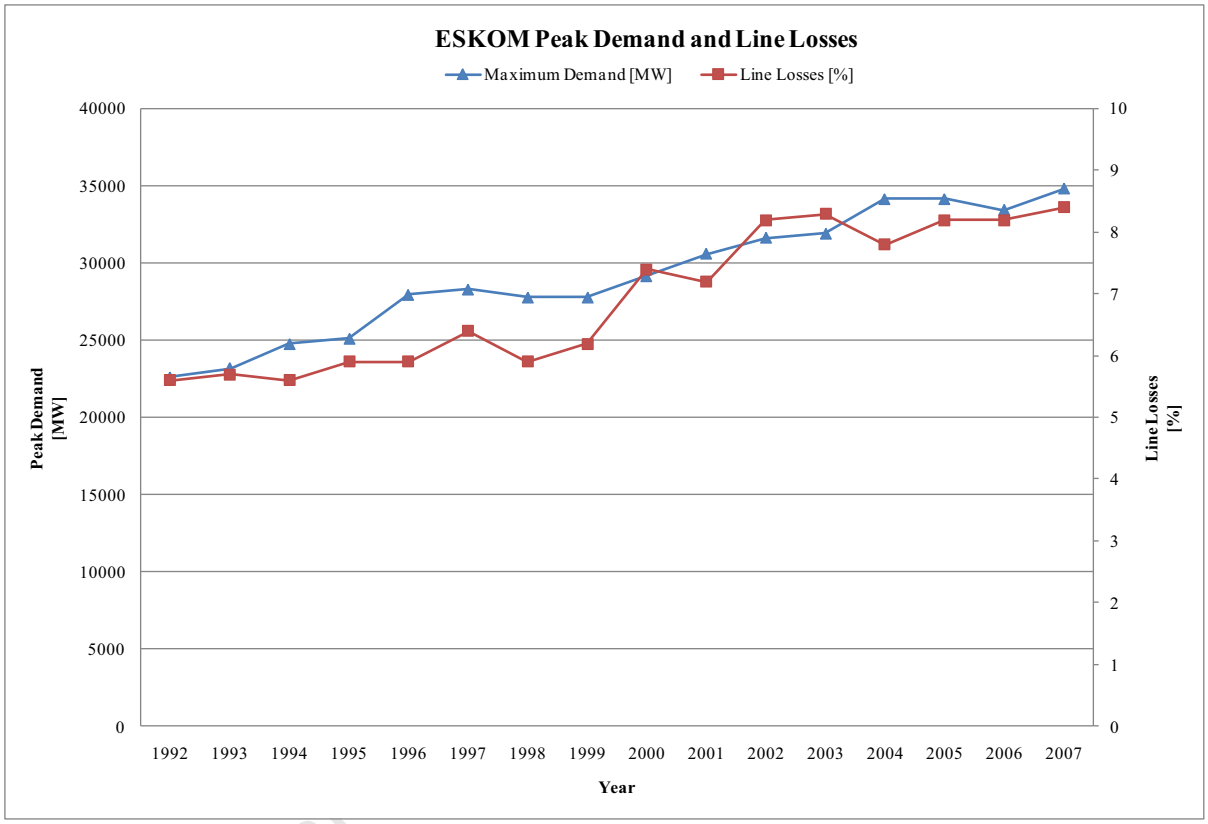

Figure 1.3: Eskom Peak Demand and Line Losses 1992 – 2007 [1]

Outages often occur during times of peak demand. This can be attributed either to the increased loading on the generation, such that demand exceeds capacity or transmission constraints, where the transmission / distribution lines are unable to carry the required power to where it is needed [1], [6].

Heavily loaded systems can experience a reactive power imbalance, which can lead to voltage collapse [7]; therefore peak demand also has an effect on system stability.

System reliability is a function of the reliability of the system's individual components. During times of peak demand, transmission equipment is heavily loaded and more likely to

be damaged or pack-up all together [8]. For example, heavily loaded transmission lines tend to sag; this makes them more susceptible to faults due to contact with trees and other structures beneath the lines. Therefore during times of peak demand, the reliability of the transmission lines is decreased, and as a result, the reliability of the entire system is also decreased.

1.2.3 SOUTH AFRICA'S TRANSMISSION SYSTEM

In South Africa the entire coastal load (Western Cape, Eastern Cape and KwaZulu Natal) constitutes approximately 34% of the country's total demand, yet only 6% of the total generating capacity is situated at the coast [9], as seen in Figure 1.4. This means that the coastal grids receive the bulk of their electricity over long transmission lines that carry power from the North-Eastern region of the country. As a result, peak demand affects transmission and distribution infrastructure most severely for these areas, particularly Cape Town.

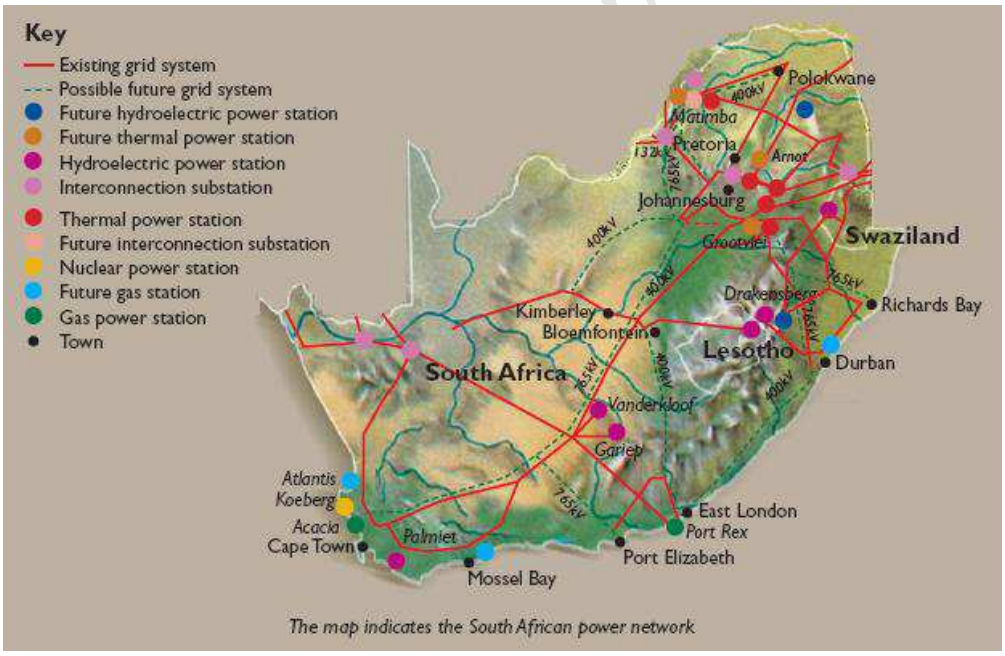

Figure 1.4: Eskom Generation and Transmission Network [1]

Maximum electricity demand in the Western Cape Province is estimated at 3550MW. Yet the maximum local generating capacity is approximately 1970MW. This means that at least 1580MW of power are being imported into the province [10]. The transmission lines that feed into the Western grid form part of a ring feed that supplies Namibia and the Southern grid as well. This means that the demand in these areas affects power availability in the

Western Cape [10, 11]. The upcoming steel smelter in the Coega development in the Eastern Cape will strain this part of the transmission grid even further with its estimated demand of ±1350MW [12].

1.2.4 RENEWABLE ENERGY IN SOUTH AFRICA

South Africa is ranked 12th in the world, in terms of Carbon Dioxide (CO_2) emissions [13]. According to the Minister of Environmental Affairs and Tourism, Marthinus van Schalkwyk, the energy sector is responsible for the bulk of emissions in South Africa. It has thus become necessary to move towards energy efficiency, and to explore cleaner energy sources [14].

1.2.4.1 Legislation

The White Paper on Renewable Energy (2003) has set a target of 10 000GWh of energy to be produced from renewable energy sources by 2013, with a focus on biomass, wind, hydro and solar. In 2004, only 70GWh were generated from renewable energy sources [15]. The Department of Minerals and Energy (DME) are far from achieving their target.

South Africa is one of the areas in the world that experiences high solar radiation, with an average of 220W/m^2 within a 24-hour period. Figure 1.5 gives a more detailed indication of the amount of solar energy that is available in South Africa [15].

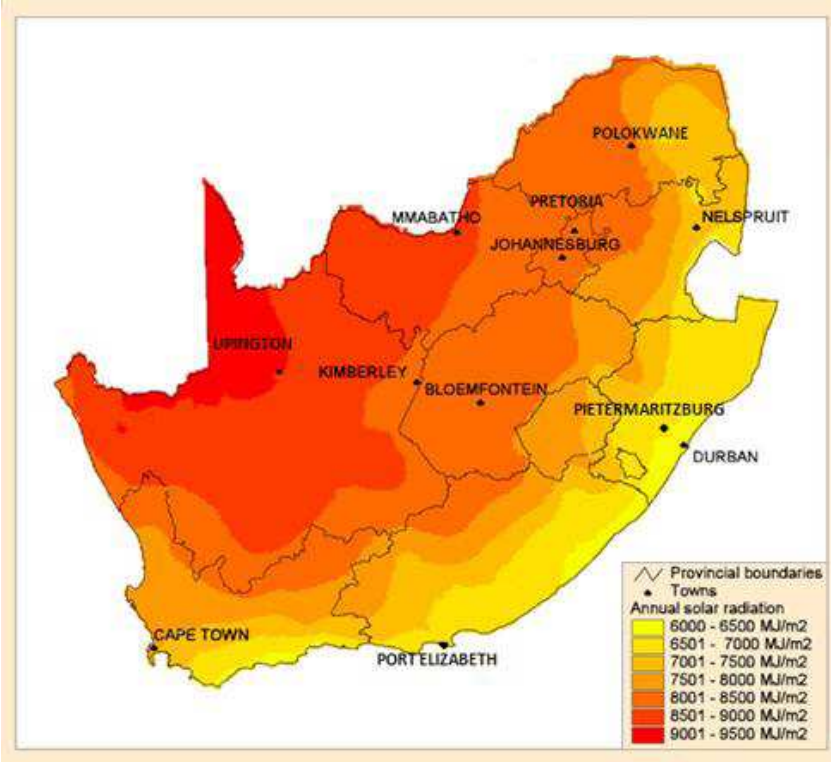

Figure 1.5: Average Annual Solar Radiation South Africa [15]

It can be seen that the amount of energy available per annum ranges from approximately 6000MJ/m^2 along the coastline to values in the region of 9500MJ/m^2 in the Northern Cape. This translates to a minimum insolation of 190W/m^2 to a maximum of approximately 300W/m^2. This is a vast renewable energy source that is yet to be fully exploited.

Figure 1.6 aims to highlight the various methods available to date, of utilising solar energy.

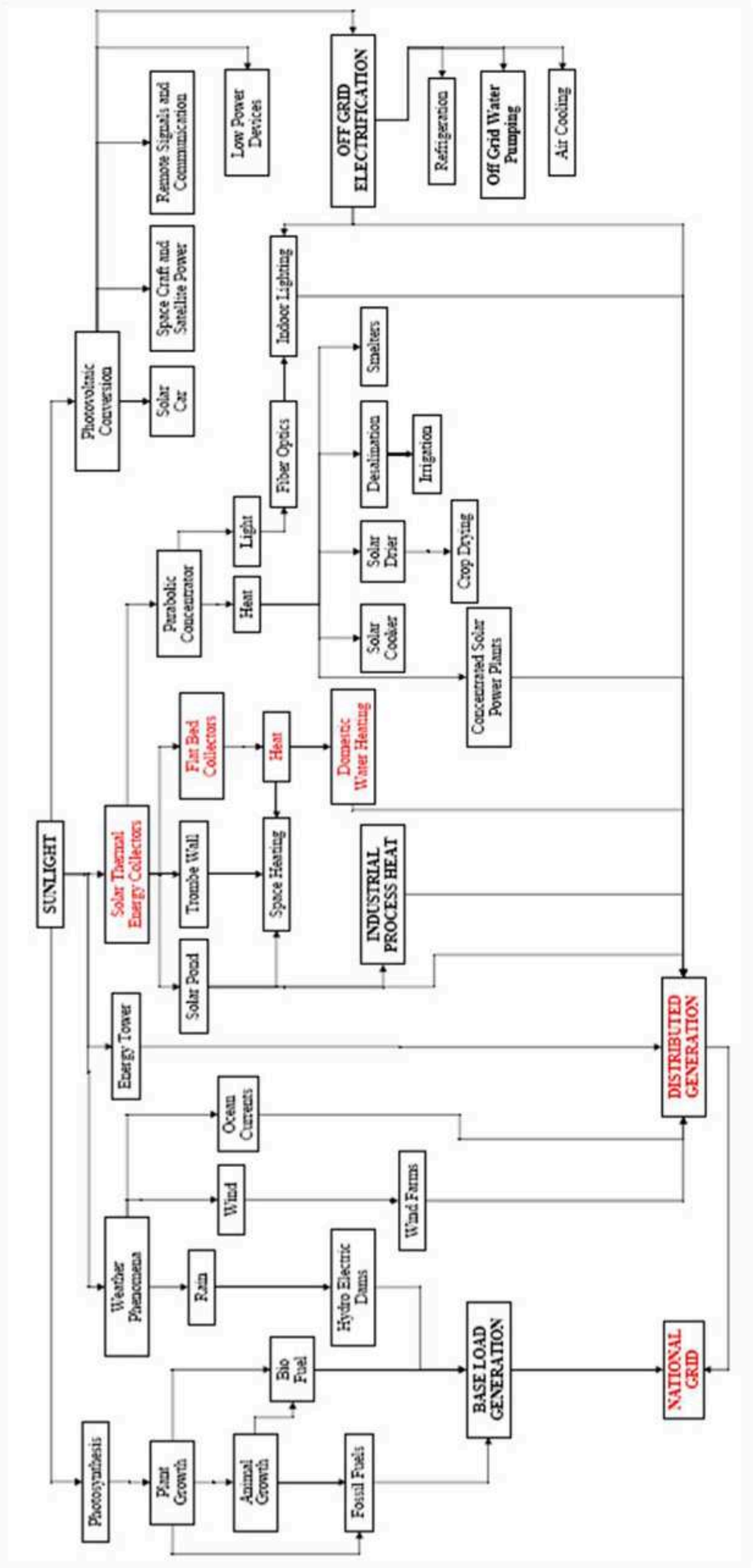

Figure 1.6: Spider diagram of the Various Uses of Solar Energy

1.3 Literature Review

About 37% of peak demand in South Africa can be attributed to residential electricity consumption [2]. In South Africa's middle to high income homes, electrical water heating accounts for 30% to 50% of electricity usage [16]. Studies by Meyer & Tshimankinda and Lane have shown that a typical South African household's hot water usage peaks during peak times, providing opportunity for peak demand reduction [17,18].

Efforts have been made to *shift* the load to off-peak times using remote control strategies. Studies have shown that although this can alleviate peak demand, it has problems such as cold-load pick up [19–21]. Solar water heating can *reduce* the amount of electricity used by a household. Dintchev found that a solar water heating system installed in a home in Pretoria, can contribute up to 87% of the household's annual water heating requirements [22].

Solar water heating initiatives have also been successfully implemented in countries such as China, Japan, Germany, Israel, Australia, Brazil, Greece, Austria, Turkey and the USA [23]. Most of these countries experience much less solar radiation than South Africa.

Studies have been conducted in the USA to find out the impact, if any, of the large scale implementation of solar water heating systems on a utility. They have found them to be beneficial. They resulted in reduction of demand and energy consumption, as well as carbon emissions. However, they also found that the impact is dependent on the utility's resource mix, weather patterns and load profile [24,25].

In South Africa, the City of Cape Town has recently drafted by-laws that will enforce the installation of solar water heaters on all new buildings where sanitary hot water is required [26]. The Department of Minerals and Energy, together with ESKOM and the Central Energy Fund (CEF) are also developing a code of practice in order to implement a nationwide solar water heating program.

1.4 Research Objectives

The benefits of large scale implementation of solar water heating in reducing grid energy consumption have been exhaustively illustrated worldwide through research and implementation. The focus of *this* research will be the impact of solar water heating on peak demand and the consequent reduction in transmission losses.

This research question is particularly important, given that:

a) Eskom is a winter peaking utility, and
b) Peak solar radiation does not coincide with the system peak demand.

The study into the impact of solar water heaters will be carried out in a number of stages. The first step will involve the simulation of the performance of solar water heating using the software packages of MeteoNorm and TRNSYS.

Secondly, solar water heating installations will be monitored, in order to validate the simulation results. The simulation results will then be used to quantify the average reduction, if any, in peak demand that a solar water heating system can bring about.

These results will then be used to determine the impact of large scale solar water heating on transmission losses experienced on the grid.

1.5 Thesis Structure

The rest of this thesis is organised as follows:

Chapter 2 gives a brief introduction to solar water heating systems. It also includes a description of the software programs used to run the simulations, and a description of the models used in the simulations.

Chapter 3 outlines the methods that were used to simulate the water heating systems and to collect data from various solar water heater installations. The research methodology

employed to model the effects of solar water heating on the transmission grid, is also presented in this section.

The simulation results are presented in Chapter 4 and in Chapter 5 the data collected from the field is presented, and used to validate the results that were presented in the previous chapter.

Chapter 6 investigates methods to improve the performance and benefits of solar water heating. A payback period analysis is also included in this section.

Chapter 7 contains a brief overview of power system modelling and the South African transmission grid. The model used to determine the transmission losses is also presented along with the results that show the effects of solar water heating on the transmission grid. Finally conclusions and recommendations are presented in Chapter 8.

CHAPTER II

2. SOLAR WATER HEATING SYSTEMS AND SIMULATION MODELS

This chapter aims to give a brief illustration of the workings of a solar water heating system. The software programs that were used to do the simulations and their models are also outlined in this section.

2.1 Solar Water Heating – How It Works

One of the ways to use the heat acquired from solar energy is solar water heating. Solar water heating is a process whereby hot water for domestic or industrial use is heated by the sun. There are several variations on the process.

All solar water-heating systems consist of three major components as shown in Figure 2.1: -

- A thermal collector system, which is placed in the sun to collect heat from the sun.
- A fluid system which transfers heat from the collector to the point of storage / usage
- A storage system, which stores the heated fluid, until it is required for use.

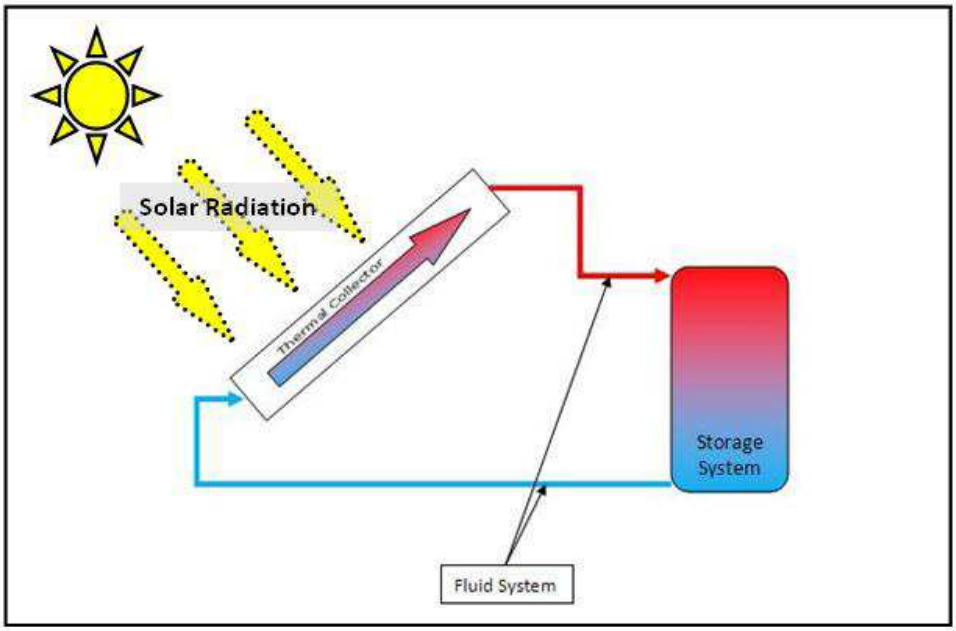

Figure 2.1: Solar Water Heating System Schematic

2.1.1 CLASSIFICATION OF SOLAR WATER HEATING SYSTEMS

Solar hot water heating systems can be separated into two categories, as shown in Figure 2.2

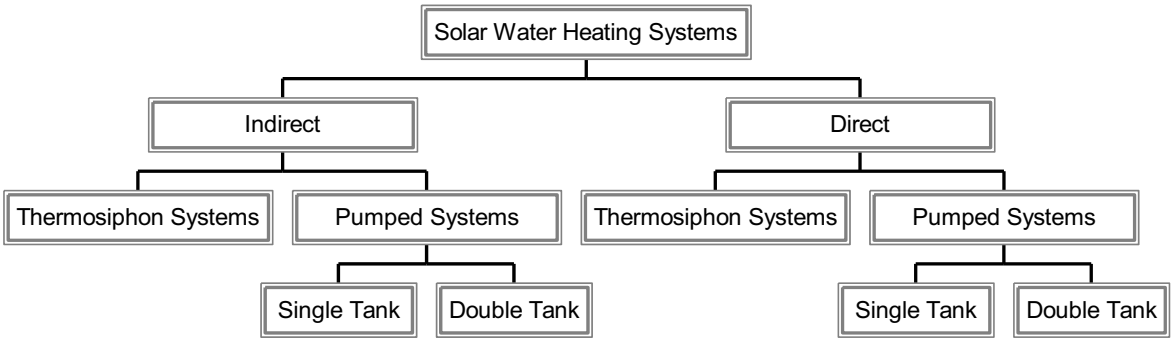

Figure 2.2: Classification of Solar Water Heating Systems [27]

In direct systems, sometimes referred to as open loop, the working fluid for the solar water heating system is the very same water that will be used in the household. These systems are best implemented in areas where temperatures do not drop below freezing, as frozen water in the pipes, could cause them to burst. Direct systems are not suited to areas with hard water either, as lime scale could build up in the pipes, lessening the efficiency of the system [28].

Indirect systems, which are also known as closed loop systems, make use of a heat exchanger circuit to heat the water. The working fluid in this case, is a freeze resistant fluid, usually glycol. These systems are used in areas where temperatures can sometimes drop below freezing. The freeze resistant fluid prevents damage from occurring to the pipes, when sub-zero conditions occur. Figure 2.3, below illustrates the difference between direct and indirect SWH systems.

Figure 2.3: Schematic of Direct and Indirect Solar Water Heating Systems [29]

The classification of SWH systems can be taken a step further, as seen in Figure 2.2 depending on the manner in which fluid circulates through the system.

Pumped systems are also known as active systems. In this instance, a pump is used to move water through the solar collector, to the storage tank. The pump is usually connected to a controller, which causes it to start pumping when the temperature of the water in the collector, exceeds that of the water in the geyser.

Pumped systems can either be of the single or double tank variety. In the single tank set up, the heat exchanger circuit and the back-up (electrical) heating element are in the same storage tank. For the double tank variation, the heat exchanger circuit is used to heat the household's water in an auxiliary tank. The pre-heated water is then pumped into the main storage tank, where the back-up heating element is located.

Thermosiphon systems, also known as passive systems, rely solely on the principle of natural convection for circulation to take place. There are no mechanical parts involved in such a system, which means they have minimal maintenance requirements. For this system to work, the geyser must be installed at a higher level than the solar collector, allowing the hot water to rise into it.

Thermosiphon systems are cheaper than pumped systems, as there are fewer components involved and little maintenance too [30]. Therefore, it is especially beneficial to implement solar water heating in areas where thermosiphon systems can work. The capital expenditure will be lower, resulting in a shorter payback period. For this reason, thermosiphon systems were chosen for the simulations.

2.1.2 SOLAR COLLECTORS

The function of a solar collector is to absorb heat from the sun, and transfer it to the working fluid as quickly, and efficiently as possible [31]. Heat naturally flows from a warmer space/material to a cooler one. Heat transfer takes place through [32]: -

- Conduction - the process of heat transfer from one body to another through direct contact.

- Convection – the process whereby a liquid/gas upon heating, expands, and rises away from the heat source taking the heat with it; leaving room for denser, colder fluid.
- Radiation – the process where energy is transferred across an empty space.

There are two main types of solar collectors used in the application of solar water heating, flat plate and evacuated tube collectors.

2.1.2.1 Flat Plate Collectors

The simplest form of collector is the flat plate collector. This type of collector consists of copper tubing and an absorber plate, in an insulated box with a glass cover. Figure 2.4 below depicts a typical flat plate collector.

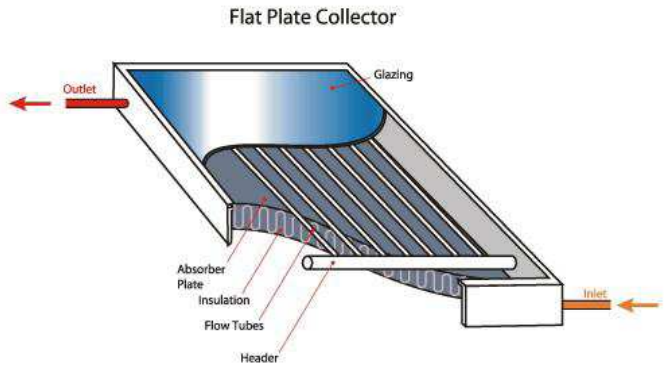

Figure 2.4: Schematic of a Flat Plate Collector [33]

The glass cover on the collector serves to trap solar radiation. The absorber plate is designed to absorb and transfer heat from the sun, to the heat transfer fluid as quickly as possible. The insulation in the box prevents heat loss from occurring.

2.1.2.2 Evacuated Tube Collectors

Evacuated-tube collectors work on the same principle as flat plate collectors in that they trap heat and transfer it to the fluid as quickly as possible. Figure 2.5 shows an evacuated tube collector. In this case, the absorber "plate" is positioned in an evacuated glass tube. The vacuum prevents heat loss through convection and radiation. The fluid then flows through tubes placed inside the glass tube. An evacuated tube collector consists of several rows of these tubes connected to a header pipe.

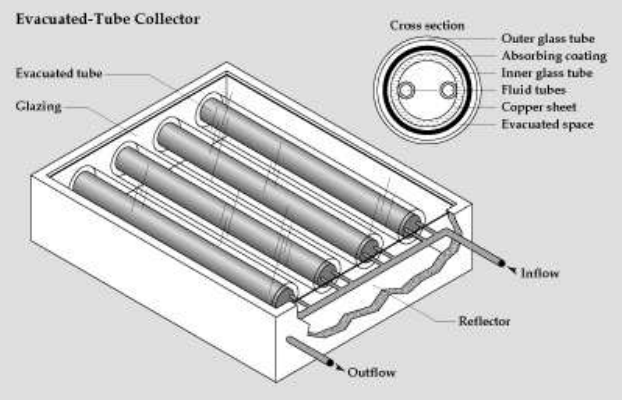

Figure 2.5: Schematic of an evacuated tube collector [34]

In both cases, water enters the collector through the inlet and rises into the flow tubes, where it is exposed to the sun and heated, before returning to the storage tank via the outlet.

Evacuated-tube collectors, have very high efficiencies, especially during winter months, however, they also have a unit area price that is approximately double that of a flat plate collector. This makes them very expensive; as a result, they are still primarily used for commercial and industrial applications [35]. Flat plate collectors will be used for the simulations during this project.

2.1.3 STORAGE OF HOT WATER

Once heated, the water is stored in a hot water geyser until it is needed. The geyser is fitted with a back up element and thermostat, to maintain the water at a certain temperature (normally between 55˚C and 65˚C) With solar water heating systems, it is important that this geyser has good heat retention properties, in order to minimize the amount of electrical energy used to keep the water at the specified temperature. Acceptable loss values as per SABS standards are shown in appendix A.

2.2 Simulating of Water Heating Systems

The performance of a solar water heating system is dependent on factors such as system location, orientation, tank-size and water usage pattern. These systems are still expensive; it has thus become necessary to find a means to determine the savings that the installation of a SWH system will bring about, prior to investment by the customer and the utility.

2.2.1 SOFTWARE PROGRAMS

South Africa consists of several different climates, from Cape Town's Mediterranean cool, wet winters; Johannesburg's dry climate; the Karoo's dry winters and the East Coast's subtropical warm winters and sultry summers [36]. It would, therefore, be important to predict the expected performance of these solar water heaters at any location around the country.

Utilities will also be interested to find out how solar water heating impacts on system demand, and energy consumption. This data is used in scheduling power plant maintenance, capacity expansion and power plant scheduling.

Monitoring households, is a prohibitively expensive exercise, thus computer simulations would be a much cheaper option. MeteoNorm and TRNSYS are two software packages that can be used in this regard.

2.2.1.1 MeteoNorm

MeteoNorm is a solar resource modeling program developed in conjunction with the Swiss Federal Office of Energy. Its primary purpose is to calculate solar radiation on a surface of arbitrary orientation. It makes use of several databases, computational models and interpolation to generate monthly, daily or hourly meteorological data for virtually any site in the world [37, 38].

The user can either select a location from a list/map or define a site. In defining the site, the user specifies latitude, longitude, altitude and terrain. The program then generates a data file containing hourly weather data for the given site. This program was used to generate the weather data, which was used during the simulation of the solar water heating system performance.

2.2.1.2 TRNSYS

TRNSYS (Transient System Simulation Program) is a transient energy simulation tool that allows the user to simulate various energy systems' performance over time. It has a library of

components that model various energy systems apparatus. The program is distributed with its source code, allowing the user to tailor existing models or create new ones, according to their requirements. Additionally, the tool permits the entry of externally generated climatic data, thus allowing the user to analyse system performance for any given location.

TRNSYS can be used to simulate the performance of several types of water heating systems. The user can vary system parameters such as location, tank size, element rating, collector area, slope, efficiency, orientation and water consumption profile to match any given scenario. The program then outputs, the system's energy and power consumption. A comparison can thus be done between the amounts of electrical energy that would go towards water heating in a household with solar water heating and one with an electric only geyser. This would give a clear picture of the energy and demand savings that the installation of a solar water heating system brings about.

2.2.2 SIMULATION MODELS [25, 39 ,40]

The most important components of a solar water heating system are the collector, and the storage tank. The rate of heat transfer from the collector to the storage tank is also an important factor in system performance. The models used to simulate these components and processes are described below.

2.2.2.1 Collector Model

There are several types of collectors available, but this research will focus solely on the use of flat plate collectors, as they are widely available and economical. Collector efficiency is suggested as the best measure of collector performance.

Collector efficiency is defined as shown in Equation 2.1 [40],

$$\eta = \frac{Q_u}{AI_T} \tag{2.1}$$

Q_U - Useful energy gain; A- collector area; I_T – Incident radiation on the collector

The efficiency is therefore, the ratio of the amount of usable energy that the collector gathers to the energy in the incoming solar radiation. The energy collected (Q_U) is defined as shown in Equation 2.2 [40]:

$$Q_u = m\, C_{PF}(T_o - T_i) \tag{2.2}$$

m – Flow rate; C_{PF} – Specific heat of fluid; T_o – Collector output temperature; T_i – collector inlet temperature

Thermosiphon systems rely solely on natural circulation to move water through the collector. In order for natural circulation to occur, the following 3 conditions must exist:

1. Temperature difference
2. Heat source lower than heat sink
3. Fluids must be in contact

The temperature difference leads to a density difference, which is the driving force for natural circulation. As water is heated, it rises; therefore, the collector (heat source) must be located below the hot water heater (heat sink) allowing heated water to rise into the tank for storage. If there are any barriers in the flow path, or if any of the three conditions are removed, then natural circulation will not take place. [41]

The flow rate of the water is determined by the collector gain. The higher the temperature produced by the collector, the faster circulation takes place. The Type 45 thermosyphon collector model in TRSNYS makes use of the Bernoulli equation to determine the flow rate of fluid through the collector. The model assumes that:

- Fluid flow in the collector is at steady state.
- the thermosyphon loop is then divided into sections, and
- the Bernoulli's equation for incompressible flow is applied to each section.

"Bernoulli's equation shown in Equation 2.3 states that the sum of all forms of energy in a fluid flowing along an enclosed path (a streamline) is the same at any two points in that path." [42]

$$\frac{1}{2}\rho v^2 + P + \rho g h = Constant \quad \textbf{(2.3)}$$

v - fluid velocity; P - fluid pressure; ρ - fluid density; g – gravitational constant; h - fluid height

The constant in Equation 2.3 is referred to as the total head of the fluid in the loop, and the terms in the equation refer to the fluid's velocity, pressure and elevation heads respectively.

As fluid moves, a reduction in total head occurs due to friction between the fluid and the pipe, turbulence and inter-particle interactions. This phenomenon is referred to as head loss. Frictional head loss can be calculated from Equation 2.4 [39]:

$$H_p = \frac{fLv^2}{2d} + \frac{kv^2}{2} \quad \textbf{(2.4)}$$

Applying Bernoulli's equation to the various nodes of the thermosyphon loop yields the relationship displayed in Equation 2.5 for the pressure drop in each node [39]:

$$\Delta P_i = \rho_i g \Delta h_i + \rho_i g h_{Li} \quad \textbf{(2.5)}$$

ΔP - change in pressure; ρ – density; g – gravitational constant; Δh – height of node; h_{Li} – frictional head loss

The TRNSYS thermosyphon model then finds a numerical solution for a flow rate which satisfies the condition in the above equation.

2.2.2.2 Storage Tank Model

The thermal storage for this system takes the form of an electric geyser. The energy storage capacity of the water in the geyser is given by Equation 2.6 [39]

$$Q_S = (mC_P)_S \Delta T_S \quad \textbf{(2.6)}$$

m – Mass of water in tank; C_P – Specific heat of water; T_S – Temperature of water in tank

In practice, the temperature of water varies in different areas of the tank. This is known as stratification. The geyser is modelled using a plug-flow approach, whereby segments of fluid at different temperature move through the tank. The size, temperature and position of the

segments are variable, and dependent on the collector flow rate, energy input from the auxiliary heater and the load flow rate.

The average temperature of the water delivered to the load by the tank is then given by Equation 2.7 [39]

$$T_d = \frac{V_h T_h + (V_L - V_h) T_1}{V_L} \tag{2.7}$$

Vh – Volume of hot fluid entering tank; Th – Temperature of fluid entering tank;
VL - Volume of cold fluid entering tank; T_1 – Temperature of fluid at the top of the tank

Water is constantly being drawn from the geyser, this leads to changes in the mass of water in the tank, and the temperature of water in the tank, as cold water flows in to replace the hot water that was drawn. Energy flow out of the tank is given by Equation 2.8 [39]

$$Q_{OUT} = m_L C_P (T_d - T_l) \tag{2.8}$$

m_L – Flow rate to load; C_P – Specific heat of water; T_D – Temperature of water to load; T_L – Temperature of cold water entering tank

There are losses that take place as water circulates in the system, as well as standing losses associated with the hot water geyser. Detailed mathematical descriptions of the models discussed can be found in appendix B. The text in the appendix was extracted from the TRNSYS-16 Manual.

CHAPTER III

3. *RESEARCH METHODOLOGY*

This chapter will cover the procedure that was used in achieving the research objectives mentioned in Chapter 1. There are 3 main steps in the methodology: the computer simulations, measurements from the field and lastly modelling the effects of solar water heating on the transmission grid.

3.1 Simulations Using MeteoNorm and TRNSYS

TRNSYS and MeteoNorm were used to run simulations for various cities around South Africa, in order to determine the annual performance of a solar water heating system.

3.1.1 WATER CONSUMPTION PROFILE

Electricity consumption for water heating is dependent on the time of hot water usage, and this varies from individual to individual. This spread makes it difficult to simulate the impact of several households using solar water heating. The typical South African water consumption profile depicted in Figure 3.1 was used as the water draw profile for the simulations.

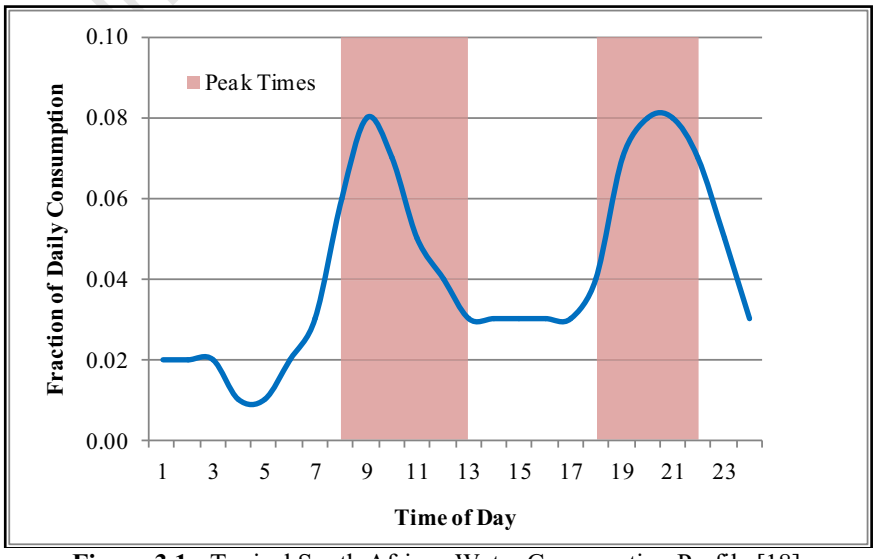

Figure 3.1: Typical South African Water Consumption Profile [18]

3.1.2 GENERATING CLIMATE DATA WITH METEONORM

The performance of a solar water heating system is highly dependent on the climate in which it is operating. Therefore, prior to commencing simulations with TRNSYS, MeteoNorm was used to generate annual climate data files for 12 cities around South Africa. Figure 3.2 shows the input screen for generating such a file in MeteoNorm. The most important parameters to note are:

- The site – this provides MeteoNorm with the latitude which is used during calculations. The sites chosen for the research project were: Cape Town, Johannesburg, Pretoria, Durban, Pietermaritzburg, Port Elizabeth, Kimberly, Upington, Bloemfontein, Mmabatho, Polokwane and Nelspruit.
- The format of the output file – MeteoNorm offers several formats for the output file; however, the TMY2 format is best suited for use with TRNSYS, in terms of compatibility.
- The orientation of the plane – is left as is, and modified in TRNSYS, so as not to skew the results due to double calculations and also to allow for more flexibility.
- The calculation required – has to produce hourly values that TRNSYS can use during the simulations.

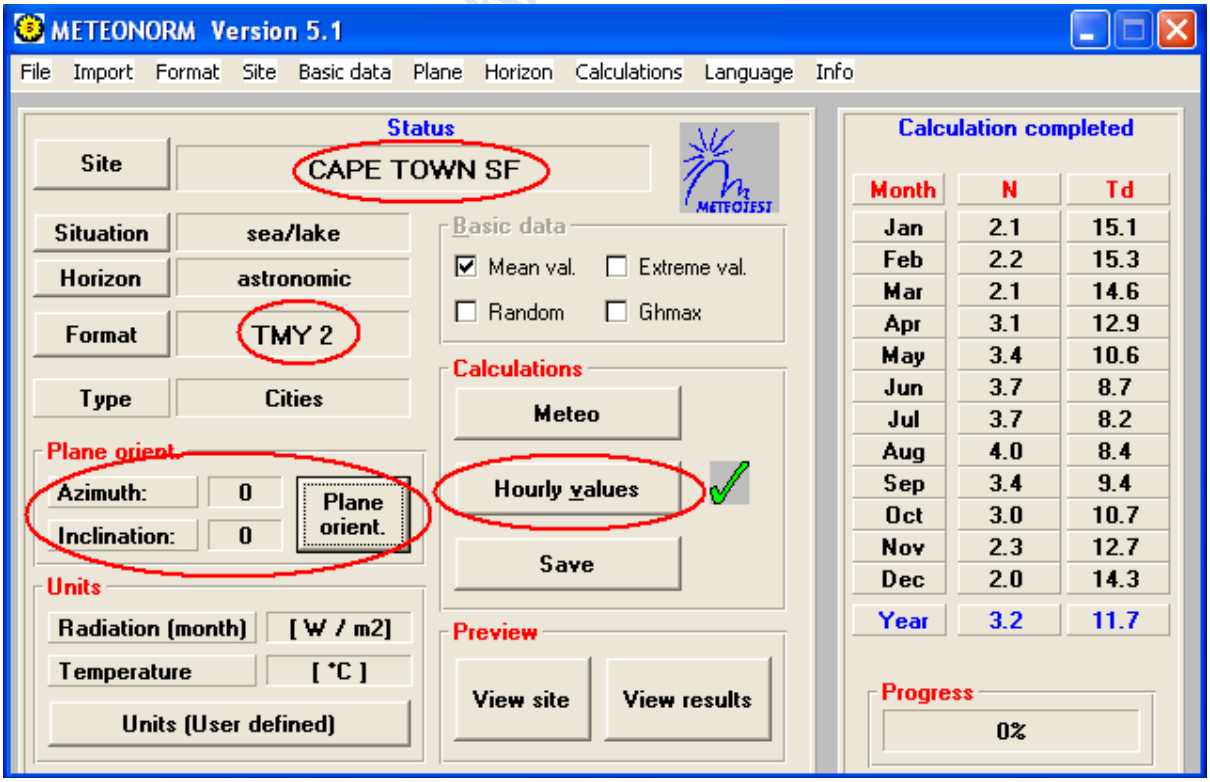

Figure 3.2: MeteoNorm Screenshot

3.1.3 TRNSYS SIMULATIONS

In order to determine the impact of a solar water heating system on peak demand, a comparison needed to be carried out between a water heating system that used electricity only (Electric Domestic Hot Water System – EDHW), and one that made use of solar energy (Solar Domestic Hot Water System – SDHW). Thus 2 simulations were done for each location; one for an EDHW system and one for an SDHW system.

3.1.3.1 Simulation Parameters and Set Up

The systems simulated in TRNSYS had parameters as set out in Table 3.1. The values were extracted from literature, and are typical values for an average South African household.

Table 3.1: Simulation System Parameters

	SDHW SYSTEM	EDHW SYSTEM
Collector Area	*2m²*	-
Intercept Efficiency	*0.706*	-
Efficiency Slope	*4.9099W/m².K*	-
Tested Flow Rate	*70kg/hr.m²*	-
Collector Slope[1]	*30°*	-
Tank Volume	*200l*	*200l*
Tank Height	*1.5m*	*1.5m*
Thermal Conductivity	*1.5kJ/hr.m.K*	*1.5kJ/hr.m.K*
Overall Loss Co-efficient	*5kJ/hr.K*	*5kJ/hr.K*
Geyser Element Rating	*3kW*	*3kW*
Thermostat Setting	*65 °C*	*65 °C*

The systems simulated in TRNSYS were set up as shown in Figure 3.3 and Figure 3.4. The component marked "Weather" allows for the input of the various climate data files generated by MeteoNorm, and the component marked "Water Draw Profile" is a link to the water consumption profile. The tee-piece and the diverter form a mixer circuit for hot and cold water. "Type 45a" is the model for the thermosyphon solar collector, and "Type 38" is a model for an electric geyser.

[1] It is recommended that the collector slope is equal to the latitude of the chosen location. The cities chosen lie between 24°S and 33°S thus a slope of 30° (typical roof angle) was chosen. It was verified that this did not adversely affect the simulation results.

The output studied was the geyser's electricity demand curve. Simulations were carried out using a time step of 15 minutes, over a period of one year. This yielded over 30'000 data points for each simulation. In order to analyse the data, average monthly geyser demand curves were compiled for each month of the year, for every simulation. A comparison was then carried out between the EDHW geyser demand and SDHW geyser demand curves, in order to establish the impact of a SDHW system on peak demand.

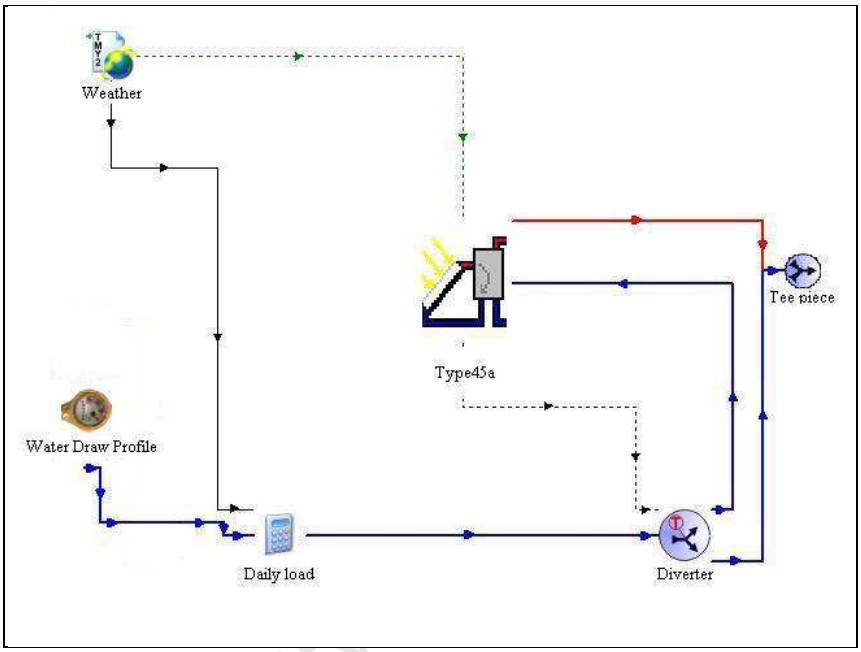

Figure 3.3: Screenshot of Solar Domestic Hot Water (SDHW) System Simulation Set Up in TRNSYS

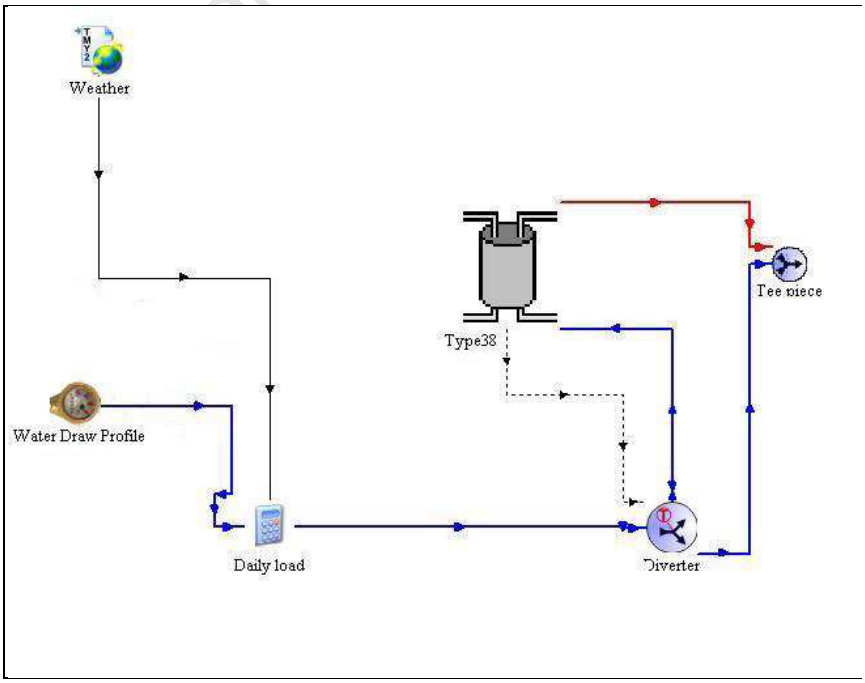

Figure 3.4: Screenshot of Electric Domestic Hot Water (EDHW) System Simulation Set Up in TRNSYS

3.2 Monitoring of Solar Water Heating Installations

Another part of the research involved the monitoring of solar water heating systems that have been installed in households around Cape Town. This was done with the help of Atlantic Solar (Pty) Limited, a Cape Town based company that deals with the design, manufacture and installation of solar water heating systems.

Atlantic Solar agreed to install data loggers at 9 of their installations. A simple schematic of the set up of the logging equipment is shown in Figure 3.5. These loggers were used to record the geyser's hourly electricity (current) consumption as well as the household's hot water usage. This data was used to compile average monthly geyser demand curves and water consumption profiles.

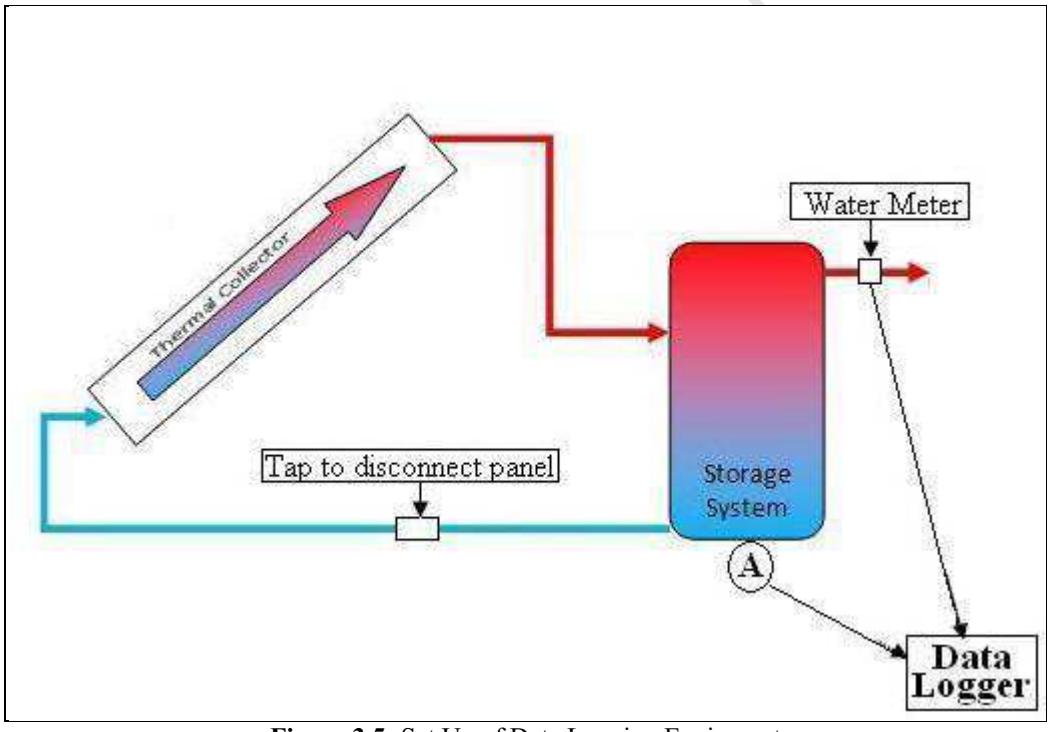

Figure 3.5: Set Up of Data Logging Equipment

As can be seen in Figure 3.5, a tap was included during the installation, which allowed for the panel to be disconnected. This would cause the household to revert to electricity only for water heating. The data obtained can then be used to create EDHW curves that allow for comparison, to assess the impact of a SDHW system on peak demand.

The data collected from the Atlantic Solar SDHW system installations was compared to the simulation results from TRNSYS[2], in order to validate the accuracy of the TRNSYS models, as well as the climatic data created by MeteoNorm.

Once the simulation results were validated, they were analysed, in order to quantify, as a percentage, the change in household electricity consumption during peak demand times, due to the use of a SDHW system. These peak demand reduction factors were then used to find out if solar water heating would have any effect on the transmission grid.

3.3 Determining the Impact of Solar Water Heating On the Transmission Grid

The final task of the project was to determine if the large scale implementation of solar water heating would have any impact on the operation of a transmission grid, particularly on the losses incurred.

A load flow study was chosen as the means of analysis. P S A T 2.0.0 software was chosen for this task. A power system model had to be developed for load flow studies. The transmission grid parameters were based on the ESKOM grid parameters, and were used to develop the model, which is outlined in greater detail in chapter 7. Load data i.e. peak demand values for the cities chosen also had to be obtained.

The peak demand reduction factors obtained from the TRNSYS simulations were used in order to examine the impact on the transmission grid, of solar water heating being implemented on a large scale in Cape Town, Johannesburg and Durban.

Load flow studies were carried out for various scenarios.

Scenario 1: This scenario served as the base case. The losses on the system in this case were representative of the losses experienced during times of peak demand, on a grid where no solar water heating had been implemented.

[2] The data collected from households was only available for the months of September – February. Only the Cape Town simulation data from these months was used during the validation process.

Scenario 2: 10% penetration of solar water heating in the residential consumer market.
Scenario 3: 50% penetration of solar water heating in the residential consumer market.
Scenario 4: 100% penetration of solar water heating in the residential consumer market.

Scenarios 2 to 4 assessed the impact of various levels of penetration of solar water heating in the residential load centres of Cape Town, Johannesburg and Durban.

The peak demand reduction factors that were derived from the TRNSYS simulations were used to alter the load data.

These load alterations were based on the assumptions that:-

- Residential Electricity Consumption = 37% of Peak Demand [2] and
- Geyser Electricity Consumption = 40% of Residential Electricity Consumption [2]

The system losses were then recalculated, and compared to the base case, in order to see if there were any changes.

CHAPTER IV

4. TRNYS SIMULATION RESULTS AND ANALYSIS

This chapter presents the results obtained from the TRNSYS simulations. Due to the large amount of information obtained, only data from selected cities has been included. The rest is presented in Appendix C. An analysis of the simulation results and derivation of household peak demand reduction factors is also included.

4.1 Simulation Results

This section presents the results from the TRNSYS simulations that were run for the cities of Cape Town, Johannesburg and Durban. These three cities were chosen due to their locations in different climatic regions, particularly with respect to solar radiation patterns. They are also the largest of the residential load centres in South Africa.

Average daily demand profiles for the SDHW and the EDHW system geysers were derived for each month. These were then plotted on the same set of axes in order to observe the difference in geyser electricity consumption, for various months in the year.

4.1.1 CAPE TOWN

Cape Town is situated on the west coast of South Africa (33˚56'S, 18˚28'E, At Sea Level), and has a Mediterranean climate. During summer, the weather is hot and dry, but winters are much cooler and wet. The simulation results are presented in Figures 4.1 to 4.3.

4.1.1.1 Summer Simulation Results

Figure 4.1 shows the average daily geyser electricity demand profiles for the months of January and February. In the figure it can be seen that the use of solar water heating has the effect of reducing both the morning and the evening peak demand of the geyser during summer. The reduction in the evening peak demand is about 90%, whereas the reduction of the morning peak is more moderate at approximately 38%.

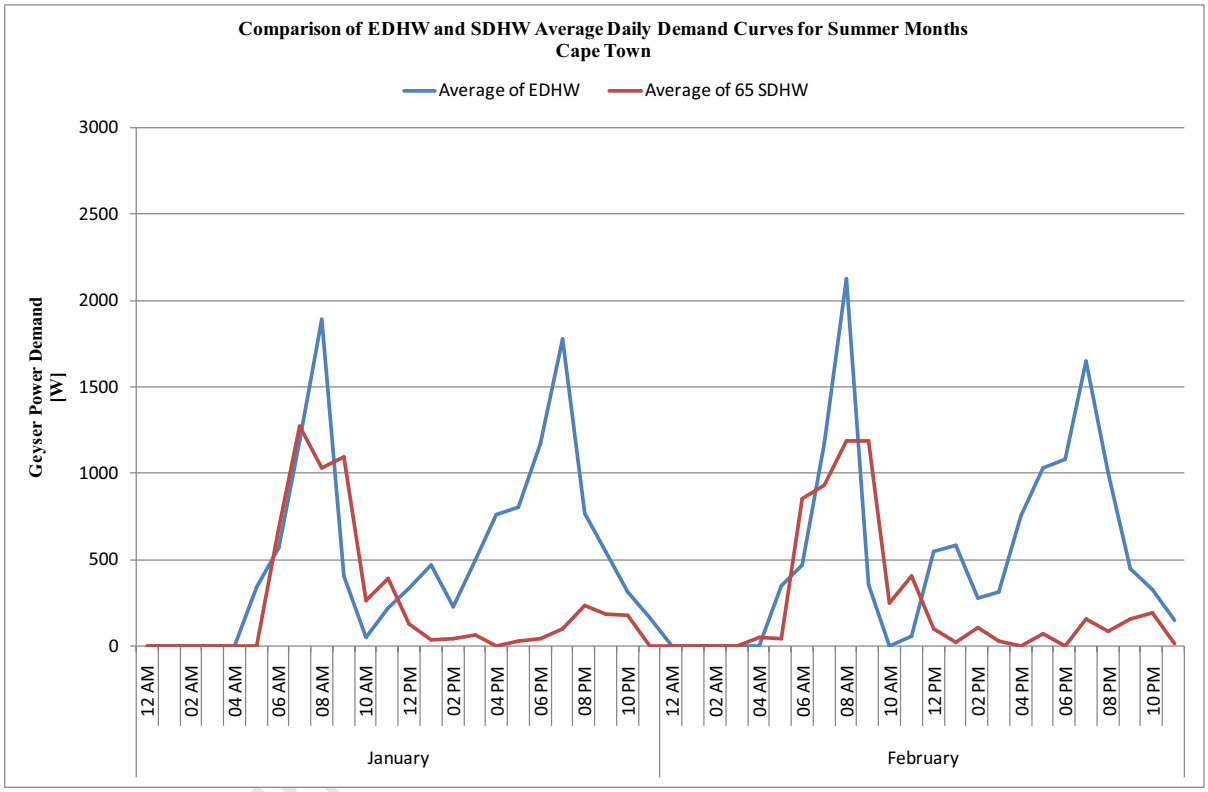

Figure 4.1: Comparison of EDHW and SDHW Average Daily Demand Curves for Summer Months in Cape Town

4.1.1.2 Winter Simulation Results

Figure 4.2 shows the average daily geyser electricity demand profiles for the months of June and July. From Figure 4.2, the SDHW system operating in Cape Town appears to have little effect on the morning peak demand of the geyser in winter. In the evening, the reduction in the geyser's peak power consumption is about 34%, which is not as extensive as it was in summer, but it is still appreciable.

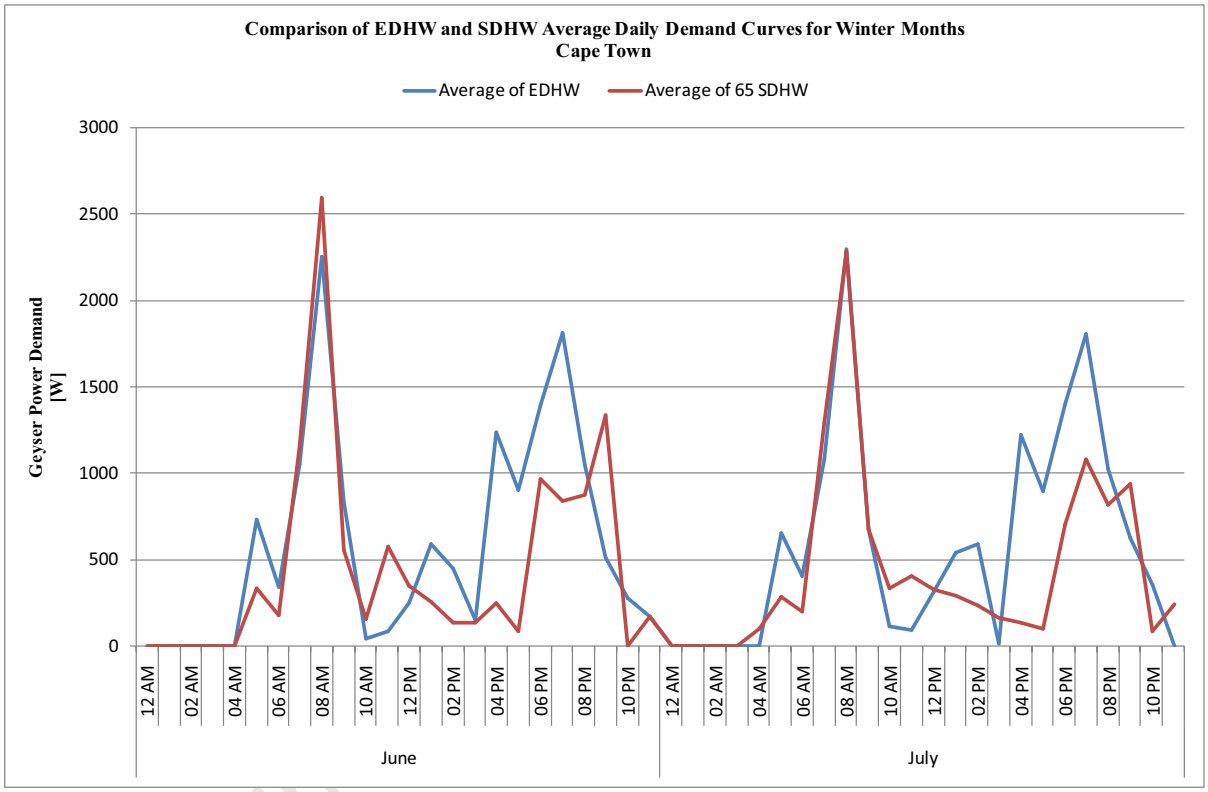

Figure 4.2: Comparison of EDHW and SDHW Average Daily Demand Curves for Winter Months in Cape Town

It is also interesting to note that the evening peak of the SDHW system geyser was deferred by an hour or two, shifting it to just outside of ESKOM's evening peak demand times of 6pm to 8pm.

4.1.1.3 Autumn and Spring Simulation Results

This simulation was carried out in order to get an idea of what happens with the SDHW system in the intermediate seasons of spring and autumn. The results are illustrated in Figure 4.3.

Once again, as seen in Figure 4.3, the SDHW system has little impact on the peak demand of the geyser in the morning. The evening peak, however, is considerably lower than that of the EDHW system. In both cases, there is a reduction of about 58%.

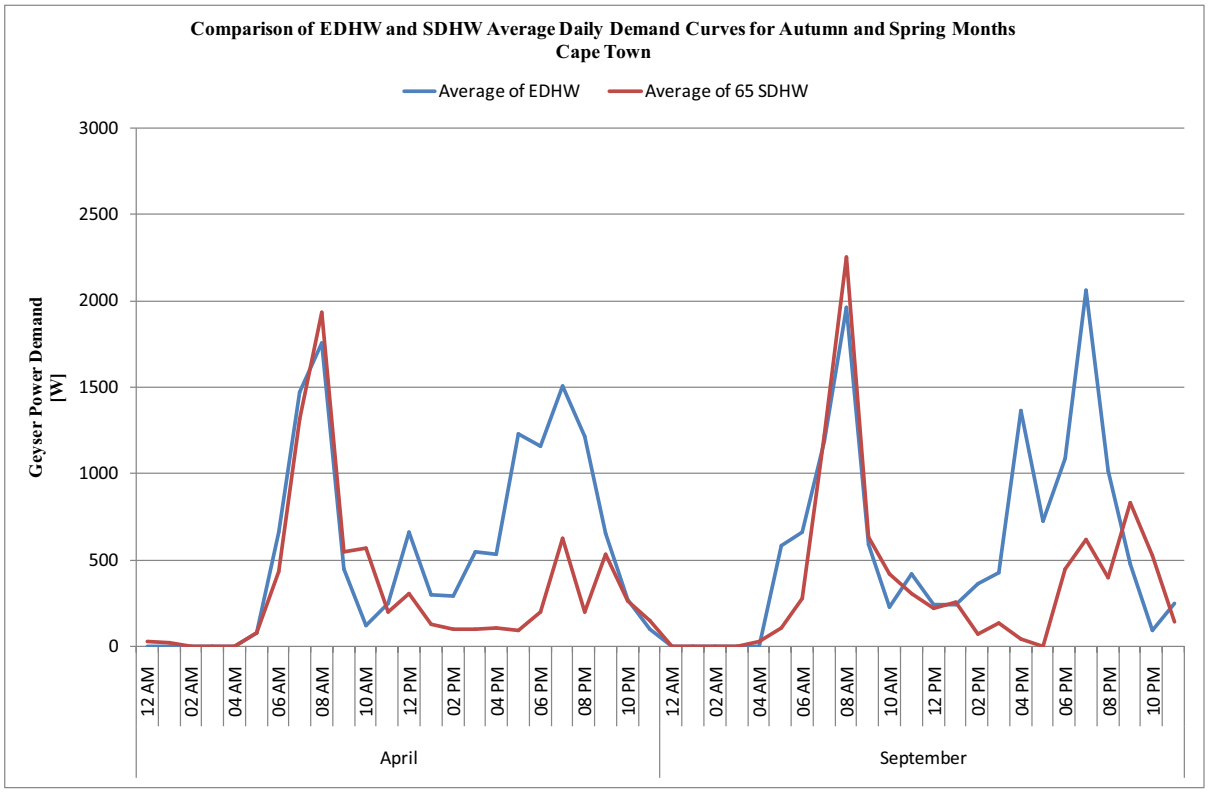

Figure 4.3: Comparison of EDHW and SDHW Average Daily Demand Curves For Autumn and Spring Months in Cape Town

4.1.2 JOHANNESBURG

Johannesburg is located in the Highveld (26˚10'S, 28˚02'E, 1676m Above Sea Level), and it experiences a dry, sunny climate all year round. The simulation results for an EDHW system and SDHW system located in this region are shown in Figures 4.4 to 4.6 below.

4.1.2.1 Summer Simulation Results

Figure 4.4 shows the average daily geyser electricity demand profiles for the months of January and February. From Figure 4.4 it can be seen that the SDHW system has little impact on the morning peak demand of the geyser. The evening peak however, has been reduced quite significantly by about 65%.

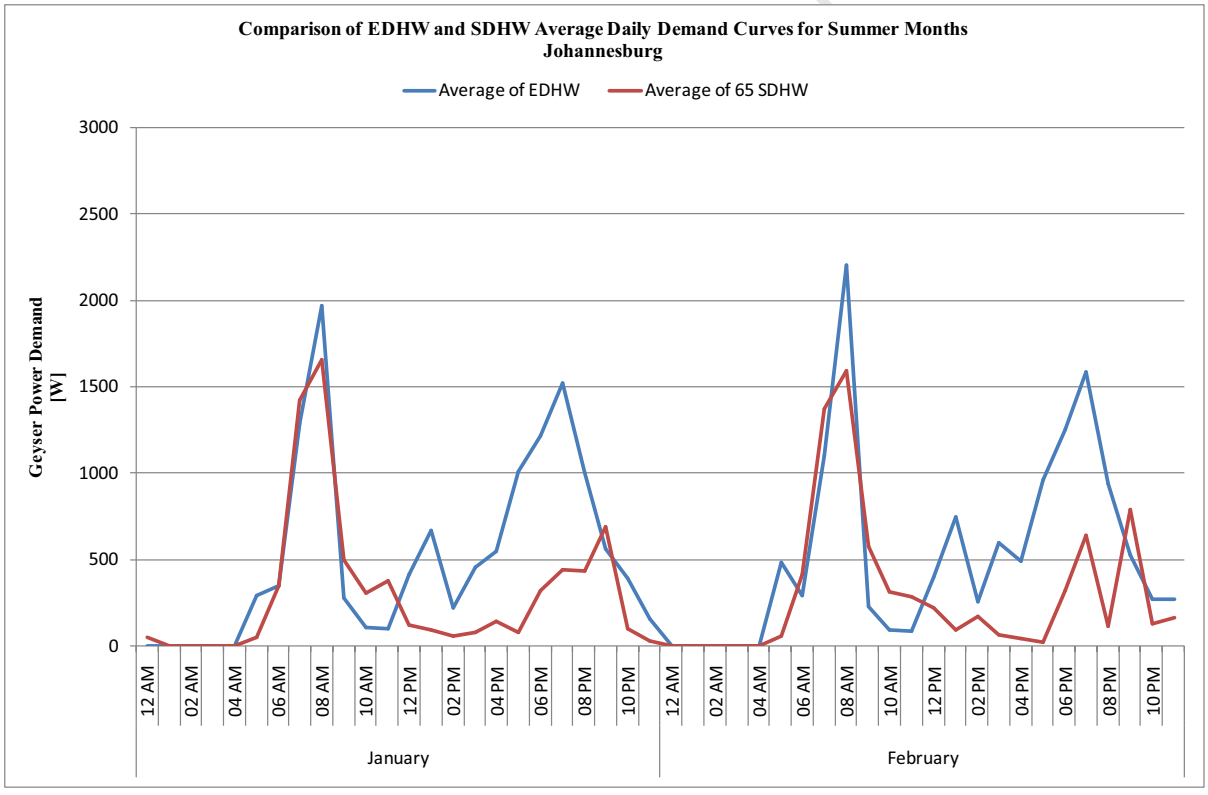

Figure 4.4: Comparison of EDHW and SDHW Average Daily Demand Curves for Summer Months in Johannesburg

4.1.2.2 Winter Simulation Results

The simulation results for June and July, shown in Figure 4.5, reveal that a SDHW system is quite effective in reducing electricity consumption in winter in Johannesburg. The evening peak demand reduction is approximately 47% which is quite appreciable. The morning peak remains largely unaffected by the use of solar water heating.

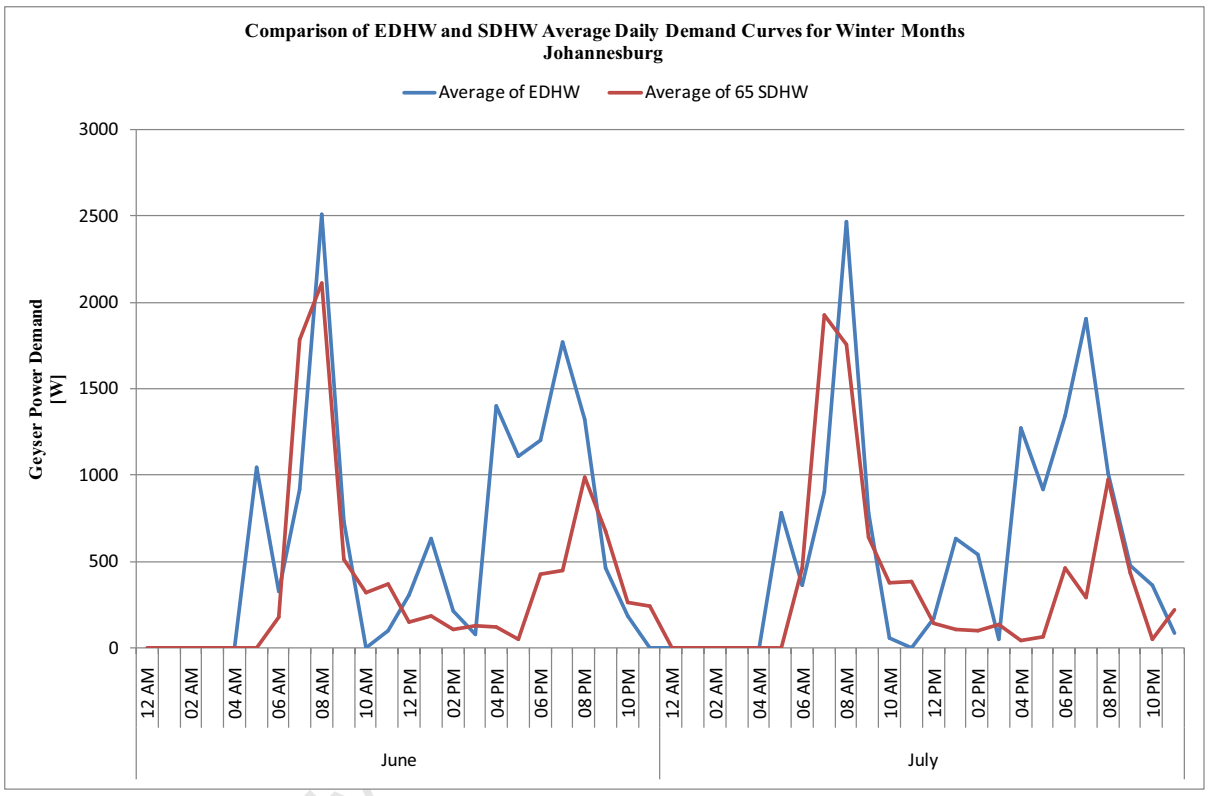

Figure 4.5: Comparison of EDHW and SDHW Average Daily Demand Curves for Winter Months in Johannesburg

4.1.2.3 Autumn and Spring Simulation Results

Figure 4.6 shows the average daily geyser electricity demand profiles for the months of April and September, autumn and spring months. From Figure 4.6, it is noticeable that the SDHW system still has a significant impact, in terms of reducing evening peak demand of the geyser during these seasons, with an average drop of about 48% in April, and 65% in September.

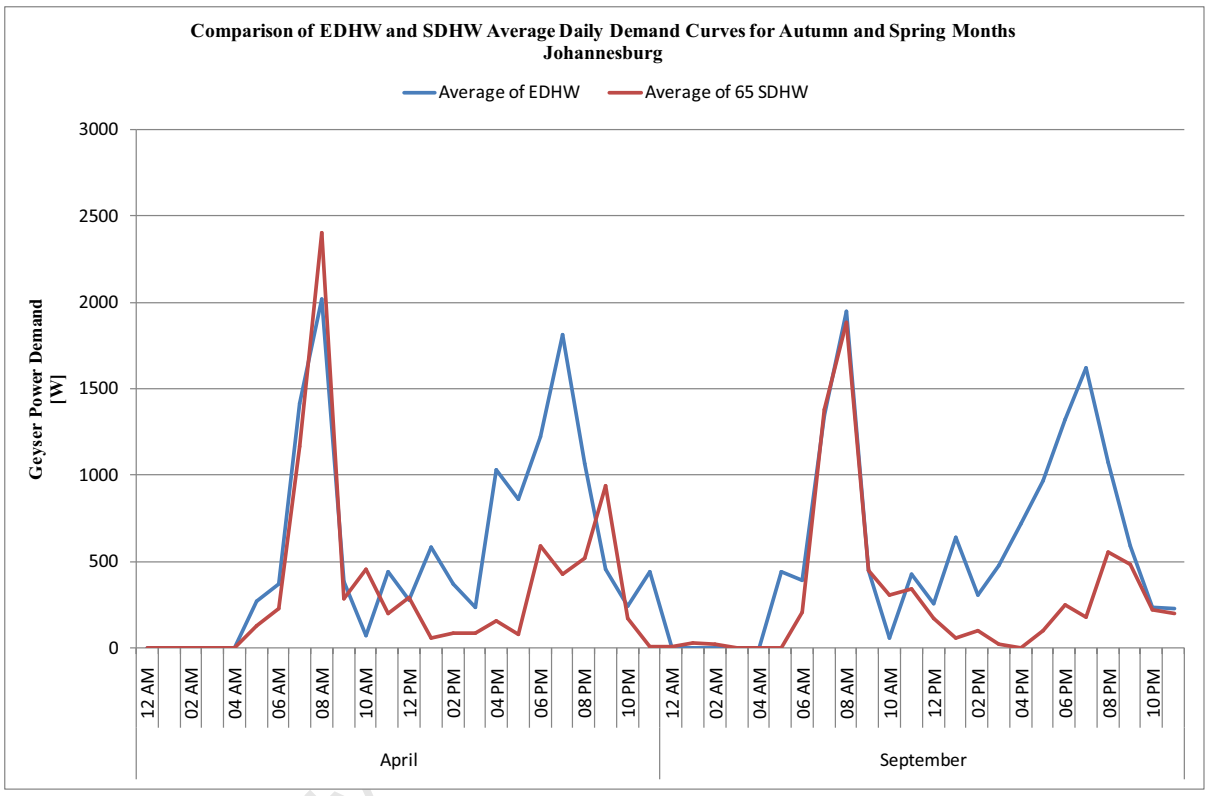

Figure 4.6: Comparison of EDHW and SDHW Average Daily Demand Curves for Autumn and Spring Months in Johannesburg

4.1.3 DURBAN

Durban is situated on the east coast (29˚53'S, 30˚60'E, At Sea Level), of South Africa. The subtropical climate of the region leads to humid summers and warm winters. The simulation results for EDHW and SDHW systems located in this city are presented in Figures 4.7 – 4.9 below.

4.1.3.1 Summer Simulation Results

The summer simulation results illusrated in Figure 4.7 show that the morning peak is slightly affected by the solar water heating system, resulting in a reduction of about 32%. The effect of the SDHW system on the evening peak is definitely more noteworthy, with an average reduction of about 60% taking place.

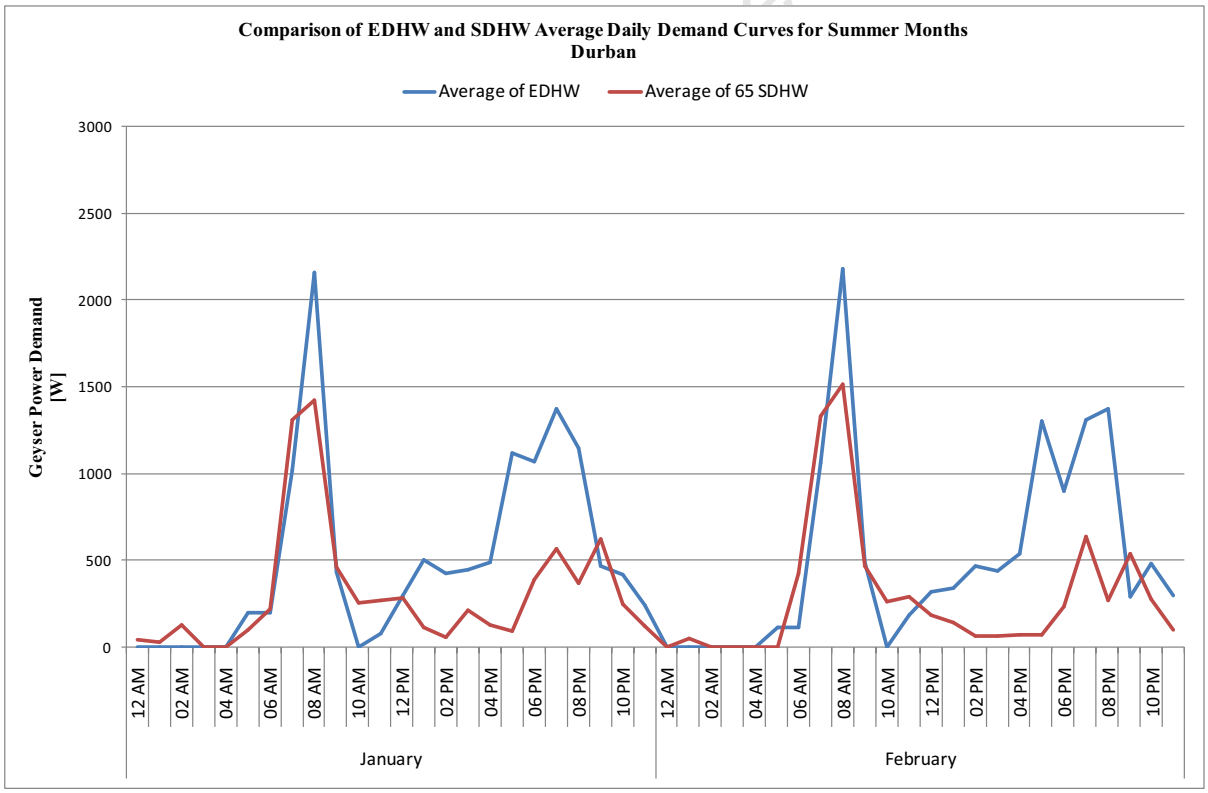

Figure 4.7: Comparison of EDHW and SDHW Average Daily Demand Curves for Summer Months in Durban

4.1.3.2 Winter Simulation Results

Figure 4.8 shows the average daily geyser electricity demand profiles for the months of June and July. From the results shown in Figure 4.8, there is a reduction of approximately 40%. Therefore, we see that in Durban, the impact of the SDHW system i.e. reduction in the geyser's evening peak is slightly lower during the winter months of June and July.

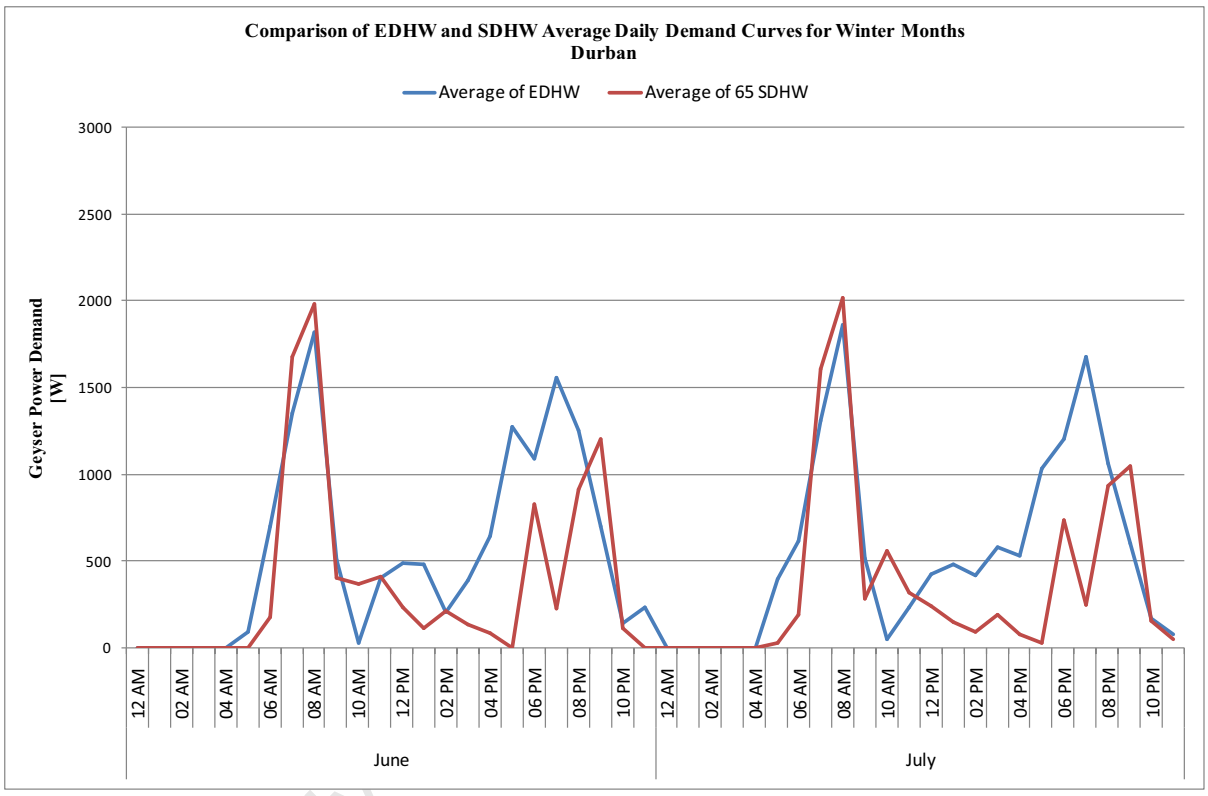

Figure 4.8: Comparison of EDHW and SDHW Average Daily Demand Curves for Winter Months in Durban

4.1.3.3 Autumn and Spring Simulation Results

From the April and September simulation results shown in Figure 4.9, there is a 52% decrease in evening peak in April, and a 57% decrease in the September evening peak. It can thus be concluded that the SDHW system still has a significant impact, in terms of reducing the evening peak demand of the geyser in the intermediate seasons of autumn and spring. The morning peak remains, for the most part unchanged by the presence of a SDHW system.

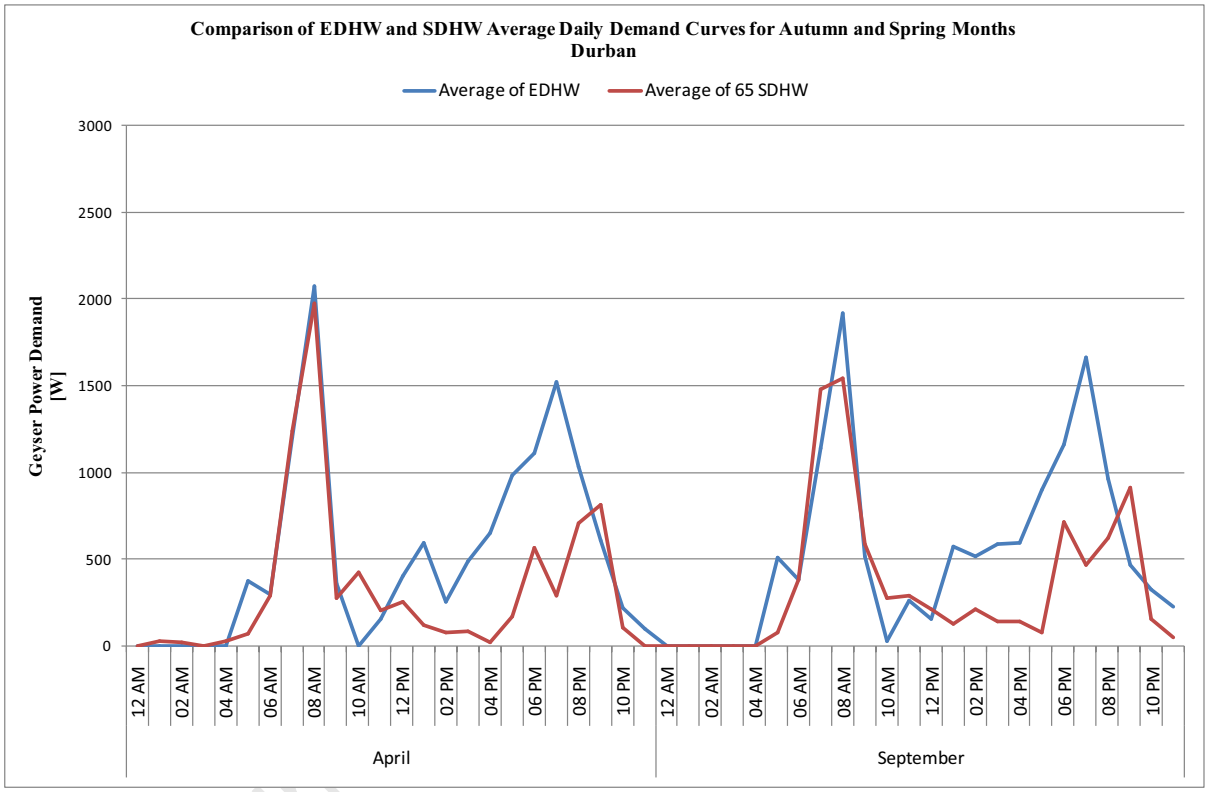

Figure 4.9: Comparison of EDHW and SDHW Average Daily Demand Curves for Autumn and Spring Months in Durban

4.1.4 SIMULATION RESULTS SUMMARY

The performance of the SDHW system can be measured by the reduction in electricity consumption that it brings about. Overall, the SDHW systems performed best during the summer months, for all three cities. The system located in Cape Town had a very good performance during summer, but in winter, the performance was drastically reduced. SDHW systems located in Durban and Johannesburg gave a more consistent performance across all 4 seasons.

4.1.4.1 Anomaly in Simulation Results

There is an anomaly that is present in all the simulation results. The simulation result shown in Figure 4.10 is used as an example. It can be seen, that in the mornings, there are times when, the demand of the SDHW system exceeds that of an EDHW system.

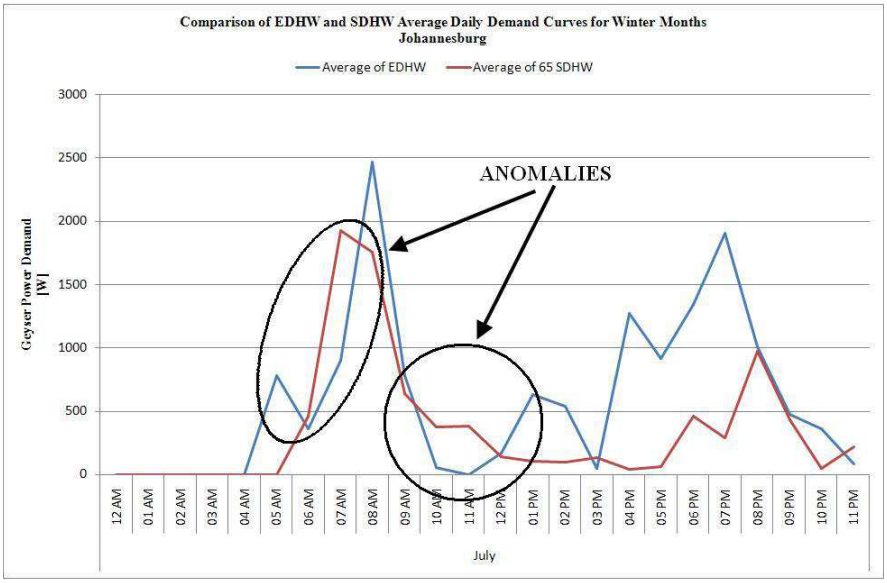

Figure 4.10: Comparison of EDHW and SDHW Average Daily Demand Curves for July in Johannesburg

This irregularity probably occurred due to the positioning of the collector inlet to the geyser and the thermostat in the geyser. In Figure 4.11, it can seen that the flow from the collector enters the geyser very close to thermostat.

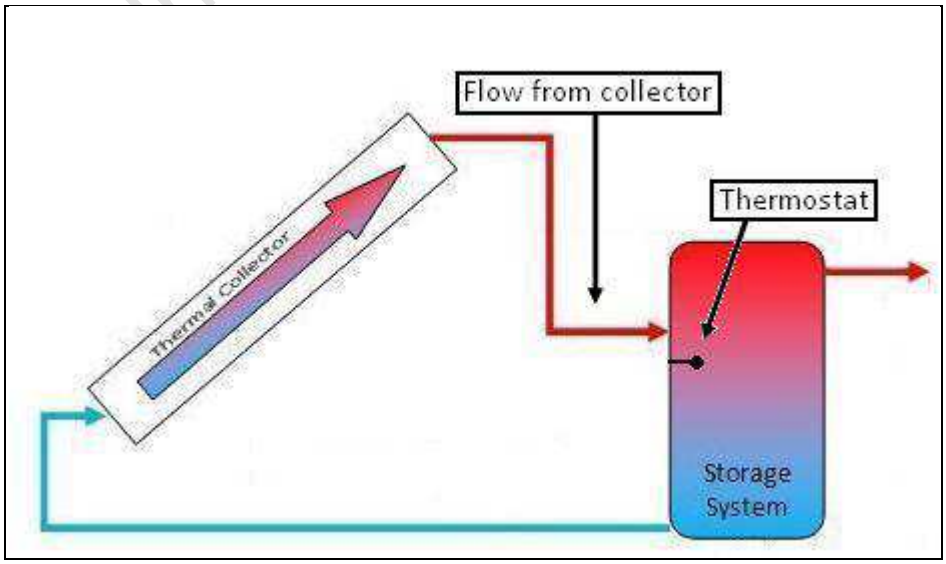

Figure 4.11: Schematic Showing Thermostat Position in Geyser

An analysis of the average tank temperature profiles, shown in Figure 4.12, can help further explain this anomaly.

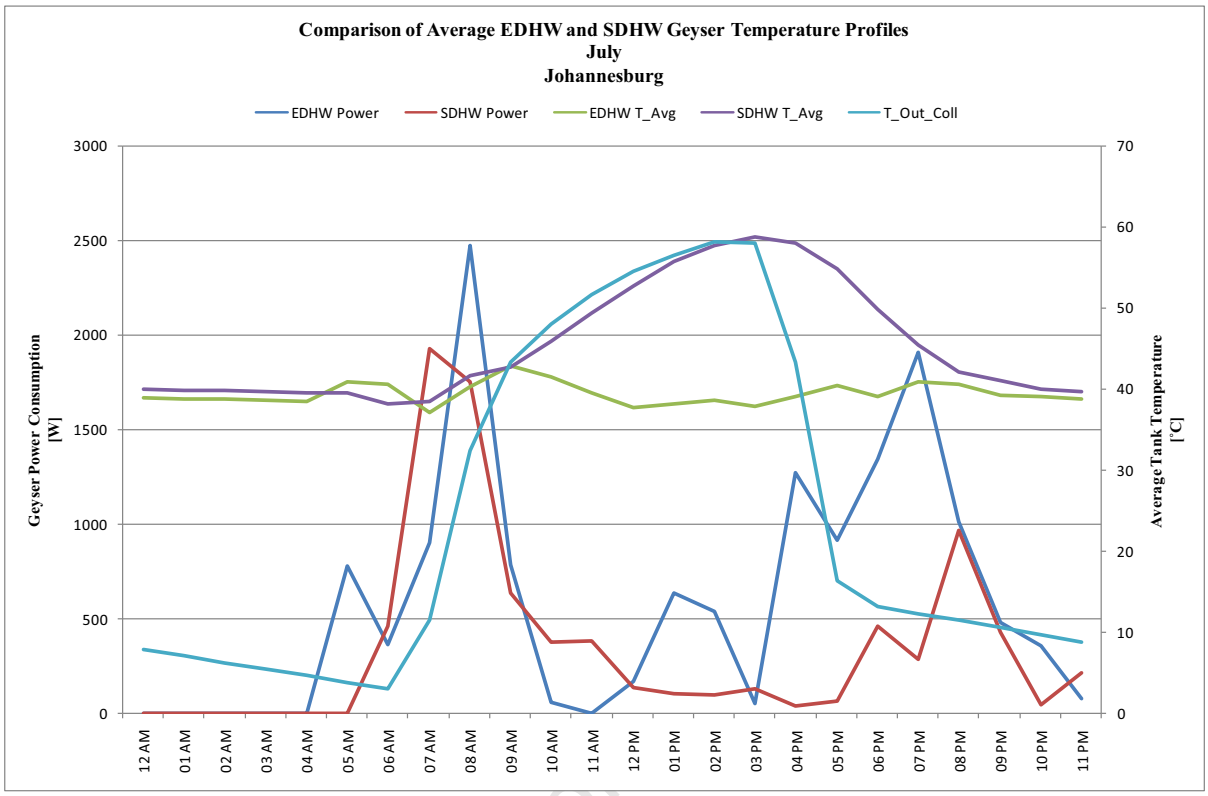

Figure 4.12: Comparison of EDHW and SDHW Average Geyser Temperature Profiles for July in Johannesburg

The curve representing the temperature of the water exiting the collector shows that early in the mornings, the water is quite cool. When it enters the geyser, it probably cools down the water around the thermostat, thus causing the geyser element to switch on, resulting in the demand curves depicted. It is however, important to note that looking at the whole 24 hour period, there is a substantial net reduction in geyser power consumption, even during winter.

This anomaly makes it difficult to determine the impact of a SDHW system on household's electrcity consumption in the morning. Therefore, only the impact of SDHW systems on evening peak demand was examined.

4.2 Analysis of Simulation Results

The aim of this section is to determine the impact of SDHW systems on residential consumers' contribution to peak demand. There are two possible methods to achieve this objective.

The first method involves incorporating the simulated geyser demand curves into a typical household electricty consumption profile, and observing the change that occurs when the EDHW system is replaced by a SDHW system.

The other method involves looking at the change in the geyser demand curves and determining the average reduction in the geyser's peak demand. Thereafter, a scaling factor would be applied in order to determine what the impact would be on a household's electrcity consumption profile. The scaling factor would be based on how much water heating contributes to electricity consumption in the household.

Both methods yield a set of Peak Demand Reduction Factors (PDRFs) for each month.

According to ESKOM [1], the evening peak period is between 6PM and 8PM. Therefore, only simulation results for 6PM, 7PM and 8PM were used during the analysis.

4.2.1 ANALYSING CHANGES IN HOUSEHOLD DEMAND PROFILE

This method of analysis involves integrating the generated geyser demand curves into a typical household demand curve. This was achieved by subtracting the simulated EDHW curve from a typical household electricity consumption profile, and adding the SDHW curve in its place.

The household electricty consumption profiles were generated using the Distribution Pre Electrification Tool (D-PET). The profiles are based on an average monthly consumption of approximately 715kWh, which is typical of a middle to high income household in South Africa.

Figure 4.13 through to Figure 4.15 show the typical daily household demand curves for January and July in Cape Town, Johannesburg and Durban.

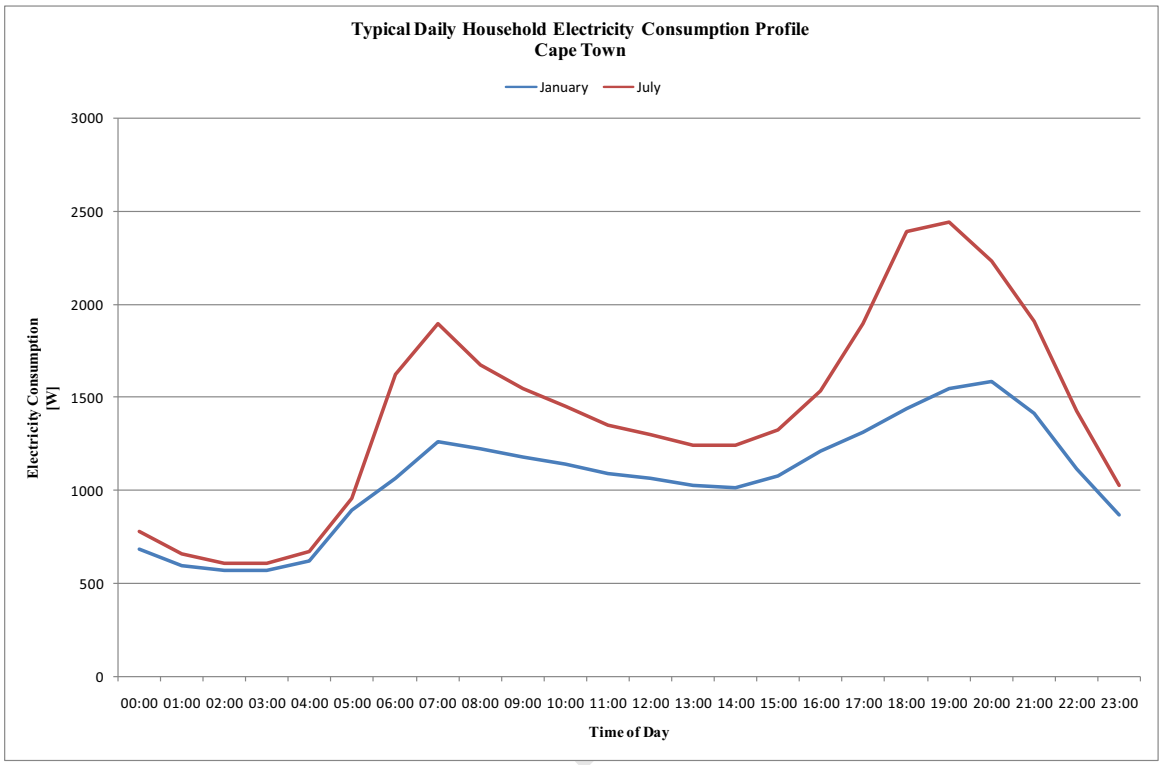

Figure 4.13: Typical Daily Household Electricity Consumption Profiles for January and July – Cape Town

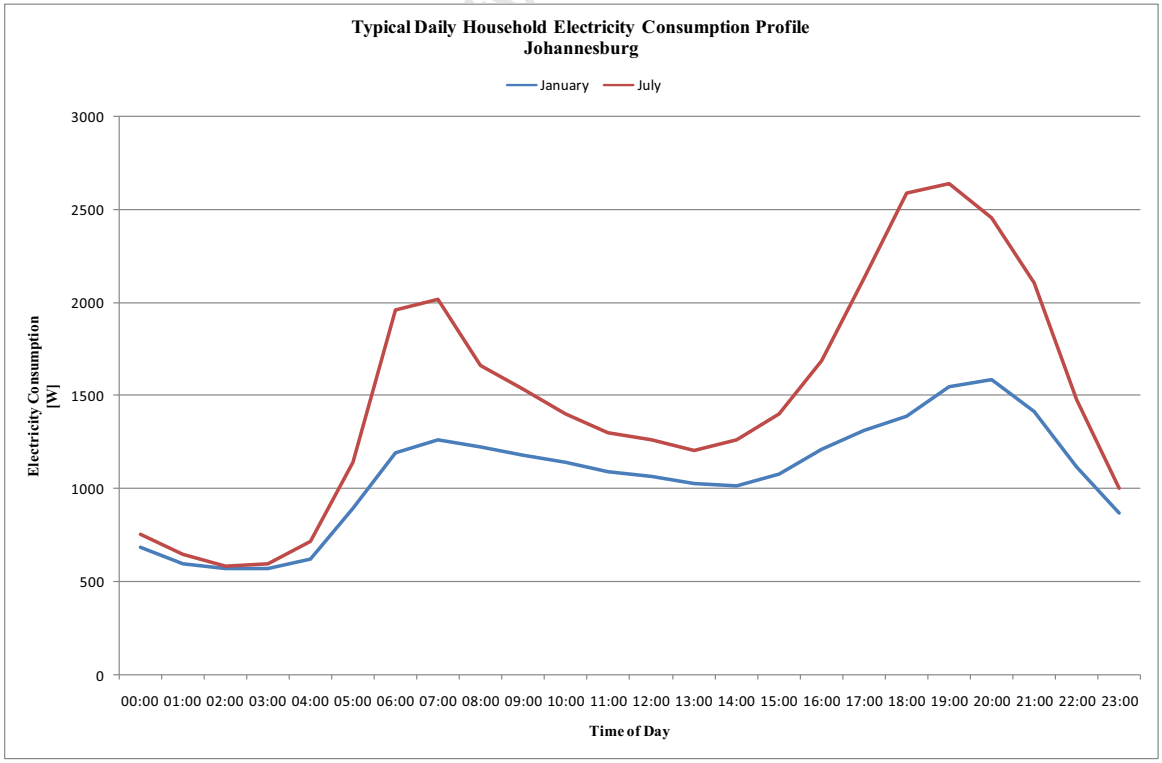

Figure 4.14: Typical Daily Household Electricity Consumption Profiles for January and July – Johannesburg

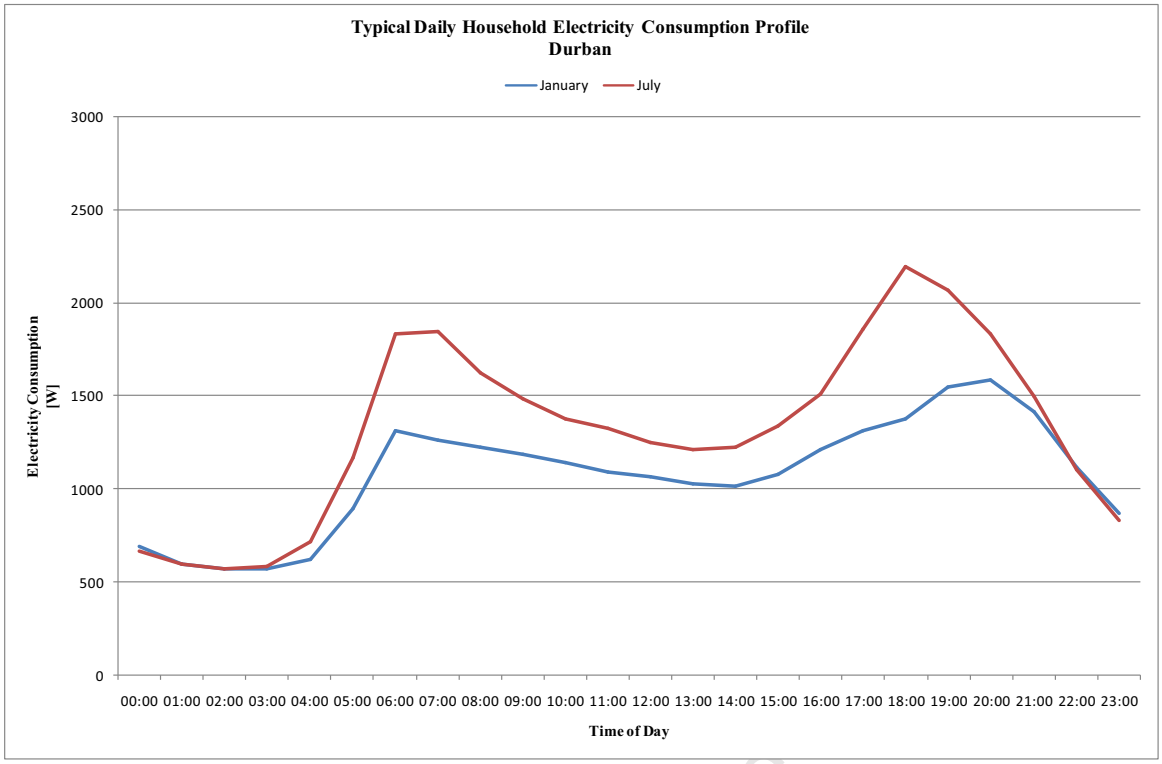

Figure 4.15: Typical Daily Household Electricity Consumption Profiles for January and July – Durban

In all the three figures, there is a marked increase in household energy consumption in winter (July). This can be attributed to space heating, as well as longer burning hours for lights. This shows that these curves account for other major users of electricity in a typical household.

The analysis will only make use of the evening portion of the household electricity consumption profile, due to the aforementioned anomaly in the simulation results. Looking specifically at the period between 6PM and 8PM, the changes depicted in Figure 4.16 to Figure 4.18 were observed.

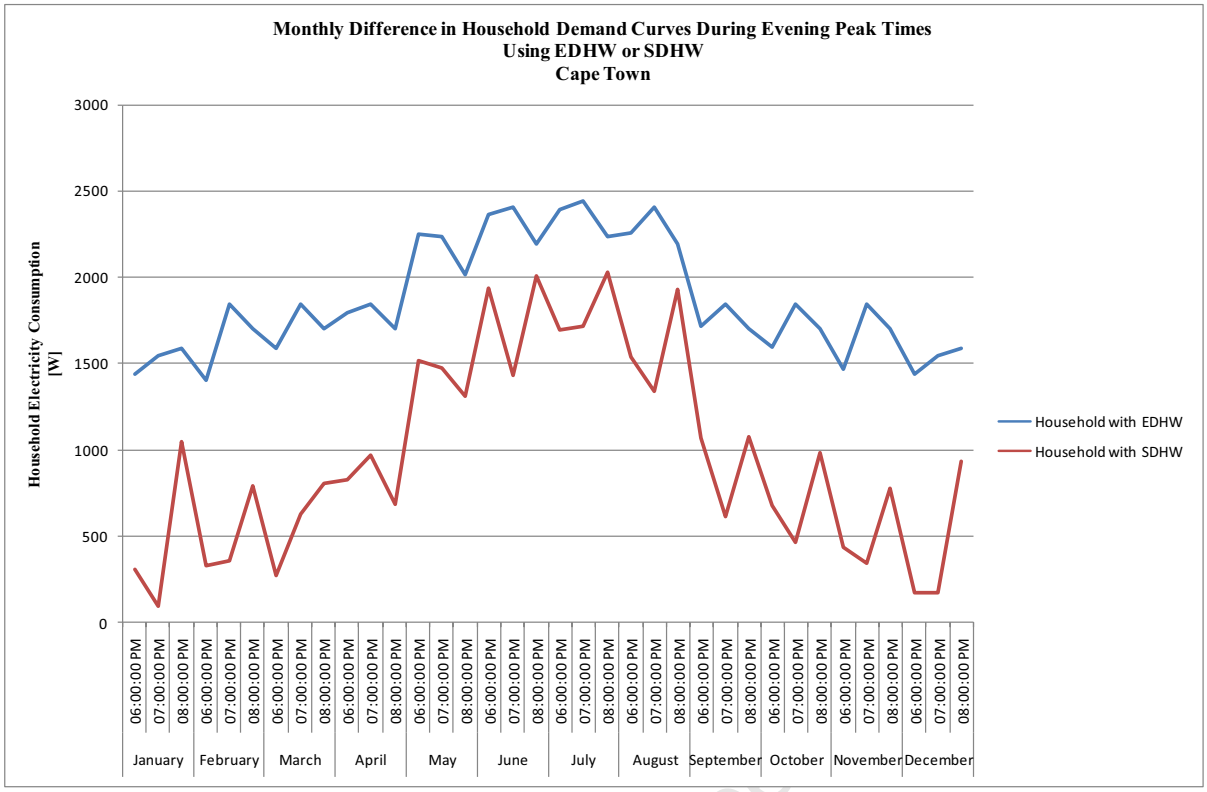

Figure 4.16: Monthly Difference in Household Demand Curves during ESKOM Evening Peak Times when using EDHW or SDHW – Cape Town

Figure 4.16, which shows results for Cape Town, reveals that there is a difference of approximately 67% in the peak of a Cape Town household demand curve for a house using a SDHW as compared to a house making use of EDHW, in the summer months (January-March, October – December). In the winter months, however, the reduction in household demand is only about 33% which is not as drastic.

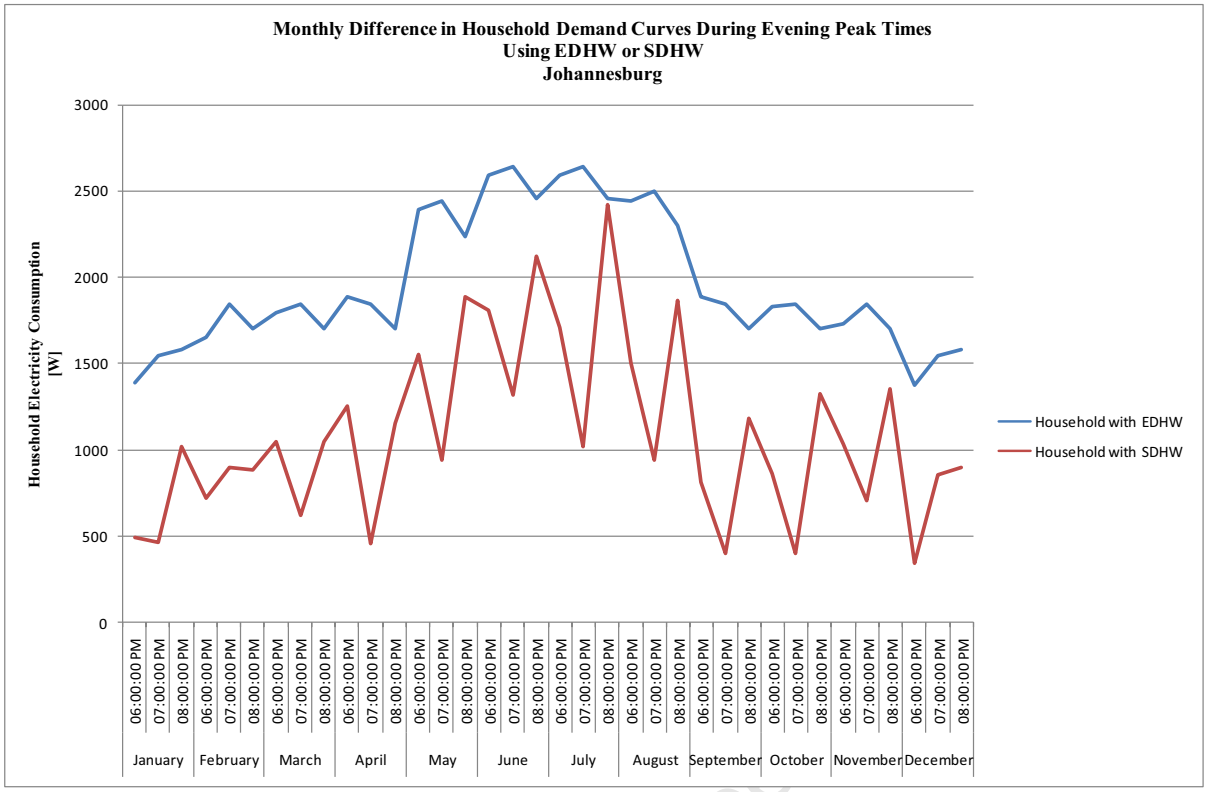

Figure 4.17: Monthly Difference in Household Demand Curves during ESKOM Evening Peak Times when using EDHW or SDHW – Johannesburg

In Johannesburg, there is also a marked difference in terms of the reduction in household consumption that the SDHW brings about in summer (50%) and winter (40%). This can clearly be seen in Figure 4.17.

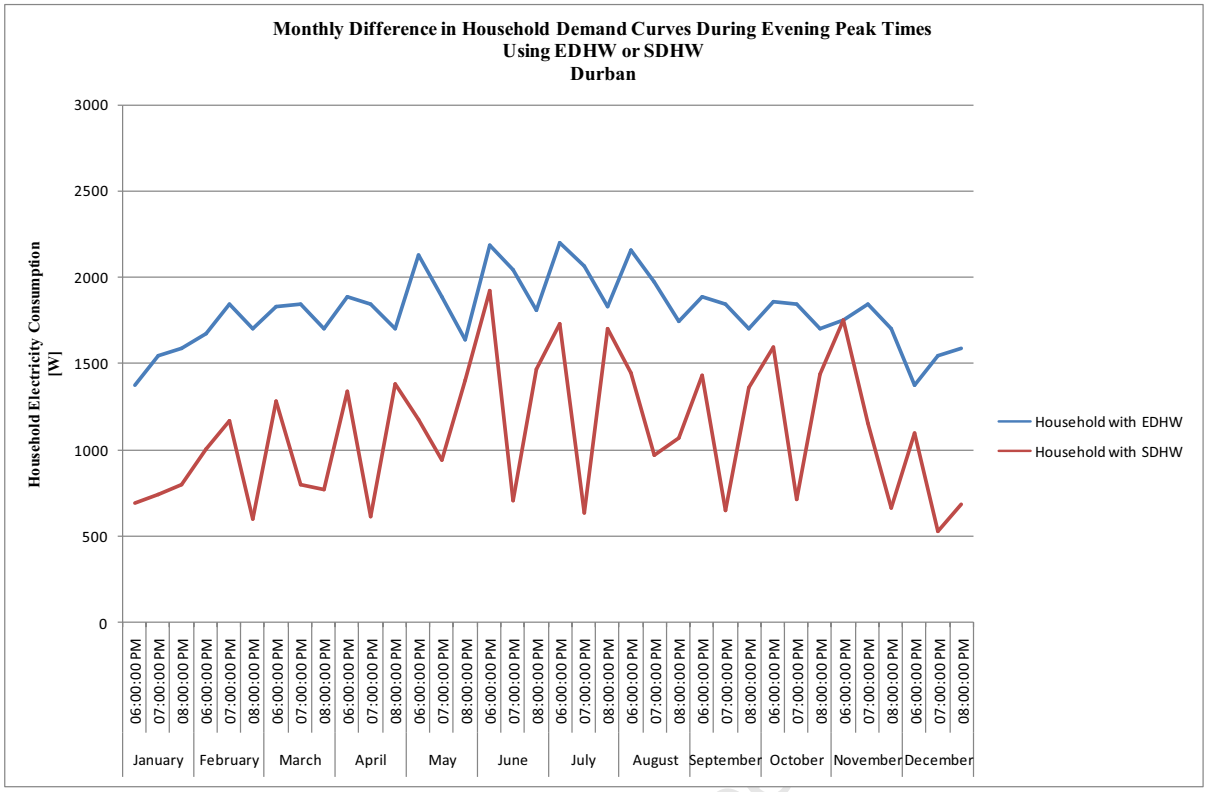

Figure 4.18: Monthly Difference in Household Demand Curves during ESKOM Evening Peak Times when using EDHW or SDHW – Durban

From the Durban results shown in Figure 4.18, it appears as though the use of SDHW in a household leads to a more or less constant reduction in the region of 40% in the household evening peak demand through out the year.

The average reduction in the household peak for each month was determined, using the simple averaging formula shown in Equation 4.1.

$$Reduction = \frac{\sum_{6PM}^{8PM} \frac{(EHW_i - SHW_i)}{EHW_i} * 100}{3} \quad \textbf{(4.1)}$$

Where *Reduction* is the reduction expressed as a percentage and EHW_i and SHW_i are the instantenous values of the *household* demand curves at time 6PM<i<8PM. The resultant changes in the household demand curve were then used to create a set of peak demand reduction factors for each city, for each month.

Figure 4.19 shows the average difference in household demand curves during peak times (peak demand reduction factors), for each month of the year, for Cape Town, Johannesburg and Durban.

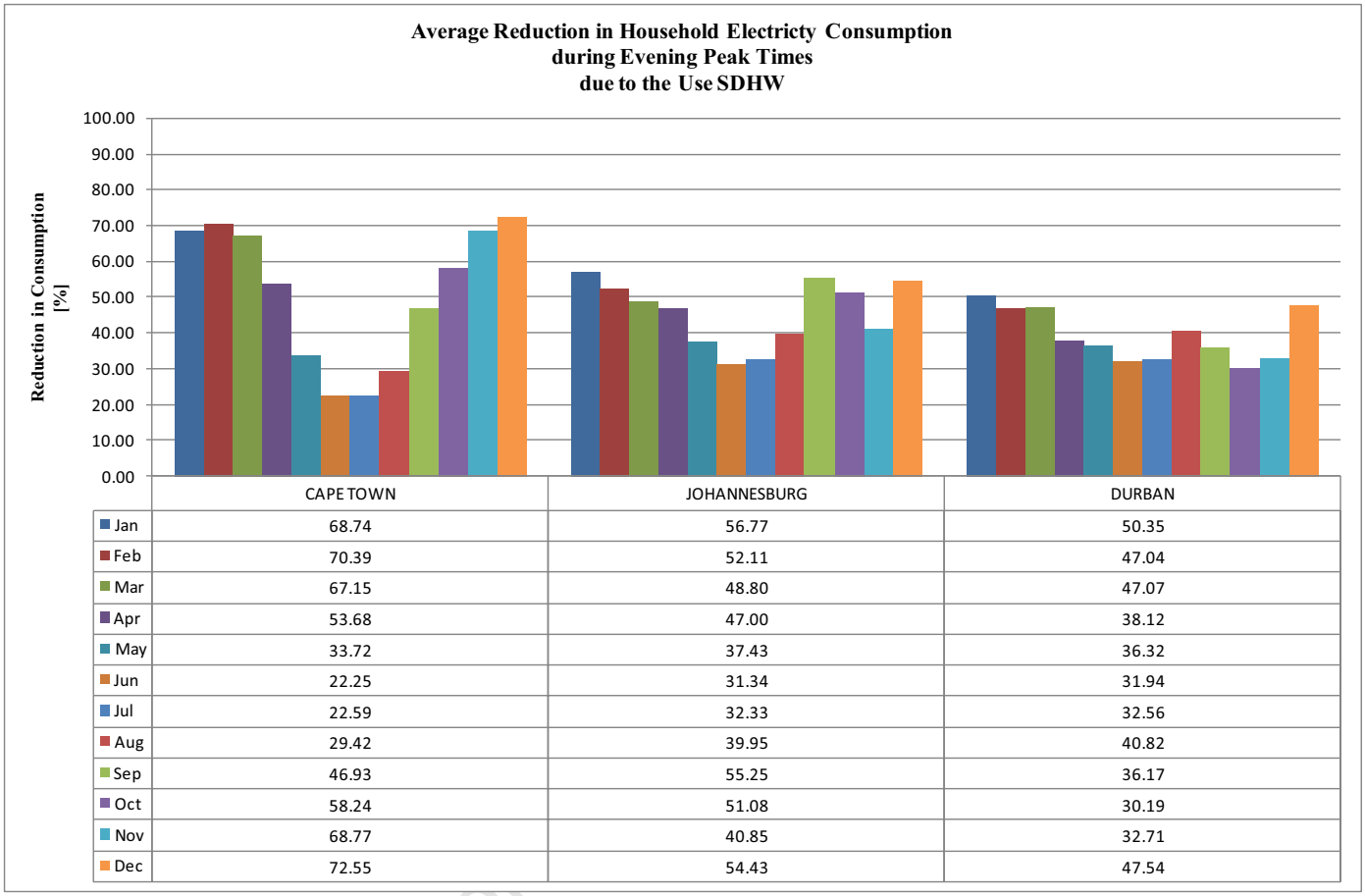

	CAPE TOWN	JOHANNESBURG	DURBAN
Jan	68.74	56.77	50.35
Feb	70.39	52.11	47.04
Mar	67.15	48.80	47.07
Apr	53.68	47.00	38.12
May	33.72	37.43	36.32
Jun	22.25	31.34	31.94
Jul	22.59	32.33	32.56
Aug	29.42	39.95	40.82
Sep	46.93	55.25	36.17
Oct	58.24	51.08	30.19
Nov	68.77	40.85	32.71
Dec	72.55	54.43	47.54

Figure 4.19: Average % Reduction in Household Electricity Consumption during Evening Peak Times, due to the Use of a SDHW System in Cape Town, Johannesburg and Durban

From Figure 4.19, we see there is a drastic difference in the impact of a SDHW system on a household's evening peak in Cape Town. It varies from approximately 70% during summer months to 22% during winter! This difference is also present in the results presented for Johannesburg, but it is not as radical, with a summer reduction in the region of 55% and a winter reduction of about 31%. In Durban, the variety between winter and summer is the smallest, ranging from 32% to 50%.

4.2.2 ANALYSING GEYSER DEMAND CURVES AND EXTRAPOLATING IMPACT ON HOUSEHOLD PEAK DEMAND

In this method of analysis, a comparison was carried out between the EDHW and SDHW system geyser demand curves during times of peak demand. The averaging formula in Equation 4.1 was used to determine the average *geyser* consumption reduction, with *Reduction* still the reduction expressed as a percentage, and EHW_i and SHW_i now being the instantenous values of the EDHW and SDHW *geyser* demand curves at time 6PM<i<8PM. The results for Cape Town, Johannesburg and Durban are shown in Table 4.1

Table 4.1: Average Monthly Reduction in Geyser Evening Peak Demand

Average Reduction in Geyser's Evening Peak Demand [%]			
	Cape Town	**Johannesburg**	**Durban**
January	87.10	67.21	63.64
February	94.02	74.27	68.84
March	92.74	68.15	69.78
April	75.10	60.03	53.71
May	55.07	61.56	53.59
June	33.88	55.12	45.45
July	36.63	51.49	45.55
August	46.61	66.58	62.02
September	63.61	73.05	48.69
October	75.08	67.86	39.84
November	91.02	54.83	41.97
December	85.94	65.43	58.09

These values apply to the geyser's electricity demand only. A scaling factor needs to be applied in order to determine the peak demand reduction factor for the household.

The contribution of water heating to total electricity consumption in a household is obviously dependent on several factors, and is expected to vary both daily and seasonally. In the mornings and evenings it will be higher, as this is when the bulk of hot water usage takes place. It is also expected to be higher in summer when water heating is the biggest load in the home, and to be reduced in winter, when space heating needs to be factored into the home's electricity usage.

On average, however, water heating constitutes 40% of electricity consumption in a household [2] [15]. This figure was used as the scaling factor to determine the impact of the geyser demand reduction, on a household's peak consumption, the results are shown in Figure 4.20.

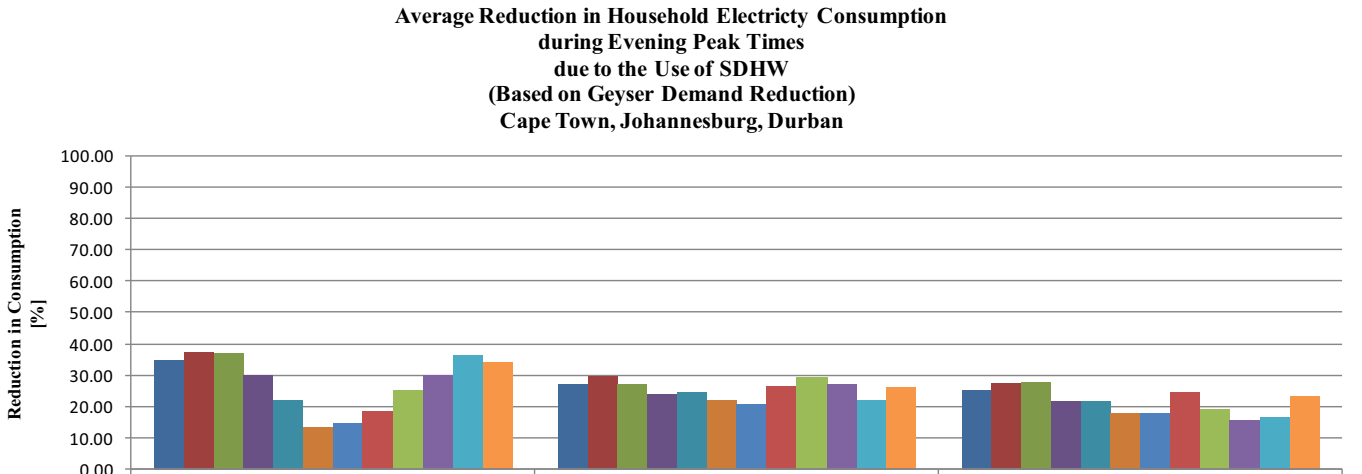

	CT	JHB	DBN
Jan	34.84	26.89	25.46
Feb	37.61	29.71	27.54
Mar	37.09	27.26	27.91
Apr	30.04	24.01	21.49
May	22.03	24.62	21.43
Jun	13.55	22.05	18.18
Jul	14.65	20.60	18.22
Aug	18.65	26.63	24.81
Sep	25.45	29.22	19.47
Oct	30.03	27.15	15.94
Nov	36.41	21.93	16.79
Dec	34.38	26.17	23.23

Figure 4.20: Average % Reduction in Household Electricity Consumption during Evening Peak Times, due to the Use of a SDHW System (Based on Geyser Demand Reduction) in Cape Town, Johannesburg and Durban

4.2.3 SUMMARY OF ANALYSIS OF SIMULATION RESULTS

Figure 4.19 and 4.20 show the possible impact of a SDHW system on one household's electricity consumption. The two methods of analysis had disparate results, probably due to errors and/or assumptions.

The second method of analysis had in in-built constraint, where the maximum possible reduction in household electricity consumption was 40%. As a result, this method yielded more conservative results. This method was utilised to determine the impact of solar water heating on the transmission grid.

The derived PDRFs (shown in Figure 4.20) were used to determine the demand reduction in MW, that various levels of penetration of solar water heating could bring about, for each month, for each *city*. The resulting value was then used to determine the impact of large scale solar water heating on a power system during peak demand.

4.3 Chapter Summary

The aim of this chapter was to present results from the simulations that were run using MeteoNorm generated data and TRNSYS. Another objective was to quantify the reduction in household peak that a SDHW system can bring about. Results for the 3 biggest residential load centers, Cape Town, Johannesburg and Durban were presented.

The results showed that the performance (in terms of geyser peak demand reduction) of a SDHW system operating in Cape Town varies radically throughout the year, doing very well in summer months and quite poorly during the winter months. The SDHW system in Johannesburg also displayed some variance in performance across the seasons, but it was not as drastic as that seen in Cape Town. The SDHW system in Durban showed the most even performance across the seasons, with the smallest variance in its performance between summer and winter.

An anomaly was present in all the simulation results, which made it difficult to determine the impact of a SDHW system on a household's morning peak. As a result, the quantification of household peak demand reduction was only carried out for the evening peak period of 6PM to 8PM.

Two possible forms of analysis to determine the impact that solar water heating has on a household's peak demand were examined. The two methods yielded very different results. The more conservative results were used in the examination of the impact of solar water heating on the transmission grid.

CHAPTER V

5. FIELD RESULTS AND VALIDATION OF TRNSYS RESULTS

In this chapter, the data that was collected from various solar water heating installations will be presented. It will be used to validate the results that were obtained in the TRNSYS simulations.

5.1 Field Results

Atlantic Solar (Pty) Limited is a Cape Town based company that deal with the design, manufacture and installation of solar water heating systems. The company installed data loggers at some of their installations around Cape Town.

These loggers recorded the electrical activity of the geyser as well as the hot water usage in the household. The data loggers were installed in 5 households, in September 2007. Data was downloaded from the households in February and March of 2008. The data loggers and the download software were all procured from MC Systems.

Unfortunately, due to the position of the geysers in their roofs, none of the homeowners were able to disconnect the solar collector bi-weekly. The data presented thus represents the scenario where water heating in the household is achieved through the use of both solar and electrical energy.

5.1.1 HOUSE 1

The system here was an indirect, pumped, double tank system. The 2kW heating element and thermostat (set at 60˚C) were located in the pre-existing (old) 40 gallon geyser. The house was quite old, and the plumbing was set-up for low pressure water usage, so the indirect pumped system was the only way to implement solar water heating in the household.

The home was occupied by two elderly people. Initially, the home owners complained that the system was not working. This was clearly reflected in the data downloaded from the logger, early in January 2008. Figure 5.1 below shows the geyser electricity consumption, as well as the hot water usage patterns when the system was not working.

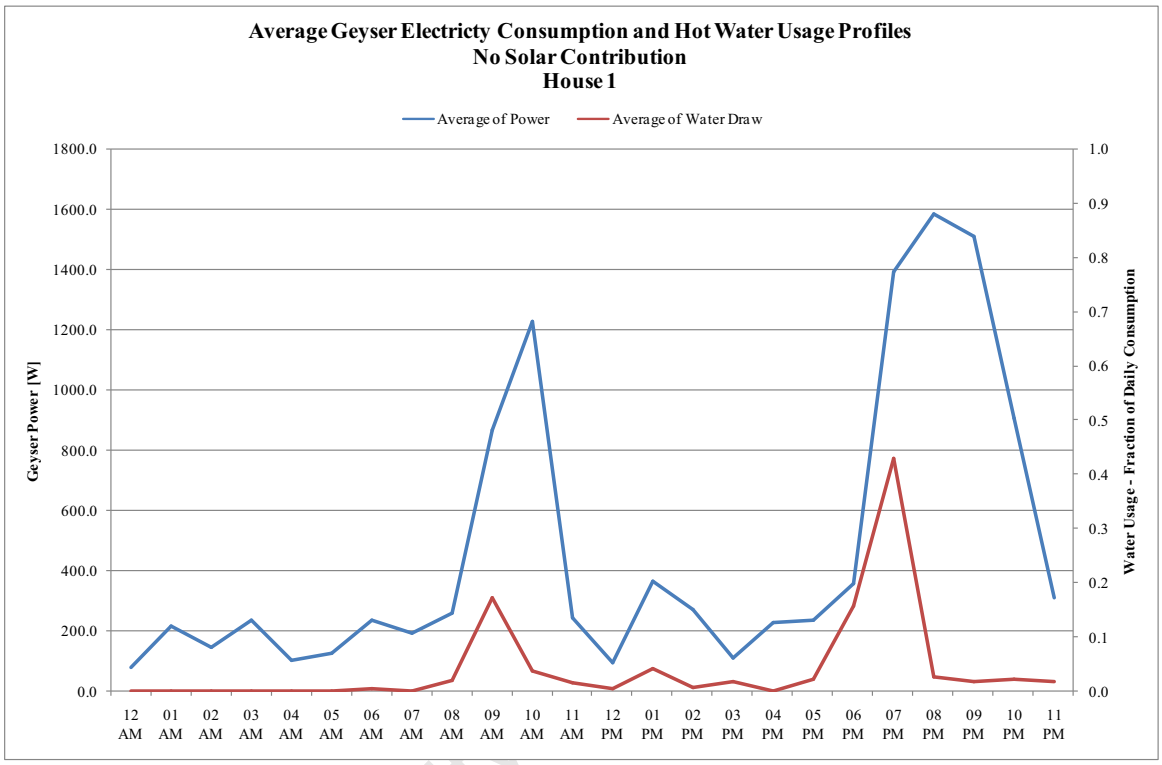

Figure 5.1: Average Geyser Consumption and Hot Water Usage Profiles with No Solar Contribution – House 1

The geyser electricity consumption peaked with the hot water usage, and judging from the evening geyser peak of 1.6kW, there appears to be no solar contribution. Late in January, Atlantic Solar fixed the system, and the solar contribution is evident in Figure 5.2, which shows the geyser electricity consumption, as well as the hot water usage patterns from the data downloaded at the end of February from the household.

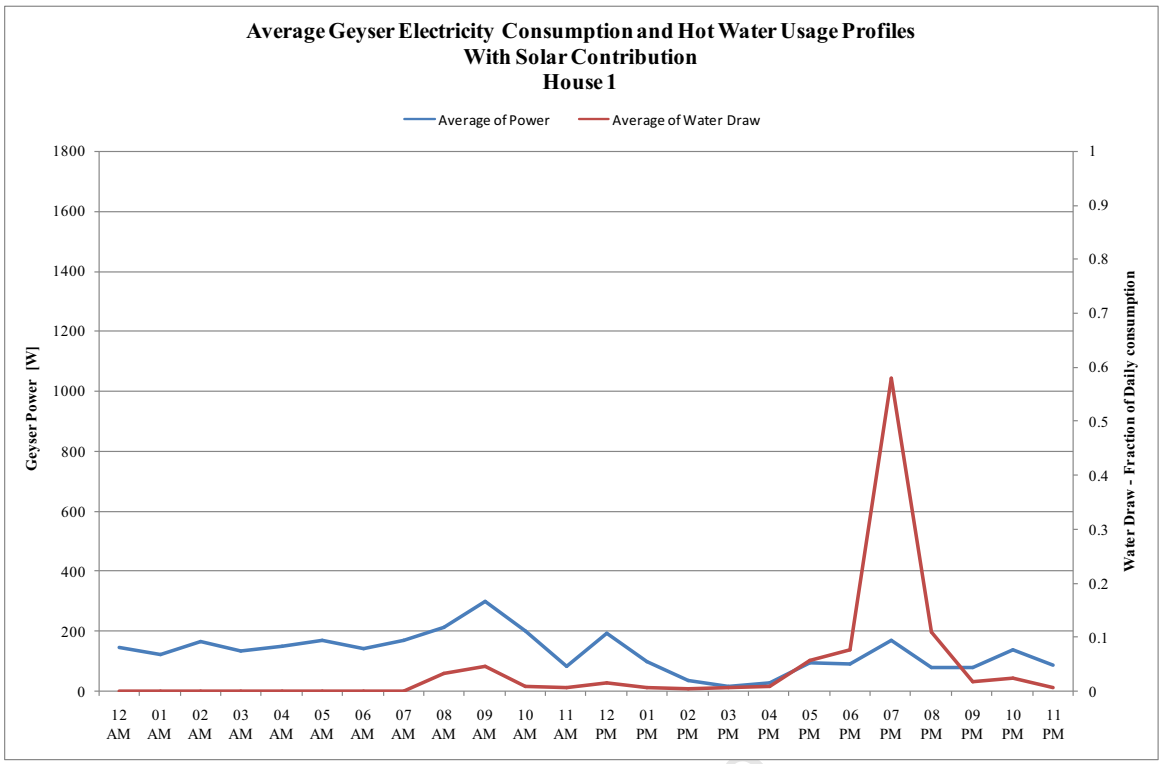

Figure 5.2: Average Geyser Consumption and Hot Water Usage Profiles with Solar Contribution – House 1

The water consumption pattern is more or less the same; however, there is a noticeable difference in the geyser electricity demand patterns.

5.1.2 HOUSE 2

The system here was a direct, close-coupled[3] thermosyphon system. This household did not use any electricity to heat water over the logging period. The homeowners said the water coming from the solar collector was very hot. As a result, they switched off the household geyser, as they did not need any electricity to supplement their water heating. It was off for the entire logging period.

Figure 5.3 shows the geyser electricity consumption, as well as the hot water usage patterns when using solar water heating.

[3] In a close-coupled system, the solar collector and the hot water storage / geyser are located right next to each other on the roof.

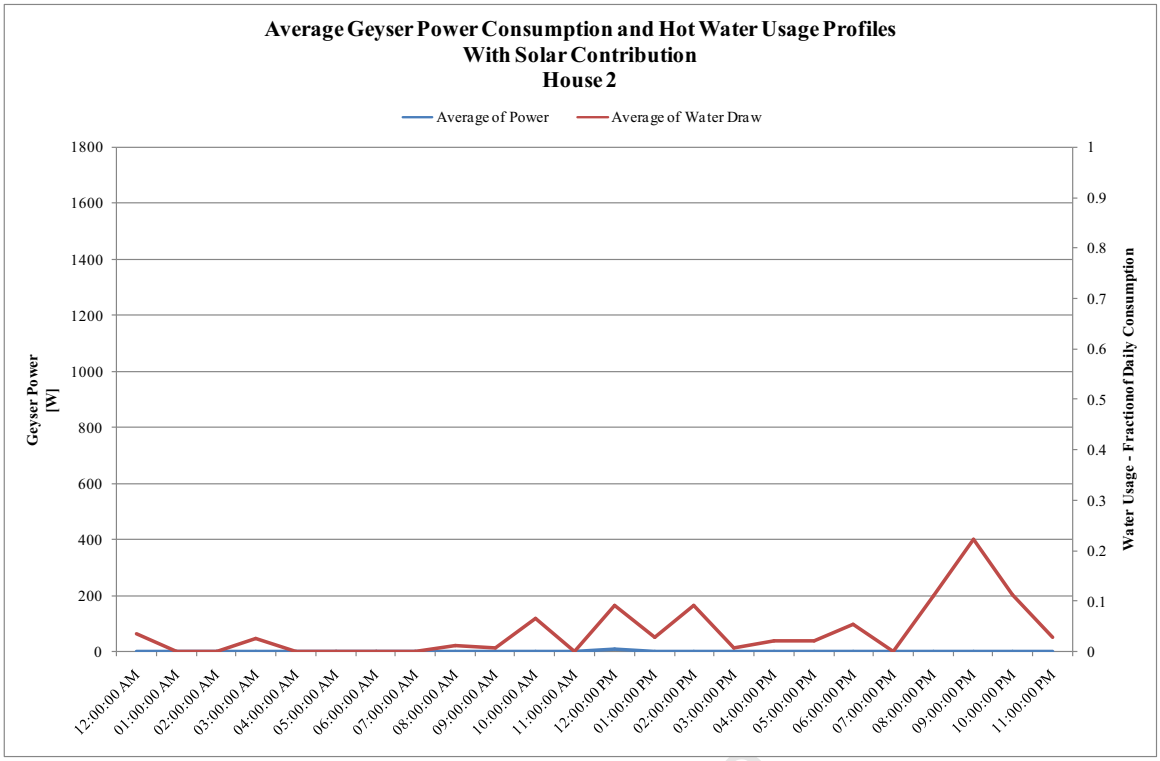

Figure 5.3: Average Geyser Consumption and Hot Water Usage Profiles with Solar Contribution – House 2

As expected, there was no activity in terms of the geyser's electricity consumption. Most hot water consumption in this household took place late in the evening.

5.1.3 HOUSE 3

The system here was a direct, thermosyphon, close-coupled system. This home was occupied by one person, a medical practitioner. She initially used it just for her practice, but she recently moved into the house, and it doubles as her office. She complained that the hot water in the household was too hot. There have been several incidents where she has burnt herself. This phenomenon is not uncommon, and has even been noted in some systems operating in the UK, in summer as well [43].

Figure 5.4 below shows the geyser's electricity consumption, as well as the hot water usage pattern when using solar water heating.

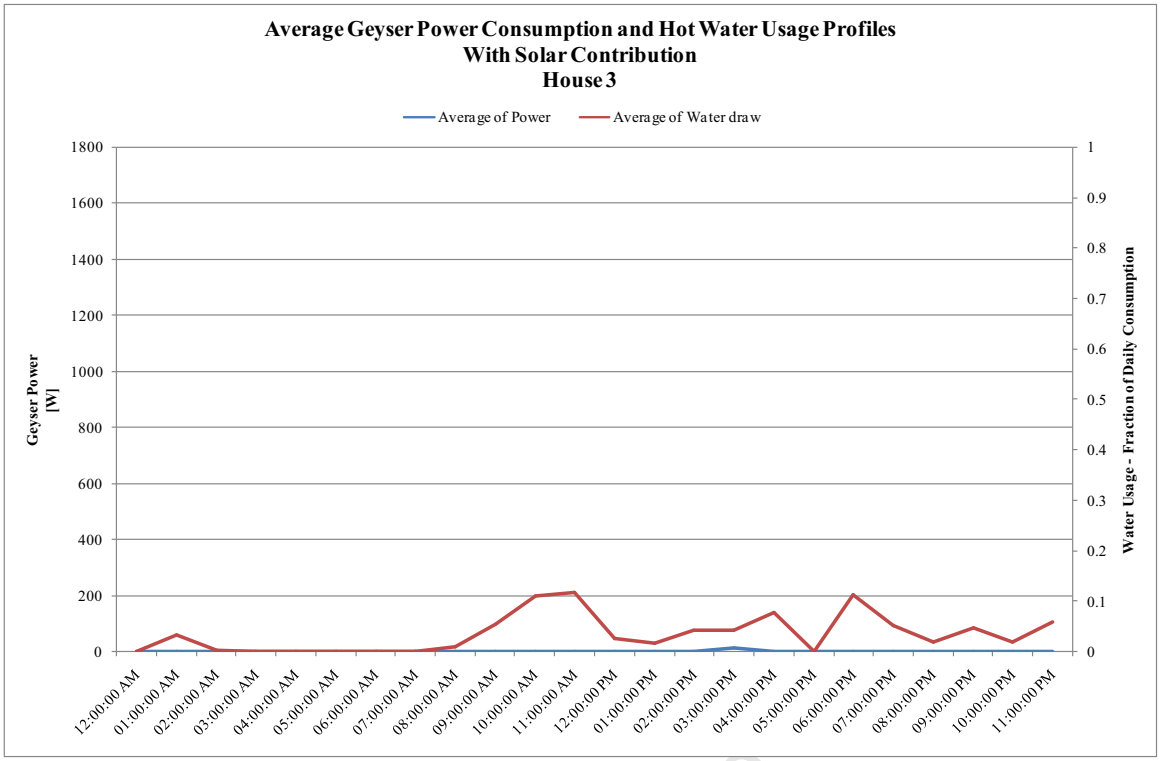

Figure 5.4: Average Geyser Consumption and Hot Water Usage Profiles with Solar Contribution – House 3

As can be seen, no electricity was used for water heating in this household. Most hot water consumption took place during the day, when solar energy was readily available.

5.1.4 HOUSE 4

The system here was an indirect thermosyphon system. This household was occupied by a family of four. The children were of primary school age. The homeowner was quite disappointed, as they were not seeing any savings after the installation of their solar water heating system. Hot water usage took place throughout the day. The geyser power demand seemed to peak with the hot water usage, albeit at low values. It later transpired that the system was faulty. It was replaced with a direct, thermosyphon system late in April 2008.

Figure 5.5 below shows the geyser electricity consumption, as well as their hot water usage patterns when using solar water heating.

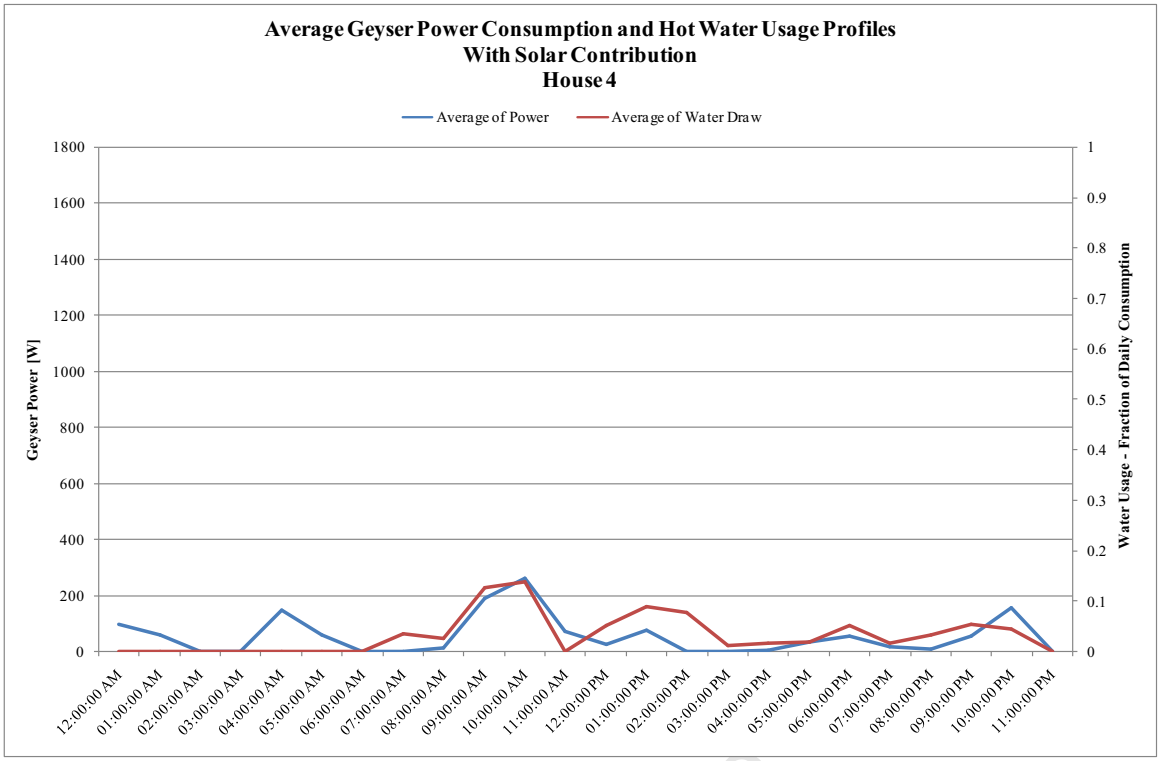

Figure 5.5: Average Geyser Consumption and Hot Water Usage Profiles with Solar Contribution – House 4

5.1.5 SUMMARY OF DATA LOGGING RESULTS

The data logging process was heavily reliant on the home owners' willingness and ability to cooperate. A number of problems were encountered with the data collection process, the most significant being the inability of the homeowners to disconnect the panel, in order to allow for the creation of EDHW demand curves. This made it difficult to quantify the reduction in geyser peak demand that the solar water heating systems brought about. A few other problems that were encountered are listed below:

- House number 1 only had valid data for two months. This is due to the fact that the system was not working for the first 5 months of logging.

- House number 2 turned off their geyser, which resulted in a data set of nil values. Had the geyser been on, they may have used electricity to heat water, especially due to the fact that most hot water consumption in the household occurred late in the evening.

- House number 4's data had to be discarded when it was revealed that system had not been operating properly for the entire logging period.

At first glance, it appears as though the monitoring of the systems was riddled with problems. However, useful data could still be extracted and used for the validation process. House number 1's non-functional system allowed for the creation of an EDHW curve. This curve could then be compared to the SDHW curve generated after the system was fixed.

Although House number 2 turned off their geyser, it is important to note that the water temperature *must* have been satisfactory in order for them to have kept it off for all that time. If the consumer is contented, the system can be considered functional. The data was thus deemed valid, and was used in the validation process.

5.2 Validation of TRNSYS Results

5.2.1 ACTUAL GEYSER DEMAND CURVES vs. TRNSYS GENERATED DEMAND CURVES

One of the ways to validate the TRNSYS results was to input the various households' water consumption patterns into the system that was simulated in TRNSYS, in order to determine how well the TRNSYS system had approximated the geyser demand of the SDHW systems. The results are presented in Figures 5.6 to 5.8.

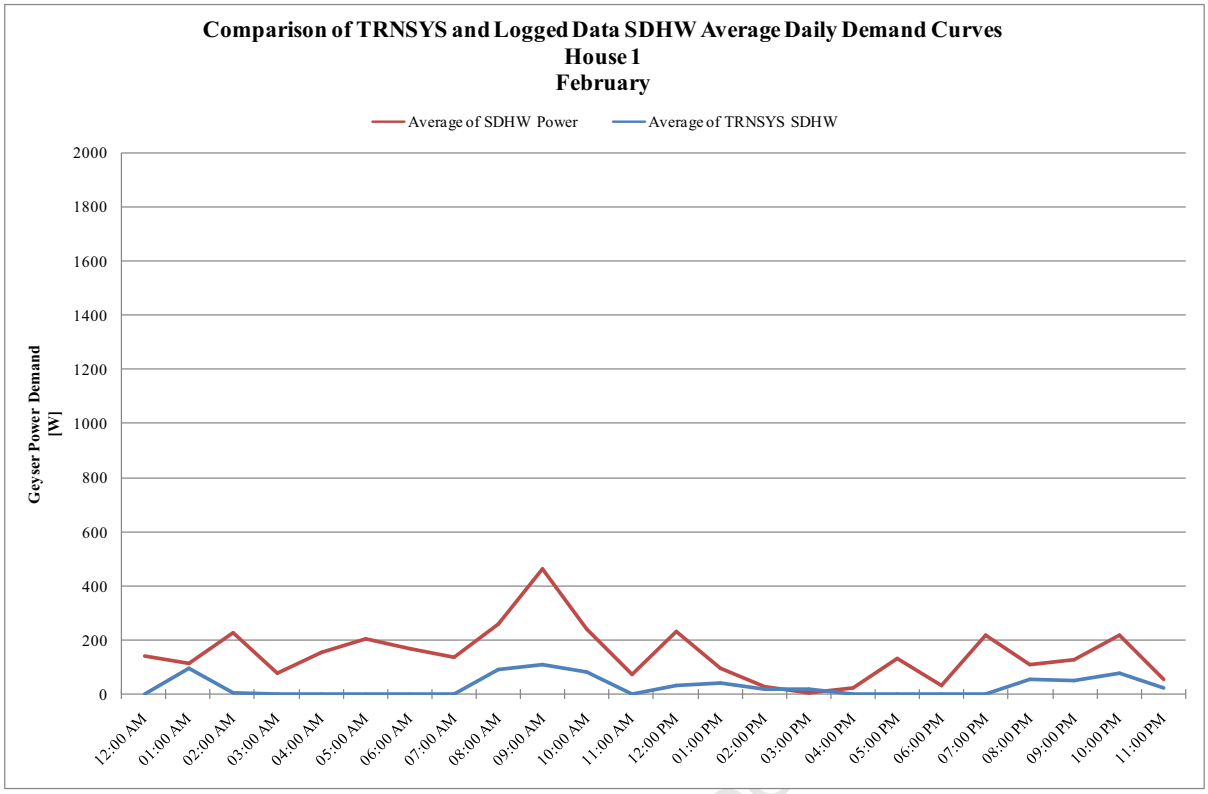

Figure 5.6: Comparison of TRNSYS Generated and Logged Average Daily Geyser Demand Curves for SDHW House 1

For House 1, in February, the average geyser demand curve that was created using the TRNSYS simulation results was lower than the actual household consumption. This can be explained by the fact that the system that was used here was an indirect, pre-feed system. This set up is prone to more losses, and is thus less efficient than the direct system that was simulated [44].

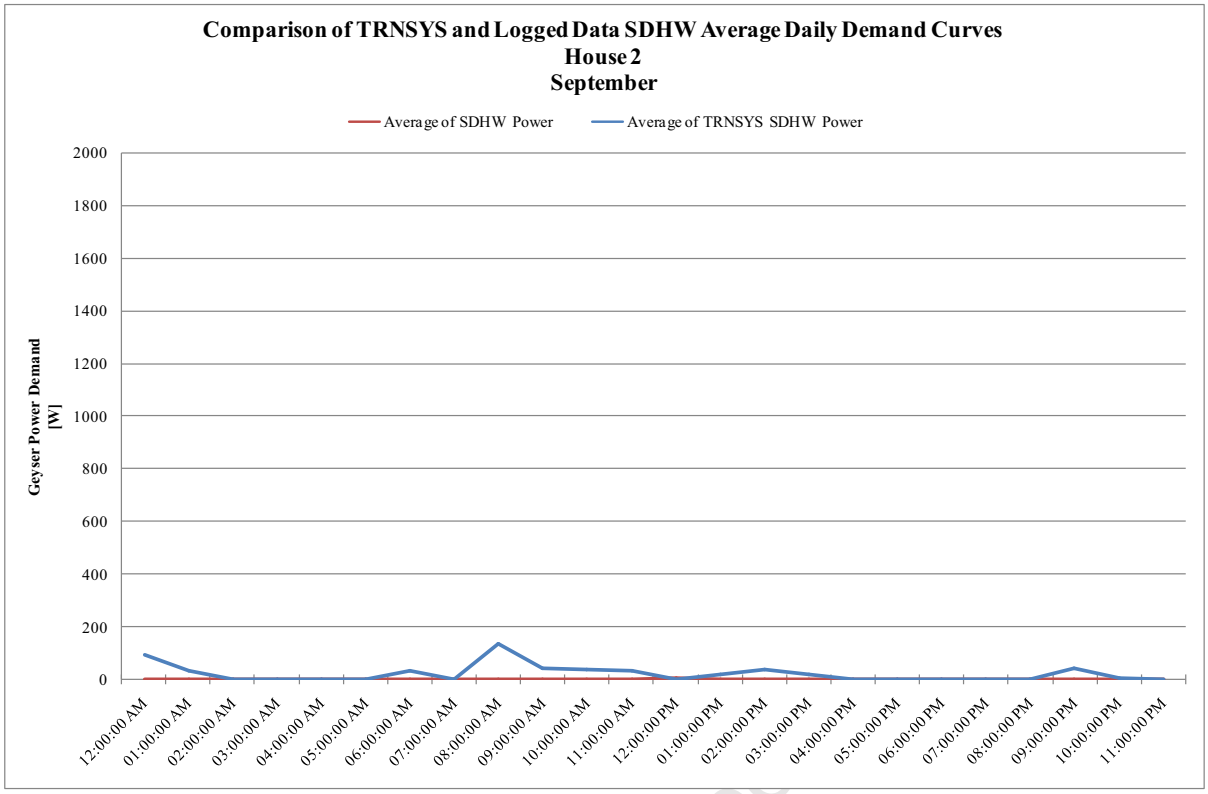

Figure 5.7: Comparison of TRNSYS Generated and Logged Average Daily Geyser Demand Curves for SDHW House 2

In Figure 5.2, it can be seen that for House 2, the approximation derived from the TRNSYS simulation was higher than the actual household's geyser demand curve. This is due to the fact that the geyser was off for the entire logging period.

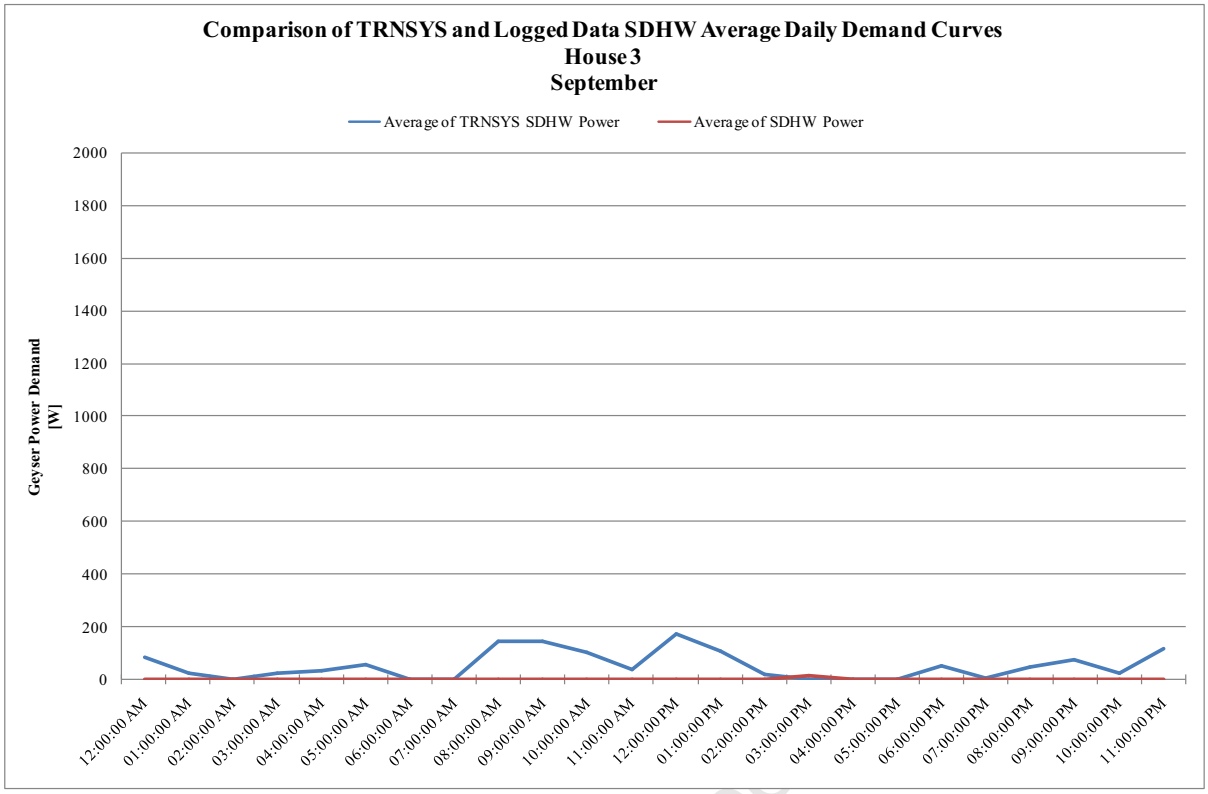

Figure 5.8: Comparison of TRNSYS Generated and Logged Average Daily Geyser Demand Curves for SDHW House 1

In the case of House 3, as seen in Figure 5.8, the TRNSYS simulated curve was also higher than the actual geyser demand curve. The system here can thus be deemed more efficient than the system that was simulated in TRNSYS.

5.2.2 ACTUAL SAVINGS vs. TRNSYS CALCULATED SAVINGS

Initially, the TRNSYS simulation results were going to be verified by comparing the savings calculated from the simulation results to the savings that the homeowners gained from their solar water heating systems. Due to the glitches encountered with the data collection process, this is only possible for one House 1.

Table 5.1 shows the average monthly reduction in the geyser evening peak values that were obtained from the TRNSYS simulations. There was an average reduction of 89.52% in the geyser evening peak demand for the summer months. In the winter months, the average reduction was 43.05%. These values were compared to the actual reduction in the household's geyser peak demand in the evening, in order to determine the validity of the TRNSYS results.

Table 5.1: Average Monthly Reduction in Geyser Evening Peak Demand – TRNSYS Prediction

Month	% Reduction in Geyser Peak Demand
January	87.10
February	94.02
March	92.74
April	75.10
May	55.07
June	33.88
July	36.63
August	46.61
September	63.61
October	75.08
November	91.02
December	85.94

Figure 5.9 shows the geyser demand curves for two scenarios. One is when electricity was being used to heat the water. The other is when both solar and electricity were being used to heat the household's water. There was a great reduction in both the morning and the evening peaks of the geyser demand, when the solar came into effect.

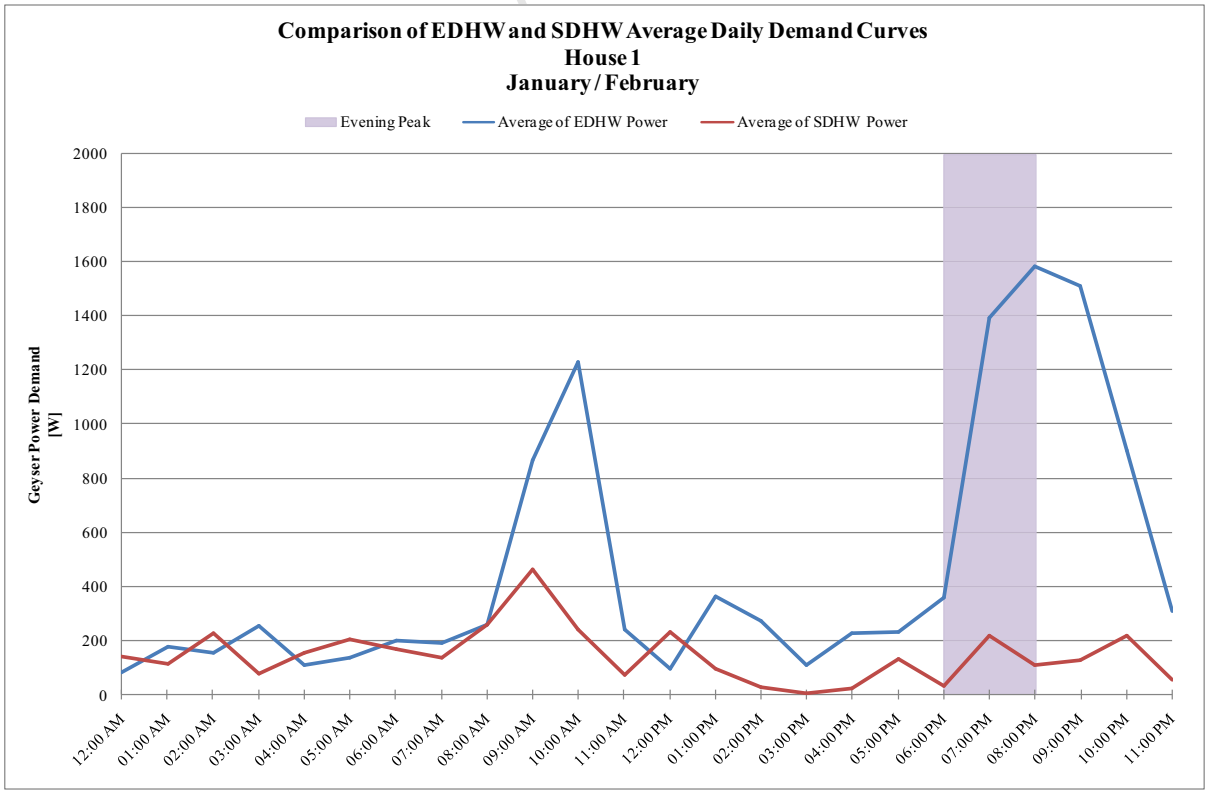

Figure 5.9: Comparison of Average Daily Geyser Demand Curves for EDHW and SDHW – House 1

A comparison needs to be carried between the evening reduction that was calculated from the TRNSYS simulation results, and the reduction which was observed in the household. Only the evening peak reduction (between 6PM and 8PM) will be examined.

Table 5.2: Calculation of Reduction in Geyser Evening Peak Demand – February

Time	EDHW Demand [W]	SDHW Demand [W]	Reduction due to SDHW
6PM	358.08	30.70	91.43%
7PM	1391.13	219.96	84.19%
8PM	1582.94	106.85	93.25%
			Average Reduction: 89.62%

Upon evaluation, it was revealed that the solar water heating system reduced the household's geyser electricity consumption by 89.62% during the evening peak period in February. This figure is very close to the 89.52% average that was calculated for summer months from TRNSYS. The 89.62% reduction is also slightly lower than the 94.02% reduction which was seen in the simulation results, for the month of February in Cape Town.

This difference can be attributed to the fact that the system here was an indirect, double tank set-up, which lent itself to more losses.

No EDHW curves were available for House 2 and House 3. However, these houses used no electricity for water heating during the logging period. It can thus be argued that they experienced a 100% reduction in geyser electricity consumption. This figure is also close to the figures for November to February predicted by TRNSYS.

It can thus be concluded that the TRNSYS results are valid.

5.3 Chapter Summary

The aim of this chapter was to present the data that was collected from various solar water heating installations. Thereafter, the data was used to validate the results that were obtained from the TRNSYS simulations.

A number of problems arose during the monitoring of the solar water heating installations. These ranged from non-functional systems, to highly efficient systems that completely

eliminated the need for electricity for water heating. This resulted in a data set that made the validation process difficult.

The data that could be used revealed that the reduction in the geyser peak demand for the household was very close to that predicted by TRNSYS. However, these results were only for summer, and the winter results still need to be validated.

CHAPTER VI

6. *SUGGESTED MEASURES TO IMPROVE PERFORMANCE AND BENEFITS OF SOLAR WATER HEATING SYSTEMS*

The installation of a solar water heating system alone can bring about savings in a household. However, there are some measures that could be taken in order to derive further benefits from the SWH system. This chapter will outline a few such measures. All measures will be illustrated with a simulation example from Cape Town, Johannesburg and Durban for the months of January (summer) and July (winter).

6.1 Introduction

The Institute of Engineering and Technology has developed an Energy Hierarchy, shown in Table 6.1, which is included in their Primer on Energy Policy. It aims to promote sustainable development by focusing on reducing energy usage, using clean methods to supply energy and avoiding "dirty" methods of energy production as much as possible [45].

Table 6.1: The IET Energy Hierarchy [45]

SUSTAINABLE  **UNSUSTAINABLE**	Energy Conservation *Changing behaviour to reduce demand*
	Energy Efficiency *Using technology to reduce demand*
	Renewable, Sustainable Energy Sources *Setting a course to replace fossil fuels*
	Conventional Energy Sources *Using low/no-carbon technologies*
	Exploitation of Conventional Energy Sources

The use of solar water heating fulfils the 2nd and 3rd levels of the hierarchy. However there are some activities which fall in the 1st level which can enhance the performance of a solar water heating system, further boosting its viability as sustainable energy solution. These suggestions require little to no capital investment by the utility.

6.2 Reduce Geyser Thermostat Setting

Geyser thermostats control the heating element's activity. If the water in the tank falls below a certain threshold, the element will be turned on, until the water temperature reaches a desired level. Thermostats are normally set at around 65˚C. If the thermostat setting were reduced, less electricity would have to be used to heat the water and thus higher energy savings could be achieved.

A scenario where the thermostat was set to room temperature (25˚C) yielded great energy savings as can be seen in Figure 6.1 to Figure 6.3; however, this is would not be ideal for the consumer. Not only does this setting mean a cold shower, it also allows certain harmful bacteria, like Legionella to survive in the geyser [46].

A reduction of 5˚C or even 10˚C of the thermostat setting on the other hand, is still sanitary and does not compromise the consumers' comfort[4]. This small reduction can bring about increased energy savings as illustrated in Table 6.2.

[4] Mr Chris Wozniak, a Technical Officer in the department, has reduced his household's thermostat to 55˚C and has found the water temperature to be acceptable.

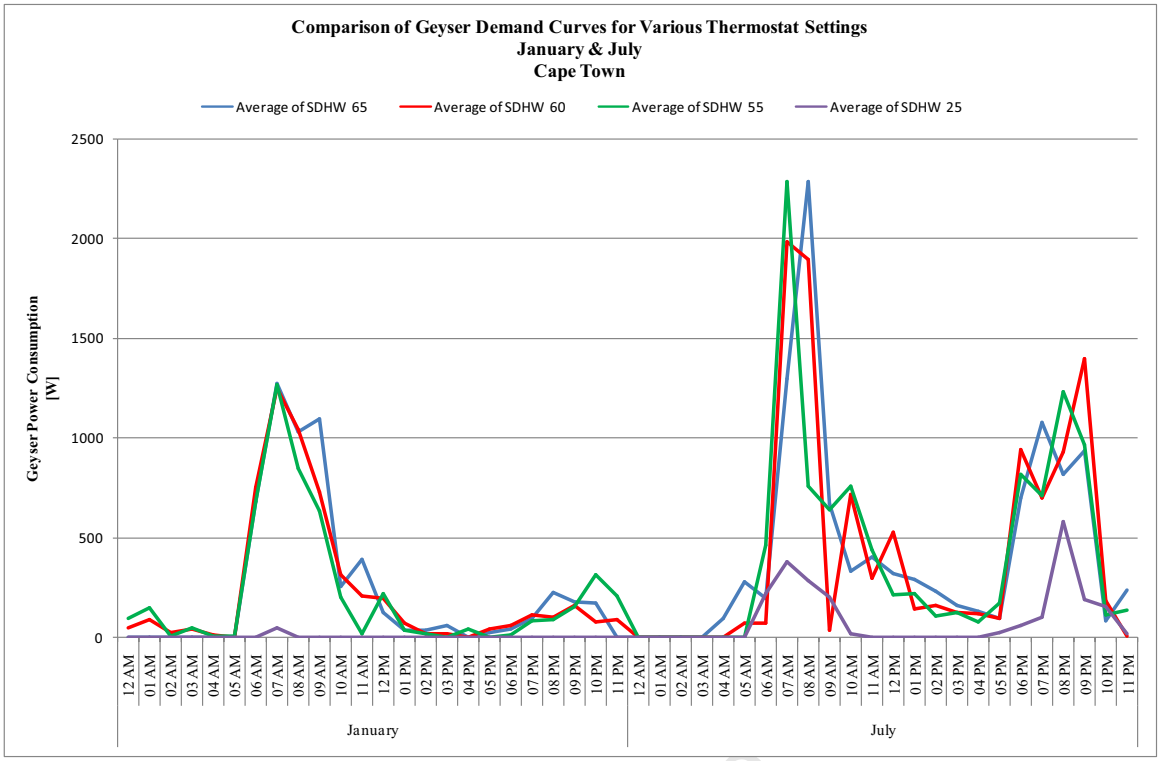

Figure 6.1: Comparison of Average Daily SDHW System Geyser Demand Curves for Various Thermostat Settings for January and July – Cape Town

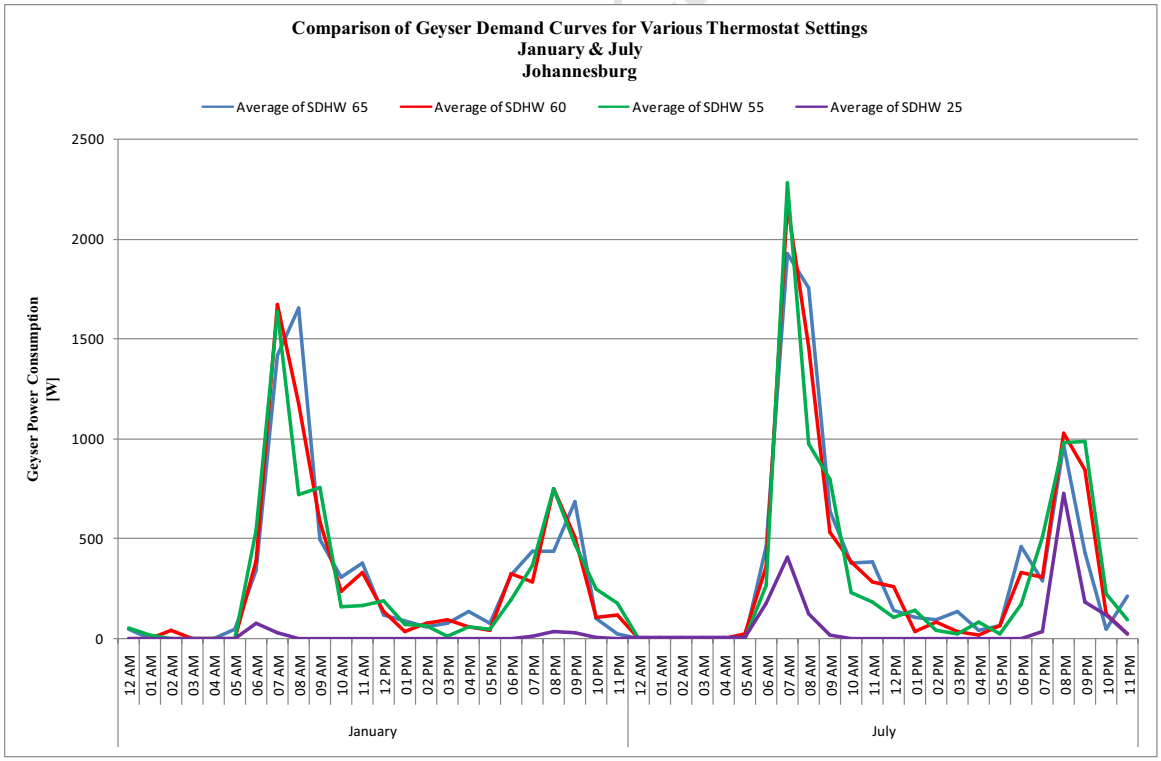

Figure 6.2: Comparison of Average Daily SDHW System Geyser Demand Curves for Various Thermostat Settings for January and July – Johannesburg

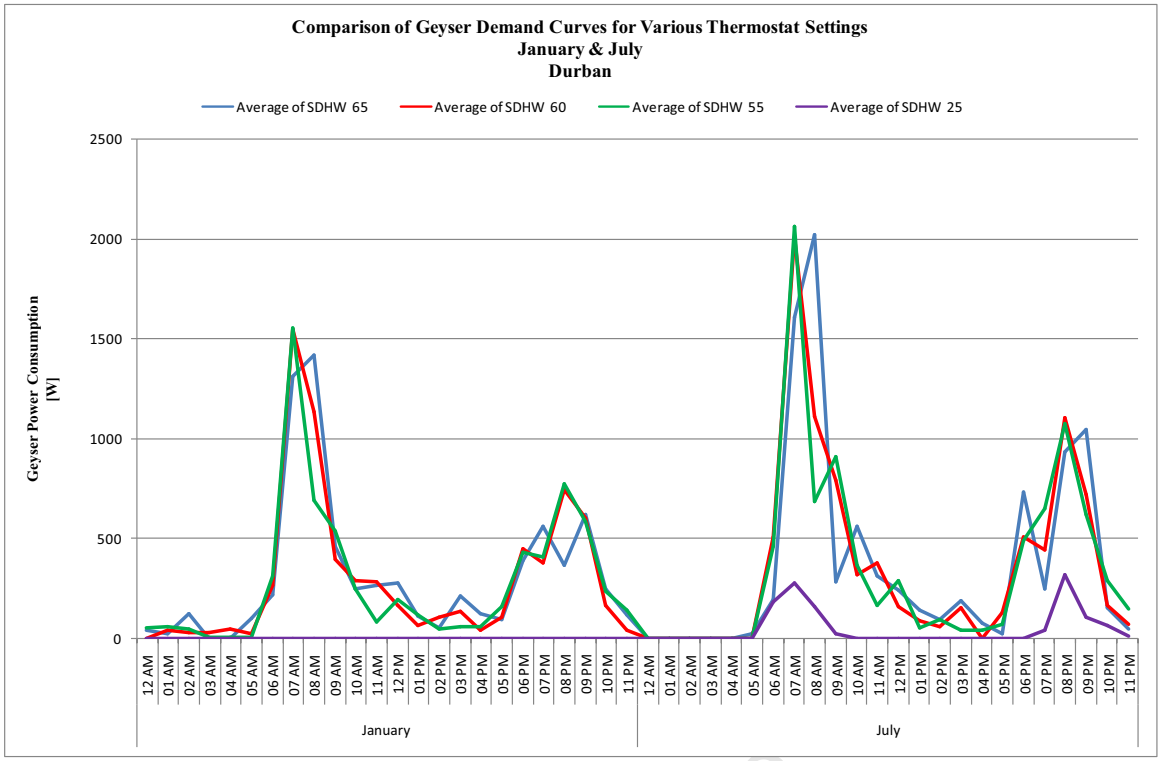

Figure 6.3: Comparison of Average Daily SDHW System Geyser Demand Curves for Various Thermostat Settings for January and July – Durban

The SDHW system geyser demand curves for 65˚C, 60˚C and 55˚C thermostat settings all have a similar shape. However, the energy consumption differs for each scenario. The monthly energy consumption for each scenario, as well as the energy savings as compared to the original SDHW system are shown in Table 6.2. The figures in brackets correspond to the savings as compared to the original SDHW system. The annual energy consumption of each system is also included.

Table 6.2: Energy Consumption (and Savings) Due to Reducing SDHW System Geyser Thermostat Setting

		SDHW 65˚C	SDHW 60˚C	SDHW 55˚C
CAPE TOWN	January	177.32kWh	169.44kWh (4.4%)	159.06kWh (10.3%)
	July	330.01kWh	322.22kWh (2.4%)	316.96kWh (4.0%)
	Annual	2917.82kWh	2820.72kWh (3.3%)	2730.59kWh (6.4%)
JOHANNESBURG	January	224.08kWh	215.84kWh (3.7%)	207.22kWh (7.5%)
	July	263.95kWh	259.05kWh (1.9%)	251.09kWh (4.9%)
	Annual	2839.74kWh	2747.83kWh (3.2%)	2655.75kWh (6.5%)
DURBAN	January	228.42kWh	218.84kWh (4.2%)	210.33kWh (7.9%)
	July	276.22kWh	269.65kWh (2.4%)	263.71kWh (4.5%)
	Annual	2926.61kWh	2833.25kWh (3.2%)	2742.72kWh (6.3%)

Based on the annual figures presented in Table 6.2, reducing the thermostat to 60˚C can increase SDHW system energy savings by approximately 3% and reducing it to 55˚C can increase the savings by a further 3% to 6%. The actual kWh value of the savings varies, depending on the location of the SDHW system.

6.3 *Increase Geyser Insulation*

Another method to increase the performance of solar water heating is to increase the geyser's insulation, through the addition of a geyser blanket. In South Africa, the insulation of geyser is given by the standing losses. In TRNSYS however, geyser insulation is defined by a factor known as the Tank Loss Coefficient (UA). The conversion is given by Equation 6.1.

$$Standing\ Losses\ = \frac{UA}{3600} * (T_s - T_a) * 24 \quad \textbf{(6.1)}$$

Where T_s is the geyser set point temperature, and T_a is the ambient temperature around the geyser

For the purpose of the simulations, T_s was chosen as 65˚C and T_a was set to 19˚C, as per manufacturer standing losses tests [47]. The standing losses for the scenarios chosen are shown in Table 6.3

Table 6.3: Geyser Insulation Ratings Used for Simulations

Tank Loss Coefficient [kJ/hr.K]	Standing Losses [kWh/day]
4	**1.23**
5	**1.53**
6	**1.84**
8	**2.45**

The energy savings achieved for Cape Town, Johannesburg and Durban, can be seen in the energy consumption data illustrated in Figure 6.4 and Figure 6.5 below.

In Figure 6.4, there is a marked increase in the geyser energy consumption in Cape Town between January and July. This can be attributed to the inclement weather experienced in the Cape during this time, which lowers the performance of a SDHW system significantly.

From the annual summary shown in Figure 6.5 it is apparent that an increase in geyser insulation can boost the energy savings yielded by a SDHW system. The savings for decreasing insulation levels, when compared against the SDHW system with a tank loss coefficient of 8kJ/hr.K, are summarised in Table 6.4.

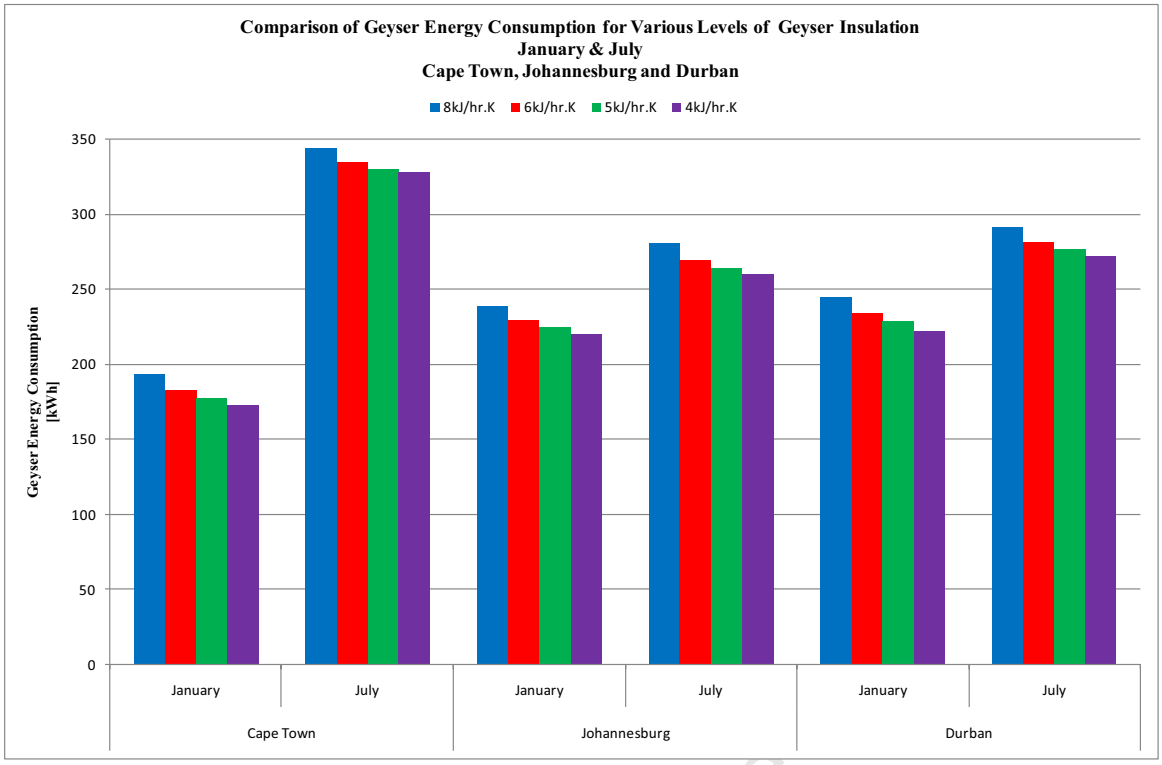

Figure 6.4: Comparison of Monthly SDHW System Energy Consumption for Different Tank Loss Coefficients for January and July – Cape Town, Johannesburg and Durban

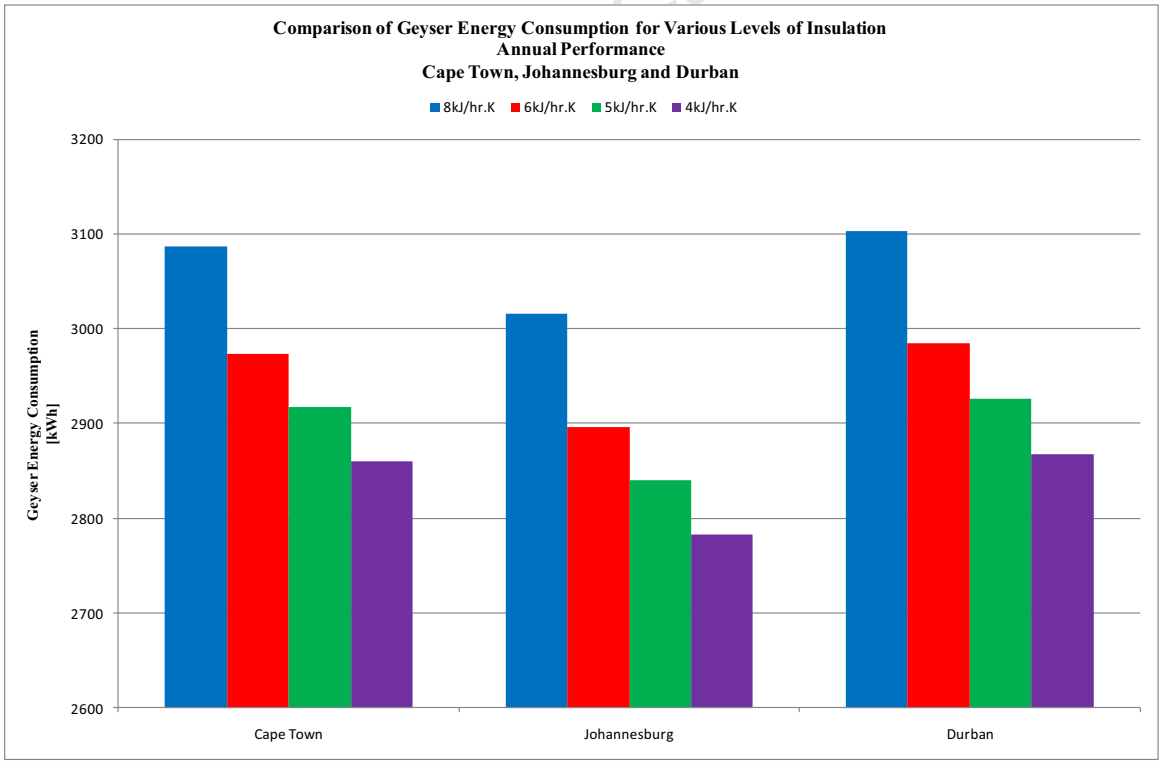

Figure 6.5: Comparison of Annual SDHW System Energy Consumption for Different Tank Loss Coefficients for Cape Town, Johannesburg and Durban

Table 6.4: Energy Savings Due to Increasing SDHW System Geyser Insulation from 8kJ/hr

		6kJ/hr.K	5kJ/hr.K	4kJ/hr.K
CAPE TOWN	January	5.37%	7.97%	10.71%
	July	2.59%	3.97%	4.87%
	Annual	3.68%	5.49%	7.35%
JOHANNESBURG	January	4.12%	6.15%	8.22%
	July	3.95%	5.69%	7.29%
	Annual	3.94%	5.83%	7.73%
DURBAN	January	4.33%	6.40%	8.97%
	July	3.51%	5.02%	6.60%
	Annual	3.80%	5.67%	7.56%

From the results in Table 6.4, it would appear that doubling the geyser insulation so that standing losses decreased from 2.45kWh/day (8kJ/hr.K) to 1.23kWh/day (4kJ/hr.K) increased the energy savings brought about by a SDHW system by approximately 7.5% annually, for all 3 cities.

6.4 Change Hot Water Usage Pattern

Another method to enhance the performance of a solar water heating system is to alter the times during which hot water is used. Judging from the general shape of the demand curves produced when using the typical South African draw profile depicted in Figure 6.6, the water consumption profile appears to be fundamental to determining savings gained by the user of a solar water heating system.

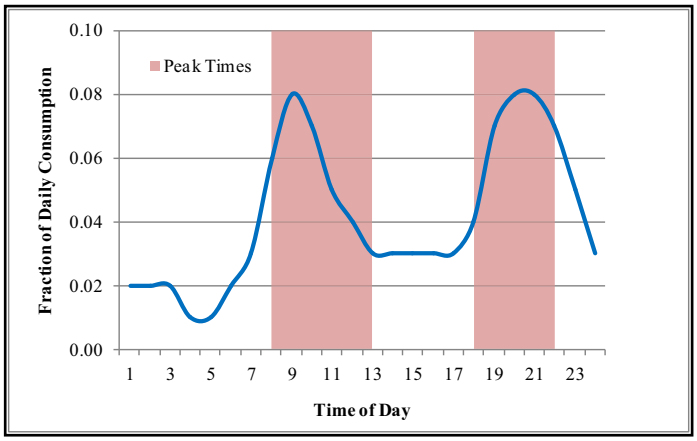

Figure 6.6: Typical South African Water Consumption Profile [18]

For example, if most hot water is used in the morning, a solar water heating system might have little to no effect, as compared to hot water usage that peaks in the evenings, especially during the summer months. This is due to the fact that most useful solar energy is only available in the afternoon.

In order to observe the impact of changing the time of hot water consumption, simulations were carried out for the hypothetical situation, where hot water usage takes place in 5 hours of the day, and is concentrated on a specific hour (x) with the distribution shown in Figure 6.7. The hours chosen for the simulations were 1AM, 3AM, 5AM, 7AM, 9AM, 11AM, 1PM, 3PM, 5PM, 7PM, 9PM AND 11PM.

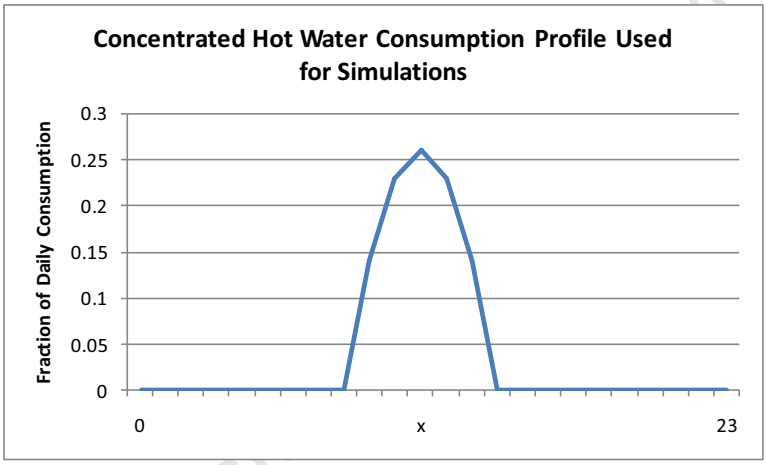

Figure 6.7: Hot Water Consumption Profile Used For Simulations

For each hypothetical scenario, simulations were carried out for an EDHW system and a SDHW system with a 65˚C thermostat setting. A comparison was then carried out for the monthly energy consumption for water heating for the two systems, in order to determine the hour of hot water usage that yielded the highest savings.

Figures 6.8 to 6.10 show the difference in energy consumption for an EDHW and an SDHW for each of the chosen hours, in the cities of Cape Town, Johannesburg and Durban.

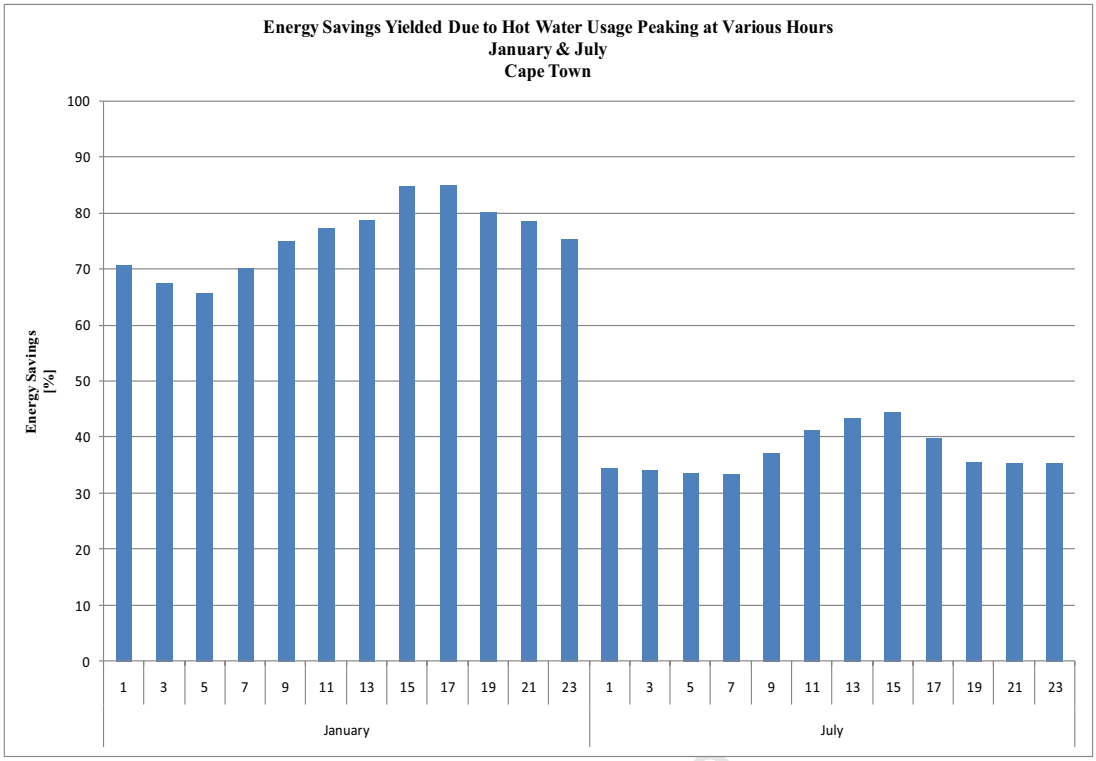

Figure 6.8: Energy Savings Yielded Due to Hot Water Consumption Peaking at Various Hours in January and July – Cape Town

In Cape Town, the highest savings were achieved between 3PM and 5PM in the summer month of January, and between 1PM and 3PM in the winter month of July.

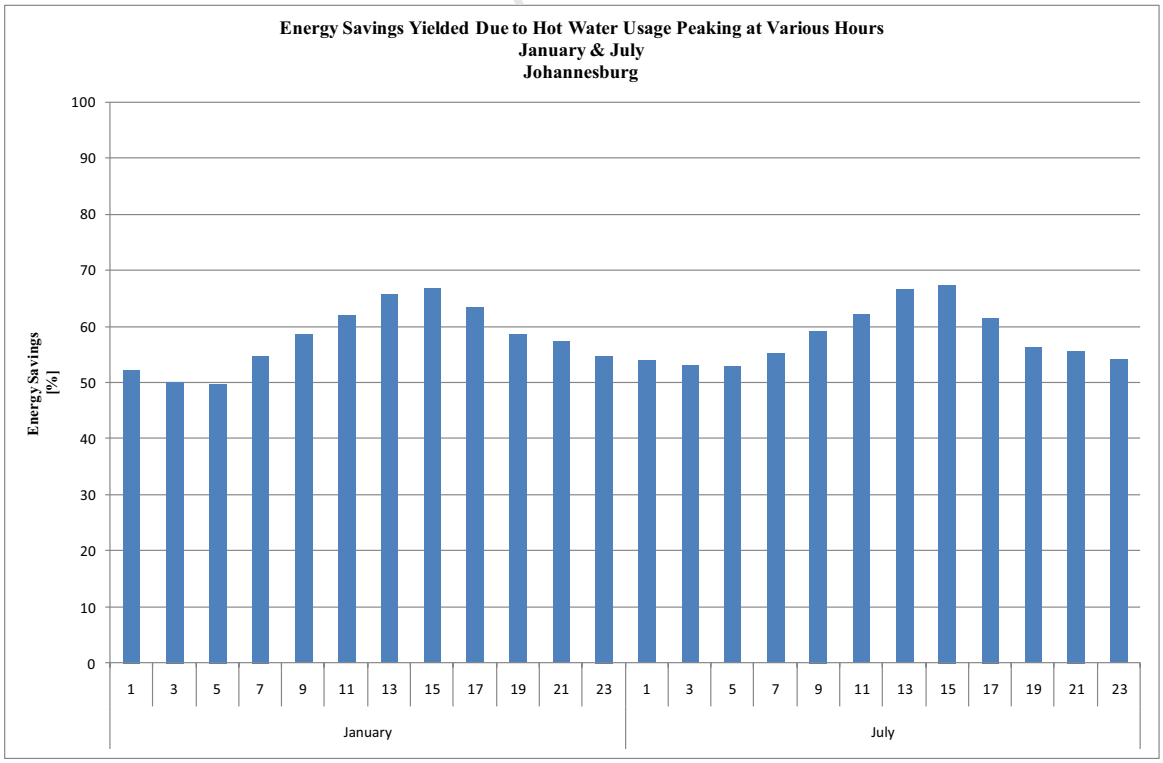

Figure 6.9: Energy Savings Yielded Due to Hot Water Consumption Peaking at Various Hours in January and July – Johannesburg

In Johannesburg, savings were at their highest in both January and July, when hot water usage peaked between 1PM and 3PM.

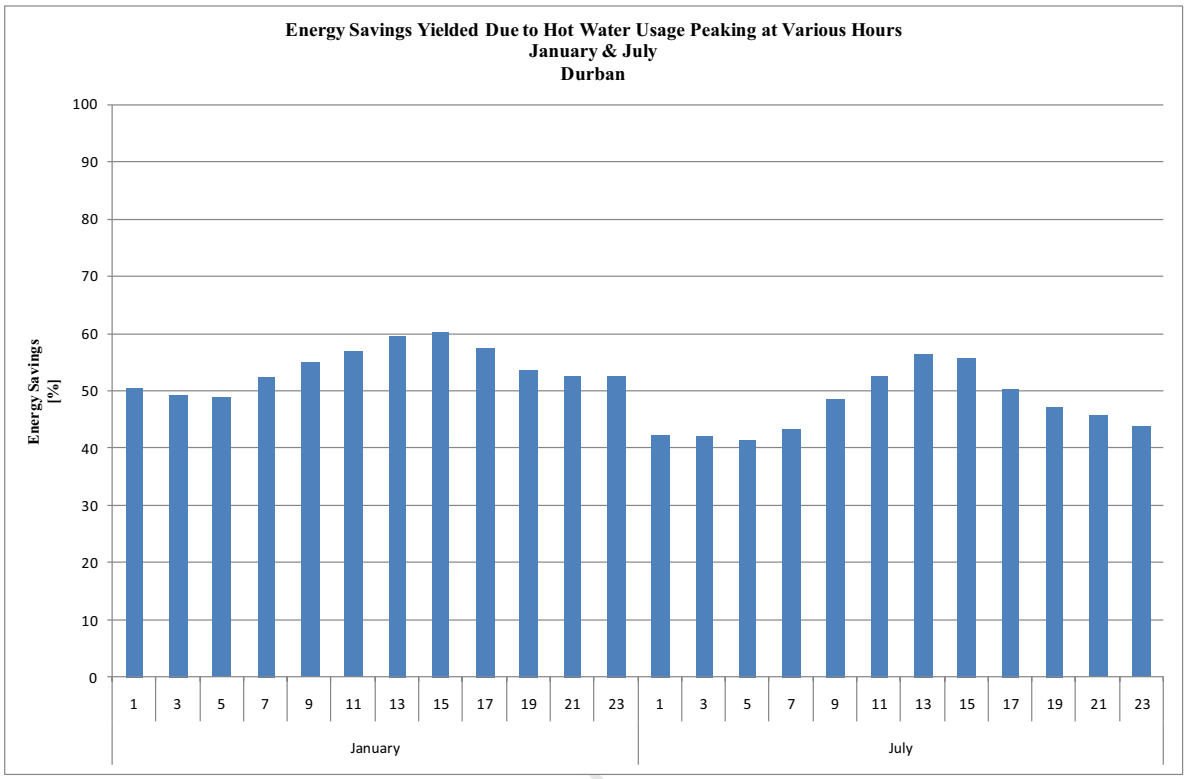

Figure 6.10: Energy Savings Yielded Due to Hot Water Consumption Peaking at Various Hours in January and July – Durban

Savings in Durban were maximised when peak hot water consumption occurred between 1PM and 3PM for winter and summer.

In general, maximum energy savings were achieved when peak hot water consumption took place early in the afternoon. It is thus concluded, that shifting most hot water usage to this part of the day, could help users of solar water heating systems realise maximum benefit from their investment. However, this may not be realistic, due to commitments such as work and school. Therefore, it is suggested that the user should aim to consume their hot water as close to these times as possible. The longer they wait after getting home, the more the savings are reduced.

Cape Town is a special case, due to the fact that its political time is derived from Durban – a whole 45 minutes ahead! As a result, the peak solar radiation actually occurs at roughly 1PM, instead of 12PM. This delay puts Cape Town consumers in a much better position to exploit SDHW systems.

6.5 Impact of Combining Measures on Energy Savings

A simulation was done in order to examine the effects of implementing all 3 measures on a SDHW system. The simulation parameters that were changed are shown in Table 6.5.

Table 6.5: Simulation Settings Changed to Implement Energy Saving Measures on a SDHW System

	SDHW	**Improved SDHW**
Thermostat Setting	65˚C	55˚C
Overall Loss Coefficient (Standing Losses)	5kJ/hr (1.53kWh/day)	4kJ/hr (1.23kWh/day)
Hot Water Consumption Evening Peak	8PM	7PM

The resulting demand curves are shown in Figure 6.11 to Figure 6.13. Table 6.6 is a summary of the energy consumption of the improved SDHW systems and its savings, as compared to the original SDHW system.

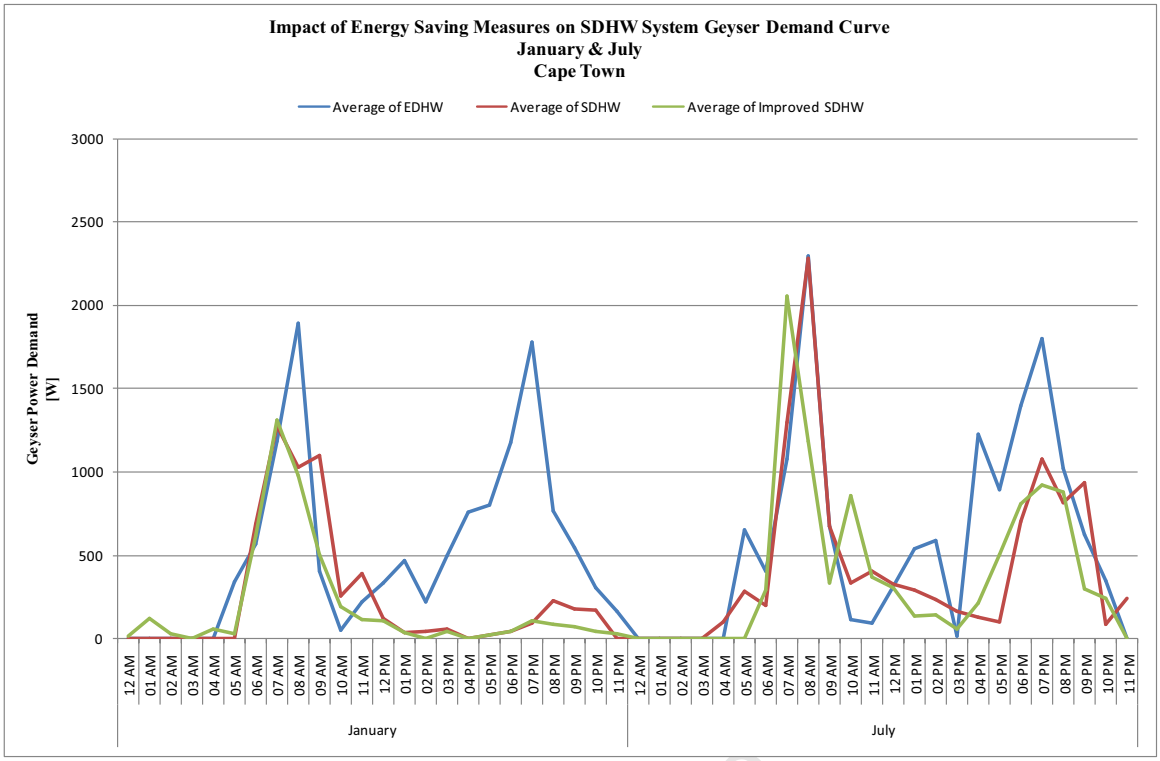

Figure 6.11: Impact of Energy Saving Measures on Average Daily SDHW Geyser Demand Curves in January and July – Cape Town

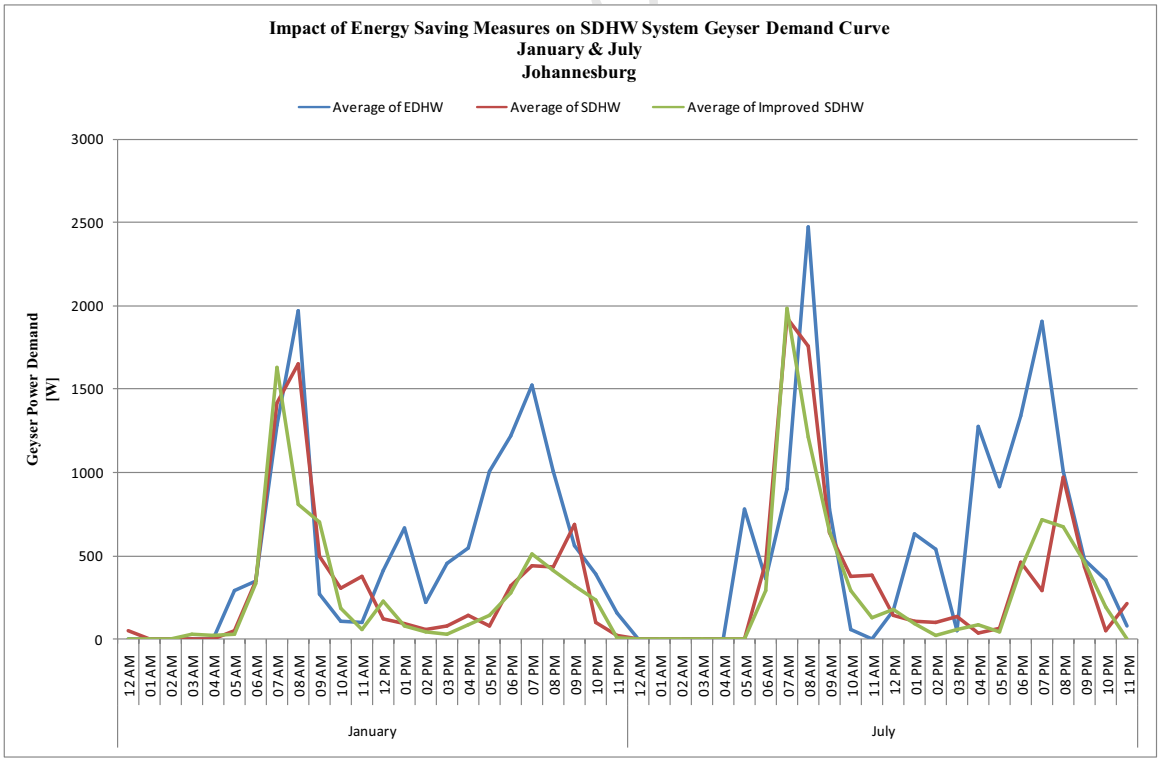

Figure 6.12: Impact of Energy Saving Measures on Average Daily SDHW Geyser Demand Curves in January and July – Johannesburg

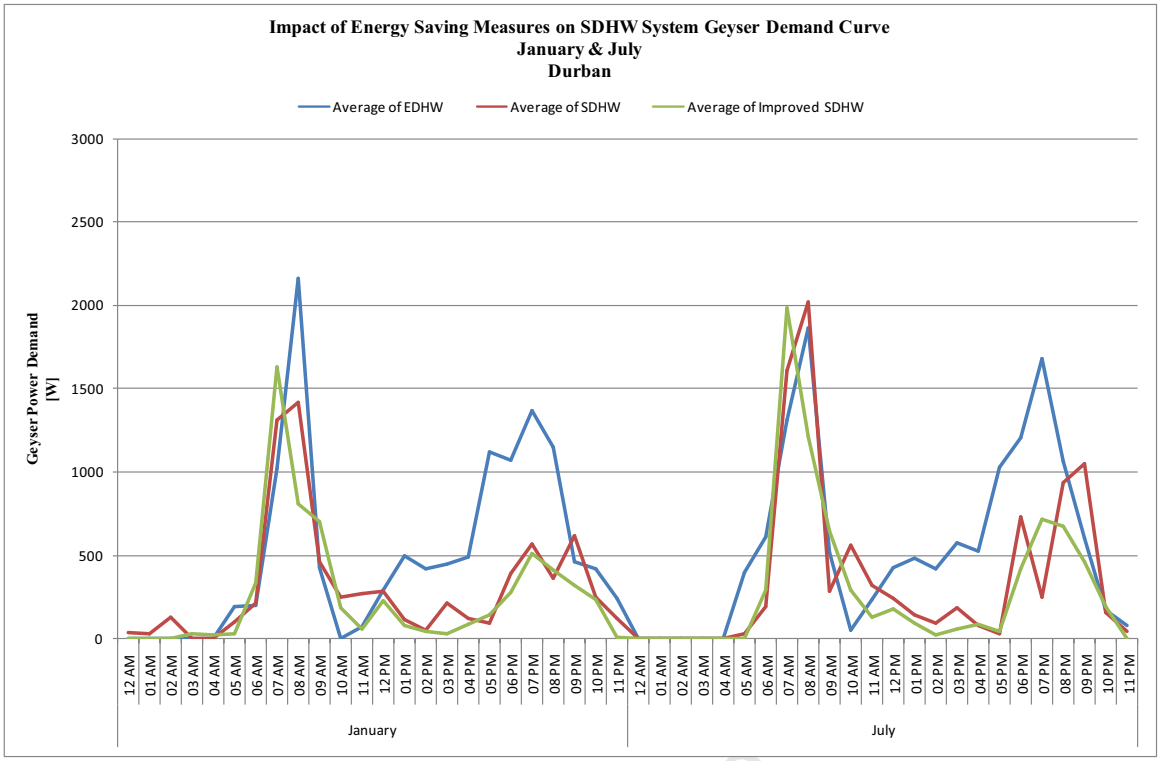

Figure 6.13: Impact of Energy Saving Measures on Average Daily SDHW Geyser Demand Curves in January and July – Durban

For all three cases, the new demand curve maintains a similar shape to that of the original SDHW system. However, there is a difference in the energy consumption of the two systems, as can be seen in Table 6.6 below. The figures in brackets indicate the energy savings of the improved system, as compared to the original SDHW that was simulated.

Table 6.6: Energy Consumption (and Savings) Due to Implementing Energy Saving Measures

		EDHW	SDHW	Improved SDHW
CAPE TOWN	January	386.13kWh	177.32kWh	140.27kWh (20.9%)
	July	435.68kWh	330.01kWh	297.00kWh (10.00%)
	Annual	4855.10kWh	2917.82kWh	2494.22kWh (14.5%)
JOHANNESBURG	January	387.47kWh	224.08kWh	190.03kWh (15.2%)
	July	436.92kWh	263.95kWh	231.75kWh (12.2%)

	Annual	4859.13kWh	2839.74kWh	2433.65kWh (14.3%)
DURBAN	January	372.98kWh	228.42kWh	192.93kWh (15.5%)
	July	409.21kWh	276.22kWh	244.49kWh (11.5%)
	Annual	4587.87kWh	2926.61kWh	2541.64kWh (13.2%)

From the results above, it can be concluded, that the implementation of all the energy saving measures discussed in this chapter can improve the energy savings brought about by the use of a solar water heating system. Across the board, there was an annual increase in savings of 13% - 14%.

This is both an appreciable saving from a consumer perspective, and definitely something a utility would be interested in, given the contribution of water heating to their overall load.

6.6 Payback Period Analysis

A payback period analysis is a simple method to show the consumer how long it will take to recover the capital costs of the SDHW systems from the savings they make. This period is dependent on the initial cost of the system, as well as the cost of electricity (which will determine the monetary value of the savings). Using the annual results presented in Table 6.6 and Equations 6.2 and 6.3, the annual cost of electricity for each system was calculated.

Annual Cost of Electricity for EDHW = Tariff*Consumption **(6.2)**

Annual Cost of Electricity for SDHW = Tariff*Consumption **(6.3)**

The annual savings were calculated using Equation 6.4.

Savings = Cost of Electricity for EDHW – Cost of Electricity for SDHW **(6.4)**

In order to determine the payback period, the annual savings were added up, until they exceeded the initial cost of the system [48]. The calculations were based on the cost of a 200l, direct, flat plate, thermosyphon system. The annual consumption of electricity for water heating was treated as constant, and the electricity tariff was increased annually by 8%.

Usually, such a system would cost about R14,650 to install, but with ESKOM's Solar Water Heating Initiative, the capital expenditure has been reduced to R12,385 [49]. The improved SDHW system will have the added cost of a geyser blanket, which is approximately R200. Table 6.7 shows the expected pay back periods (in years) for systems operating in Cape Town, Johannesburg and Durban.

Table 6.7: Estimated Payback Period (in years) for SDHW Systems

	SDHW SYSTEM	IMPROVED SDHW SYSTEM
CAPE TOWN	10.20	8.96
JOHANNESBURG	9.53	8.44
DURBAN	10.92	9.53

There are few important points to note about these payback periods. Firstly, they are based on electricity prices as at April 2008. With the 50% increase that ESKOM requested soon to be implemented, tariffs are likely to rise. This will shorten the payback period.

Another driver for the payback period will be the initial cost of the system. The increasing cost of electricity is likely to drive up demand for SDHW systems. This trend could cause the initial cost of a SDHW system to decrease, further decreasing the payback period.

Lastly, the payback period was also calculated based on the assumption that the consumer will purchase an entire solar water heating system. If it is possible to retrofit the existing geyser with a solar thermal panel, the payback period could be reduced even further.

From Table 6.7 it is evident that the implementation of the measures discussed in this chapter can reduce the payback period for a SDHW system.

6.7 Chapter Summary

It has been established that SDHW systems can reduce the amount of electrical energy used for water heating in a household. In this chapter, it has been shown that even more energy can be saved by implementing a few behavioural and operational changes. The changes discussed require little to no capital investment on the part of the utility, and are beneficial to both the utility and the consumer.

From a consumer perspective, putting these measures into practice requires little effort on their part. Turning down a thermostat and installing a geyser blanket are both quick, once-off procedures. Changing the hot water consumption pattern might be a bit more difficult, due to several external factors which drive hot water usage. However, the promise of such significant energy savings would probably prove incentive enough for them to try.

CHAPTER VII

7. EFFECTS OF SOLAR WATER HEATING ON THE TRANSMISSION GRID

This chapter presents a brief introduction to power system operations. Thereafter, the potential impact of solar water heating on a transmission grid is explored through load flow studies on a power system model that is loosely based on the ESKOM transmission grid.

7.1 Electric Power System Operation

A power system is a collection of circuits and electrical and mechanical equipment used to generate, transmit and distribute electricity.

A power system can be divided into 3 major parts: generation, transmission and distribution. Generation comprises all the power stations and is responsible for the production of electrical energy. The transmission system is responsible for transferring large amounts of power from the power stations to the loads. It also acts as a bridge between power systems, providing support during emergencies. The transmission network operates at very high voltages in order to minimise losses; therefore, substations are erected where the voltage is stepped down to a more appropriate value for the end use. Distribution then supplies the power from the substation to the consumers [3].

7.1.1 OVERVIEW

A utility that runs a power system is a business whose ultimate goal is to make money. Therefore, they look to keep operating costs to a minimum while maintaining the system's reliability at an acceptable level. Achieving a balance between the two involves load forecasting, and scheduling of generating plants to meet the expected demand. This process is known as operations planning. It can be done for hours, days, weeks and even years. Another important activity in running a power system is real time control. As the name suggests, this process deals with the system's actual response to demand and equipment failure. This normally takes place in a centralised control centre [3].

7.1.2 LOAD FORECASTING

Accurate load forecasting is essential to the running of a power system. It affects activities from generation scheduling to the addition of system infrastructure. There are a number of factors that affect the system load such as time of day, weather, load history and the types and numbers of customers. Load forecasting takes place in the short term (hours and days) medium term (weeks and years) and the long term (several years) [50].

Short term forecasting has a large impact on a power system's reliability. Accurate forecasts in this time frame can help avert system overloading and black outs. Factors that affect this type of load forecast particularly are time of day and weather. These influence the consumers' behaviour and power consumption patterns [50].

7.1.3 GENERATION SCHEDULING

A utility stands to make maximum profit if it figures out the combination of generating plants that have the lowest operating costs and still meet the power demand. This combination is likely to change as the load fluctuates and generating costs rise and fall. It is also affected by the composition of the power system, which changes due to the addition, maintenance downtime and decommissioning of infrastructure [51].

Generating costs are affected by the power plant's efficiency, and the cost of fuel used by the power plant. This cost can be expressed as Rands per Megawatt Hour (R/MWh). It is obtained by multiplying the heat rate[5] of the fuel - Gigajoules per Megawatt Hour [GJ/MWh] plant by the fuel cost – Rands per Gigajoule [R/GJ].

Generation scheduling is also affected by the capacity of transmission infrastructure [50].

There are two important issues when it comes to reliability of a power system. The first is the adequacy of the generating capacity. In other words, is it capable of meeting demand at all times? The other, is the reliability of the transmission system, specifically, can it deliver power to where it is needed? Security of supply is essential. In South Africa, ESKOM owns

[5] The heat rate is indicative of the energy content of the fuel

majority of the power stations, and is the only licensed transmission system operator. Therefore a large part of the responsibility for security of supply lies with the utility [52].

7.2 Potential Impact of Solar Water Heating on a Transmission Grid

A power system model had to be developed, in order to observe the impact of the reduction in geyser demand, on a power system that supplies, residential, commercial and industrial consumers. The power system model was based on the ESKOM generation and transmission grid shown in Figure 7.1. The grid is characterised by long transmission lines that connect consumers to the generating hub in the north-east.

Unfortunately, due to confidentiality laws [53], an exact model could not be obtained from ESKOM in order to determine the impact on their system. But, after these studies, a framework will have been established to carry out such an investigation in the future.

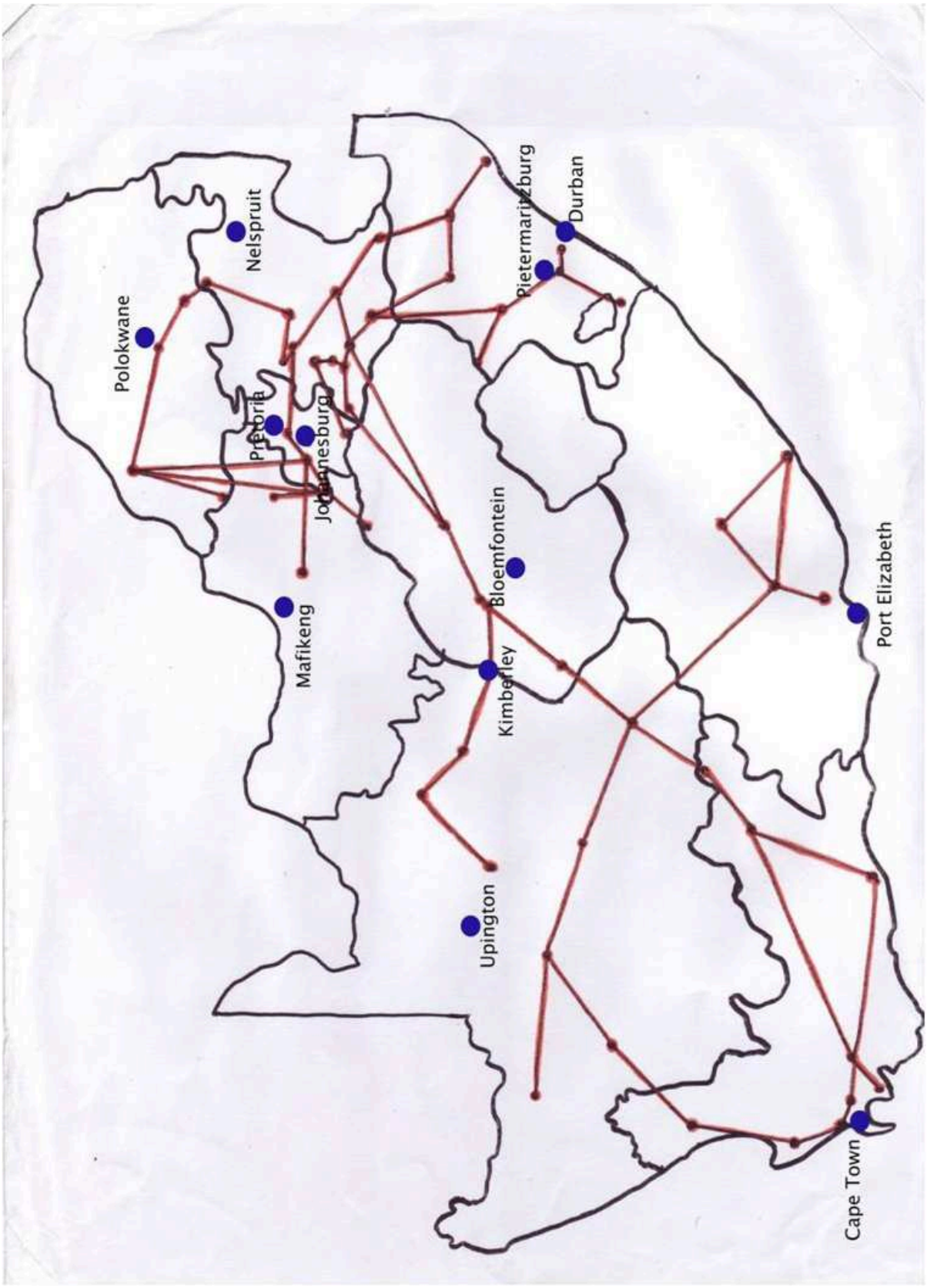

Figure 7.1: ESKOM Transmission Grid – 400kV and above

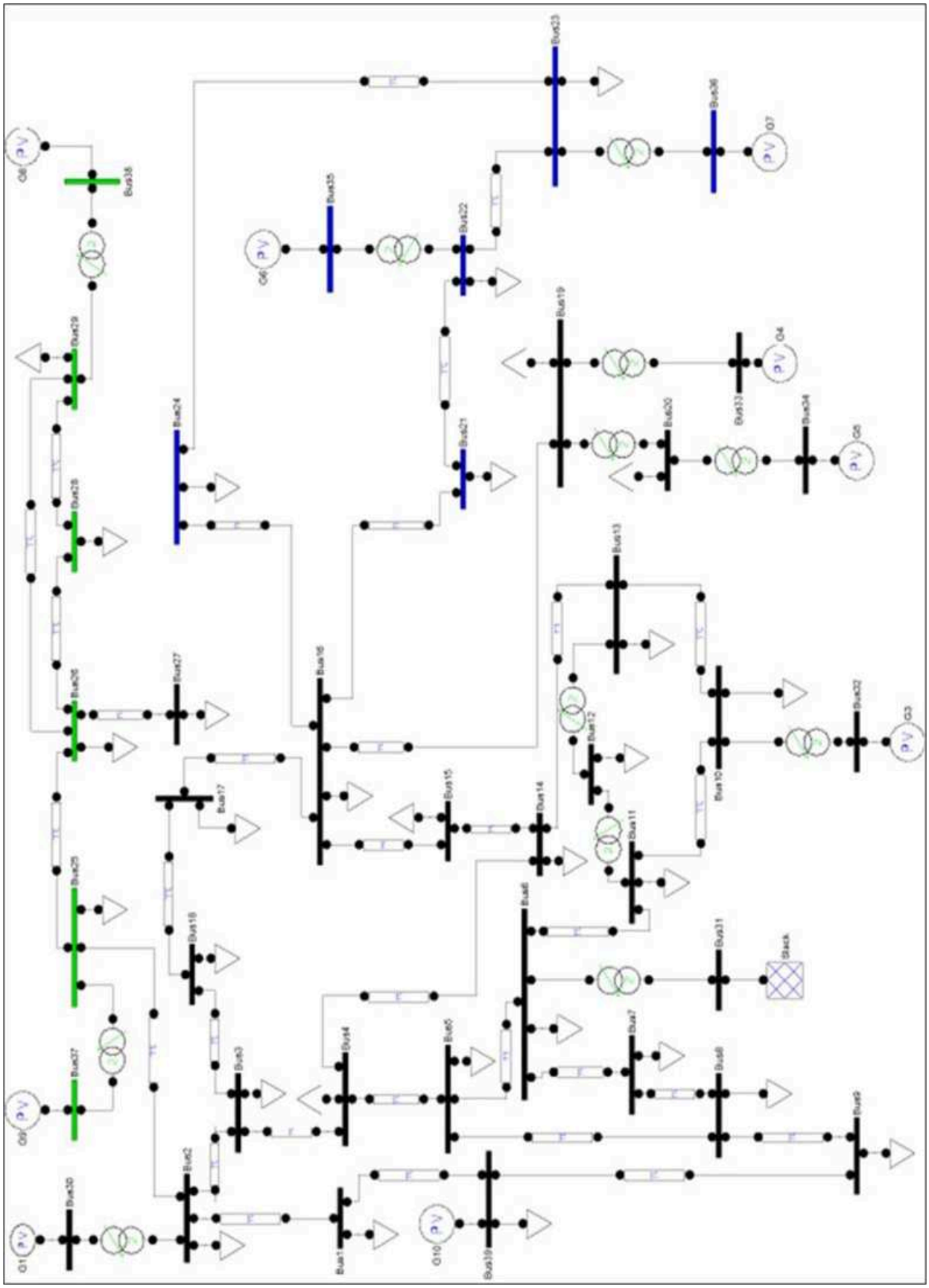

Figure 7.2: Modified IEEE 39 Bus Test System Used for Load Flow Studies

The power system model used was a modified version of the IEEE 39 Bus test system [54], as depicted in Figure 7.2. The full system parameters are outlined in Appendix D.

The system was divided into 3 distinct areas, as outlined in Table 7.1.

Table 7.1: Power System Set Up

	Bus Colour Code	**Load - P [p.u]**	**Generation - P [p.u]**
Area 1	Black	217.09	308.95
Area 2	Blue	57.00	8.66
Area 3	Green	54.24	25.96

Area 1 is equivalent to the generating hub in Mpumalanga, along with Gauteng and other parts of the Highveld. Area 2 is equivalent to the Eastern coast of South Africa, and includes the load centres of Durban and Richards Bay. Area 3 covers the entire Western and Southern regions of South Africa, including Cape Town, Port Elizabeth and Kimberley.

7.2.1 LOAD FLOW STUDY METHODOLGY AND RESULTS

In order to determine the impact of solar water heating on the power system, the load on the system was varied, according to the methodology outlined below. The initial loading on the system is summarised in Table 7.2 below.

Table 7.2: System Loads for Base Case Scenario – No Solar Water Heating Implemented

Bus Number	Active Power [p.u]	Reactive Power [p.u]
3	17.19	0.1284
4	26.69	9.8252
7	12.48	4.4854
8	27.87	9.398
12	0.453	4.699
15	17.087	8.1699
16	17.567	1.7247
18	8.4368	1.6019
20	33.533	5.5
21	6.3393	2.6606
22	20.17	7.5939
23	27.662	9.4555
24	3.4578	-1.033
25	9.2208	1.9429

26	4.3392	0.5306
27	11.9328	3.2061
28	7.0512	0.9447
29	21.696	2.0586
39	58.951	13.349

The marked loads were chosen to represent the cities that were identified for the simulation studies as follows:

Area 1 - Bus 39 - "Johannesburg"
Area 2 - Bus 23 - "Durban"
Area 3 - Bus 29 - "Cape Town"

Load flow studies were carried out for various scenarios.

Scenario 1: This scenario served as the base case. The losses on the system in this case were representative of the losses experienced during times of peak demand, on a grid where no solar water heating had been implemented.
Scenario 2: 10% penetration of solar water heating in the residential consumer market.
Scenario 3: 50% penetration of solar water heating in the residential consumer market.
Scenario 4: 100% penetration of solar water heating in the residential consumer market.

Scenarios 2 to 4 assessed the impact of various levels of penetration of solar water heating in the residential load centres of Cape Town, Johannesburg and Durban.

The values of the loads at these busses were altered based on the summer and winter peak demand reduction factors that were derived in chapter 4. These load changes were based on the following assumptions.

- Residential Electricity Consumption constitutes 37% of Peak Demand [2]
- Geyser Electricity Consumption constitutes 40% of Residential Electricity Consumption [2]

For example:

In the case of Cape Town, a solar water heating system reduced geyser peak consumption by 89% in summer. (This figure was calculated from the TRNYS simulation results, and validated by the field data.)

The following calculations were carried out in order to determine the change in load in the case where there is 50% penetration of solar water heating in the residential consumer market.

According to Table 7.2 above,

$$Initial\ Cape\ Town\ Load = 21.696 + 2.0586i\ p.u = 21.793/5.4^{\circ}$$

37% of this load can be attributed to residential consumers….

$$Residential\ Load = \mathbf{0.37} * 21.793/5.4^{\circ} = 8.064/5.4^{\circ}$$

At **50%** penetration, half of this load will be affected by solar water heating…

$$Load\ Affected\ by\ SDHW = \mathbf{0.5} * 8.064/5.4^{\circ} = 4.0317/5.4^{\circ}$$

40% of this load can be attributed to geyser demand…

$$Geyser\ Demand = \mathbf{0.4} * 4.0317/5.4^{\circ} = 1.613/5.4^{\circ}$$

This demand will be reduced by **89%**...

$$Geyser\ Demand\ Reduction = \mathbf{0.89} * 1.613/5.4^{\circ} = 1.4353/5.4^{\circ}$$

The new residential load is then given by the old load, less the reduction, which is…

$$New\ Residential\ Load = 6.628/5.4^{\circ}$$

Similarly, the new Cape Town Load will be…

$$New\ Cape\ Town\ Load = 20.358/5.4^{\circ}$$

The procedure outlined above, was used for each of the scenarios mentioned, in order to calculate the values of the loads at the selected busses. These values can be seen in the detailed load flow results included in Appendix E. Once the load values were changed, a load flow was run, and the system losses were then recalculated, and compared to the base case, in order to see if there were any changes. The results are presented in this section. All values are in p.u. on a 100MVA base.

The focus during the load flow studies was the impact on a change in the loads in each of these areas on the real power losses on the system, particularly on the tie-lines between the areas.

7.2.1.1 Impact of 10% Penetration of SDHW Systems

This section explores the scenario where 10% of the residential electricity consumers in Cape Town, Johannesburg and Durban all implement solar water heating in their households. Table 7.3 shows the changes that occur in the system's overall loading, generation and losses. The figures in brackets represent the reduction in load / losses as compared to the base case.

Table 7.3: Impact of 10% Penetration of SDHW Systems on Power System

	Base Case No SDHW	**SDHW in Summer**	**SDHW in Winter**
TOTAL LOAD	**328.33**	**327.32**	**327.54**
(Reduction in Total System Load)		(0.31%)	(0.24%)
Area 1 Load	217.09	216.58	216.63
Area 2 Load	57.00	56.78	56.81
Area 3 Load	54.24	53.95	54.10
TOTAL GENERATION	**343.57**	**342.47**	**342.72**
Area1 Generation	308.95	307.85	308.10
Area2 Generation	8.66	8.66	8.66
Area3 Generation	25.96	25.96	25.96
TOTAL LOSSES	**15.24**	**15.15**	**15.18**
(Reduction in System Losses)		(0.59%)	(0.39%)

From the figures in Table 7.2, it can be seen that the impact of SDHW systems on the transmission grid, in terms of load and loss reduction will vary depending on the season. A load reduction of 0.31% in summer reduced the losses on the system by 0.59% and a load reduction of 0.24%, for winter, still had a significant loss reduction of 0.39%.

Table 7.4 shows the impact of the load reduction on the real power transmission and real power losses in the lines that connect the areas.

Table 7.4: Impact of 10% Penetration of SDHW Systems on Line Flows

		Base Case No SDHW	SDHW in Summer	SDHW in Winter
A1 – A3 Bus 2-Bus 25	Line Loading	31.11	30.77	30.94
	Line Losses	1.11	1.09	1.10
A1-A2 Bus 21- Bus 22	Line Loading	17.14	17.03	17.05
	Line Losses	0.29	0.28	0.29
A1-A2 Bus 24- Bus 23	Line Loading	22.36	22.22	22.24
	Line Losses	0.42	0.42	0.42

From Table 7.4 it can be seen that, there is decreased loading on the inter area tie lines for both the summer and winter scenarios. There is also a reduction in the value of the line losses on the line connecting area 1 to area 3 for both scenarios.

7.2.1.2 Impact of 50% Penetration of SDHW Systems

This section explores the scenario where the penetration of residential SDHW systems in Cape Town, Johannesburg and Durban has increased to 50%. Table 7.5 shows the impact on the power system for both summer and winter.

In this case, the resultant load reduction of 1.56% in summer reduced the value of losses on the system by 2.62% and the load reduction of 1.22% in winter led to a loss reduction of 1.77%.

Table 7.5: Impact of 50% Penetration of SDHW Systems on Power System

	Base Case No SDHW	SDHW in Summer	SDHW in Winter
TOTAL LOAD	**328.33**	**323.22**	**324.32**
(Reduction in Total System Load)		(1.56%)	(1.22%)
Area 1 Load	217.09	214.52	214.76
Area 2 Load	57.00	55.89	56.02
Area 3 Load	54.24	52.81	53.54
TOTAL GENERATION	**343.57**	**338.06**	**339.29**
Area1 Generation	308.95	303.44	304.67
Area2 Generation	8.66	8.66	8.66
Area3 Generation	25.96	25.96	25.96
TOTAL LOSSES	**15.24**	**14.84**	**14.97**
(Reduction in System Losses)		(2.62%)	(1.77%)

Table 7.6 shows the impact of the load reduction on the real power flow and real power losses in the transmission lines that connect the areas.

Table 7.6: Impact of 50% Penetration of SDHW Systems on Line Flows

		Base Case No SDHW	SDHW in Summer	SDHW in Winter
A1 – A3 Bus 2-Bus 25	Line Loading	31.11	29.43	30.29
	Line Losses	1.11	1.01	1.06
A1-A2 Bus 21- Bus 22	Line Loading	17.14	16.62	16.68
	Line Losses	0.29	0.27	0.28
A1-A2 Bus 24- Bus 23	Line Loading	22.36	21.68	21.76
	Line Losses	0.42	0.40	0.40

From Table 7.6 it can be seen that an increase in the penetration of SDHW systems on the power system decreased loading and losses on the inter area tie lines further, for both the summer and winter scenarios.

7.2.1.3 Impact of 100% Penetration of SDHW Systems

In this section, the assumption is that 100% of the residential electricity consumers in Cape Town, Johannesburg and Durban implemented solar water heating in their households. Table 7.7 shows the resultant changes to the system's overall loading, generation and losses.

Table 7.7: Impact of 100% Penetration of SDHW Systems on Power System

	Base Case No SDHW	**SDHW in Summer**	**SDHW in Winter**
TOTAL LOAD	**328.33**	**318.03**	**320.26**
(Reduction in Total System Load)		(3.14%)	(2.46%)
Area 1 Load	217.09	211.89	212.37
Area 2 Load	57.00	54.76	55.03
Area 3 Load	54.24	51.38	52.86
TOTAL GENERATION	**343.57**	**332.53**	**335.0**
Area1 Generation	308.95	297.91	300.38
Area2 Generation	8.66	8.66	8.66
Area3 Generation	25.96	25.96	25.96
TOTAL LOSSES	**15.24**	**14.50**	**14.73**
(Reduction in System Losses)		(4.86%)	(3.35%)

From the table, it can be seen, that a load reduction of 3.14% reduced the value of losses on the system by 4.86%. Also, a load reduction of 2.46% led to a loss reduction of 3.35%.

Table 7.8: Impact of 100% Penetration of SDHW Systems on Line Flows

		Base Case No SDHW	SDHW in Summer	SDHW in Winter
A1 – A3 Bus 2-Bus 25	Line Loading	31.11	27.77	29.48
	Line Losses	1.11	0.93	1.02
A1-A2 Bus 21- Bus 22	Line Loading	17.14	16.10	16.23
	Line Losses	0.29	0.26	0.26
A1-A2 Bus 24- Bus 23	Line Loading	22.36	20.99	21.16
	Line Losses	0.42	0.38	0.39

The most interesting result to note in Table 7.8 is how drastically the line losses have been reduced for all the tie lines. In the line connecting area 1 to area 3, there is a 16% reduction in line losses for the summer scenario, and an 8% reduction in winter. The tie lines for area 1 and 2 have an average reduction in losses of about 8%.

7.3 Chapter Summary

The aim of this chapter was to examine the possible impact of SDHW systems on a power system, particularly on transmission losses. A power system model, loosely based on the ESKOM grid, was used to carry out load flow studies. The studies were based on various levels of penetration of SDHW systems in the 3 major residential load centres of South Africa.

The results from the load flow studies revealed that SDHW systems could indeed impact on a power system's losses. Even with a penetration level of just 10%, the SDHW systems managed to reduce losses on the transmission grid by 0.59% in summer and 0.39% in winter. These are seemingly insignificant figures, but when dealing with a large power system, the value of the MW savings becomes significant. In this case, system losses were reduced from 1524MW to 1515MW. As the penetration level increased, so did the reduction in transmission losses that the SDHW systems brought about. At 100% penetration, the losses on the system had been reduced to 1450MW! On the ESKOM power system, this level of penetration would amount to 1800MW reduction in transmission losses.

Another result of interest from the load flow studies was the power flow in the transmission lines that connected the various areas. It was revealed that the SDHW systems reduced both the loading and the losses on these long transmission lines.

It can thus be concluded that the large scale implementation of SDHW systems can impact on transmission losses on a power system. Although the results presented here were not specific to the ESKOM grid, they still present a strong case for the use of SDHW systems in order to reduce transmission line loading and losses, especially during times of peak demand.

CHAPTER VIII

8. CONCLUSIONS AND RECOMMENDATIONS

The aim of this thesis was to investigate the impact of solar water heating on ESKOM's grid, particularly on the losses incurred during times of peak demand. This chapter will present conclusions and recommendations, based on the previous chapters.

8.1 Conclusions

The South African electricity sector is facing a major crisis at the moment. Electricity usage has risen to a point where the generation and transmission infrastructure are no longer capable of satisfying the demand. This has led to compulsory load shedding, along with a call from ESKOM for consumers to reduce their electricity usage by 10%.

Residential consumers account for 37% of the electricity consumption during peak demand. With water heating being responsible for approximately 40% of residential electricity usage, it is definitely a key area where consumption can be cut down. Furthermore, the abundance of sunshine in South Africa makes solar water-heating a practical means of achieving this goal. Studies have already shown that solar water heaters can reduce electricity usage in a household.

The main contribution of this research was to establish the impact that these systems could have on peak demand.

Simulations were carried out using TRNSYS and MeteoNorm, in order to determine the reduction in electricity consumption that a solar water-heating system could bring about. Not only did the simulation results cement the fact that solar water-heating does reduce energy consumption. They also showed that, based on the typical South African water usage profile, solar water heating can reduce the demand of a geyser during the evening peak period of 6PM to 8PM. This would ultimately reduce the acute burden imposed on the transmission infrastructure by peak demand. It was also shown that the actual reduction was dependent on the time of year, as well as the location in South Africa. The best results were obtained in

summer months, with a reduction of up to 94% in Cape Town during February. In June the solar water-heating system resulted in a reduction of 34% of the geyser's peak demand in the evening. Cape Town showed the largest variation between the summer and winter reductions, with Durban showing a reduction of 70% in March and 45% in June.

In order to validate the simulation results, a number of solar water-heating installations around Cape Town were monitored over a period of 6 months. Although a number of problems were encountered with the monitoring of the systems, the overall results showed that the homeowners had experienced a great reduction in their electricity usage for water heating. A comparison of the field results and the simulation results showed a close correlation. There was very little difference in the reduction in the evening geyser peak that was predicted (94%) and that which was measured (89%) for the summer months.

Some of the problems encountered with the logging process helped highlight the fact that consumer behaviour can have an impact on the energy savings brought about by a solar water heater. Subsequently, a number of simulations were run to find out if a few behavioural changes could have an impact on the benefits derived from a solar water heating system. The changes investigated were a lower thermostat setting, the installation of a geyser blanket and aiming to use most hot water as early in the evening as possible. The results showed that a user who implemented these changes could increase their savings by up to 14%.

Lastly, a power system model, with similarities to the ESKOM grid was developed. Using a number of assumptions, the validated simulation results were used to estimate the load reduction that would take place with increasing penetration levels of solar water heating in Cape Town, Johannesburg and Durban. Load flows were then carried out in order to determine the impact on transmission line loading and losses. Each case revealed the substantial savings that could be realised, in transmission losses, as more and more residential consumers switched to solar water heating. At 100% penetration, there was an improvement of 5%.

On ESKOM's power system, these savings would amount to approximately 180MW, which is the capacity of an Open Cycle Gas Turbine (OCGT) generation unit. A unit of this nature costs millions, and takes 2 to 3 years to come online after being commissioned. Further capital expenditure would also have to go into upgrading the transmission grid to carry the

extra power. Lastly, the addition of fossil-fuel based generation onto the grid also brings with it more carbon emissions, which are harmful to the environment.

All in all, the research conducted made it clear that solar water heating has the potential to reduce both the demand and transmission losses on a power system. It is thus recommended as a means of mitigating these phenomena, especially during times of peak demand. This will allow the power system to operate more efficiently. The reduced strain on the system can also prolong the life of transmission equipment, and postpone the need for investment in new generation and transmission infrastructure.

8.2 Recommendations

Ideally, this project would have presented the actual results of the impact of large-scale solar water heating on the ESKOM grid. However, this study had to be carried out on a generic power system, due to the fact that ESKOM system data is currently protected by confidentiality laws and could not be obtained. In order to accurately quantify the expected impact on ESKOM's grid, it is recommended that current energy policy be re-examined to allow more access to the country's energy database to researchers who are tasked to find solutions. This would make it possible for a similar investigation be carried out, using the ESKOM transmission model. This project has established the framework for such a study.

The programs used to run the simulations are well established modelling tools. However, it is good practice to validate simulation results. Due to time constraints, this process only took place for summer months. It is essential that the winter simulation results are also compared to field data, in order to confirm that they too are accurate.

During the collection of field data, it became clear that the user's behavioural patterns can influence the savings they derive from their solar water heating system. A number of simulations also showed that by making a few changes, a user could potentially increase their savings substantially. It is thus recommended that the utility makes users aware of the simple steps highlighted in this thesis, which they can take in order to maximise the savings they achieve with their solar water heating system. This can be achieved through various forms of public communication. Not only would this benefit the consumer, it would reduce demand on the power system even further, which would benefit the utility too.

REFERENCES

[1] Eskom Holdings Limited., *Eskom Annual Report 2007.* Johannesburg : Eskom, 2007. Annual .

[2] ESKOM., *ESKOM DSM.* [Online] http://www.eskomdsm.co.za.

[3] McGraw-Hill, Parker, Sybil P and Licker, Mark D., *McGraw Hill Dictionary of Scientific and Technical Terms.* 6th Edition. s.l. : The McGraw Hill Companies, Inc., 2003. ISBN 007042313X.

[4] Glover, J. Duncan and Sarma, Mulukutla S., *Power System Analysis and Design.* 3rd Edition. California : Brooks/Cole, 2002.

[5] United States Alumoweld Company, Inc., Alumoweld: ACSR CORE WIRE. *Alumoweld.* [Online] Wire World, 06 March 1999. [Cited: 11 March 2008.] http://www.wireworld.com/alumoweld/apps/corewire.html.

[6] Pollack, Martin., Eskom has innovative ideas to reduce power cuts. *City of Cape Town Website.* [Online] City of Cape Town, 2 June 2006. http://www.capetown.gov.za/clusters/viewarticle3.asp?conid=12733 .

[7] UKZN - Department of Electrical Engineering., "4SS2SLIDES_7." *System Stability Voltage Stability Kundur Chapter 14.* [Online] [Cited: 12 February 2008.] coursemain.ee.ukzn.ac.za/enel4ssh2/notes/4SS2SLIDES_7.pdf.

[8] Tennesse Valley Authority., Why Is The Algood Transmission Line Needed? *TVA: Cookeville, Tennessee, Power Supply Upgrade.* [Online] Tenessee Valley Authority. [Cited: 12 February 2008.] http://www.tva.gov/power/projects/cookeville_tn/index.htm

[9] Haricharun, Harun., "Nuclear Power As An Energy Option for South ." *South African Government Department of Environmental Affairs and Tourism.* [Online] 19 October 2005. http://www.environment.gov.za/HotIssues/2005/climateChange/presentations/91October_science/12H00/(4)dst%20climate%20change%20rev3.pdf.

[10] ESKOM., "An Overview of the Western Cape Recovery Plan." *Western Cape Newspaper Insert.* Cape Town : s.n., April 2006.

[11] ESKOM. "ESKOM." *Western Cape Recovery Plan.* [Online] 31 March 2006. http://www.eskom.co.za/live/monster.php?URL=%2Fcontent%2FIntegration+Plan+Ver12.0%7E1.doc&Src=Item+1201.

[12] Benjamin, Chantelle and LeRoux, Mathabo., Information Centre. *Coega Development Corporation.* [Online] Coega Development Corporation, 25 January 2008. [Cited: 15

February 2008.]
http://www.coega.co.za/iNetNewsView.asp?cID=536&id=243&node0id=79.

[13] Energy Information Administration., "Energy Information Administration - EIA - Official Energy Statistics from the U.S. Government." *Energy Emissions Data and Environmental Analysis of Energy Data.* [Online] 01 February 2008. [Cited: 08 February 2008.] http://www.eia.doe.gov/pub/international/iealf/tableh1co2.xls.

[14] Reddy, Trusha., ISS Today 1 Feb: South Africa's "Energy Crisis" vs "Climate Crisis" Stand-Off. *Institute For Security Studies.* [Online] 01 February 2008. [Cited: 02 February 2008.] http://www.iss.co.za/static/templates/tmpl_html.php?node_id=2942 .

[15] Department of Minerals and Energy., Department of Minerals and Energy: Energy. *Department of Minerals and Energy Website.* [Online] DME. [Cited: 9 October 2007.] http://www.dme.gov.za/energy/renewable.stm.

[16] Sustainable Energy Africa, City of Cape Town., *State of Energy Report for Cape Town.* Cape Town : Galeforce Communication, 2003.

[17] Lane, I.E., *Demand Side Management Options for the Domestic Sector. Report Prepared for the Department of Minerals and Energy Affairs.* Pretoria : Department of Minerals and Energy, 1996. ED9207.

[18] Meyer, J P and Tshimankinda, M., "Domestic Hot Water Consumption in South African Houses For Developed and Developing Communities." International Journal of Energy Research, 1997, pp. 667-673.

[19] Lane, I E and Beute, N., "A Model of The Domestic Hot Water Load." *IEEE Transactions on Power Systems.* 1996, Vol. 11, 4, pp. 1850-1855.

[20] Delport, G J., "The Geyser Gadgets That Work / Do Not Work." Cape Town : Cape Peninsula University of Technology, 2005. Domestic Use of Energy Proceedings 2005.

[21] Britz, Eugene, Delport, Johan and Nell, Chris., "The Influence of The Come-Back Load Because of Hot Water Load Control." Cape Town : Cape Peninsula University of Technology, 2006. Domestic Use of Energy Conference Proceedings.

[22] Dintchev, O D., "Solar Water Heating as a Mechanism to Reduce Domestic Electrical Energy Consumption and its Contribution Towards South African Maximum Demand." Cape Town : Cape Peninsula University of Technology, 2006. Domestic Use of Energy International Conference - April 2006.

[23] Weiss, W, Bergmann, I and Faninger, G., "Solar Heat Worldwide - Markets and Contribution to The Energy Supply 2004." *International Energy Agency.* [Online] 13 February 2007. http://www.iea.org/impagr/cip/pdf/SHCWorldwide2006.pdf .

[24] Cragan, Keary E, Klein, Sanford A and Beckman, William A., "Impact on a Utility, Utility Customers and the Environment of an Ensemble of Solar Domestic Hot Water Systems." [ed.] R Campbell-Howe and B Wilkins-Crowder. Minneapolis, Minnesota : American Solar Energy Society, 1995. Proceedings of Solar '95 - The 1995 American Solar Energy Society Annual Conference. pp. 95-99.

[25] Grater, J, Beckman, W A and Mitchell, J W., "Impact of Solar Water Heating Systems on An Electric Utility." Washington, DC : American Solar Energy Society, 1993. Proceedings of Solar '93 - The 1993 American Solar Energy Society Annual Conference. pp. 165-170.

[26] City of Cape Town., *City of Cape Town: Solar Water Heating By-Law. Draft 10.* [Document] Cape Town, Western Cape, South Africa : s.n., 12 March 2007.

[27] SERI - Solar Energy Research Institute (Now NREL)., *Engineering Principles & Concepts for Active Solar Systems.* New York : Hemisphere Publishing Corporation, 1988. p. 57. ISBN-0-89116-855-9.

[28] Jones, Dylan Tudor., "Domestic Solar Heat Hot Water System Installation Option." Cape Town : Cape Peninsula University of Technology, 2006. Domestic Use Of Energy Conference Proceedings 2006.

[29] Provey, Joe., Solar Hot-Water Heating Systems Roundup - Popular Mechanics:. *Popular Mechanics.* [Online] Popular Mechanics, February 2006. [Cited: 07 June 2006.] http://www.popularmechanics.com/home_journal/home_improvement/2270791.html?page=2.

[30] US Department of Energy - Energy Efficiency and Renewable Energy., *A Consumer's Guide - Heat Your Water With The Sun.* s.l. : US Department of Energy, 2003.

[31] Norton, Brian and Lo, Steve., "Anatomy of a Solar Collector." *Renewable Energy Focus.* May/June 2006, Vol. 7, 3, pp. 32-35.

[32] Go Solar Company., Solar Heating Theory, Solar Temperature and Energy Knowledge is Important. *Solar Energy Panels Power Electric and Heating Systems.* [Online] Go Solar Company, 22 February 2004. [Cited: 12 January 2008.] http://www.solarexpert.co/Heat-theory.html.

[33] Southface., How Solar Thermal Works. *Solar Roadmap Home Page.* [Online] Southface, 2005. http://www.southface.org/solar/solar-roadmap/solar_how-to/solar-how_solar_works.htm.

[34] US Department of Energy., Solar Energy Technologies Program: Solar Collectors. *US Department of Energy - Energy Efficiency and Renewable Energy.* [Online] US

Department of Energy, 2006. [Cited: 13 July 2006.] http://www1.eere.energy.gov/solar/sh_basics_collectors.html.

[35] Darling, David., Evacuated Tube Collectors. *The Encylopedia of Alternative Energy and Sustainable Living.* [Online] 16 October 2007. [Cited: 14 January 2008.] http://www.daviddarling.info/encyclopedia/E/AE_evacuated_tube_collector.html.

[36] South Africa - Travel.Net., Climate in South Africa. *South Africa - Travel.Net - Online Travel Guide.* [Online] [Cited: 3 December 2007.] http://www.southafrica-travel.net/climate/eklima_f.htm.

[37] MeteoTest, Remund, Jan and Kunz, Stefan., *MeteoNorm Handbook, Part I, Review and Software.* Switzerland : MeteoTest, 2003.

[38] Sebitosi, Adoniya Ben., *Application of Advances of Automotive Technologies to Electrification in Rural Sub-Saharan Africa - Chapter 8 - pp.128-162.* PhD Dissertation : UCT Department of Electrical Engineering, 2004.

[39] Solar Energy Laboratory, University of Wisconsin-Madison., "05 Mathematical Reference." *TRNSYS 16 Documentation.* [User Manual]. Wisconsin, United States of America : Solar Energy Laboratory, 2006. pp. 329-340,375-379.

[40] Duffie, John A and Beckman, William A., *Solar Engineering of Thermal Processes.* New York : Wiley, 1991. ISBN 0471510564 9780471510567.

[41] Engineer's Edge., Conditions Required for Natural Circulation. *Fluid Flow Hydraulic and Pneumatic, Engineers Edge.* [Online] Engineer's Edge, 2007. [Cited: 27 June 2007.] http://www.engineersedge.com/fluid_flow/conditions_required_natural_circulation.htm

[42] Bernoulli's Principle. *Wikipedia.* [Online] Wikipedia. [Cited: 27 June 2007.] http://en.wikipedia.org/wiki/Bernoulli's_equation.

[43] Goodall, Chris., "Living a Low Carbon Life." [ed.] Dickon Ross. *E&T - Engineering and Technology.* 2008, Vol. 3, 6, pp. 49-51.

[44] US Department of Energy., Solar Hot Water Heating. *DOE Building Technologies Program.* [Online] US Department of Energy - Energy Efficiency and Renewable Energy, 13 June 2006. [Cited: 9 April 2008.] http://www.eere.energy.gov/buildings/info/components/waterheating/solarhot.html#indirect.

[45] The Institution of Engineering and Technology., "The IET Energy Principles." *The IET Knowledge Network.* July 2007.

[46] Wikipedia., Legionella. *Wikipedia, The Free Encylopedia.* [Online] Wikimedia Foundation, Inc, 19 February 2008. [Cited: 25 February 2008.] http://en.wikipedia.org/wiki/Legionella.

[47] Harris, Anton, Uken, Ernst and Kilfoil, Mark., "Domestic Energy Savings With Geyser Blankets." Cape Town : Cape Peninsula University of Technology, 2007. Proceedings of the 15th Conference on the Domestic Use of Energy. pp. 153-157. ISBN 0-9584901-6-3.

[48] Drury, Colin. *Management and Cost Accounting*. 6th Edition. London. Thomson Learning. 2004

[49] Eskom Demand Side Management., "Accredited Participating Suppliers List." *Eskom DSM.* [Online] 2008. [Cited: 12 March 2008.] http://www.eskomdsm.co.za/2008_05_07%20Accredited%20participating%20suppliers%20list.pdf.

[50] Feinberg, E A and Genethliou, D., "Load forecasting." [book auth.] J H Chow, F F Wu and J J Momoh. *Applied Mathematics foRestructured Electric Power Systems: Optimization, Control, and Computational Intelligence.* s.l. : Springer , 2005, p. Chapter 12.

[51] Energy Exemplar., Power System Modelling 101. *PLEXOS Wiki.* [Online] Wiki, 20 June 2007. Cited: 2007 August 15.] http://www.plexos.info/wiki/index.php?n=Main.Introduction.

[52] Wilson, Duncan and Adams, Ivan., *Review of Security of Supply in South Africa.* A Report to : The Department of Public Enterprise, July 2006.

[53] Cooper, C and Prinsloo, J., *Digest of South African Energy Statistics.* Pretoria : Department of Minerals and Energy, 2002. http://www.dme.gov.za/pdfs/energy/planning/digest_energy_05.pdf. ISBN 0-9584376-4-5.

[54] Pai, M A., *Energy Function Analysis For Power System Stability.* Dordrecht : Kluwer Academic Publishers, 1989.

APPENDIX A

A. STANDARD HEAT LOSSES OF WATER CYLINDERS

This appendix presents the SABS Standards for Geyser Standing Losses

Geyser Capacity [Ltrs.]	SABS Standing Losses [kWh/day]
50	1.62
100	2.16
150	2.59
200	3.02
250	3.46
300	N/A

APPENDIX B

B. MATHEMATICAL DESCRIPTIONS OF TRNSYS MODELS

This appendix presents the full mathematical descriptions of the TRNSYS models that were used in running simulations. The text has been extracted from the TRNSYS User Manual – Volume 5.

B.1. Nomenclature

Symbol	***Units***	***Description***
A	[m²]	Total collector array aperture or gross area (consistent with $F_R(\tau\alpha)$,F_RU_L, $F_RU_{L/T}$ and G_{test})
a_0	-	Intercept (maximum) of the collector efficiency (Equation B.13)
a_1	[kJ/h-m²-K]	Negative of the first-order coefficient in collector efficiency equation
a_2	[kJ/h-m²-K²]	Negative of the second-order coefficient in collector efficiency equation
A_a	[m²]	Aperture area of a single collector module
A_r	[m²]	Absorber area of a single collector module
b_0	-	Negative of the 1st-order coefficient in the Incident Angle Modifier curvefit equation (Equation B.13)
b_1	-	Negative of the 2nd-order coefficient in the IAM curve fit equation
C_{min}	[kJ/h-K]	Minimum capacitance rate (mass flow times specific heat) of heat exchanger flow streams
C_{pf}	[kJ/kg-K]	Specific heat of collector fluid
d_H	[m]	Diameter of collector headers
d_i, d_o	[m]	Diameter of collector inlet and outlet pipes
d_R	[m]	Diameter of collector risers
f	-	Friction factor for flow in pipes
F_{av}	-	Modified value of F_R when the efficiency is given in terms of T_{av}, not T_i
F_o	-	Modified value of F_R when the efficiency is given in terms of T_o, not T_i
F_R	-	Overall collector heat removal efficiency factor
$F_R(\tau\alpha)$	-	Intercept efficiency corrected for non-normal incidence
$F_R(\tau\alpha)_n$	-	Intercept of the collector efficiency versus $(T_{ci} - T_a)/IT$ curve
F_RU_L	-	Slope of the collector efficiency versus $(T_{ci} - T_a)/IT$ curve
$F'U_L$	-	Product of the collector efficiency factor, F', and heat loss coefficient, U_L
g	[m/s²]	Gravitational constant
G	[kg/hr.m²]	Collector flow rate per unit area
G_{test}	[kg/hr.m²]	Collector flow rate per unit area at test conditions at which F_RU_L and $F_R(\tau\alpha)_n$ were determined

H_a	[m]	Height of auxiliary heater above bottom of tank
H_c	[m]	Vertical distance between outlet and inlet of collectors
h_{Li}	-	Frictional head loss in the piping
H_o	[m]	Vertical distance between outlet of tank and inlet to collector
H_R	[m]	Height of collector return above bottom of tank
H_r	[m]	Height of entry of hot stream (above bottom of tank)
H_t	[m]	Height of tank
H_t	[m]	Height of tank
H_{th}	[m]	Height of auxiliary thermostat above bottom of tank
I	[kJ/h-m²]	Global (total) horizontal radiation
I_{bT}	[kJ/h-m²]	Beam radiation incident on the solar collector
I_d	[kJ/h-m²]	Diffuse horizontal radiation
Ig	[kJ/h-m²]	Diffuse reflected ground radiation per unit area
I_T	[kJ/h-m²]	Global radiation incident on the solar collector (Tilted surface)
k	[kJ/hr.m.K]	Thermal conductivity
k_i, k_o	-	Number of velocity heads lost by flow in bends, tees, and restrictions of inlet and outlet piping
k_w	[kJ/hr.m.K]	Effective thermal conductivity of water and tank
L_h	[m]	Length of collector headers
L_i, L_o	[m]	Length of inlet and outlet piping
LU	-	Fortran logical unit containing collector frictional head loss data
m_h	[kg/hr]	Mass flow rate of hot stream entering tank
m_L	[kg/hr]	Load flow rate
N_{B1},N_{B2}	-	Number of equivalent right angle bends in inlet and outlet connecting pipes
NDATA	-	Number of lines of data in LU
N_R	-	Number of parallel collector risers
N_S	-	Number of identical collectors in series
N_x	-	Number of equal sized collector nodes
Q_{aux}	[kJ/hr]	Rate of auxiliary energy input to tank
Q_{env}	[kJ/hr]	Rate of energy loss from tank
Q_{he}	[kJ/hr]	Maximum rate of energy input to tank by auxiliary
Q_{in}	[kJ/hr]	Rate of energy input to tank from hot fluid stream
Q_{sup}	[kJ/hr]	Rate of energy supplied to load by tank
Q_u	[kJ/hr]	Rate of useful energy collection
r	-	Ratio of collector heat removal efficiency factor, FR, to the value at test conditions
Re	-	Reynolds number for flow in pipes
ri	-	Ratio of insulation thickness (see Parameter 33 description)
r_i	-	Ratio of insulation thickness of top to sides of upright tanks or top to bottom insulation ratio for horizontal tanks
T	[°C]	Average tank temperature

T_a	[°C]	Ambient (air) temperature
Ta	[°C]	Ambient temperature
T_{av}	[°C]	Average collector fluid temperature
Tci	[°C]	Collector inlet temperature
Tck	[°C]	Temperature of k^{th} node in collector
Tco	[°C]	Collector outlet temperature
T_D	[°C]	Temperature of water delivered by tank to load
T_{env}	[°C]	Environmental temperature for losses
Th	[°C]	Temperature of hot fluid entering tank
T_i	[°C]	Inlet temperature of fluid to collector
Ti	[°C]	Temperature of i^{th} segment
T_I	[°C]	Initial temperature of preheat portion of tank
T_L	[°C]	Temperature of load stream entering tank
T_o	[°C]	Outlet temperature of fluid from collector
T_p	[°C]	Average temperature of fluid in a pipe
T_{pi}	[°C]	Temperature of inlet fluid to pipe
T_{po}	[°C]	Pipe outlet fluid temperature
T_R	[°C]	Temperature of fluid return to heat source
T_{set}	[°C]	Thermostat set temperature
UA	[kJ/hr.K]	Overall UA value of tank
U_i, U_o	[kJ/hr.m^2.K]	Loss coefficients for inlet and outlet pipes (based on pipe surface area)
U_L	[kJ/h.m².K]	Overall thermal loss coefficient of the collector per unit area
$U_{L/T}$	[kJ/h.m².K²]	Thermal loss coefficient dependency on T (see Equation B.5)
v	[m/s]	Velocity of fluid in pipes
Vh	[m/s]	Velocity of fluid at entry to inlet header and at exit of outlet header
Vh	[m^3]	Volume of fluid entering tank from heat source over a time interval Δt
Vi	[m^3]	Volume of i^{th} segment
VL	[m^3]	Volume of fluid entering tank from load over a time interval Δt
Vt	[m^3]	Tank volume
γ_{htr}	-	Optional control function input (0 to 1) that disables or enables auxiliary heater
ΔE	[kJ]	Change in internal energy storage
Δt	[s]	Simulation time step
ΔT_{db}	[˚C]	Thermostat temperature dead band
ρ	[kg/m^3]	Fluid density
$\dot{m}_{test}$	[kg/h]	Flow rate at test conditions
$\dot{m}$	[kg/h]	Flow rate at use conditions
α	-	Short-wave absorptance of the absorber plate
β	[°]	Collector slope above the horizontal plane
θ	[°]	Incidence angle for beam radiation
τ	-	Short-wave transmittance of the collector cover(s)

β	-	Collector slope measured from horizontal
$(\tau\alpha)$	-	Product of the cover transmittance and the absorber absorptance
$(\tau\alpha)_b$	-	$(\tau\alpha)$ for beam radiation (depends on the incidence angle θ)
$(\tau\alpha)_g$	-	$(\tau\alpha)$ for ground reflected radiation
$(\tau\alpha)_n$	-	$(\tau\alpha)$ at normal incidence
$(\tau\alpha)_s$	-	$(\tau\alpha)$ for sky diffuse radiation
ρg	-	Ground reflectance
ρ_s	[kg/m^3]	Density of working fluid at standard conditions
$(UA)_f$	[kJ/hr.K]	Overall conductance for heat loss to flue of gas heater
$(UA)_p$	[kJ/hr.K]	Conductance for heat loss from pipes
ρ_i	[kg/m^3]	Density of ith node
Δh_i	[m]	Height of the ith node
ΔP_h	[Pa]	Pressure change across collector inlet and outlet headers
ΔP_i	[Pa]	Change in pressure across the ith node
$\frac{(\tau\alpha)}{(\tau\alpha)_n}, \frac{(\tau\alpha)_b}{(\tau\alpha)_n}, \frac{(\tau\alpha)_s}{(\tau\alpha)_n}, \frac{(\tau\alpha)_g}{(\tau\alpha)_n}$		Incidence angle modifiers for total, beam, sky diffuse and ground diffuse radiation

B.2. Type1: Flat-Plate Collector (Quadratic Efficiency)

This component models the thermal performance of a variety of collector types using theory. The total collector array may consist of collectors connected in series and in parallel. The thermal performance of the total collector array is determined by the number of modules in series and the characteristics of each module. The user must provide results from standard tests of efficiency versus a ratio of fluid temperature minus ambient temperature to radiation ($\Delta T/IT$). The fluid temperature may be an inlet, average, or outlet temperature. The model assumes that the efficiency vs. $\Delta T/IT$ curve can be modelled as a quadratic equation. Corrections are applied to the slope, intercept, and curvature parameters to account for the presence of a heat exchanger, identical collectors in series, and flow rates other than those at test conditions.

There are four possibilities for considering the effects of off-normal solar incidence. Optical modes 2 and 3 require test data for single-axis incidence angle modifiers. Optical mode 4 determines modifiers from properties of the covers. In the fifth optical mode, the user must enter bi-axial incidence angle modifier data. This is useful for considering non-optically

symmetric collectors such as evacuated tubes, etc. If the optical mode is set to 1, no off-normal incidence effects are considered.

B.2.1. MATHEMATICAL DESCRIPTION

A general equation for solar thermal collector efficiency can be obtained from the Hottel - Whillier equation [[5]] as:

$$\eta = \frac{Q_U}{AI_T} = \frac{\dot{m}C_{pf}(T_o - T_i)}{AI_T} = F_R(\tau\alpha)_n - F_R U_L \frac{(T_i - T_{a)}}{I_T} \quad \text{(B.1)}$$

The loss coefficient U_L is not exactly constant, so a better expression is obtained by taking into account a linear dependency of U_L versus $(T_i - T_a)$:

$$\eta = \frac{Q_U}{AI_T} = F_R(\tau\alpha)_n - F_R U_L \frac{(T_i - T_a)}{I_T} - F_R U_{L/T} \frac{(T_i - T_a)^2}{I_T} \quad \text{(B.2)}$$

Equation B.2 can be rewritten as:

$$\eta = a_0 - a_1 \frac{(\Delta T)}{I_T} - a_2 \frac{(\Delta T)^2}{I_T} \quad \text{(B.3)}$$

Which is the general solar collector thermal efficiency equation used in Type 1. The thermal efficiency is defined by 3 parameters: a_0, a_1 and a_2. Those 3 parameters are available for collectors tested according to ASHRAE standards and rated by SRCC [[1], [2]], as well as for collectors tested according to the recent European Standards on solar collectors [[3]]. Many examples of collector parameters can be found on the internet (e.g. [[4]]).

Note: It is important to make sure that collector area entered as a parameter matches the area used when determining the values of a_0, a_1 and a_2. Typically, efficiency curves are provided for gross area in the US and aperture area in Europe

In Equation B.3, ΔT is equal to $(T_i - T_a)$. Collector test reports sometimes provide the efficiency curve using a different temperature difference:

$$\Delta T = \begin{cases} \Delta T_i = T_i - T_a \\ \Delta T_{av} = T_{av} - T_a \\ \Delta T_o = T_o - T_a \end{cases} \quad \text{(B.4)}$$

The 1st formulation is usually preferred in the US, while the 2nd one is used in most European documents. Equation B.2 can use any of those definitions of the temperature difference and the user can specify the a_0, a_1 and a_2 coefficients using any of the definitions. If the coefficients are given in terms of the average or the outlet temperature, correction factors are applied. Those correction factors have been derived for linear efficiency curves (Equation. B.1), so Equation. B.2 must first be converted to that form by performing some manipulations. A modified first-order collector efficiency coefficient is defined:

$$U'_L = U_L + U_{L/T}(T_i - T_a) \quad \text{(B.5)}$$

Which gives:

$$\eta = \frac{Q_U}{AI_T} = F_R(\tau\alpha)_n - F_R U'_L \frac{(T_i - T_a)}{I_T} \quad \text{(B.6)}$$

The correction factors are then given by [[5]]:

$$\left.\begin{aligned} F_R(\tau\alpha) &= F_{av}(\tau\alpha)_n \left(\frac{\dot{m}_{test} c_{pf}}{\dot{m}_{test} c_{pf} + \frac{F_{av} U'_L}{2}} \right) \\ \text{AND} \\ F_R U'_L &= F_{av} U'_L \left(\frac{\dot{m}_{test} c_{pf}}{\dot{m}_{test} c_{pf} + \frac{F_{av} U'_L}{2}} \right) \end{aligned}\right\} \quad \text{(B.7)}$$

$$\left.\begin{aligned} F_R(\tau\alpha) &= F_o(\tau\alpha)_n\left(\frac{\dot{m}_{test}c_{pf}}{\dot{m}_{test}c_{pf}+F_oU'_L}\right) \\ &\text{AND} \\ F_RU'_L &= F_oU'_L\left(\frac{\dot{m}_{test}c_{pf}}{\dot{m}_{test}c_{pf}+F_oU'_L}\right) \end{aligned}\right\} \quad \text{(B.8)}$$

B.2.2. CORRECTIONS TO THE IDEAL EFFICIENCY CURVE

Analytical corrections are applied to the collector parameters to account for:

- Operation at flow rates other than the value at test conditions
- Ns identical collectors mounted in series
- Non-normal solar incidence

These modifications are outlined in [[5]] and summarized as follows.

B.2.2.1. Flow Rate Correction

In order to account for conditions when the collector is operated at a flow rate other than the value at which it was tested, both $F_R\,(\tau\alpha)_n$ and F_RU_L' are corrected to account for changes in F_R. The ratio, r_1, by which they are corrected, is given by:

$$r_1 = \frac{F_RU'_L\,|_{use}}{F_RU'_L\,|_{test}} = \frac{F_R(\tau\alpha)_n\,|_{use}}{F_R(\tau\alpha)_n\,|_{test}} = \frac{\dfrac{\dot{m}C_{pf}}{AF'U_L}\left(1-e^{-AF'U_L/\dot{m}C_{pf}}\right)|_{use}}{\dfrac{\dot{m}C_{pf}}{AF'U_L}\left(1-e^{-AF'U_L/\dot{m}C_{pf}}\right)|_{test}} \quad \text{(B.9)}$$

To use this equation, it is necessary to estimate $F'U_L$. That quantity can be calculated from the test conditions:

$$F'U_L = -\frac{\dot{m}C_{pf}}{A}\ln\left(1-\frac{F_R U'_L A}{\dot{m}C_{pf}}\right) \tag{B.10}$$

For liquid collectors, $F'U_L$ calculated from the test conditions is approximately equal to $F'U_L$ at use conditions and can be used in both the numerator and denominator of Equation. B.9.

B.2.2.2. Series Collectors

Both FR $(\tau\alpha)_n$ and F_RU_L' are analytically modified to account for identical collectors mounted in series. The ratio, r_2, by which they are corrected, is:

$$r_2 = \frac{1-\left(1-\frac{AF_RU'_L}{\dot{m}C_{pf}}\right)^{N_s}}{N_s\frac{AF_RU'_L}{\dot{m}C_{pf}}} \tag{B.11}$$

B.2.2.3. Incidence Angle Modifier (IAM)

Collector tests are generally performed on clear days at normal incidence so that the transmittance - absorptance product $(\tau\alpha)$ is nearly the normal incidence value for beam radiation, $(\tau\alpha)_n$. The intercept efficiency, $F_R(\tau\alpha)_n$, is corrected for non-normal solar incidence by the factor $(\tau\alpha)/(\tau\alpha)_n$. By definition, $(\tau\alpha)$ is the ratio of the total absorbed radiation to the incident radiation. Thus, a general expression for $(\tau\alpha)/(\tau\alpha)_n$ is:

$$\frac{(\tau\alpha)_b}{(\tau\alpha)_n} = \frac{I_{bT}\frac{(\tau\alpha)_b}{(\tau\alpha)_n} + I_d\left(\frac{1+\cos\beta}{2}\right)\frac{(\tau\alpha)_d}{(\tau\alpha)_n} + \rho_g I\left(\frac{1-\cos\beta}{2}\right)\frac{(\tau\alpha)_g}{(\tau\alpha)_n}}{I_T} \tag{B.12}$$

For flat-plate collectors, $(\tau\alpha)_b/(\tau\alpha)_n$ can be approximated from ASHRAE test results [[1]] as:

$$\frac{(\tau\alpha)_b}{(\tau\alpha)_n} = 1 - b_0\left(\frac{1}{\cos\theta} - 1\right) - b_1\left(\frac{1}{\cos\theta} - 1\right)^2 \quad \text{(B.13)}$$

Note: Some collector tests only provide the IAM value at one incidence angle, typically 50°. In such case, it is recommended to use Optical Mode 2, assume that $b_1 = 0$ and calculate b_0 using Equation B.3.

B.2.2.4. Type 1 Optical Modes

5 optical modes can be selected to Input the IAM data:

- Optical mode 1: perfect IAM $(\tau\alpha)/(\tau\alpha)_n=1$ for any incidence angle
- Optical mode 2: the user specifies the values of b_0 and b_1 in Equation B.13.
- Optical mode 3: values of $(\tau\alpha)_b/(\tau\alpha)_n$ versus θ are supplied in an external data file but the collector is assumed to be symmetrical so only one direction is provided in the data file (see here below).
- Optical mode 4: the function routine TAU_ALPHA (see Volume 08, Programmer's guide) is used to estimate incidence angle modifiers for beam radiation in terms of incidence angle and cover properties.
- Optical mode 5: values of $(\tau\alpha)_b/ (\tau\alpha)_n$ versus θ are supplied in an external data file for both the longitudinal and transversal directions (see here below). Note that this mode is usually used to simulate evacuated collectors, for which it is recommended to use Type 71.

The incidence angle modifiers for both sky, $(\tau\alpha)_s/ (\tau\alpha)_n$, and ground diffuse, $(\tau\alpha)_g/ (\tau\alpha)_n$, are determined in modes 2-4 by defining equivalent incidence angles for beam radiation that give the same transmittance as for diffuse radiation [[5]]. The effective incidence angles for sky diffuse and ground reflected radiations are:

$$\theta_{sky} = 59.68 - 0.1388\ \beta + 0.001497\ \beta^2 \quad \text{(in degrees)} \quad \text{(B.14)}$$

$$\theta_{gnd} = 90.00 - 0.5788\ \beta + 0.002693\ \beta^2 \quad \text{(in degrees)} \quad \text{(B.15)}$$

B.2.3. EXTERNAL DATA FILES

Type 1 can optionally read the incidence angle modifier (IAM) data from an external data file. These data are read and interpolated by subroutine DYNAMICDATA (See Volume 08, Programmer's Guide). The data consists of between 2 and 10 values of incidence angles and modifiers. This section will only describe the data file used in Optical Mode 3. Optical Mode 5 (bi-directional IAM's) is typically used for evacuated tube collectors, for which it is recommended to use Type 71. The data file used in Optical Mode 5 is the same as the data file used by Type 71.

B.2.3.1. Data File For Optical Mode 3

Type 1 optionally reads the IAM values from a data file. An example is provided in "Examples\Data Files". The data file format is as follows ($2 \leq Na \leq 10$):

```
<Incidence angle 1> <Incidence angle 2> etc.            Na values [0; 90]
<IAM 1>                                                 IAM for angle  1
<IAM 2>                                                 IAM for angle  1
…
<IAM Na>                                                IAM for angle  Na
```

The principle of the data file is that the first line gives the values of the independent variable (incident angle) that will be used in the "IAM map". Then the dependent variable (IAM) is provided for all values of the independent variable. Data are read in free format.

Example

```
   0     10   20   30   40   50   60   70   80   90   ! Angle values
1.000               ! IAM for incident angle     1 ( 0)
0.997               ! IAM for incident angle     2 (10)
0.988               ! IAM for incident angle     3 (20)
…
0.644               ! IAM for incident angle     8 (70)
0.120               ! IAM for incident angle     9 (80)
0.000               ! IAM for incident angle    10 (90)
```

B.3. Type 45: Thermosyphon Collector with Integral Collector Storage

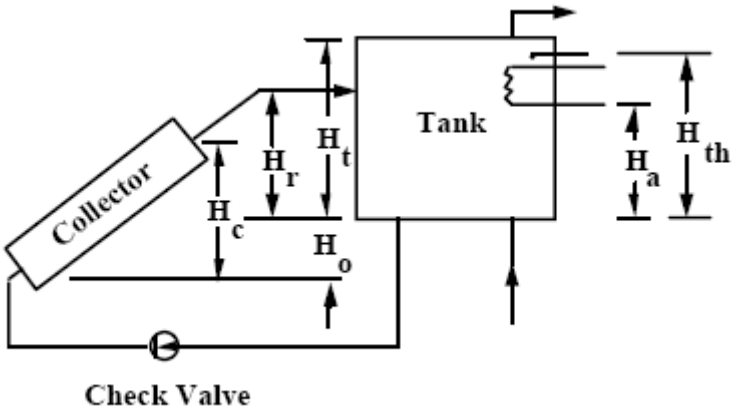

Figure B.1: Thermosyphon System Schematic

This component models the thermosyphon system depicted in Figure B.1. The system consists of a flat-plate solar collector, a stratified storage tank (either vertical or horizontal cylinder), and a check valve to prevent reverse flow, and water as the working fluid. Flow in the loop is assumed to be steady state. The system is analyzed by dividing the thermosyphon loop into a number of segments normal to the flow direction and applying Bernoulli's equation for incompressible flow to each segment. The flow rate is obtained by numerical solution of the resulting set of equations. The stratification in the storage tank is modeled using the Type 38 Algebraic tank component. The advantage of the Type 38 model over fixed node models (Type 4) is that large simulation time steps can be used. A time step of 1 hour in the Type 38 tank model is sufficient for many stratified tank systems, whereas simulation time steps of a few minutes are necessary in a Type 4 model with a large number of fixed nodes

B.3.1. MATHEMATICAL DESCRIPTION

Application of Bernoulli's equation to any node, i, in the thermosyphon loop results in the following expression for pressure drop:

$$\Delta P_i = \rho_i g \Delta h_i + \rho_i g h_{Li} \tag{B.16}$$

At any instant of the time, the sum of the pressure changes around the loop is zero:

$$\sum_{i=1}^{i=N} \rho_i \Delta h_i = \sum_{i=1}^{i=N} \rho_i h_{Li} \tag{B.17}$$

The thermosiphon model involves the numerical solution for the flow rate that satisfies the above equation. The density of the fluid is evaluated at the local temperature using a correlation for water. Temperatures and frictional head losses in each node of the collector and pipes are determined as described below.

The collector inlet and outlet pipes are each considered to be single nodes, with negligible thermal capacitance.

A first law analysis yields the following expressions for average and outlet temperatures of these pipes:

$$\overline{T}_p = T_a + (T_{pi} - T_a) \cdot \frac{\dot{m} C_p}{(UA)_p} \cdot \left(1 - \exp\left(- \frac{(UA)_p}{\dot{m} C_p} \right) \right) \tag{B.18}$$

$$T_{po} = T_a + (T_{pi} - T_a) \cdot \exp\left(- \frac{(UA)_p}{\dot{m} C_p} \right) \tag{B.19}$$

B.3.1.1. Friction Head Loss

Frictional head loss in either pipe is given as:

$$H_p = \frac{fLv^2}{2d} + \frac{kv^2}{2} \tag{B.20}$$

where the friction factor, f, is

f = 64/ Re for Re $\leq$ 2000

f = 0.032 for Re > 2000

A correction is also applied to allow for the additional friction due to developing flow in the connecting pipes [[7]].

The program can evaluate the collector pressure drop or pressure drop versus flow rate for the collector (and a check value etc.) can be entered as a data file. Friction pressure drop versus flow rate data entered by the user is not adjusted to allow for the variation of water viscosity with temperature. The friction head in each section of the thermosyphon loop is evaluated as follows.

1. Entry from tank to connecting pipe to collector
   k = .5
2. Developing flow in the connecting pipes (and collector risers if collector pressure drop versus flow rate data is not specified) [[7]].
   f = f [1 + .038/(L/Re/d).964]
3. Losses due to bends in connecting pipes
   a. Right angle bend
      Equivalent length of pipe increased by 30 d for Re ≤ 2000
      Or k = 1.0 for Re ≥ 2000
   b. 45° bend
      Equivalent length at pipe increased by 20 d for Re ≤ 2000
      Or k = 0.6 for Re > 2000
4. Cross section change at junction of connecting pipes and header (and riser entry and exit to header if collector friction data is not specified)
   a. Sudden Expansion
      $k = 0.667 (D_1/D_2)^4 - 2.667 (D_1/D_2)^2 + 2.0$
   b. Sudden Contraction
      $k = -0.3259 (D_2/D_1)^4 - 0.1784 (D_2/D_1)^2 + 0.5$

   where D_1 = inlet diameter, D_2 = outlet diameter
5. Collector header pressure drop (if collector friction data is not specified) - average of pressure change along inlet and outlet headers for equal mass flow in each riser:

$$S_1 = \sum_{i=1}^{N_R} \frac{N_R - i + 1}{N_R^2} \tag{B.21}$$

$$S_2 = \sum_{i=1}^{N_R} \frac{N_R - i + 1}{N_R^2} \tag{B.22}$$

$$A_{11} = \frac{fL_h V_h^2}{2d_h} \tag{B.23}$$

where f = 64/Re with Re based on inlet header velocity and temperature

A12 = A11 with f = 64/Re (B.24)

Based on outlet header, velocity and temperature;

$$A_2 = \frac{\rho V_h^2}{2} \tag{B.25}$$

$$P_h = (-S_1 A_{11} + 2(S_2 A_2) + S_1 A_{12})^{/2} \tag{B.26}$$

6. Loss at entry of flow into tank

k = 1

Friction head loss in the tank is neglected. If pressure drop versus flow rate data for the collector (and check value etc.) is entered via an external file, the program only evaluates friction loss in the connecting pipes, connections to the tank and bends.

If pressure drop versus flow rate data are supplied, they are read and interpolated by subroutine DYNAMICDATA (See Volume 08, Programmer's Guide). The data consist of between 2 and 10 values of flow rate and head loss (meters of water). All values of flow rate are listed first, in increasing order, followed by values of pressure drop (free format) loss in meters of water. For numerical stability, the first data line should correspond to zero head loss at zero flow rate.

B.3.1.2. Thermosyphon Head

The net weight of fluid in the collector is found by dividing the collector into Nx (user specified) equally sized nodes. The thermal performance is modeled according to the Hottel-Whillier equation [[7]]. The temperature at the midpoint of any collector node, k, is:

$$T_{ck} = T_a + \frac{I_T F_R(\tau\alpha)}{F_R U_L} + \left(T_{ci} - T_a - \frac{I_T F_R(\tau\alpha)}{F_R U_L} \right) \cdot \exp\left[\frac{F'U_L}{G \cdot C_p} \cdot \frac{(k - 1/2)}{N_x} \right] \tag{B.27}$$

The collector parameter $F'U_L$ is calculated from the value of F_RU_L and G at test conditions:

$$F'U_L = -G_{test} \cdot C_p \ln\left(1 - \frac{F_R U_L}{G_{test} C_p} \right) \tag{B.28}$$

This procedure neglects changes in F' and U_L due to changes in the fluid heat transfer coefficient. The parameter $F_R(\tau\alpha)$ is determined from the intercept efficiency at normal incidence $F_R(\tau\alpha)_n$, using an incidence angle modifier, $(\tau\alpha)/(\tau\alpha)_n$. In general,

$$\frac{(\tau\alpha)}{(\tau\alpha)_n} = \frac{I_{bT} \frac{(\tau\alpha)_b}{(\tau\alpha)_n} + I_d \frac{1+\cos\beta}{2} \frac{(\tau\alpha)_s}{(\tau\alpha)_n} + I_g \frac{1-\cos\beta}{2} \frac{(\tau\alpha)_g}{(\tau\alpha)_n}}{I_T} \tag{B.29}$$

The incidence angle modifier for beam radiation is given in terms of incidence angle and a user specified constant, b_0, (ASHRAE 93 test result) as:

$$\frac{(\tau\alpha)_b}{(\tau\alpha)_n} = 1 - b_0 \left(\frac{1}{\cos\theta} - 1 \right) \tag{B.30}$$

For sky and ground diffuse radiation, the incidence angle modifiers are also determined using the above relation but at effective incidence angles as defined by Brandemuehl (2)

The overall useful energy collection is:

$$Q_u = rA_c(F_R(\tau\alpha)I_T - F_R U_L(T_{ci} - T_a)) \tag{B.31}$$

Where:

$$r = \frac{F_R\big|_{use}}{F_R\big|_{test}} = \frac{G\left(1 - \exp\left(-\frac{F'U_L}{GC_p}\right)\right)}{G_{test}\left(1 - \exp\left(-\frac{F'U_L}{G_{test}C_p}\right)\right)} \tag{B.32}$$

From a simple energy balance, the collector outlet temperature is:

$$T_{co} = Q_u / \dot{m}C_p + T_{ci} \tag{B.33}$$

Thermal stratification in the storage tank is modeled using the Type 38 Algebraic Tank component.

B.4. Type 38: Algebraic Tank (Plug-Flow)

This component models the behavior of a temperature stratified storage tank using variable size segments of fluid. The size of segments is governed by the simulation time step, the magnitude of collector and load flow rates, heat losses and auxiliary input. The main advantage over fixed node simulation techniques (e.g. Type 4) is that temperature stratification can be modeled with small segments in the temperature gradient zone without the need to use small simulation time steps to obtain a "good" solution. This model is most appropriate for tanks that exhibit a large degree of stratification.

There are two modes of operation. In mode 1, the tank has fixed inlet positions and the flow mixes with adjacent segments if its temperature is within 1/2 degree. Otherwise a new segment is created and temperature inversions are corrected by mixing appropriate segments above or below the inlets. In mode 2, the tank has variable inlet positions and new segments are inserted at the levels, which produce no temperature inversions. This allows a maximum degree of stratification and is equivalent to the Type 4 model with a large number of nodes.

This "plug-flow" tank model is very similar to the extended SOLSYS model outlined in reference [[6]] with the additional features:

- An optional auxiliary heater subject to temperature and/or time control,
- conduction between segments,
- upright or horizontal cylindrical tanks, and
- different insulation thicknesses on the top and sides of upright tanks or eccentric location of the tank in the insulation jacket for horizontal tanks.

Only one unit of Type 38 can be used per simulation.

B.4.1. MATHEMATICAL DESCRIPTION

Figure B.2 illustrates the concept of this tank model. In this example, the tank is initially divided into four segments of volume V_i and temperature T_i, so that no temperature inversions are present. In one time period, the heat source delivers a volume of liquid, V_h, equal to $\dot{m}_h \Delta t/\rho$ at a temperature T_h. Assuming T_h is greater than T_1, then a new segment is added at the top of the tank and the existing profile is shifted. At the same time, the fluid enters from the load with a volume, V_L, equal to $\dot{m}_l \Delta t/\rho$ and temperature of T_L. If T_L is less than T_4, then a segment is added at the bottom of the tank and the profile is shifted once more. The net shift of the profile in the tank is equal to the difference between the total heat source volume and load volume or $(\dot{m}_h - \dot{m}_l)\Delta t/\rho$. The segments and/or fraction of segments whose positions fall outside the bounds of the tank are returned to the heat source and load. The average temperature delivered to load for the example of Figure B.2 is:

$$T_D = \frac{V_h T_h + (V_L - V_h) T_1}{V_L} \tag{B.34}$$

and the average heat source return temperature, T_R, is equal to T_L. In general, for N segments the average delivery and heat source return temperatures are computed as follows:

If $V_h < V_L$, then

$T_R = T_L$

$$T_D = \frac{\left(V_h T_h + \sum_{i=1}^{k-1} T_i V_i + a\, T_k V_k\right)}{V_L} \tag{B.35}$$

where a and k must satisfy

$0 \leq a \leq 1$

$$V_h + \sum_{i=1}^{k-1} V_i + aV_k = V_L \tag{B.36}$$

If $V_h > V_L$, then

TD = Th

$$T_R = \frac{(V_L T_L + \sum_{i=k+1}^{N} T_i V_i + a\, T_k V_k)}{V_h} \tag{B.37}$$

where a and k must satisfy

$0 \leq a \leq 1$

$$V_L + \sum_{i=k+1}^{N} T_i V_i + a\, T_k V_k = V_h \tag{B.38}$$

In mode 1, the average delivery and heat source return temperatures are computed after the profile has been corrected for temperature inversions. Segments are combined until the equilibrium temperatures result in no temperature inversions. This process begins at each inlet and proceeds in the direction of the inversion.

The optional auxiliary heater is modeled as in the Type 4 component. If necessary, the segment containing the auxiliary is split into two segments at the actual position of the auxiliary. The auxiliary is on if the temperature of the segment containing the thermostat is

either less than T_{set} - Δt_{db} or if the auxiliary was on for the previous time interval and the thermostat temperature is less than T_{set}. The segment containing the auxiliary is heated first, until it reaches the temperature of the segment above. These two segments are then heated together until they reach the temperature of the segment above them. This process continues until either the maximum heater input is used or the set temperature is reached. If a load flow is occurring and auxiliary is able to heat the top segment, then the delivered fluid is heated with a linear temperature profile.

Storage losses from the tank and conduction between segments are evaluated before the temperature profile has been adjusted for flows and auxiliary heat input. This is accomplished by solving the following differential equation for each segment:

$$\rho C_p V_i \frac{dT_i}{dt} = -(UA)_i(T_i - T_{env}) + (kA)_{i-1}\frac{(T_{i-1} - T_i)}{\Delta h_{i-1}} - (kA)_i\frac{(T_i - T_{i+1})}{\Delta h_{i+1}} \quad \text{(B.39)}$$

where Δh_{i-1} = separation between centers of segments i-1 and i, and Δh_{i+1} = separation between centers of segments i and i+1.

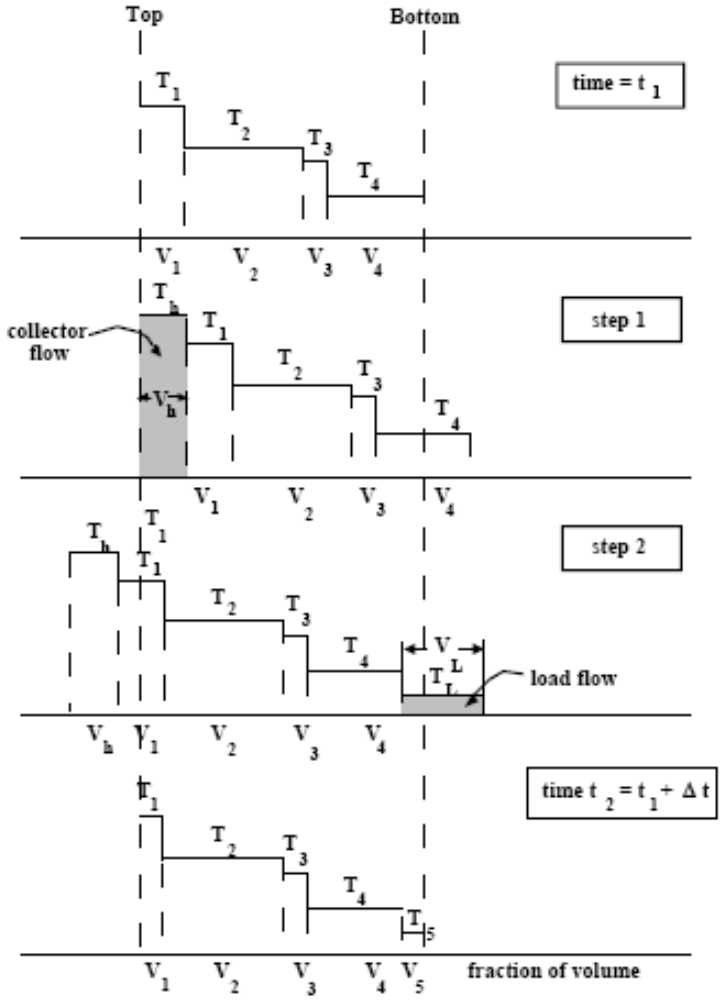

Figure B.2: Example of the Extended SOLSYS SYSTEM (adapted from [[6]])

When conduction is included, the set of coupled differential equations is solved by successive substitution. Conduction down the walls of the tank can be included by using an effective conductivity.

The overall conductance for heat loss from any segment, (UA)i depends upon its surface area and a user-supplied overall loss conductance UA. In addition an optional conductance for heat loss to a gas heater flue when the auxiliary is not operating can also be specified.

The total loss from the tank is:

$$\dot{Q}_{env} = \sum_{i=1}^{N} (UA)_i (T_i - T_{env}) \qquad \text{(B.40)}$$

The energy input to the tank due to the hot inlet stream is

$$\dot{Q}_{in} = \dot{m}C_p(T_h - T_R) \tag{B.41}$$

The energy supplied to the load is

$$Q_{sup} = m_L C_p(T_D - T_L) \tag{B.42}$$

The change in internal energy of storage is

$$\Delta E = \rho C_p \left(\sum_{i=1}^{N} V_i T_i - \sum_{i=1}^{N} V_i T_i \Big|_{t=TIME0} \right) \tag{B.43}$$

B.5. References

[1] ASHRAE, 2003 - Standard 93-2003: Methods of testing to determine the performance of solar collectors, ASHRAE, Atlanta

[2] Solar Rating and Certification Corporation, 1995. SRCC Standard 100. Test Methods and Minimum Standards for Certifying Solar Collectors. Available on www.solar-ratings.org

[3] CEN, 2001. EN 12975-2:2001. Thermal solar systems and components - Solar collectors - Part 2: Test methods. European Committee for Standardization, Brussels, Belgium. (www.cenorm.be)

[4] SPF, 2004 - Institut für Solartechnik SPF, online collector test reports on www.spf.ch

[5] Duffie J.A. and Beckman W.A., 1991. Solar Engineering of Thermal Processes - Second Edition, Wiley-Interscience, New York

[6] Kuhn, J.K. VanFuchs, G.F., and Zob, A.P., "Developing and Upgrading of Solar System Thermal Energy Storage Simulation Models," Draft Report for DOE, Boeing Computer Services Company, August 31 (1980).

[7] Morrison, G. L. and D. B. J. Ranatunga. 1980. Thermosyphon Circulation in Solar Collectors. Solar Energy. Vol. 24, pp. 191-198.

APPENDIX C

C. SIMULATION RESULTS FOR OTHER CITIES

This appendix presents the simulation results for Port Elizabeth, Pretoria, Pietermaritzburg, Bloemfontein, Kimberley, Upington, Polokwane, Nelspruit and Mmabatho.

C.1. Port Elizabeth

Port Elizabeth is located on the south-western coast of South Africa (33˚58'S, 25˚36'E, 38m Above Sea Level), and it experiences a subtropical climate. The simulation results for an EDHW system and SDHW system located in this region are presented below.

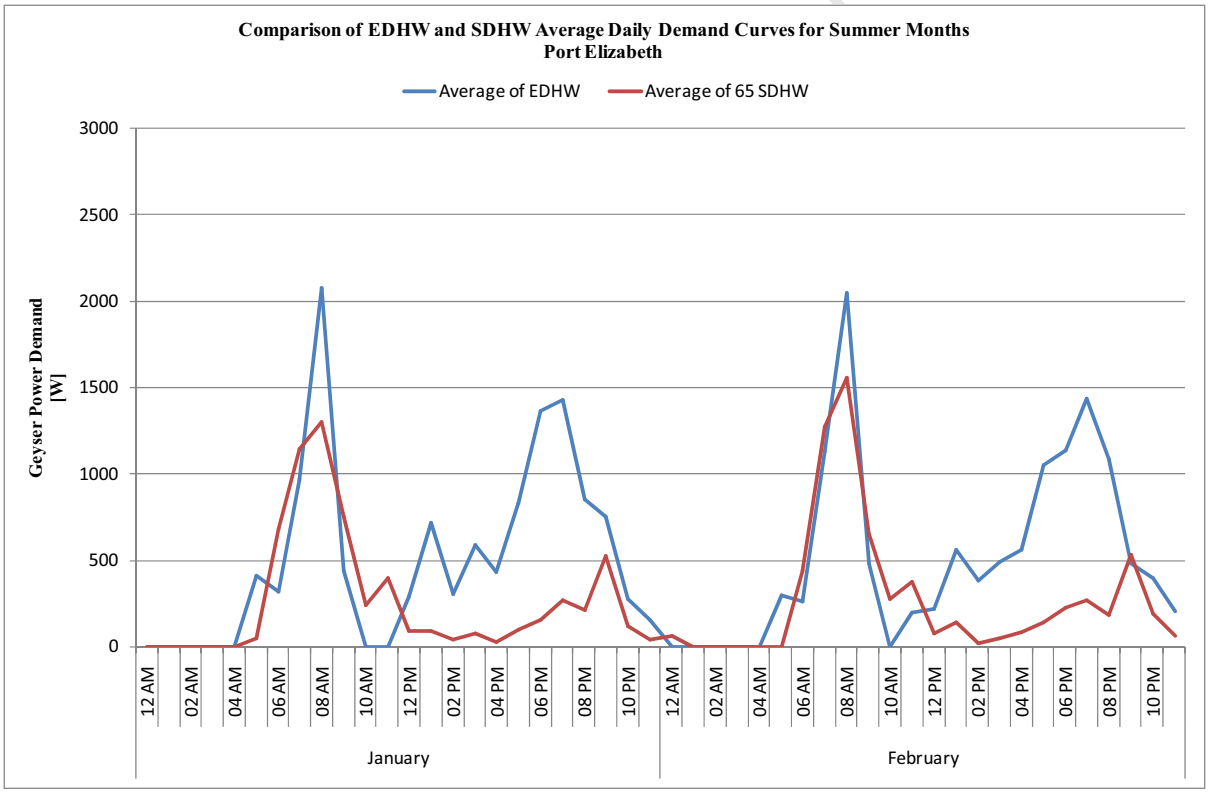

Figure C.1: Comparison of EDHW and SDHW Average Daily Demand Curves for Summer Months in Port Elizabeth

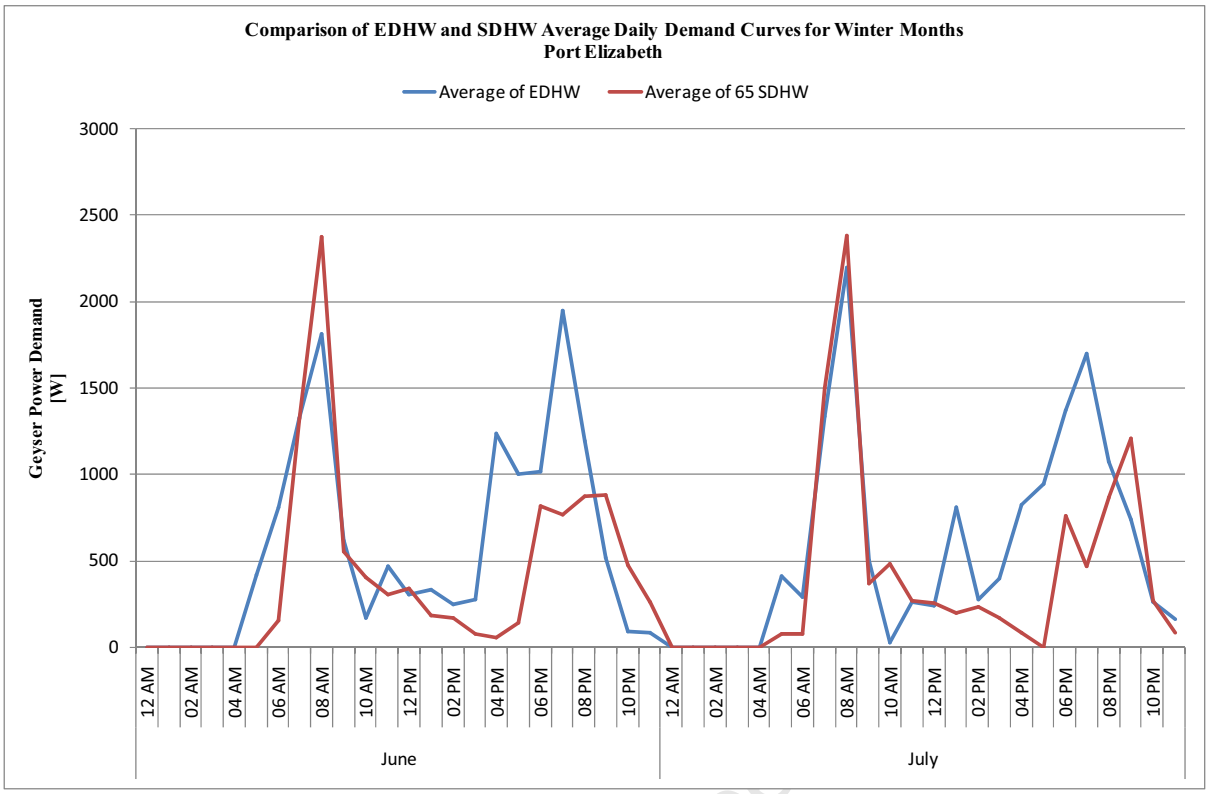

Figure C.2: Comparison of EDHW and SDHW Average Daily Demand Curves for Winter Months in Port Elizabeth

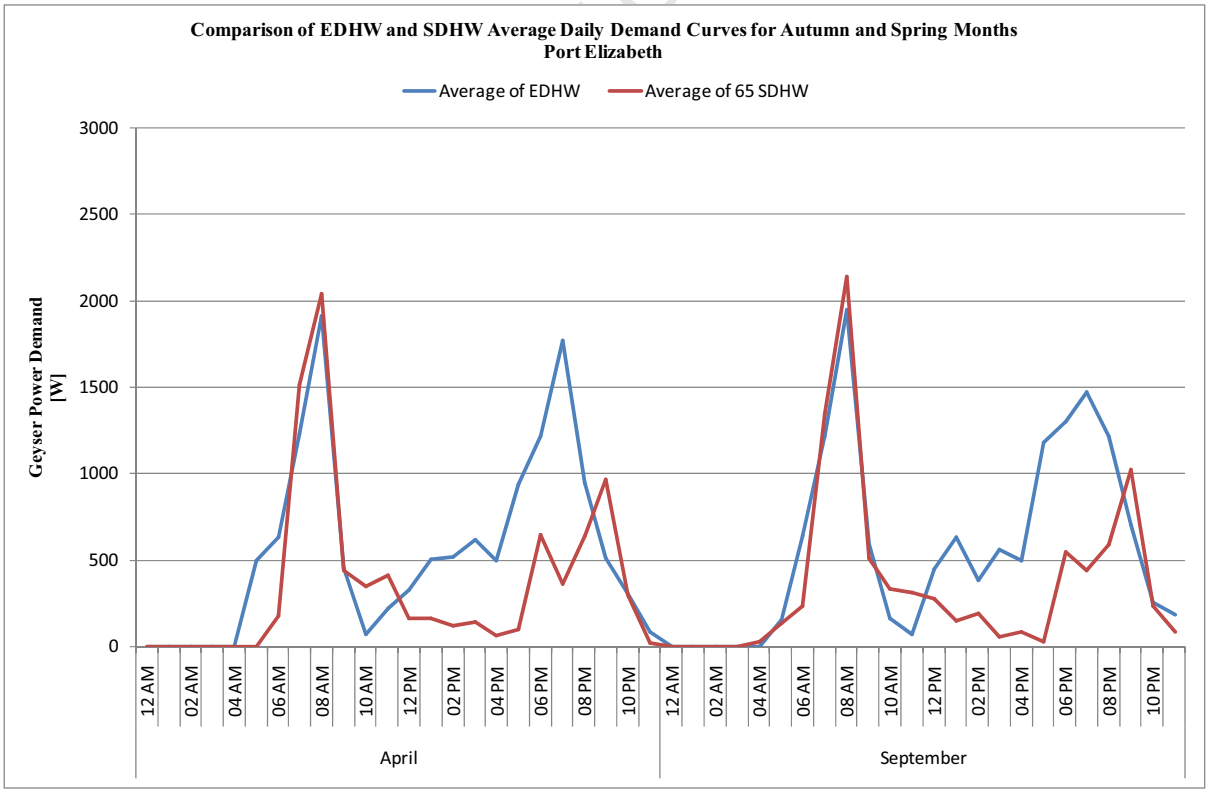

Figure C.3: Comparison of EDHW and SDHW Average Daily Demand Curves for Autumn and Spring Months in Port Elizabeth

C.2. Pretoria

Pretoria is located in the Highveld (25˚45'S, 28˚12'E, 1402m Above Sea Level), and it experiences a dry, sunny climate all year round. The simulation results for an EDHW system and SDHW system located in this region are presented below.

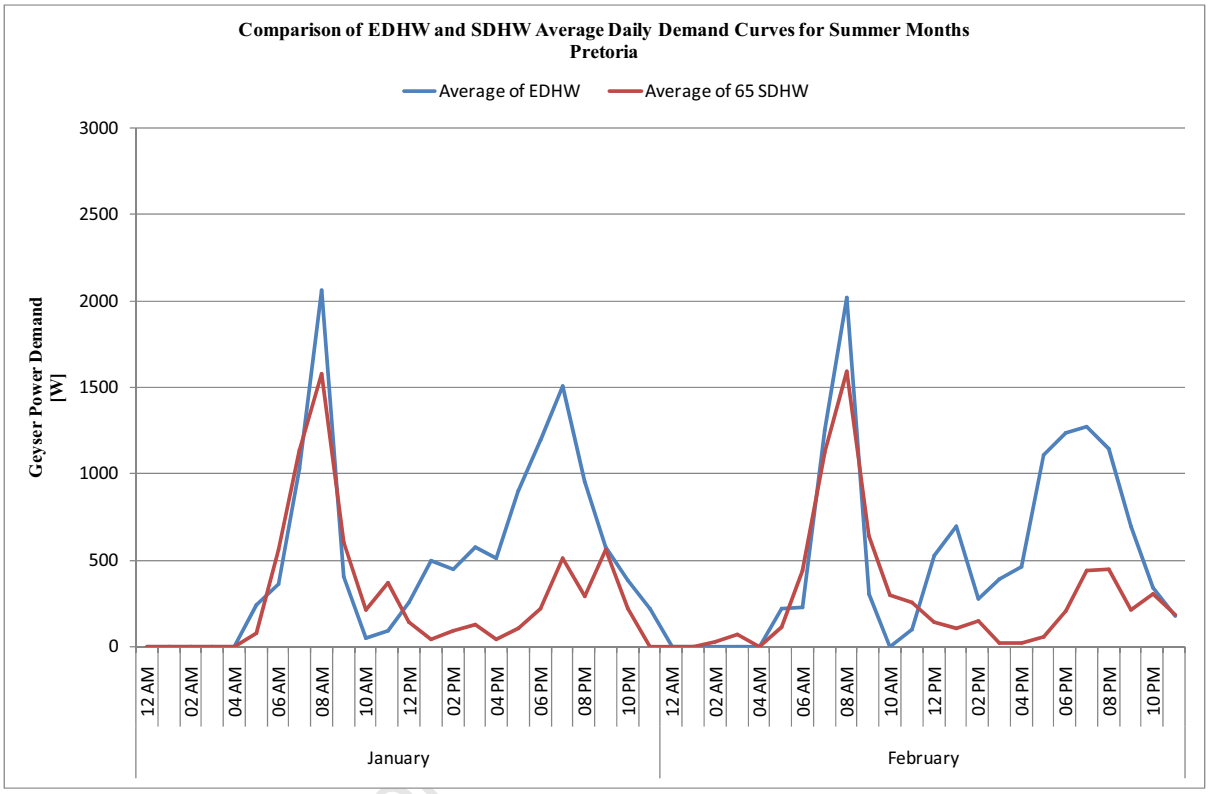

Figure C.4: Comparison of EDHW and SDHW Average Daily Demand Curves for Summer Months in Pretoria

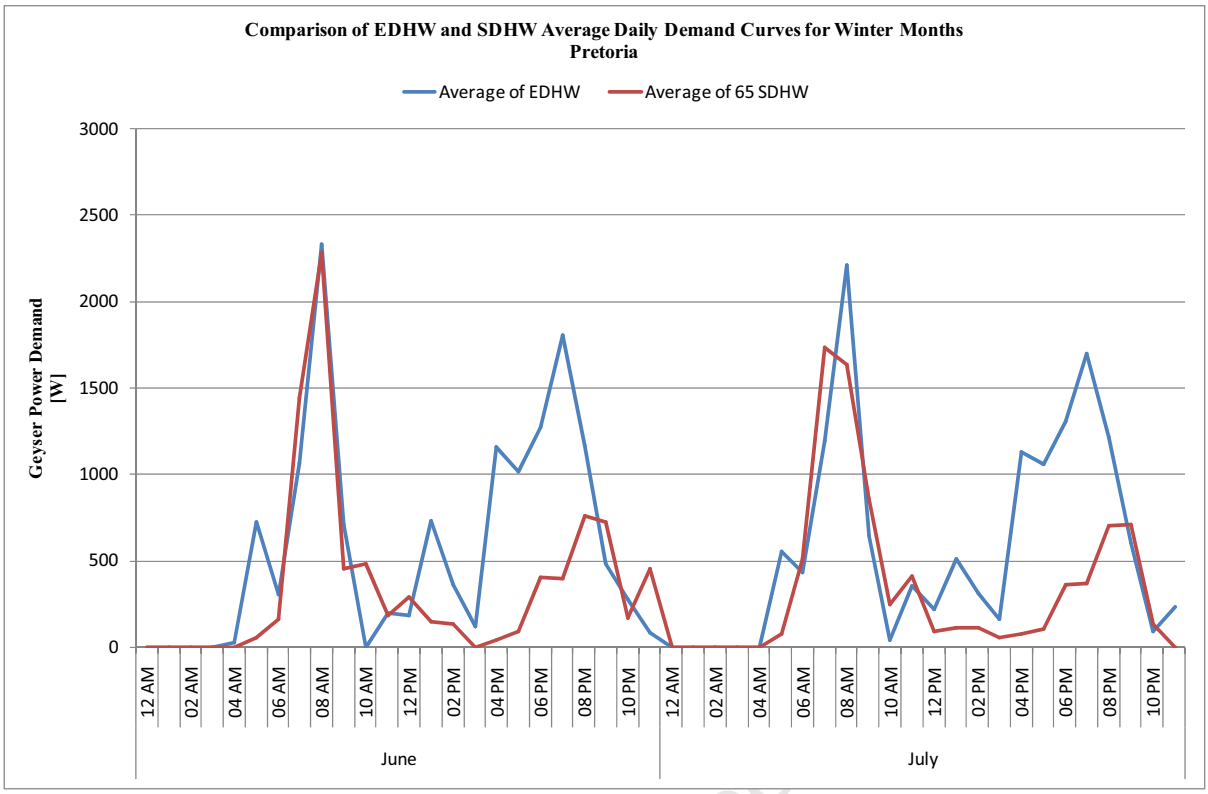

Figure C.5: Comparison of EDHW and SDHW Average Daily Demand Curves for Winer Months in Pretoria

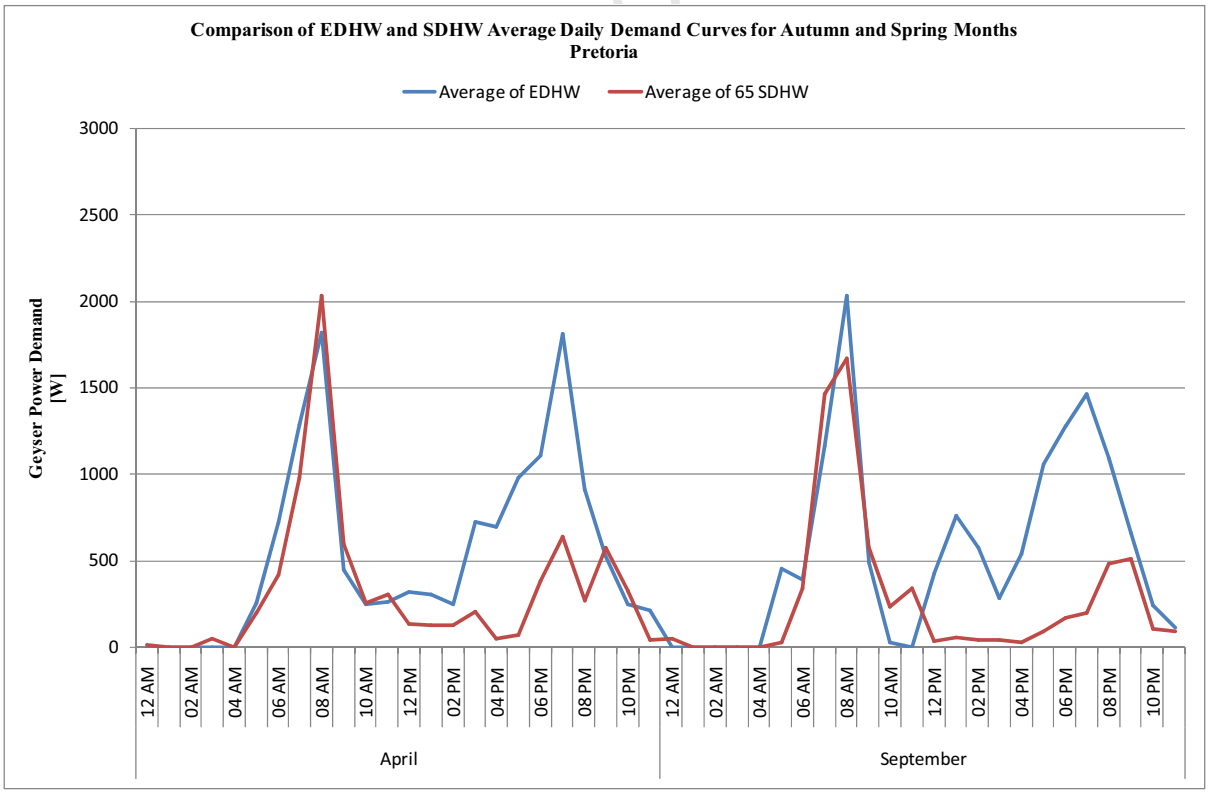

Figure C.6: Comparison of EDHW and SDHW Average Daily Demand Curves for Autumn and Spring Months in Pretoria

C.3. Pietermaritzburg

Pietermaritzburg is located slightly inland of the East coast (29˚36'S, 30˚24'E, 838m Above Sea Level), and it experiences a pleasant climate with few extremes. The simulation results for an EDHW system and SDHW system located in this region are presented below.

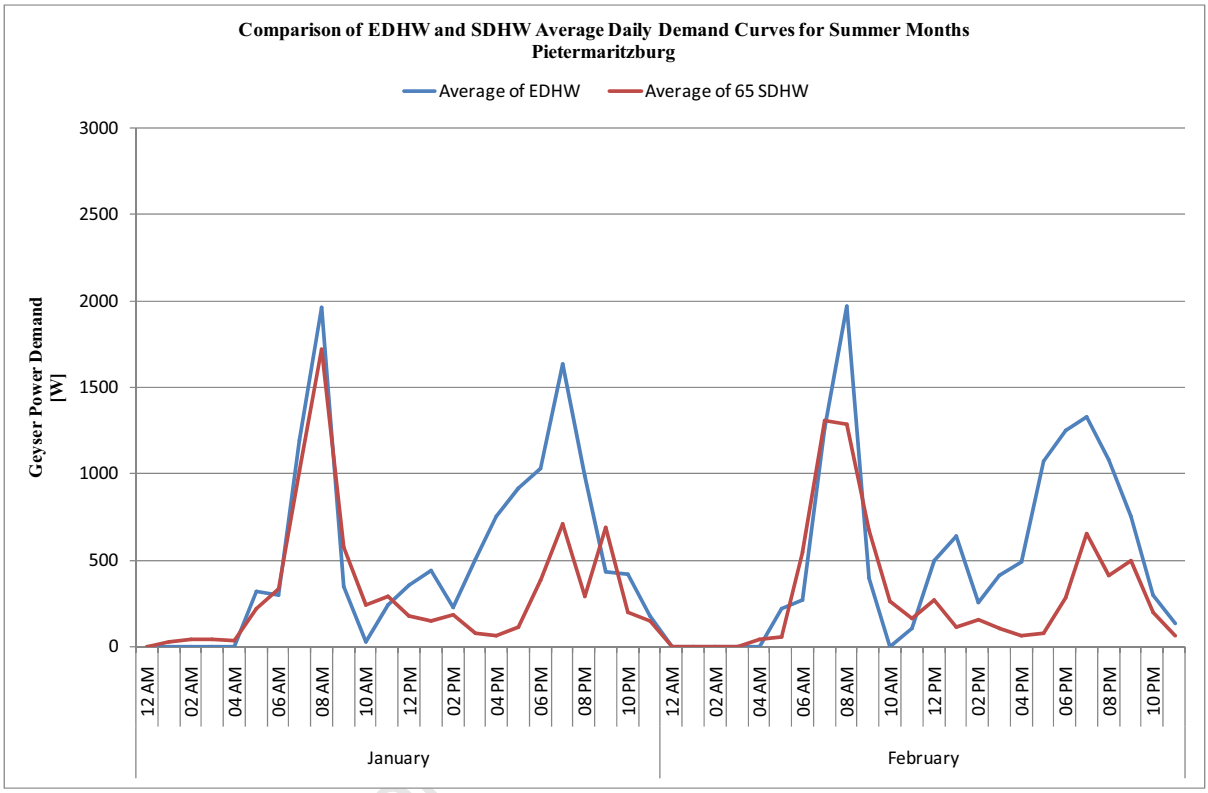

Figure C.7: Comparison of EDHW and SDHW Average Daily Demand Curves for Summer Months in Pietermaritzburg

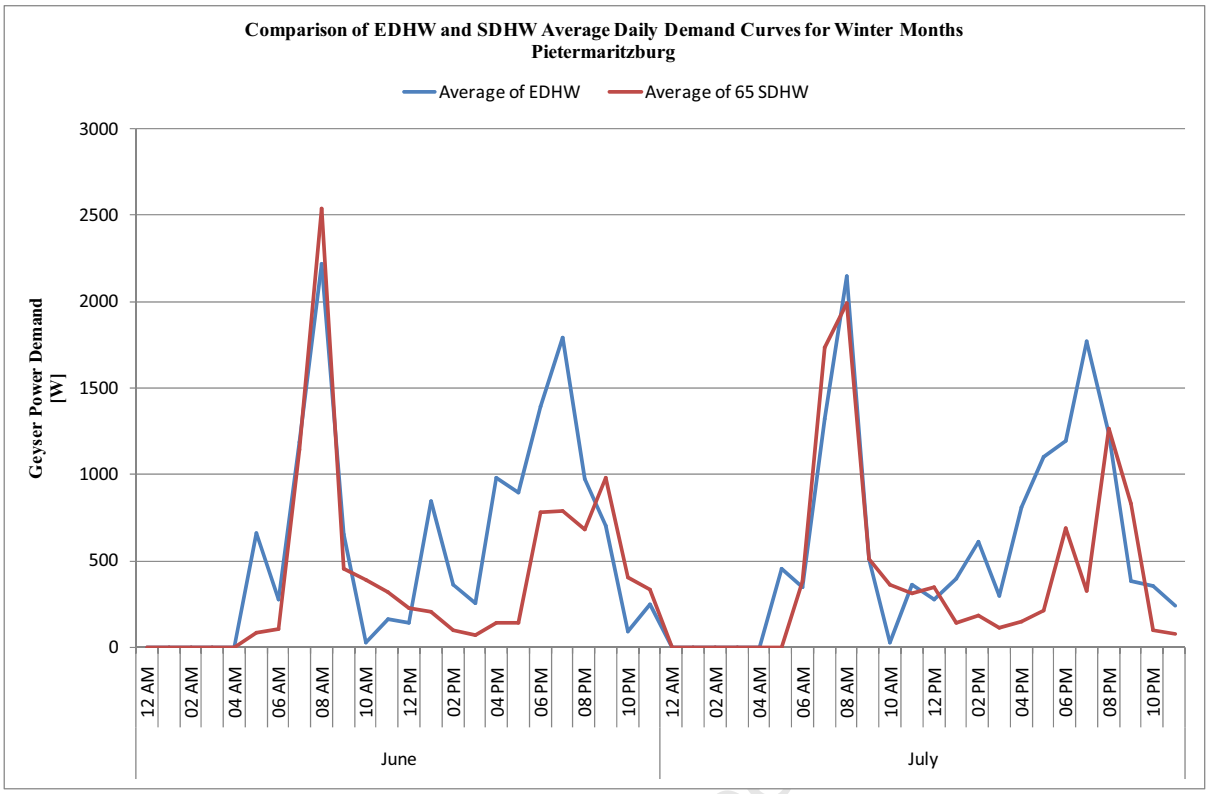

Figure C.8: Comparison of EDHW and SDHW Average Daily Demand Curves for Winter Months in Pietermaritzburg

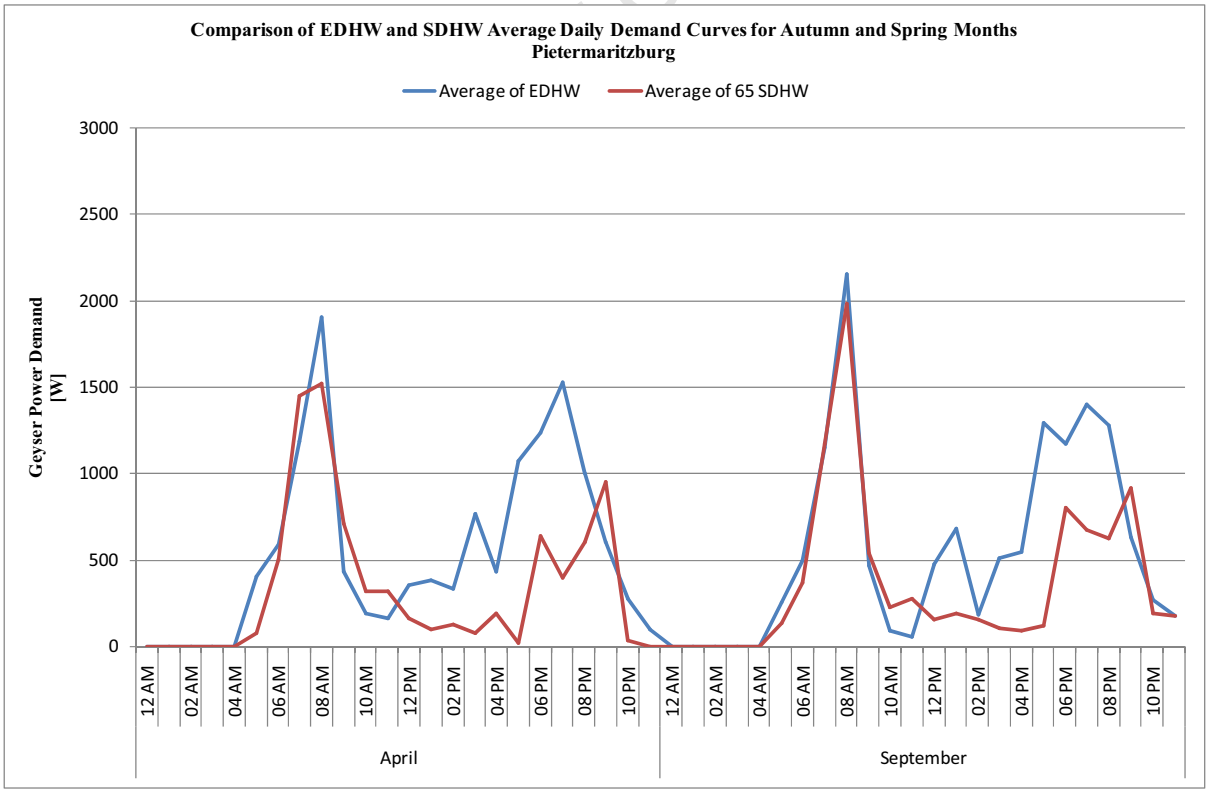

Figure C.9: Comparison of EDHW and SDHW Average Daily Demand Curves for Autumn and Spring Months in Pietermaritzburg

C.4. Bloemfontein

Bloemfontein is located in the Free State, on the interior plateau (29˚07'S, 26˚14'E, 1387m Above Sea Level), and it experiences a hot, arid climate with summer rain and cold winters. The simulation results for an EDHW system and SDHW system located in this region are presented below.

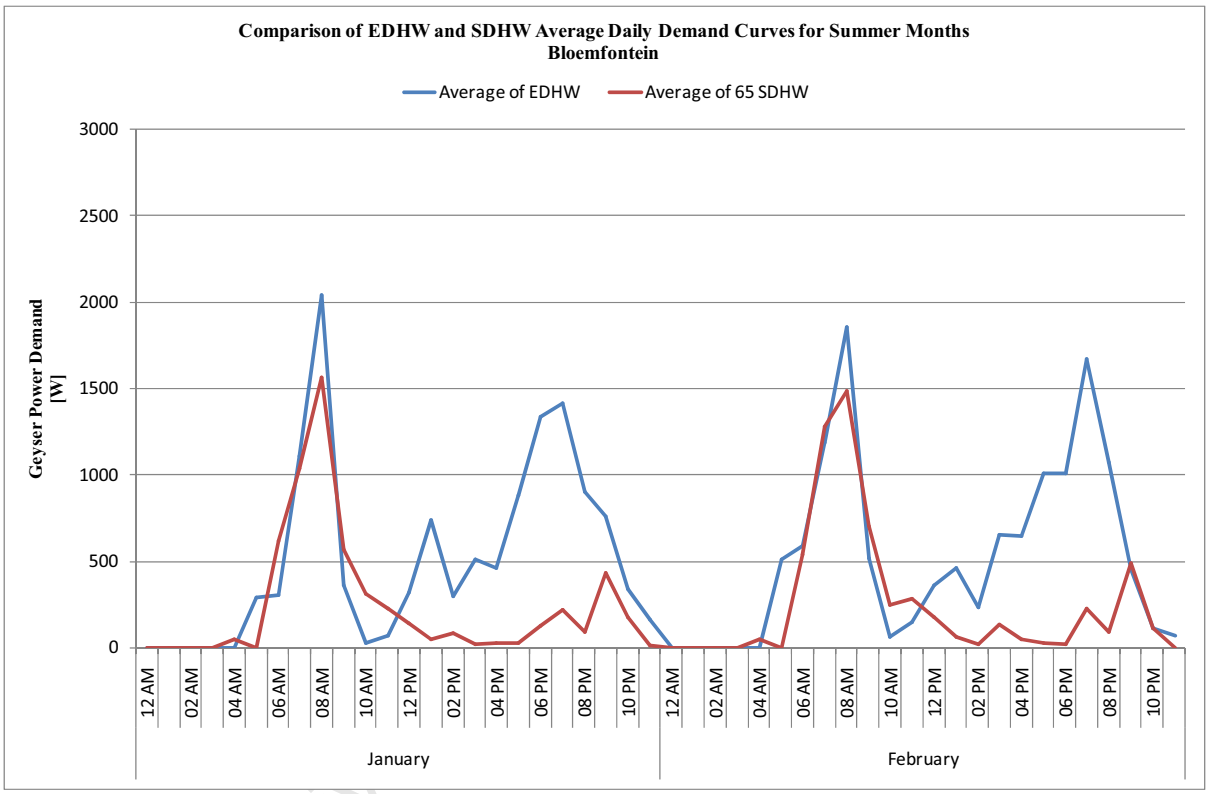

Figure C.10: Comparison of EDHW and SDHW Average Daily Demand Curves for Summer Months in Bloemfontein

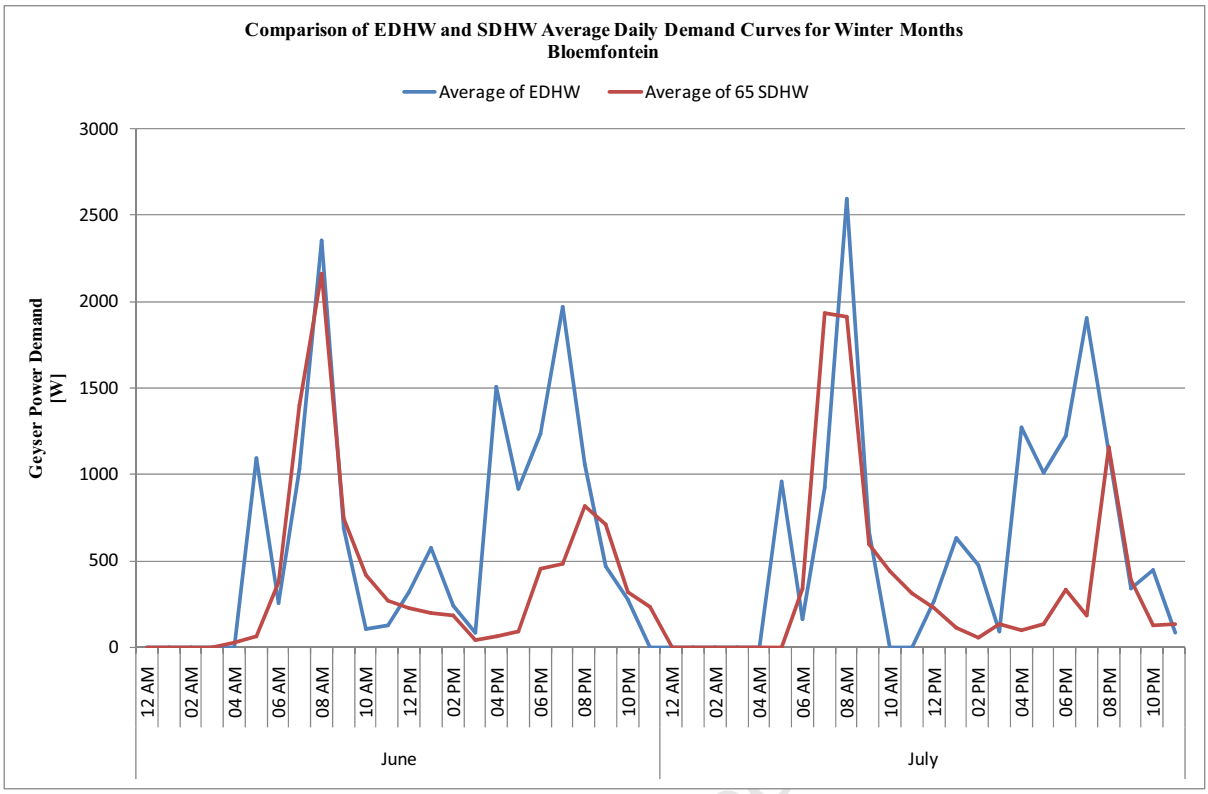

Figure C.11: Comparison of EDHW and SDHW Average Daily Demand Curves for Winter Months in Bloemfontein

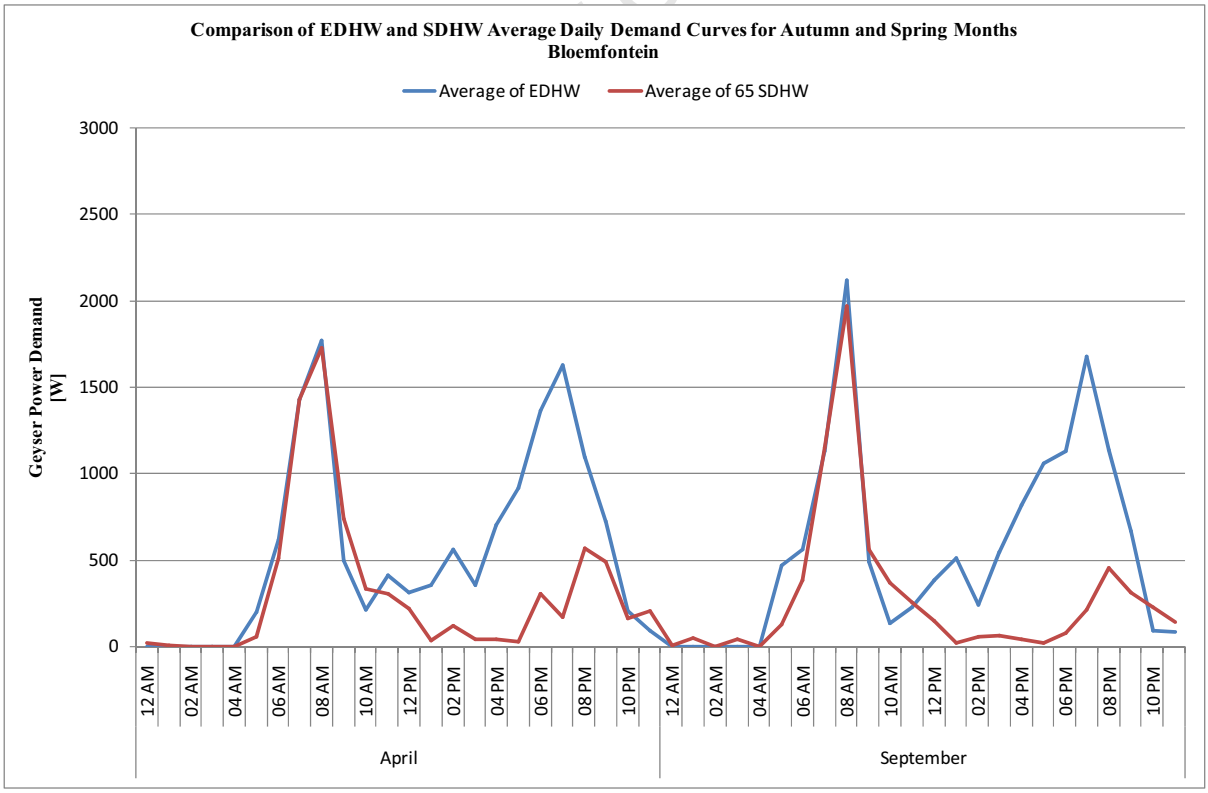

Figure C.12: Comparison of EDHW and SDHW Average Daily Demand Curves for Autumn and Spring Months in Bloemfontein

C.5. Kimberley

Kimberley is located in the Northern Cape on the interior plateau (28˚45'S, 24˚46'E, 11196m Above Sea Level). This semi-desert area experiences a dry, hot climate with very hot summers. The simulation results for an EDHW system and SDHW system located in this region are presented below.

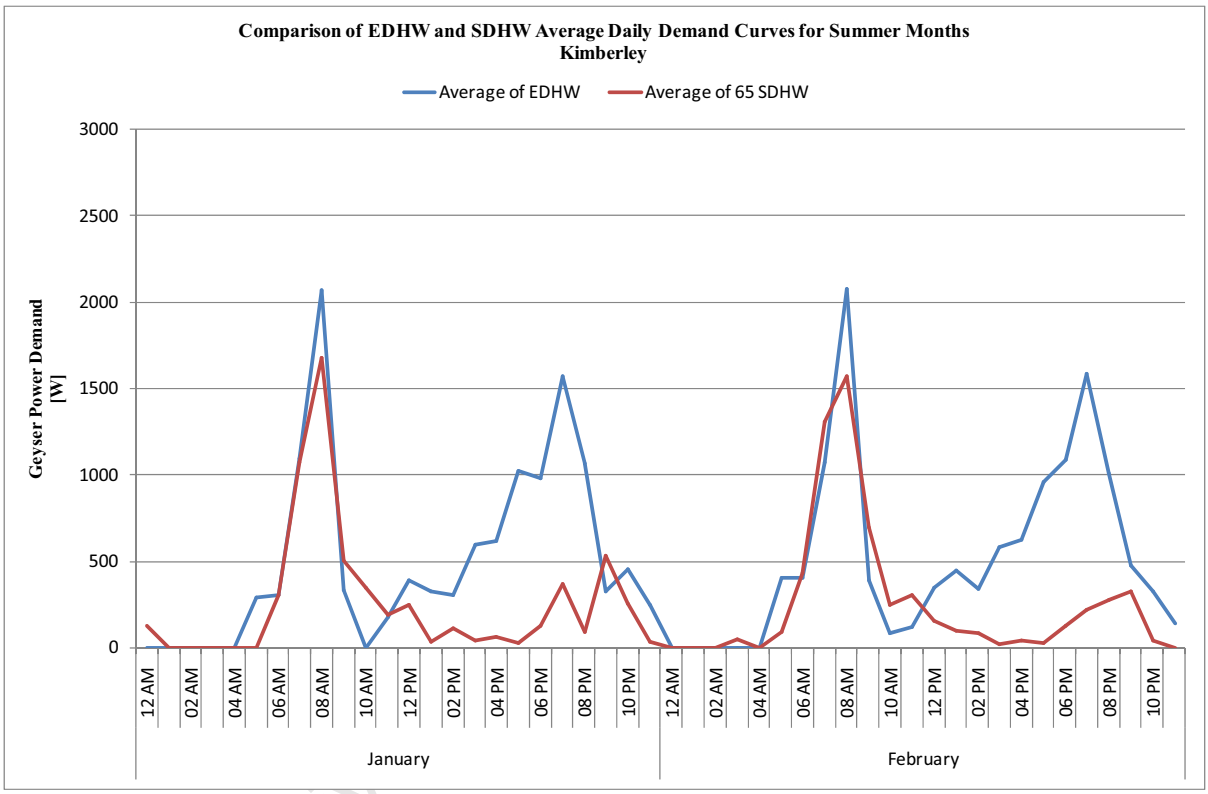

Figure C.13: Comparison of EDHW and SDHW Average Daily Demand Curves for Summer Months in Kimberley

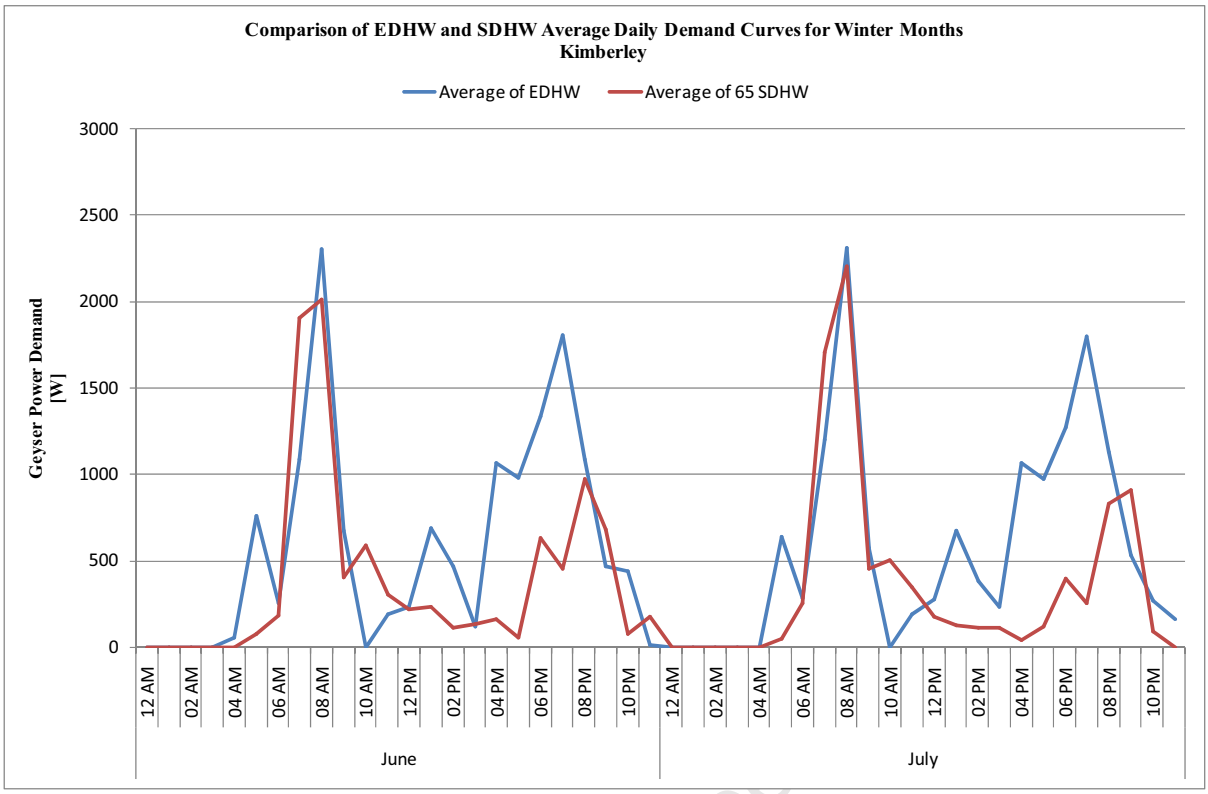

Figure C.14: Comparison of EDHW and SDHW Average Daily Demand Curves for Winter Months in Kimberley

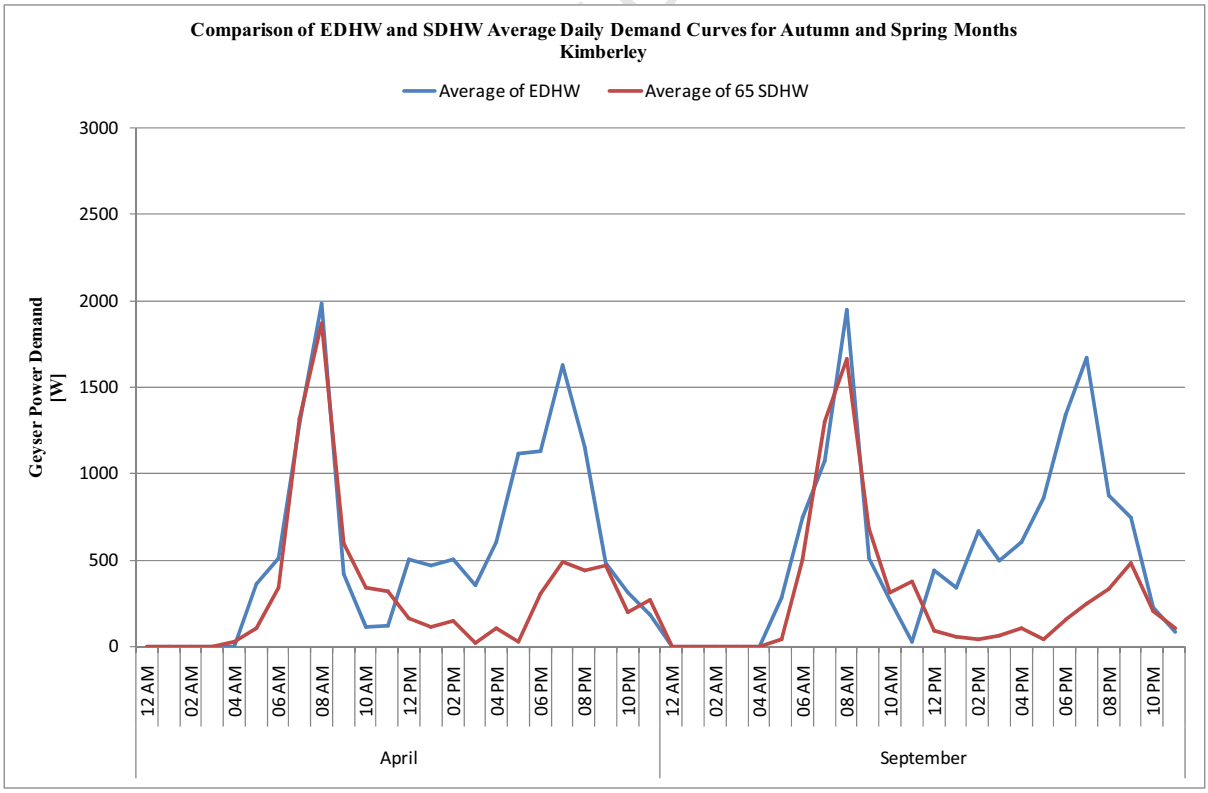

Figure C.15: Comparison of EDHW and SDHW Average Daily Demand Curves for Autumn and Spring Months in Kimberley

C.6. Upington

Upington is located in the Northern Cape on the interior plateau (28˚26'S, 21˚16'E, 814m Above Sea Level). This semi-desert area experiences a dry, hot climate with very hot summers. The simulation results for an EDHW system and SDHW system located in this region are presented below.

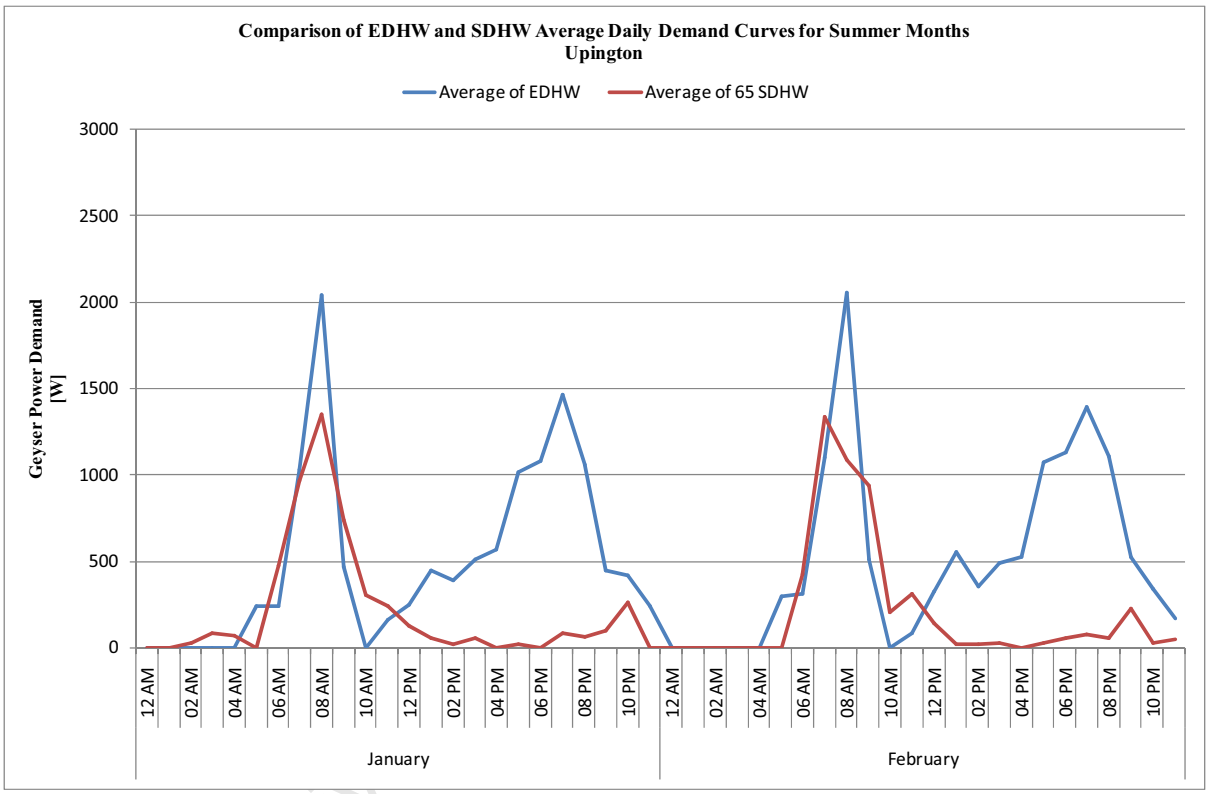

Figure C.16: Comparison of EDHW and SDHW Average Daily Demand Curves for Summer Months in Upington

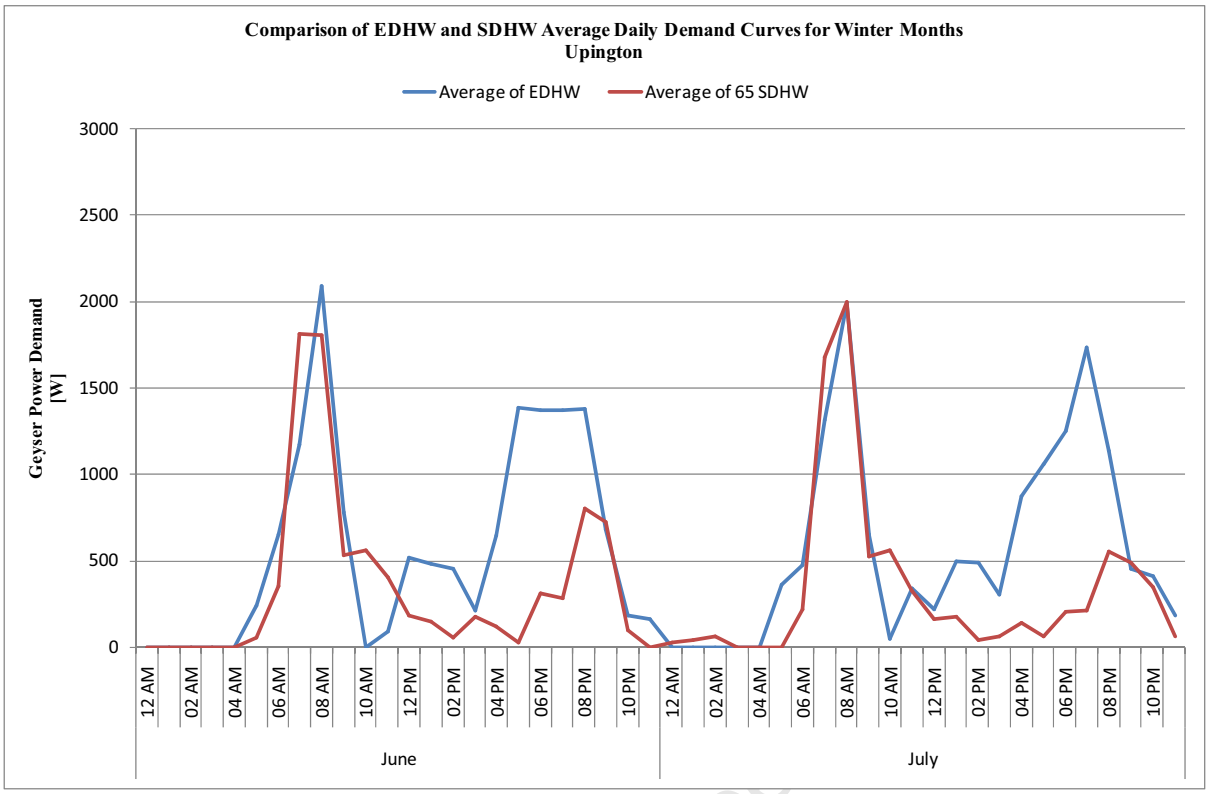

Figure C.17: Comparison of EDHW and SDHW Average Daily Demand Curves for Winter Months in Upington

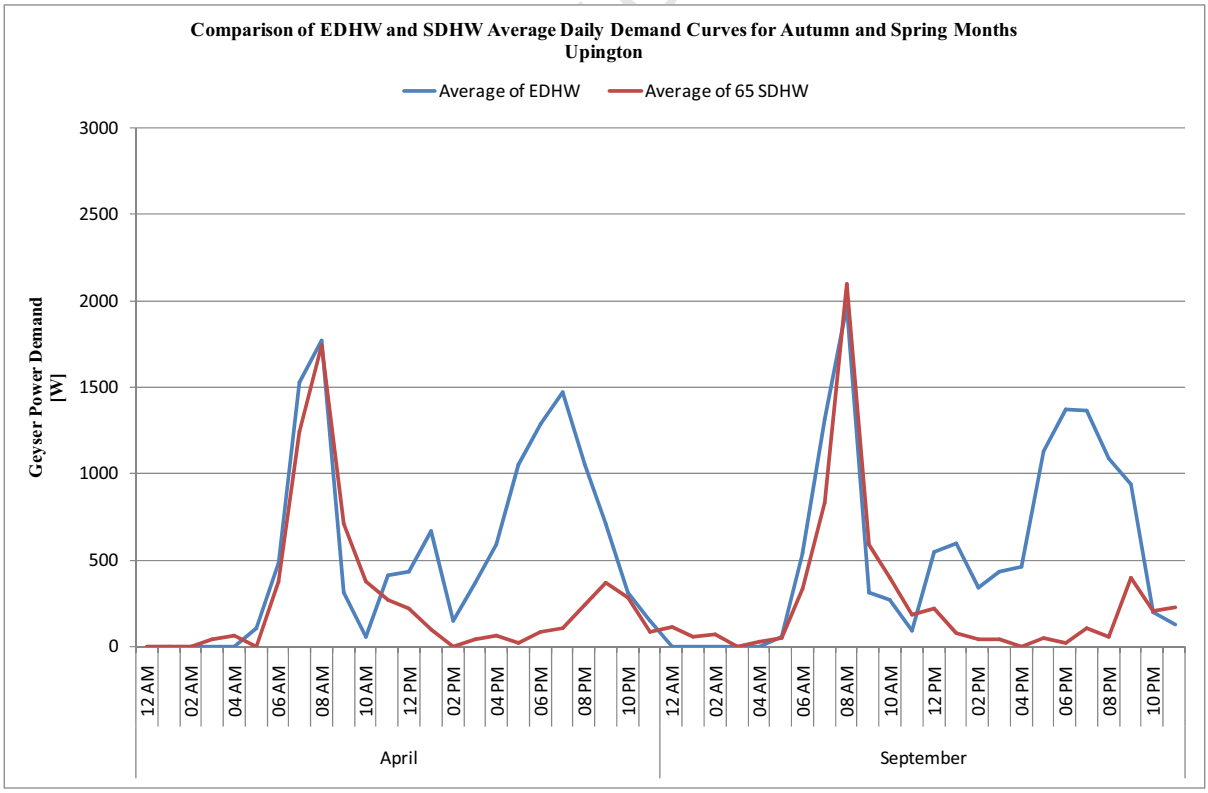

Figure C.18: Comparison of EDHW and SDHW Average Daily Demand Curves for Autumn and Spring Months in Upington

C.7. Polokwane

Polokwane is located on the Escarpment, (23˚52'S, 29˚27'E, 1230m Above Sea Level), and it experiences a dry climate all year round. The simulation results for an EDHW system and SDHW system located in this region are presented below.

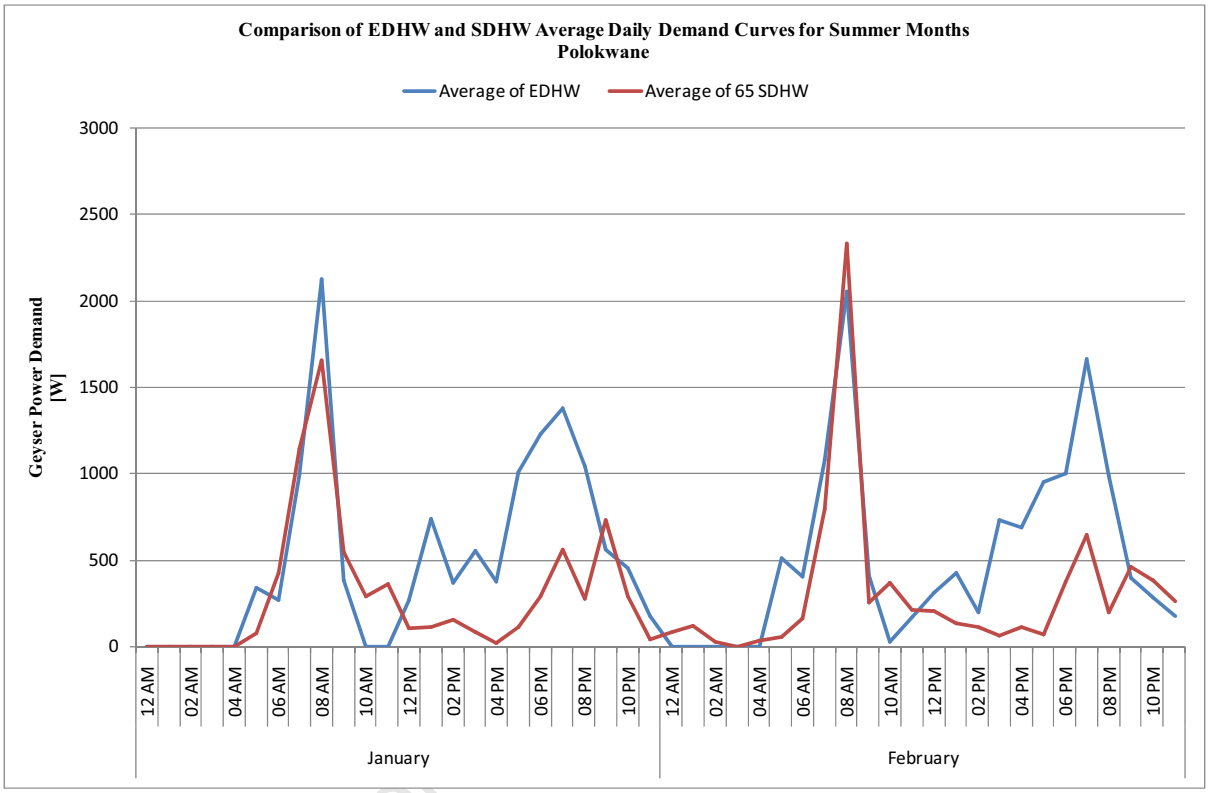

Figure C.19: Comparison of EDHW and SDHW Average Daily Demand Curves for Summer Months in Polokwane

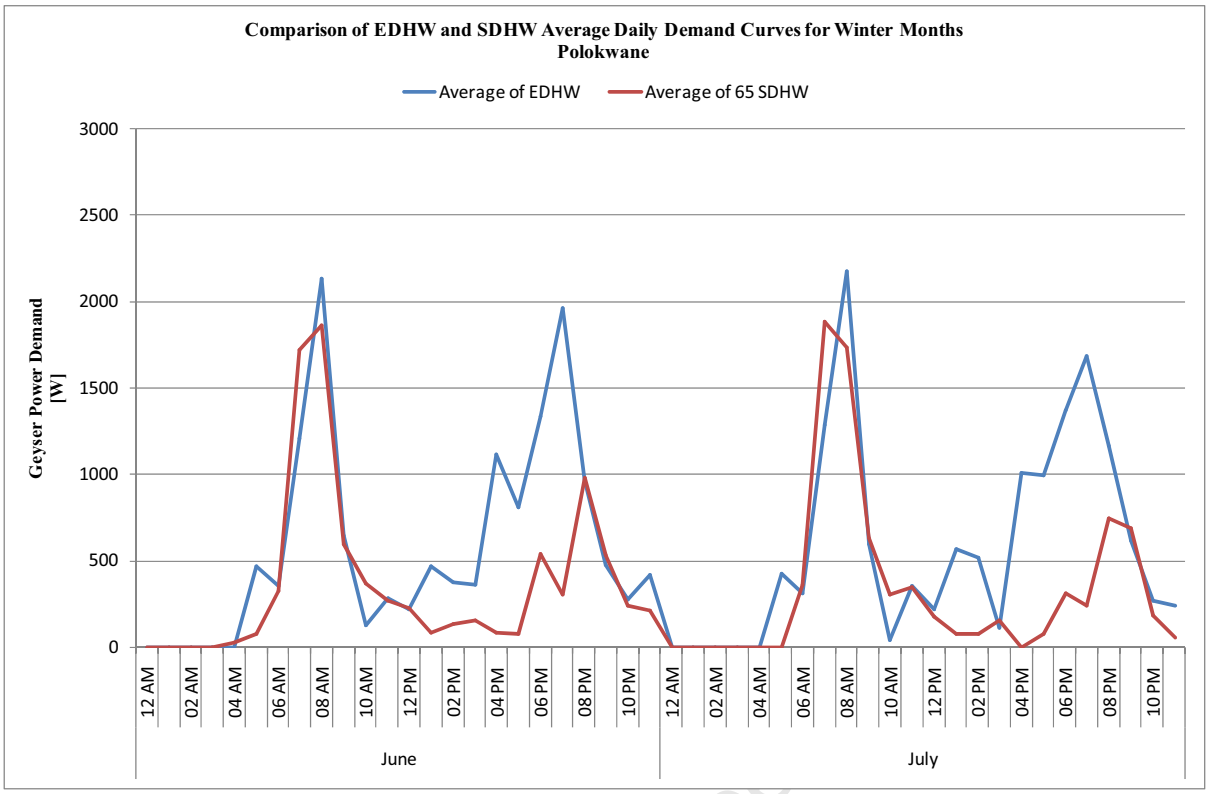

Figure C.20: Comparison of EDHW and SDHW Average Daily Demand Curves for Winter Months in Polokwane

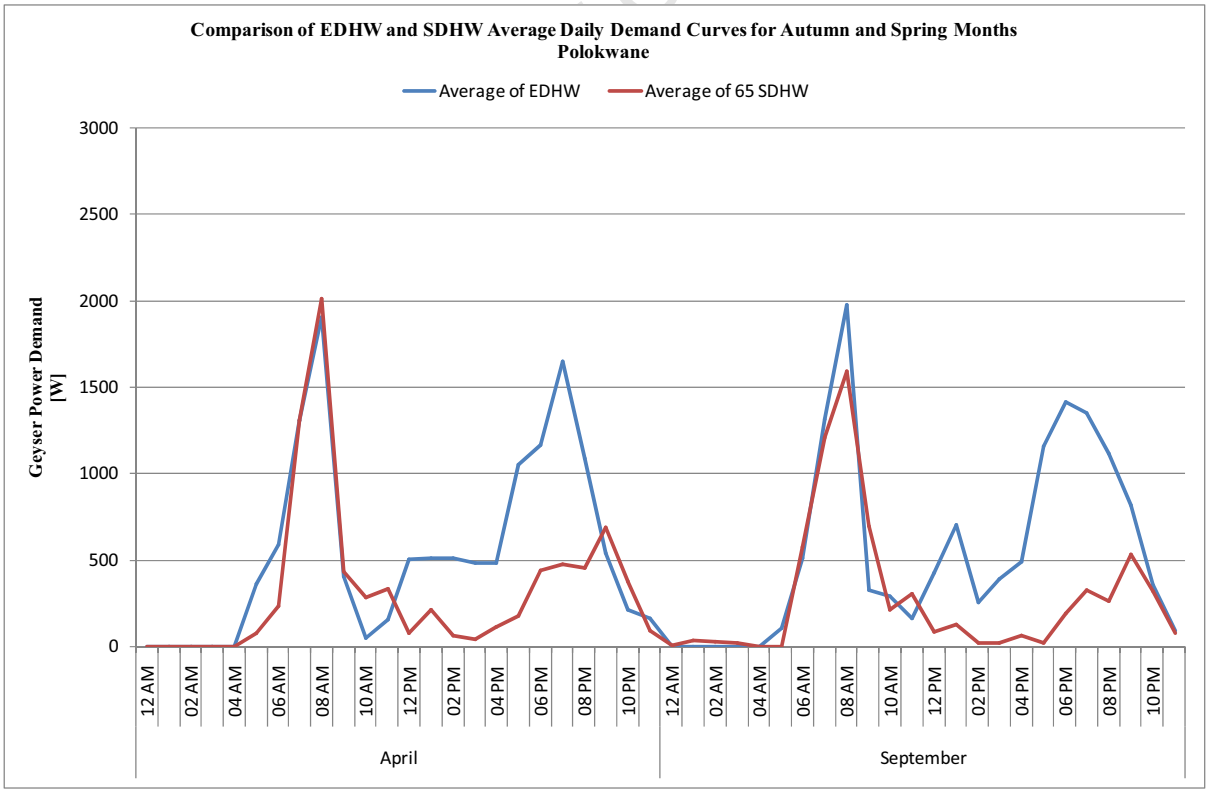

Figure C.21: Comparison of EDHW and SDHW Average Daily Demand Curves for Autumn and Spring Months in Polokwane

C.8. Nelspruit

Nelspruit is located in the Lowveld (25˚18'S, 30˚56'E, 676m Above Sea Level), and it experiences a subtropical climate. The simulation results for an EDHW system and SDHW system located in this region are presented below.

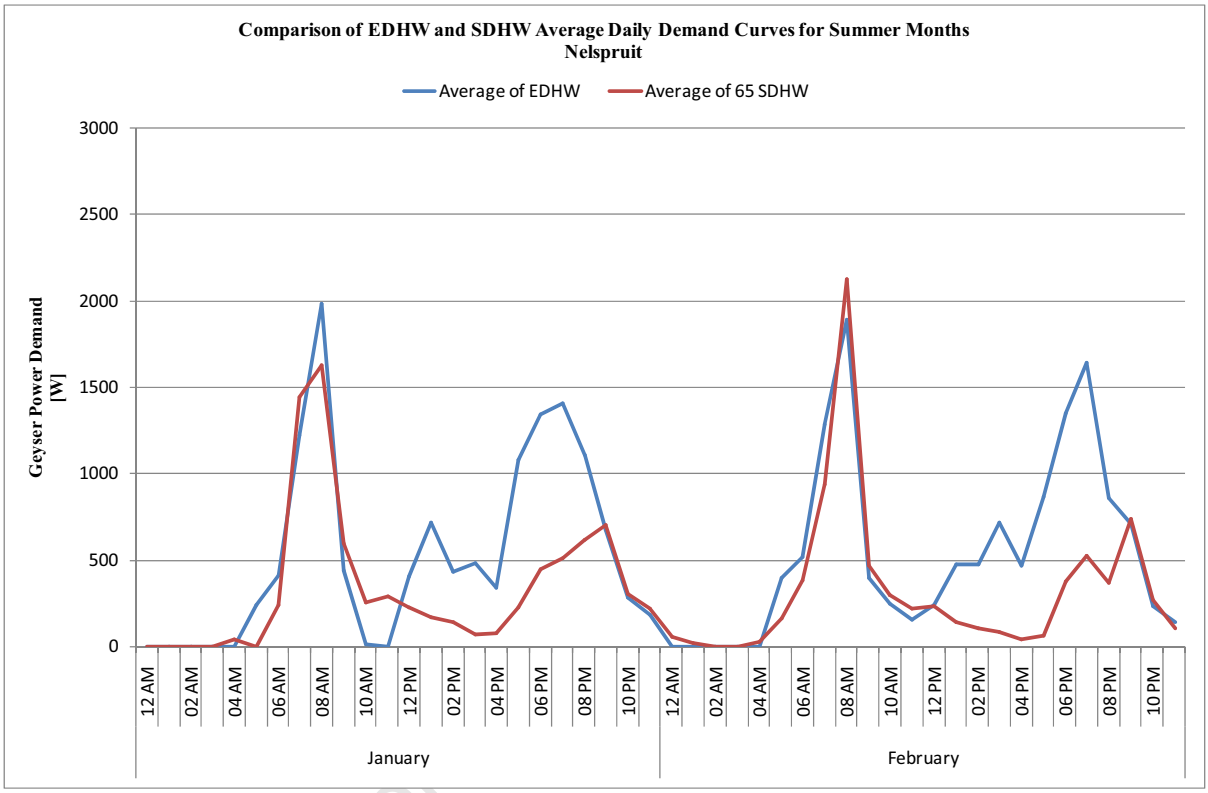

Figure C.22: Comparison of EDHW and SDHW Average Daily Demand Curves for Summer Months in Nelspruit

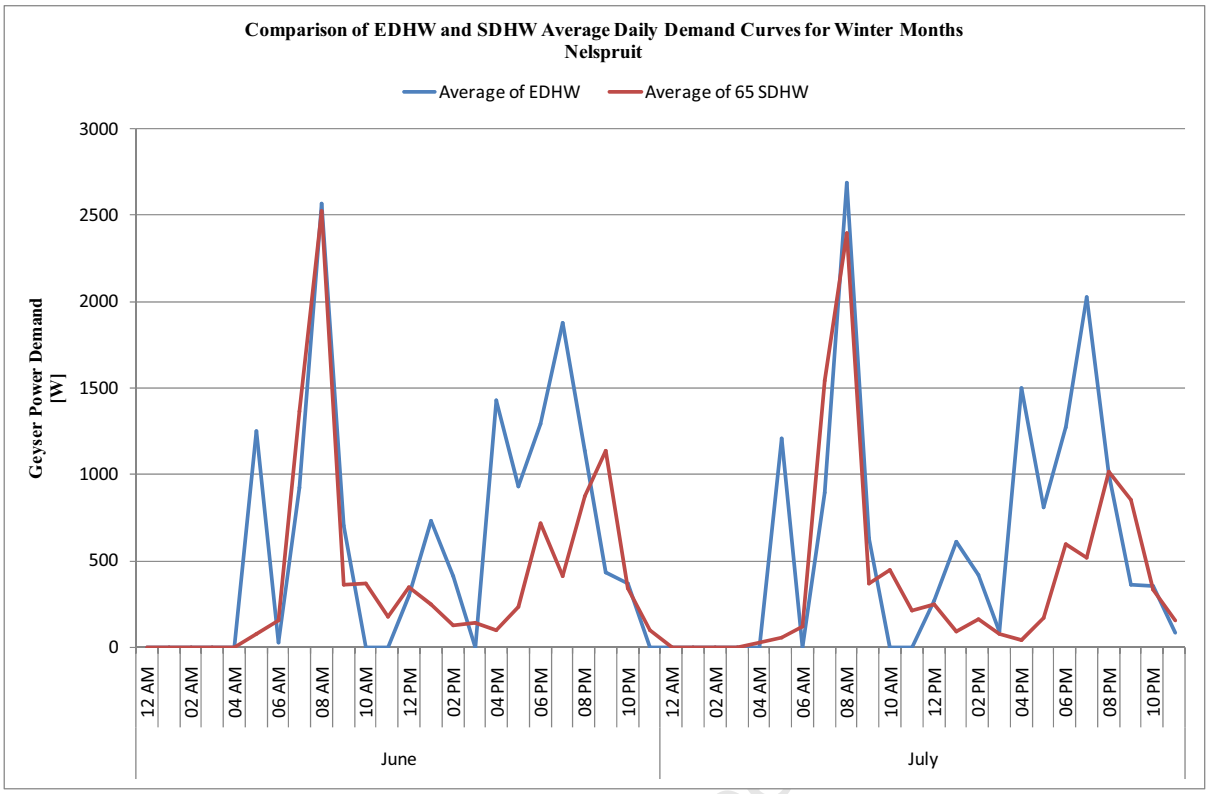

Figure C.23: Comparison of EDHW and SDHW Average Daily Demand Curves for Winter Months in Nelspruit

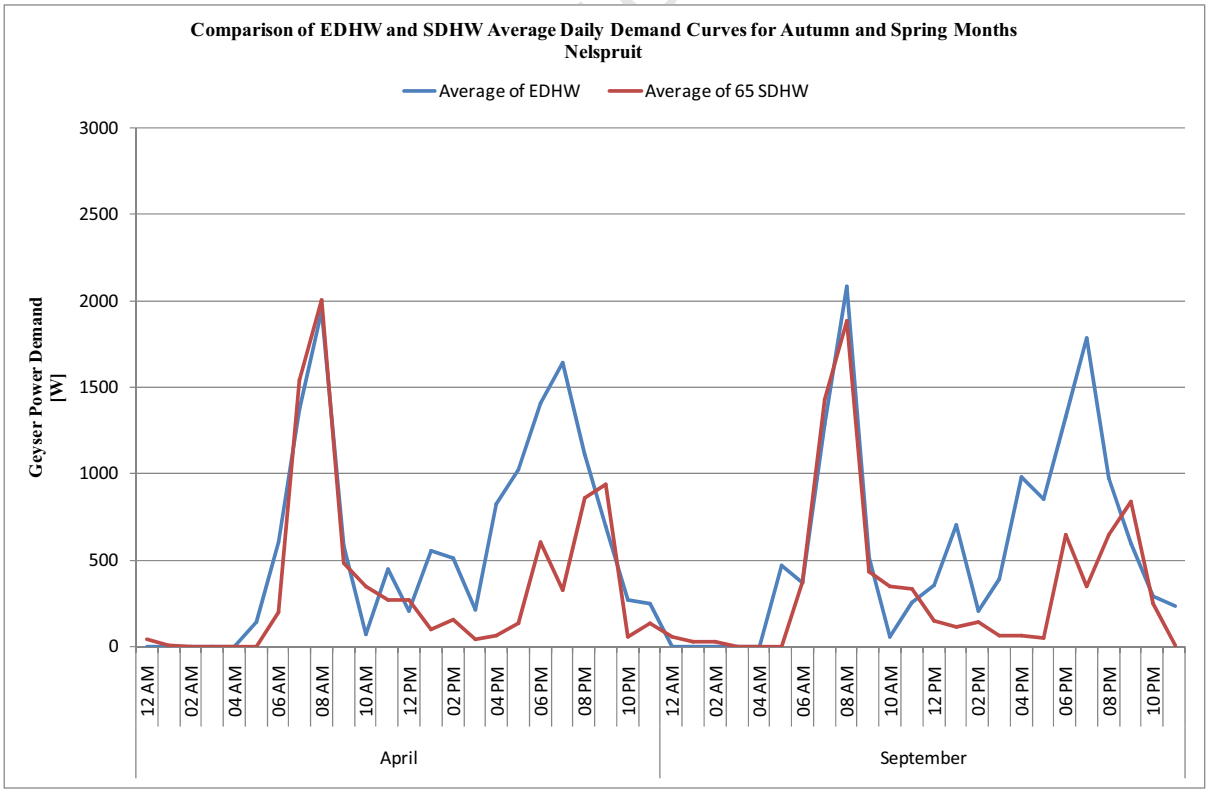

Figure C.24: Comparison of EDHW and SDHW Average Daily Demand Curves for Autumn and Spring Months in Nelspruit

C.9. Mmabatho

Mmabatho is located in the North West province, in the southern parts of the Kalahari Desert (25˚47'S, 25˚32'E, 1281m Above Sea Level). In this region winter is dry and sunny, and summer is hot. The simulation results for an EDHW system and SDHW system located in this region are presented below.

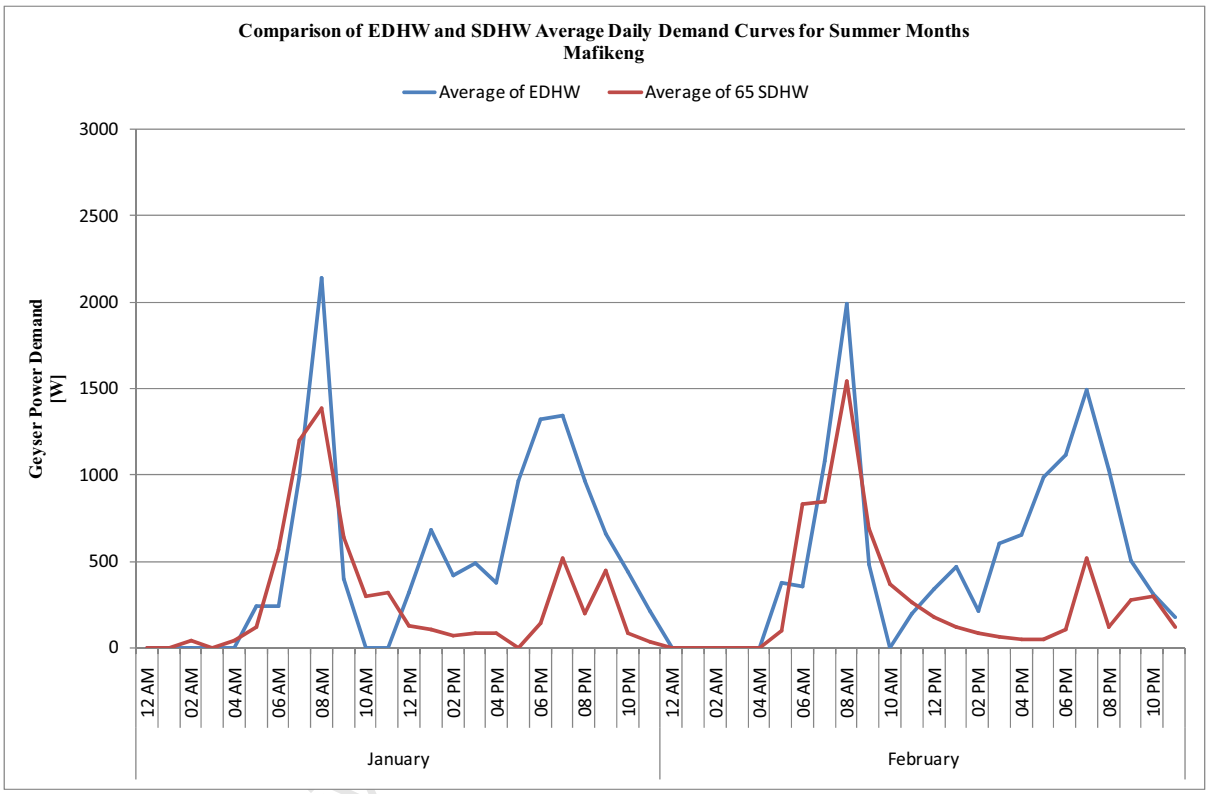

Figure C.25: Comparison of EDHW and SDHW Average Daily Demand Curves for Summer Months in Mmabatho

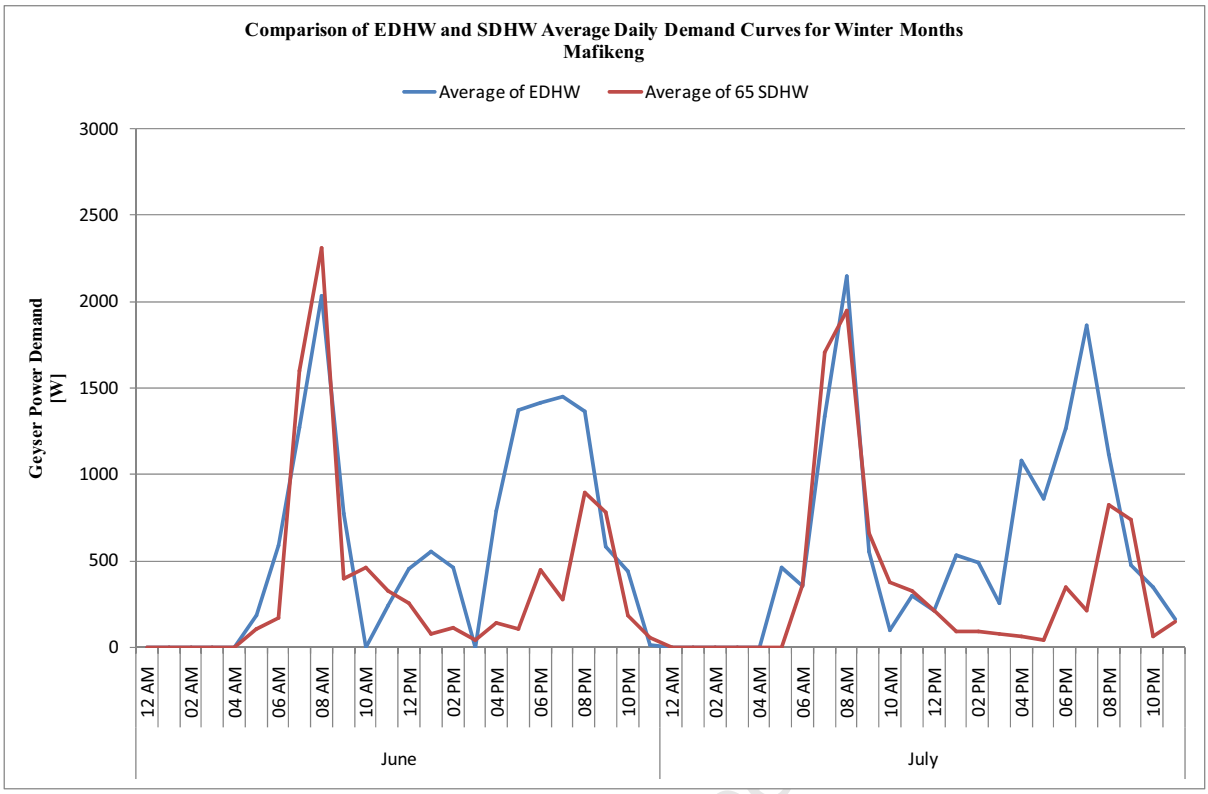

Figure C.26: Comparison of EDHW and SDHW Average Daily Demand Curves for Winter Months in Mmabatho

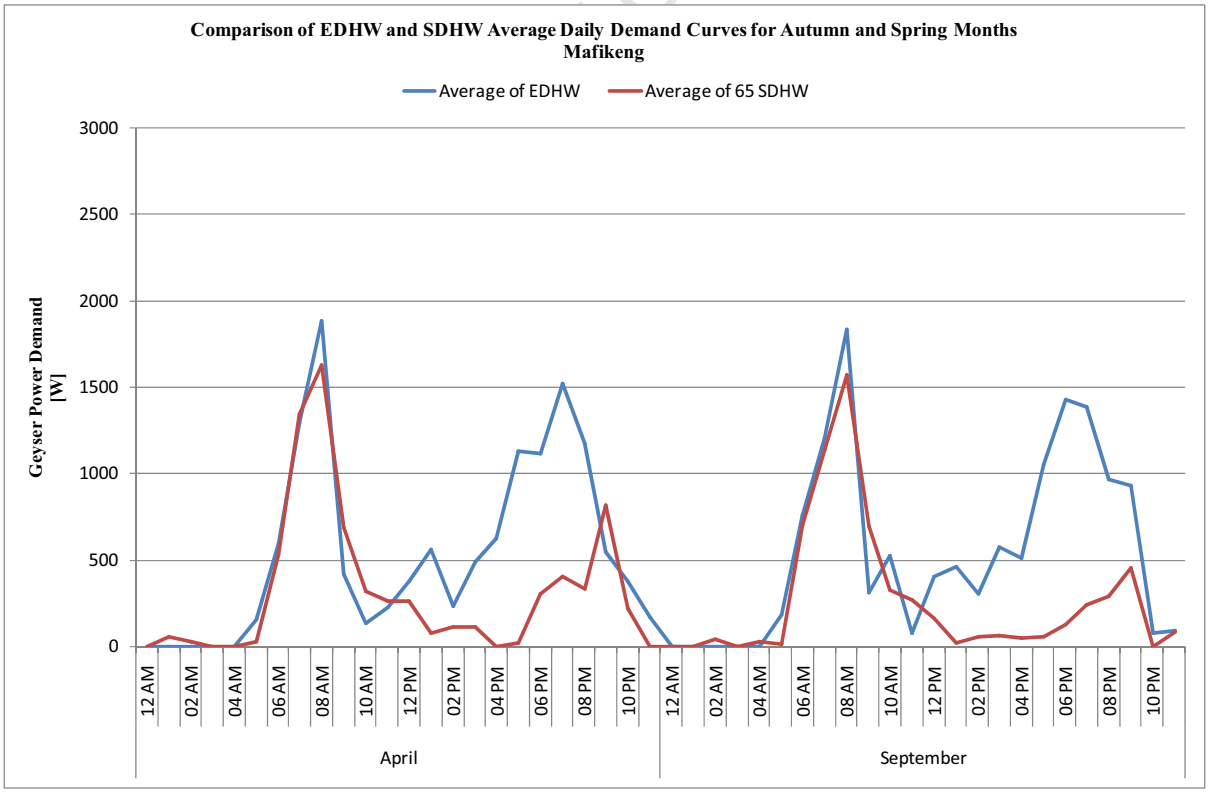

Figure C.27: Comparison of EDHW and SDHW Average Daily Demand Curves for Autumn and Spring Months in Mmabatho

Figures C.28 to C.30 show the average reduction in household electricity consumption during evening peak times due to the use of solar water heating in the Port Elizabeth, Pretoria, Pietermaritzburg, Bloemfontein, Kimberley, Upington, Polokwane, Nelspruit and Mmabatho

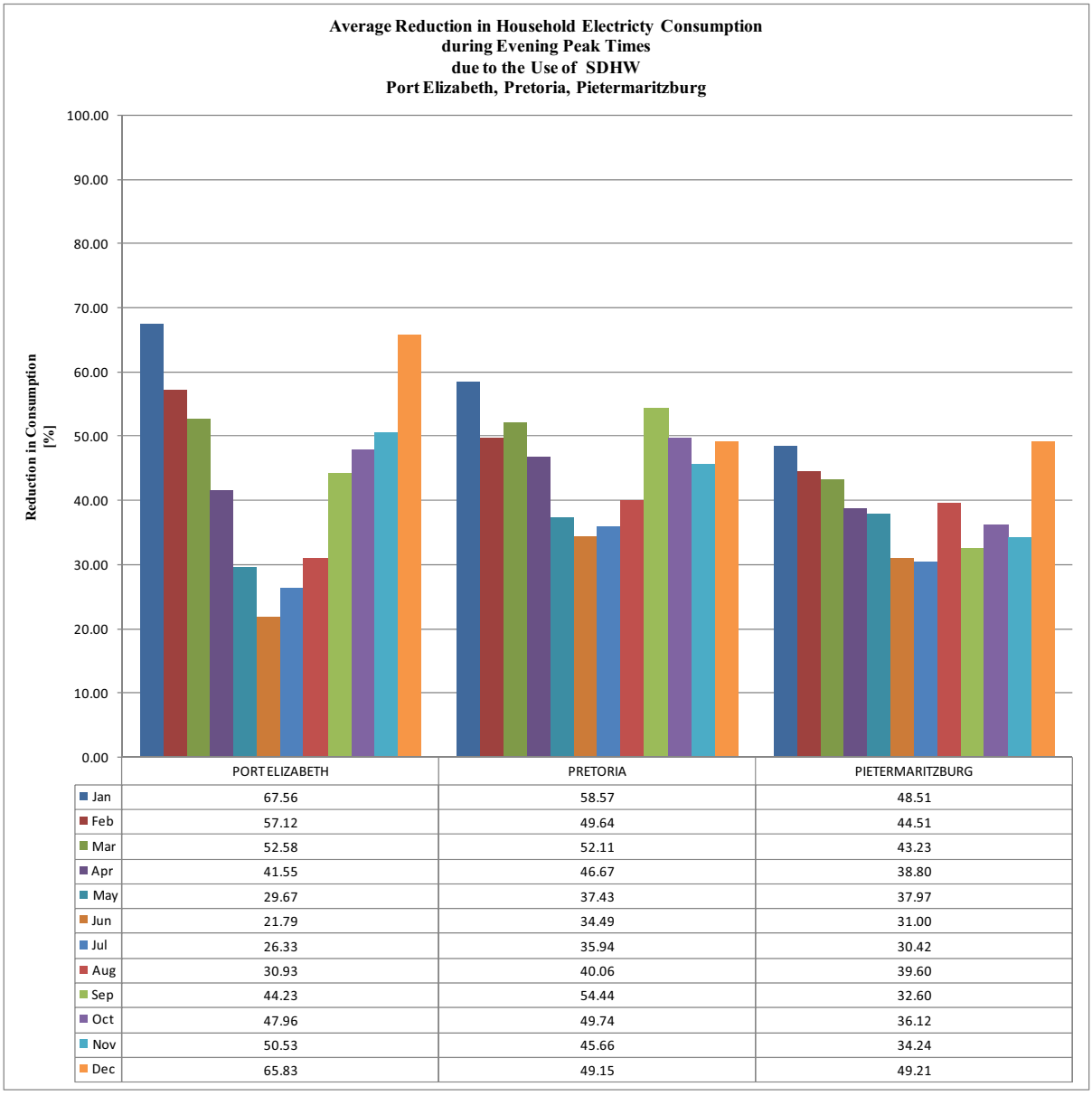

	PORT ELIZABETH	PRETORIA	PIETERMARITZBURG
Jan	67.56	58.57	48.51
Feb	57.12	49.64	44.51
Mar	52.58	52.11	43.23
Apr	41.55	46.67	38.80
May	29.67	37.43	37.97
Jun	21.79	34.49	31.00
Jul	26.33	35.94	30.42
Aug	30.93	40.06	39.60
Sep	44.23	54.44	32.60
Oct	47.96	49.74	36.12
Nov	50.53	45.66	34.24
Dec	65.83	49.15	49.21

Figure C.28: Average % Reduction in Household Electricity Consumption during Evening Peak Times, due to the Use of a SDHW System in Port Elizabeth, Pretoria and Pietermaritzburg

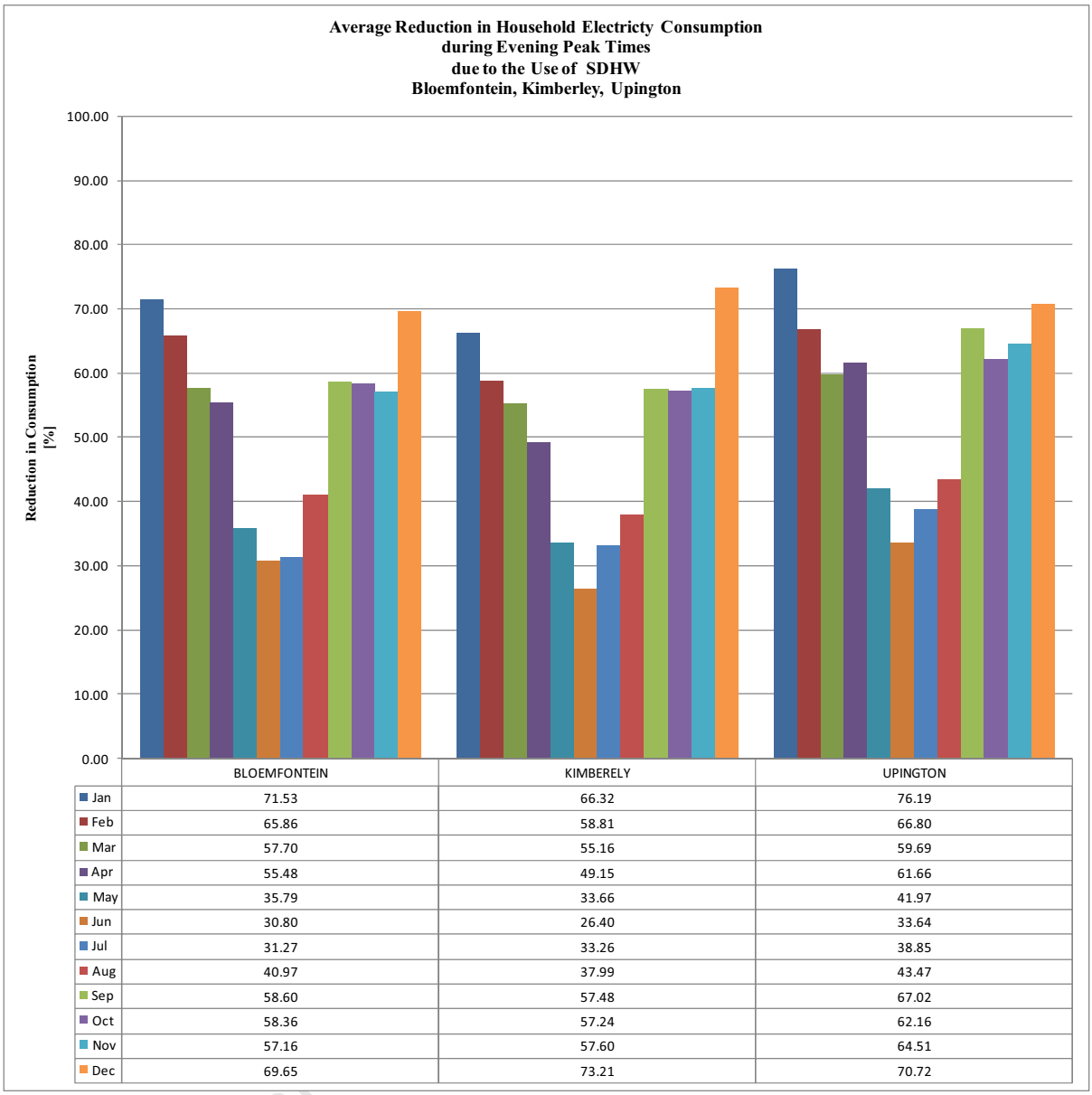

	BLOEMFONTEIN	KIMBERELY	UPINGTON
Jan	71.53	66.32	76.19
Feb	65.86	58.81	66.80
Mar	57.70	55.16	59.69
Apr	55.48	49.15	61.66
May	35.79	33.66	41.97
Jun	30.80	26.40	33.64
Jul	31.27	33.26	38.85
Aug	40.97	37.99	43.47
Sep	58.60	57.48	67.02
Oct	58.36	57.24	62.16
Nov	57.16	57.60	64.51
Dec	69.65	73.21	70.72

Figure C.29: Average % Reduction in Household Electricity Consumption during Evening Peak Times, due to the Use of a SDHW System in Bloemfontein, Kimberley and Upington

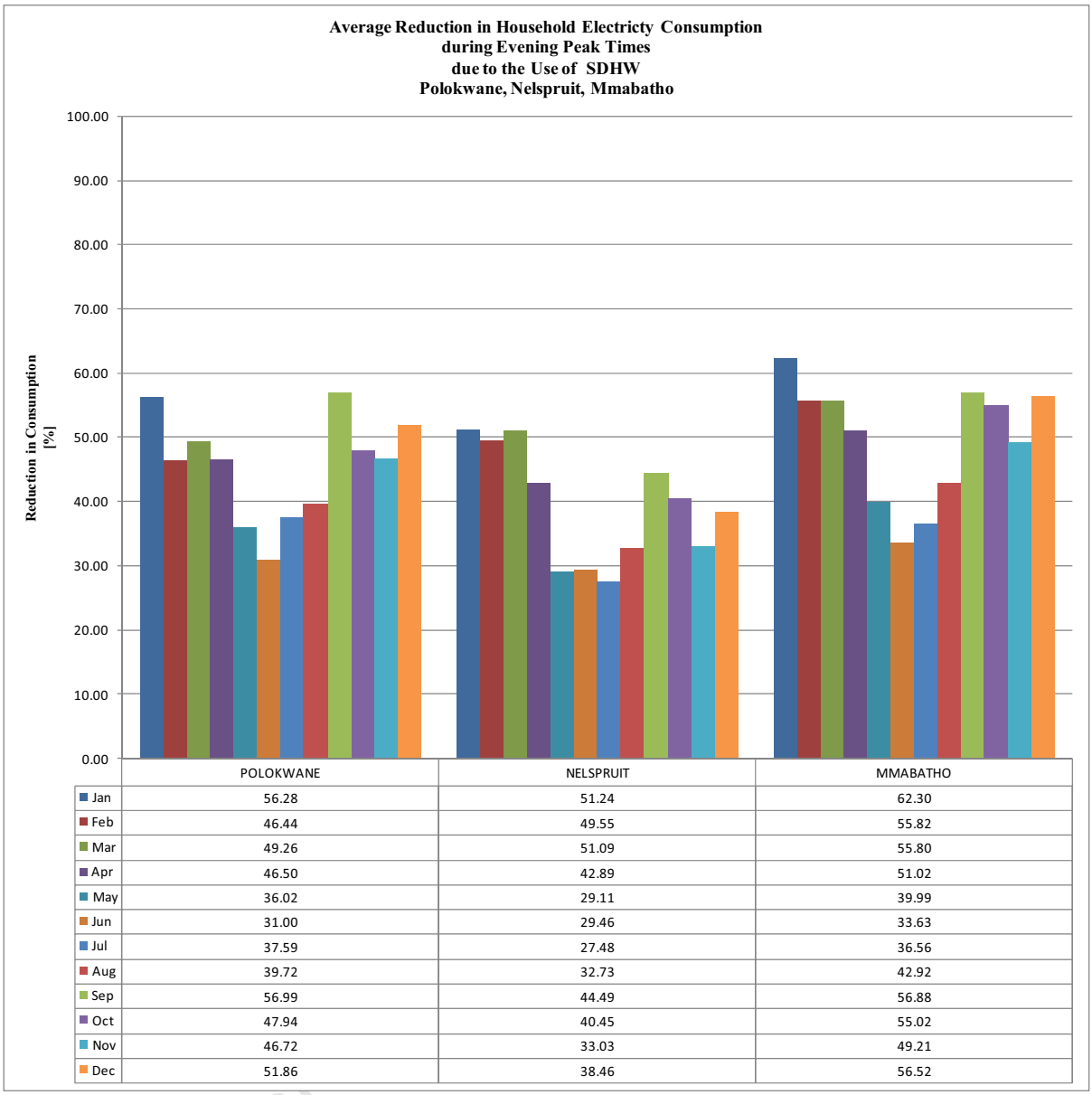

	POLOKWANE	NELSPRUIT	MMABATHO
Jan	56.28	51.24	62.30
Feb	46.44	49.55	55.82
Mar	49.26	51.09	55.80
Apr	46.50	42.89	51.02
May	36.02	29.11	39.99
Jun	31.00	29.46	33.63
Jul	37.59	27.48	36.56
Aug	39.72	32.73	42.92
Sep	56.99	44.49	56.88
Oct	47.94	40.45	55.02
Nov	46.72	33.03	49.21
Dec	51.86	38.46	56.52

Figure C.30: Average % Reduction in Household Electricity Consumption during Evening Peak Times, due to the Use of a SDHW System in Polokwane, Nelspruit and Mmabatho

APPENDIX D

D. POWER SYSTEM PARAMETERS

This appendix presents detailed system parameters of the system that was used to run the load flow studies in Matlab® using the PSAT.2.0.0 toolbox.

PSAT is an open source power system analysis toolbox for Matlab®. The toolbox has a Simulink® library which allows for the creation of one line network diagrams. Figure D.1 shows the one-line diagram for the modified IEEE 39-bus system that was used for the load flow studies.

PSAT extracted all the system information from the Simulink® model to create an m-file which was then used to run a load flow, using the Newton-Rhapson method.

The parameters of the system busses, lines, generators and loads are included in the following pages.

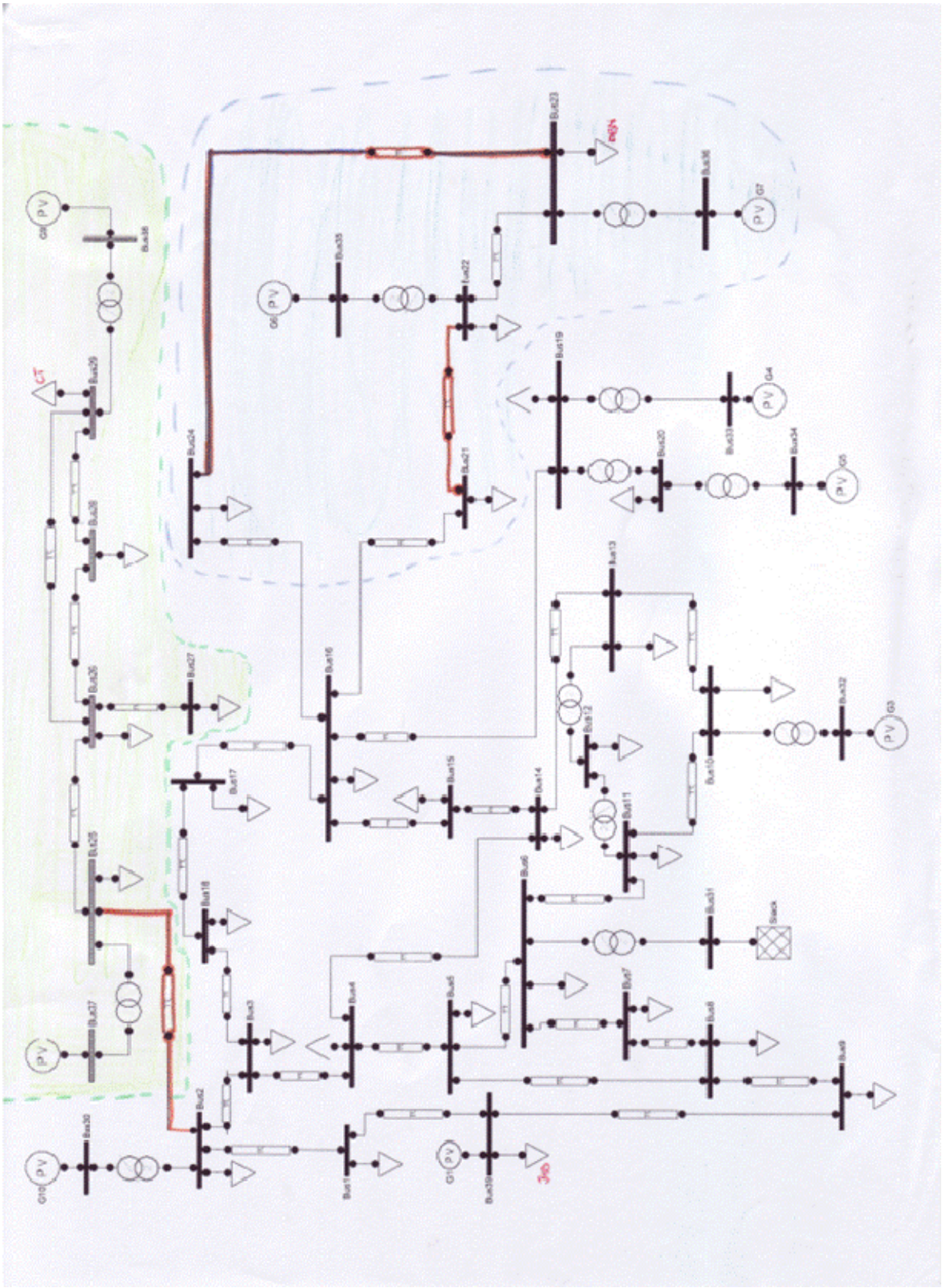

Figure D.1: Simulink® Screenshot of Modified IEEE 39 Bus System used for Load Flow Studies

BUS PARAMETERS

Bus Number	Voltage [p.u.]	Phase [rad]
1	1.048	-0.1646
2	1.0505	-0.1203
3	1.0341	-0.1698
4	1.0116	-0.1838
5	1.0165	-0.1637
6	1.0172	-0.1515
7	1.0067	-0.1892
8	1.0057	-0.1979
9	1.0322	-0.1946
10	1.0235	-0.1101
11	1.0201	-0.1243
12	1.0072	-0.1246
13	1.0207	-0.1225
14	1.0181	-0.1511
15	1.0194	-0.1581
16	1.0346	-0.1337
17	1.0365	-0.151
18	1.0343	-0.1656
19	1.0509	-0.0531
20	0.9914	-0.0777
21	1.0337	-0.0918
22	1.0509	-0.0143
23	1.0459	-0.0178
24	1.0399	-0.1316
25	1.0587	-0.0962
26	1.0536	-0.1182
27	1.0399	-0.1532
28	1.0509	-0.0571
29	1.0505	-0.0089
30	1.0475	-0.078
31	0.982	0
32	0.9831	0.0284
33	0.9972	0.038
34	1.0123	0.0129
35	1.0493	0.0723
36	1.0635	0.1192
37	1.0278	0.022
38	1.0265	0.1143
39	1.03	-0.1913

Modified IEEE 39 Bus System Parameters

LINE PARAMETERS

From Bus	To Bus	Resistance	Reactance	Susceptance	Tap Ratio
		[p.u.]	[p.u.]	[p.u.]	
1	2	0.000254545	0.002989086	0.05081446	0
1	39	0.000181818	0.00454545	0,1363635	0
2	3	0.000236364	0.002745459	0.04676371	0
2	25	0.000929091	0.001141454	0.01937818	0
2	30	0	0.003290909	0	1.025
3	4	0.000236364	0.003872733	0.04025461	0
3	18	0.0002	0.002418182	0.03887273	0
4	14	0.000145455	0.002345462	0.02512735	0
4	5	0.000145455	0.00232728	0.02440008	0
6	5	0.0000364	0.000472727	0.007890901	0
5	8	0.000145455	0.00203637	0.02683645	0
6	7	0.000109091	0.001672729	0.02054547	0
6	11	0.000127273	0.001490912	0.0252546	0
7	8	0.0000727	0.000836364	0.01418182	0
8	9	0.000290909	0.004591303	0.04811382	0
9	39	0.000181818	0.00454545	0.2181816	0
10	11	0.0000727	0.000781818	0.01325455	0
10	13	0.0000727	0.000781818	0.01325455	0
10	32	0	0.003636364	0	1.07
12	11	0.000290909	0.007909091	0	1.006
12	13	0.000290909	0.007909091	0	1. 006
13	14	0.000163636	0.00183636	0.0313272	0
14	15	0.000327273	0.003945458	0.06654551	0
15	16	0.000163636	0.001709087	0.03109084	0
16	17	0.000127273	0.001618185	0.02440005	0
16	19	0.000750909	0.009151703	0.142677	0
16	21	0.000145455	0.002454553	0.04632742	0
16	24	0.0000545	0.001072728	0.01236365	0
17	18	0.000127273	0.001490912	0.02398187	0
19	20	0.000127273	0.002509091	0	1.06
19	33	0.000127273	0.002581818	0	1. 070
20	34	0.000163636	0.003272727	0	1.009
21	22	0.000470909	0.008240907	0.1509852	0
22	23	0.000109091	0.001745456	0.03356366	0
22	35	0	0.0026	0	1.025
23	24	0.000470909	0.007491734	0.07727188	0
23	36	0.0000909	0.004945455	0	1
25	26	0.000623636	0.006294828	0.09976683	0
25	37	0.000109091	0.004218182	0	1. 025
26	27	0.000254545	0.002672723	0.04356356	0
26	28	0.001018182	0.01122368	0.1847408	0
26	29	0.001272727	0.01395534	0.2297607	0
28	29	0.000534545	0.005765453	0.09507271	0
29	38	0.000145455	0.002836364	0	1.025
6	31	0	0.004545455	0	1.07

Modified IEEE 39 Bus System Parameters

GENERATOR PARAMETERS

Bus Number	MW	Voltage	Phase	Max Mvar	Min Mvar	Slack Bus
	[p.u.]	[p.u.]	[rad]	[p.u.]	[p.u.]	
30	34.88	1.0475	-0.0780	44	-27.5	n
31	20	1	0.9820	44	-27.5	y
32	56.88	0.9831	0.0284	44	-27.5	n
33	55.89	0.9972	0.0380	44	-27.5	n
34	66.78	1.0265	0.0129	44	-27.5	n
35	4.65	1.0493	0.0723	22	-16.5	n
36	4.01	1.0635	0.1192	22	-16.5	n
37	6.59	1.0278	0.0220	22	-16.5	n
38	19.37	1.0123	0.1143	22	-16.5	n
39	76.13	1.03	-0.1913	83	-55	n

LOAD PARAMETERS

Bus Number	P Load [p.u.]	Q Load [p.u.]
1	0	0
2	0	0
3	17.19	0.1284
4	26.69	9.8252
5	0	0
6	0	0
7	12.48	4.4854
8	27.87	9.398
9	0	0
10	0	0
11	0	0
12	0.453	4.699
13	0	0
14	0	0
15	17.087	8.1699
16	17.567	1.7247
17	0	0
18	8.4368	1.6019
19	0	0
20	33.533	5.5
21	6.3393	2.6606
22	20.17	7.5939
23	27.662	9.4555
24	3.4578	-1.033
25	9.2208	1.9429
26	4.3392	0.5306
27	11.9328	3.2061
28	7.0512	0.9447
29	21.696	2.0586
39	58.951	13.349

APPENDIX E

E. DETAILED LOAD FLOW RESULTS

E.1. Load Flow Results for Base Case

POWER FLOW REPORT

P S A T 2.0.0

Author: Federico Milano, (c) 2002-2007
e-mail: fmilano@thunderbox.uwaterloo.ca
website: http://thunderbox.uwaterloo.ca/~fmilano
File: C:\Program Files\MATLAB\R2006b\work\IEEE 39 Models\BaseCase.mdl
Date: 23-Apr-2008 11:58:47

NETWORK STATISTICS

Buses:	39
Lines:	33
Transformers:	12
Generators:	10
Loads:	30

SOLUTION STATISTICS

Number of iterations:	7
Maximum P mismatch [p.u.]	0
Maximum Q mismatch [p.u.]	0
Power rate [MVA]	100

POWER FLOW RESULTS

Bus	V [p.u.]	Phase [rad]	P gen [p.u.]	Q gen [p.u.]	P load [p.u.]	Q load [p.u.]
Bus1	1.001	-0.07584	0	0	0	0
Bus10	1.0094	-0.00027	0	0	0	0
Bus11	1.0037	-0.02535	0	0	0	0
Bus12	0.99026	-0.0225	0	0	0.453	4.699
Bus13	0.99049	-0.01738	0	0	0	0
Bus14	0.95031	-0.05914	0	0	0	0
Bus15	0.86807	-0.0854	0	0	15.8961	7.6005
Bus16	0.85053	-0.06246	0	0	15.6887	1.5403
Bus17	0.87348	-0.07589	0	0	0	0
Bus18	0.89467	-0.08781	0	0	8.3371	1.583
Bus19	1.008	1.0158	0	0	0	0
Bus2	0.97764	-0.01143	0	0	0	0
Bus20	0.93249	1.0908	0	0	33.533	5.5
Bus21	0.87415	-0.14098	0	0	5.9804	2.51
Bus22	1.0032	-0.30994	0	0	20.17	7.5939
Bus23	0.98118	-0.31091	0	0	27.662	9.4555
Bus24	0.86483	-0.10135	0	0	3.1929	0.95385

Bus25	0.96485	-0.06219	0	0	9.2208	1.9429
Bus26	0.94365	-0.33931	0	0	4.3392	0.5306
Bus27	0.93064	-0.37471	0	0	11.9328	3.2061
Bus28	0.99191	-0.48143	0	0	7.0512	0.9447
Bus29	1.0303	-0.50878	0	0	21.696	2.0586
Bus3	0.93527	-0.08205	0	0	17.19	0.1284
Bus30	1.03	0.22766	76.13	10.0401	0	0
Bus31	0.982	0	18.3947	31.4498	0	0
Bus32	0.9831	0.1828	56.88	41.1759	0	0
Bus33	0.9972	1.1349	55.89	59.5259	0	0
Bus34	1.0265	1.3101	66.78	39.7406	0	0
Bus35	1.0493	-0.29901	4.65	42.0983	0	0
Bus36	1.0635	-0.29345	4.01	17.6621	0	0
Bus37	1.0123	0.01484	19.37	25.1046	0	0
Bus38	1.0278	-0.49441	6.59	18.5479	0	0
Bus39	1.0475	-0.16529	34.88	33.0631	58.951	13.349
Bus4	0.95103	-0.10066	0	0	26.69	9.8252
Bus5	0.99021	-0.08633	0	0	0	0
Bus6	0.99991	-0.07444	0	0	0	0
Bus7	0.98633	-0.11611	0	0	12.48	4.4854
Bus8	0.98428	-0.12674	0	0	27.87	9.398
Bus9	1.016	-0.1471	0	0	0	0

LINE FLOWS

From Bus	To Bus	Line	P Flow [p.u.]	Q Flow [p.u.]	P Loss [p.u.]	Q Loss [p.u.]
Bus1	Bus2	1	-20.2033	10.1947	0.13023	1.4795
Bus39	Bus1	2	-20.1106	12.3683	0.09267	2.1737
Bus11	Bus10	3	-32.843	-3.8271	0.07889	0.83498
Bus10	Bus13	4	23.9581	22.3607	0.07665	0.81109
Bus14	Bus13	5	-23.0269	-18.3054	0.1567	1.729
Bus14	Bus15	6	7.0896	19.2627	0.1531	1.7906
Bus15	Bus16	7	-8.9596	9.8716	0.03864	0.38065
Bus17	Bus16	8	-5.1548	12.827	0.03192	0.38769
Bus19	Bus16	9	87.4297	59.4784	8.2702	100.6685
Bus16	Bus21	10	23.2466	8.6481	0.12364	2.052
Bus16	Bus24	11	26.0393	-12.1521	0.0622	1.2152
Bus18	Bus17	12	-5.1229	13.1812	0.03184	0.35423
Bus2	Bus25	13	31.1075	13.309	1.1126	1.3486
Bus2	Bus3	14	24.689	13.7731	0.1978	2.2548
Bus21	Bus22	15	17.1425	-13.2101	0.2877	4.9011
Bus22	Bus23	16	1.3348	1Z.5555	0.01733	0.24418
Bus23	Bus24	17	-22.3609	19.0836	0.42342	6.6701
Bus25	Bus26	18	40.0471	4.7546	1.0898	10.9094
Bus26	Bus27	19	11.9776	3.6386	0.04483	0.4325
Bus26	Bus28	20	11.4265	4.3356	0.16998	1.7006
Bus26	Bus29	21	11.214	5.9884	0.22925	2.2895
Bus28	Bus29	22	4.2053	6.9808	0.03573	0.28815
Bus3	Bus18	23	3.2711	15.42	0.05693	0.65581
Bus4	Bus3	24	-4.0213	4.1374	0.00874	0.10737

Bus4	Bus14	25	-15.8962	1.5965	0.04105	0.63928
Bus5	Bus4	26	6.8187	16.2761	0.04625	0.71706
Bus8	Bus5	27	-19.413	1.1029	0.05676	0.76849
Bus6	Bus11	28	-32.9457	1.057	0.13831	1.5949
Bus6	Bus5	29	26.3264	18.6315	0.03788	0.48408
Bus7	Bus6	30	-24.9405	-5.8793	0.07361	1.1085
Bus8	Bus7	31	-12.4487	-1.2725	0.01175	0.1214
Bus9	Bus8	32	-3.9722	7.2822	0.0195	0.25955
Bus9	Bus39	33	3.9722	-7.2822	0.01183	0.06355
Bus25	Bus37	34	-19.273	-21.3552	0.09697	3.7495
Bus29	Bus38	35	-6.5417	-17.6054	0.04833	0.94247
Bus12	Bus13	36	-0.69712	-1.4932	0.00081	0.0219
Bus12	Bus11	37	0.24412	-3.2058	0.00307	0.08337
Bus23	Bus36	38	-3.9836	-16.2278	0.02636	1.4343
Bus30	Bus2	39	76.13	10.0401	0	18.2912
Bus6	Bus31	40	-18.3947	-26.6763	0	4.7735
Bus10	Bus32	41	-56.88	-27.0227	0	14.1532
Bus20	Bus34	42	-65.8752	-21.6446	0.9048	18.0961
Bus19	Bus33	43	-55.239	-46.3203	0.65098	13.2056
Bus19	Bus20	44	-32.1907	-13.1581	0.15149	2.9865
Bus22	Bus35	45	-4.65	-38.2605	0	3.8377

LINE FLOWS

From Bus	To Bus	Line	P Flow [p.u.]	Q Flow [p.u.]	P Loss [p.u.]	Q Loss [p.u.]
Bus2	Bus1	1	20.3335	-8.7152	0.13023	1.4795
Bus1	Bus39	2	20.2033	-10.1947	0.09267	2.1737
Bus10	Bus11	3	32.9219	4.6621	0.07889	0.83498
Bus13	Bus10	4	-23.8815	-21.5496	0.07665	0.81109
Bus13	Bus14	5	23.1836	20.0344	0.1567	1.729
Bus15	Bus14	6	-6.9365	-17.4721	0.1531	1.7906
Bus16	Bus15	7	8.9983	-9.4909	0.03864	0.38065
Bus16	Bus17	8	5.1867	-12.4393	0.03192	0.38769
Bus16	Bus19	9	-79.1596	41.1901	8.2702	100.6685
Bus21	Bus16	10	-23.1229	10.7001	0.12364	2.052
Bus24	Bus16	11	-25.9771	13.3673	0.0622	1.2152
Bus17	Bus18	12	5.1548	-12.827	0.03184	0.35423
Bus25	Bus2	13	-29.9949	14.6577	1.1126	1.3486
Bus3	Bus2	14	-24.4912	-11.5184	0.1978	2.2548
Bus22	Bus21	15	-16.8548	18.1112	0.2877	4.9011
Bus23	Bus22	16	-1.3175	-12.3113	0.01733	0.24418
Bus24	Bus23	17	22.7843	-12.4135	0.42342	6.6701
Bus26	Bus25	18	-38.9573	6.1547	1.0898	10.9094
Bus27	Bus26	19	-11.9328	-3.2061	0.04483	0.4325
Bus28	Bus26	20	-11.2565	6.0361	0.16998	1.7006
Bus29	Bus26	21	-10.9847	8.2779	0.22925	2.2895
Bus29	Bus28	22	-4.1696	7.269	0.03573	0.28815
Bus18	Bus3	23	-3.2142	-14.7642	0.05693	0.65581
Bus3	Bus4	24	4.0301	-4.03	0.00874	0.10737

Bus14	Bus4	25	15.9372	-0.95721	0.04105	0.63928
Bus4	Bus5	26	-6.7725	-15.5591	0.04625	0.71706
Bus5	Bus8	27	19.4698	1.8714	0.05676	0.76849
Bus11	Bus6	28	33.084	0.53795	0.13831	1.5949
Bus5	Bus6	29	-26.2885	-18.1475	0.03788	0.48408
Bus6	Bus7	30	25.0141	6.9878	0.07361	1.1085
Bus7	Bus8	31	12.4605	1.3939	0.01175	0.1214
Bus8	Bus9	32	3.9917	-7.0226	0.0195	0.25955
Bus39	Bus9	33	-3.9604	7.3457	0.01183	0.06355
Bus37	Bus25	34	19.37	25.1046	0.09697	3.7495
Bus38	Bus29	35	6.59	18.5479	0.04833	0.94247
Bus13	Bus12	36	0.69792	1.5151	0.00081	0.0219
Bus11	Bus12	37	-0.24105	3.2892	0.00307	0.08337
Bus36	Bus23	38	4.01	17.6621	0.02636	1.4343
Bus2	Bus30	39	-76.13	8.2511	0	18.2912
Bus31	Bus6	40	18.3947	31.4498	0	4.7735
Bus32	Bus10	41	56.88	41.1759	0	14.1532
Bus34	Bus20	42	66.78	39.7406	0.9048	18.0961
Bus33	Bus19	43	55.89	59.5259	0.65098	13.2056
Bus20	Bus19	44	32.3422	16.1446	0.15149	2.9865
Bus35	Bus22	45	4.65	42.0983	0	3.8377

GLOBAL SUMMARY REPORT

TOTAL GENERATION

REAL POWER [p.u.]	343.5747
REACTIVE POWER [p.u.]	318.4083

TOTAL LOAD

REAL POWER [p.u.]	328.3342
REACTIVE POWER [p.u.]	85.3972

TOTAL LOSSES

REAL POWER [p.u.]	15.2405
REACTIVE POWER [p.u.]	233.0111

E.2. Load Flow Results for 10% Penetration in Summer

POWER FLOW REPORT

P S A T 2.0.0

Author: Federico Milano, (c) 2002-2007
e-mail: fmilano@thunderbox.uwaterloo.ca
website: http://thunderbox.uwaterloo.ca/~fmilano
File: C:\Program Files\MATLAB\R2006b\work\IEEE 39 Models\Geyser_S_10.mdl
Date: 23-Apr-2008 12:59:22

NETWORK STATISTICS

Buses:	39
Lines:	33
Transformers:	12
Generators:	10
Loads:	30

SOLUTION STATISTICS

Number of iterations:	7
Maximum P mismatch [p.u.]	0
Maximum Q mismatch [p.u.]	0
Power rate [MVA]	100

POWER FLOW RESULTS

Bus	V [p.u.]	phase [rad]	P gen [p.u.]	Q gen [p.u.]	P load [p.u.]	Q load [p.u.]
Bus1	1.0012	-0.06678	0	0	0	0
Bus10	1.0096	0.00471	0	0	0	0
Bus11	1.004	-0.02052	0	0	0	0
Bus12	0.99054	-0.01751	0	0	0.453	4.699
Bus13	0.99078	-0.01222	0	0	0	0
Bus14	0.9507	-0.05349	0	0	0	0
Bus15	0.86868	-0.07867	0	0	15.9186	7.6112
Bus16	0.85125	-0.05522	0	0	15.7155	1.5429
Bus17	0.87408	-0.06857	0	0	0	0
Bus18	0.89516	-0.08044	0	0	8.3463	1.5847
Bus19	1.0083	1.0212	0	0	0	0
Bus2	0.97787	-0.00269	0	0	0	0
Bus20	0.93266	1.0962	0	0	33.533	5.5
Bus21	0.87485	-0.13329	0	0	5.99	2.514
Bus22	1.0036	-0.30105	0	0	20.17	7.5939
Bus23	0.98166	-0.30185	0	0	27.4246	9.3743
Bus24	0.86557	-0.09384	0	0	3.1983	-0.95548
Bus25	0.96546	-0.05306	0	0	9.2208	1.9429
Bus26	0.94488	-0.32747	0	0	4.3392	0.5306

Bus27	0.93189	-0.36278	0	0	11.9328	3.2061
Bus28	0.99279	-0.46765	0	0	7.0512	0.9447
Bus29	1.0309	-0.4942	0	0	21.4102	2.0315
Bus3	0.93558	-0.07458	0	0	17.19	0.1284
Bus30	1.03	0.23633	76.13	9.9623	0	0
Bus31	0.982	0	17.292	31.3033	0	0
Bus32	0.9831	0.18774	56.88	41.0992	0	0
Bus33	0.9972	1.1403	55.89	59.3961	0	0
Bus34	1.0265	1.3155	66.78	39.6864	0	0
Bus35	1.0493	-0.29012	4.65	41.946	0	0
Bus36	1.0635	-0.28438	4.01	17.5573	0	0
Bus37	1.0123	0.02394	19.37	24.9523	0	0
Bus38	1.0278	-0.47981	6.59	18.3389	0	0
Bus39	1.0475	-0.15581	34.88	32.805	58.3839	13.2206
Bus4	0.95137	-0.09493	0	0	26.69	9.8252
Bus5	0.99051	-0.08155	0	0	0	0
Bus6	1.0002	-0.06996	0	0	0	0
Bus7	0.98663	-0.11113	0	0	12.48	4.4854
Bus8	0.98459	-0.12151	0	0	27.87	9.398
Bus9	1.0162	-0.13967	0	0	0	0

LINE FLOWS

From Bus	To Bus	Line	P Flow [p.u.]	Q Flow [p.u.]	P Loss [p.u.]	Q Loss [p.u.]
Bus1	Bus2	1	-20.1101	10.163	0.12906	1.4658
Bus39	Bus1	2	-20.0183	12.3159	0.09184	2.1529
Bus11	Bus10	3	-33.0617	-3.8007	0.07988	0.84558
Bus10	Bus13	4	23.7384	22.3179	0.07573	0.80118
Bus14	Bus13	5	-22.7886	-18.2947	0.15452	1.7046
Bus14	Bus15	6	6.8681	19.2305	0.15141	1.7701
Bus15	Bus16	7	-9.2018	9.8492	0.03945	0.38901
Bus17	Bus16	8	-5.1363	12.7685	0.03159	0.38352
Bus19	Bus16	9	87.4321	59.3419	8.2537	100.4673
Bus16	Bus21	10	23.1507	-8.6509	0.12255	2.0335
Bus16	Bus24	11	25.9031	-12.1724	0.0616	1.2034
Bus18	Bus17	12	-5.1048	13.1189	0.03151	0.3504
Bus2	Bus25	13	30.7699	-13.3676	1.0933	1.3249
Bus2	Bus3	14	25.1209	13.7407	0.20281	2.3129
Bus21	Bus22	15	17.0382	-13.1984	0.28485	4.8511
Bus22	Bus23	16	1.2333	12.4923	0.01711	0.24076
Bus23	Bus24	17	-22.2244	19.0164	0.41877	6.5961
Bus25	Bus26	18	39.7296	4.5959	1.0705	10.7143
Bus26	Bus27	19	11.9775	3.6372	0.04471	0.43114
Bus26	Bus28	20	11.2932	-4.3208	0.16593	1.6556
Bus26	Bus29	21	11.0492	-5.9654	0.22304	2.221
Bus28	Bus29	22	4.0761	-6.9212	0.03464	0.27624
Bus3	Bus18	23	3.298	15.3538	0.05647	0.65017
Bus4	Bus3	24	-4.4204	4.1775	0.0097	0.12309
Bus4	Bus14	25	-15.8795	1.573	0.04093	0.63722

Bus5	Bus4	26	6.4356	16.2806	0.04549	0.7049
Bus8	Bus5	27	-19.2108	-1.1209	0.05556	0.75165
Bus6	Bus11	28	-33.1841	1.104	0.14026	1.6177
Bus6	Bus5	29	25.7387	18.6223	0.03673	0.46919
Bus7	Bus6	30	-24.6653	-5.8934	0.07206	1.0846
Bus8	Bus7	31	-12.1741	-1.2925	0.01124	0.11552
Bus9	Bus8	32	-3.4967	7.2245	0.01825	0.23987
Bus9	Bus39	33	3.4967	-7.2245	0.01106	0.04411
Bus25	Bus37	34	-19.2738	-21.2313	0.09623	3.721
Bus29	Bus38	35	-6.5426	-17.4152	0.04737	0.92372
Bus12	Bus13	36	-0.71873	-1.4953	0.00082	0.02219
Bus12	Bus11	37	0.26573	-3.2038	0.00306	0.08331
Bus23	Bus36	38	-3.9839	-16.1391	0.02607	1.4182
Bus30	Bus2	39	76.13	9.9623	0	18.2864
Bus6	Bus31	40	-17.292	-26.7044	0	4.599
Bus10	Bus32	41	-56.88	-26.9642	0	14.135
Bus20	Bus34	42	-65.8758	-21.6033	0.90416	18.0832
Bus19	Bus33	43	-55.2405	-46.2211	0.64947	13.175
Bus19	Bus20	44	-32.1916	-13.1208	0.15129	2.9825
Bus22	Bus35	45	-4.65	-38.1357	0	3.8104

LINE FLOWS

From Bus	To Bus	Line	P Flow [p.u.]	Q Flow [p.u.]	P Loss [p.u.]	Q Loss [p.u.]
Bus2	Bus1	1	20.2392	-8.6972	0.12906	1.4658
Bus1	Bus39	2	20.1101	-10.163	0.09184	2.1529
Bus10	Bus11	3	33.1416	4.6463	0.07988	0.84558
Bus13	Bus10	4	-23.6627	-21.5167	0.07573	0.80118
Bus13	Bus14	5	22.9431	19.9992	0.15452	1.7046
Bus15	Bus14	6	-6.7167	-17.4604	0.15141	1.7701
Bus16	Bus15	7	9.2413	-9.4602	0.03945	0.38901
Bus16	Bus17	8	5.1679	-12.385	0.03159	0.38352
Bus16	Bus19	9	-79.1784	41.1255	8.2537	100.4673
Bus21	Bus16	10	-23.0282	10.6843	0.12255	2.0335
Bus24	Bus16	11	-25.8415	13.3758	0.0616	1.2034
Bus17	Bus18	12	5.1363	-12.7685	0.03151	0.3504
Bus25	Bus2	13	-29.6766	14.6925	1.0933	1.3249
Bus3	Bus2	14	-24.9181	-11.4278	0.20281	2.3129
Bus22	Bus21	15	-16.7533	18.0495	0.28485	4.8511
Bus23	Bus22	16	-1.2162	-12.2516	0.01711	0.24076
Bus24	Bus23	17	22.6432	-12.4203	0.41877	6.5961
Bus26	Bus25	18	-38.6591	6.1184	1.0705	10.7143
Bus27	Bus26	19	-11.9328	-3.2061	0.04471	0.43114
Bus28	Bus26	20	-11.1273	5.9765	0.16593	1.6556
Bus29	Bus26	21	-10.8262	8.1863	0.22304	2.221
Bus29	Bus28	22	-4.0414	7.1974	0.03464	0.27624
Bus18	Bus3	23	-3.2416	-14.7036	0.05647	0.65017
Bus3	Bus4	24	4.4301	-4.0544	0.0097	0.12309

Bus14	Bus4	25	15.9205	-0.93579	0.04093	0.63722
Bus4	Bus5	26	-6.3901	-15.5757	0.04549	0.7049
Bus5	Bus8	27	19.2664	1.8725	0.05556	0.75165
Bus11	Bus6	28	33.3244	0.51365	0.14026	1.6177
Bus5	Bus6	29	-25.702	-18.1531	0.03673	0.46919
Bus6	Bus7	30	24.7374	6.9781	0.07206	1.0846
Bus7	Bus8	31	12.1853	1.408	0.01124	0.11552
Bus8	Bus9	32	3.5149	-6.9846	0.01825	0.23987
Bus39	Bus9	33	-3.4856	7.2686	0.01106	0.04411
Bus37	Bus25	34	19.37	24.9523	0.09623	3.721
Bus38	Bus29	35	6.59	18.3389	0.04737	0.92372
Bus13	Bus12	36	0.71955	1.5174	0.00082	0.02219
Bus11	Bus12	37	-0.26267	3.2871	0.00306	0.08331
Bus36	Bus23	38	4.01	17.5573	0.02607	1.4182
Bus2	Bus30	39	-76.13	8.3241	0	18.2864
Bus31	Bus6	40	17.292	31.3033	0	4.599
Bus32	Bus10	41	56.88	41.0992	0	14.135
Bus34	Bus20	42	66.78	39.6864	0.90416	18.0832
Bus33	Bus19	43	55.89	59.3961	0.64947	13.175
Bus20	Bus19	44	32.3428	16.1033	0.15129	2.9825
Bus35	Bus22	45	4.65	41.946	0	3.8104

GLOBAL SUMMARY REPORT

TOTAL GENERATION

REAL POWER [p.u.]	342.472
REACTIVE POWER [p.u.]	317.0469

TOTAL LOAD

REAL POWER [p.u.]	327.3173
REACTIVE POWER [p.u.]	85.178

TOTAL LOSSES

REAL POWER [p.u.]	15.1547
REACTIVE POWER [p.u.]	231.8689

E.3. Load Flow Results for 10% Penetration in Winter

POWER FLOW REPORT

P S A T 2.0.0

Author: Federico Milano, (c) 2002-2007
e-mail: fmilano@thunderbox.uwaterloo.ca
website: http://thunderbox.uwaterloo.ca/~fmilano
File: C:\Program Files\MATLAB\R2006b\work\IEEE 39 Models\Geyser_W_10.mdl
Date: 23-Apr-2008 13:40:08

NETWORK STATISTICS

Buses:	39
Lines:	33
Transformers:	12
Generators:	10
Loads:	30

SOLUTION STATISTICS

Number of iterations:	7
Maximum P mismatch [p.u.]	0
Maximum Q mismatch [p.u.]	0
Power rate [MVA]	100

POWER FLOW RESULTS

Bus	V [p.u.]	phase [rad]	P gen [p.u.]	Q gen [p.u.]	P load [p.u.]	Q load [p.u.]
Bus1	1.0011	-0.06888	0	0	0	0
Bus10	1.0096	0.00358	0	0	0	0
Bus11	1.0039	-0.02161	0	0	0	0
Bus12	0.99049	-0.01864	0	0	0.453	4.699
Bus13	0.99073	-0.01339	0	0	0	0
Bus14	0.95064	-0.05477	0	0	0	0
Bus15	0.86859	-0.08018	0	0	15.9152	7.6096
Bus16	0.85114	-0.05684	0	0	15.7115	1.5425
Bus17	0.87399	-0.07025	0	0	0	0
Bus18	0.89508	-0.08216	0	0	8.3449	1.5844
Bus19	1.0082	1.0199	0	0	0	0
Bus2	0.9778	-0.00489	0	0	0	0
Bus20	0.93264	1.0948	0	0	33.533	5.5
Bus21	0.87475	-0.13496	0	0	5.9886	2.5134
Bus22	1.0035	-0.30287	0	0	20.17	7.5939
Bus23	0.9816	-0.3037	0	0	27.4532	9.3841
Bus24	0.86546	-0.09549	0	0	3.1975	-0.95524
Bus25	0.96518	-0.05545	0	0	9.2208	1.9429
Bus26	0.94427	-0.33124	0	0	4.3392	0.5306

Bus27	0.93127	-0.36659	0	0	11.9328	3.2061
Bus28	0.99235	-0.47241	0	0	7.0512	0.9447
Bus29	1.0306	-0.49938	0	0	21.5579	2.0455
Bus3	0.93552	-0.07638	0	0	17.19	0.1284
Bus30	1.03	0.23415	76.13	9.9861	0	0
Bus31	0.982	0	17.5391	31.3322	0	0
Bus32	0.9831	0.18662	56.88	41.112	0	0
Bus33	0.9972	1.1389	55.89	59.4152	0	0
Bus34	1.0265	1.3141	66.78	39.6944	0	0
Bus35	1.0493	-0.29195	4.65	41.9666	0	0
Bus36	1.0635	-0.28623	4.01	17.5712	0	0
Bus37	1.0123	0.02156	19.37	25.0211	0	0
Bus38	1.0278	-0.48499	6.59	18.4435	0	0
Bus39	1.0475	-0.15776	34.88	32.8329	58.4362	13.2324
Bus4	0.95131	-0.09625	0	0	26.69	9.8252
Bus5	0.99046	-0.08262	0	0	0	0
Bus6	1.0001	-0.07096	0	0	0	0
Bus7	0.98658	-0.11223	0	0	12.48	4.4854
Bus8	0.98453	-0.12266	0	0	27.87	9.398
Bus9	1.0161	-0.14123	0	0	0	0

LINE FLOWS

From Bus	To Bus	Line	P Flow [p.u.]	Q Flow [p.u.]	P Loss [p.u.]	Q Loss [p.u.]
Bus1	Bus2	1	-20.0736	10.171	0.12874	1.462
Bus39	Bus1	2	-19.982	12.3181	0.09161	2.1471
Bus11	Bus10	3	-33.0091	-3.8066	0.07964	0.84299
Bus10	Bus13	4	23.7913	22.3244	0.07594	0.8034
Bus14	Bus13	5	-22.846	-18.2939	0.15501	1.7101
Bus14	Bus15	6	6.9149	19.2329	0.15169	1.7736
Bus15	Bus16	7	-9.152	9.8497	0.03926	0.38705
Bus17	Bus16	8	-5.1597	12.7772	0.03168	0.38459
Bus19	Bus16	9	87.4317	59.3619	8.2561	100.4969
Bus16	Bus21	10	23.1621	-8.6514	0.12269	2.0358
Bus16	Bus24	11	25.9194	-12.1709	0.06168	1.2049
Bus18	Bus17	12	-5.1281	13.1285	0.0316	0.35138
Bus2	Bus25	13	30.9437	-13.329	1.1029	1.3367
Bus2	Bus3	14	24.984	13.7362	0.20111	2.2932
Bus21	Bus22	15	17.0508	-13.2006	0.28522	4.8576
Bus22	Bus23	16	1.2456	12.5004	0.01714	0.2412
Bus23	Bus24	17	-22.2409	19.026	0.41936	6.6055
Bus25	Bus26	18	39.8935	4.6787	1.0804	10.8139
Bus26	Bus27	19	11.9776	3.6379	0.04477	0.43181
Bus26	Bus28	20	11.3621	-4.3275	0.16799	1.6785
Bus26	Bus29	21	11.1343	-5.9761	0.2262	2.2558
Bus28	Bus29	22	4.1429	-6.9508	0.03519	0.28224
Bus3	Bus18	23	3.2733	15.3636	0.05651	0.65065
Bus4	Bus3	24	-4.3101	4.1676	0.00943	0.11865
Bus4	Bus14	25	-15.8901	1.5772	0.04099	0.63821

Bus5	Bus4	26	6.5355	16.2778	0.04568	0.70784
Bus8	Bus5	27	-19.246	-1.1179	0.05577	0.75456
Bus6	Bus11	28	-33.1268	1.0929	0.13979	1.6121
Bus6	Bus5	29	25.8742	18.6229	0.03699	0.47255
Bus7	Bus6	30	-24.7193	-5.8907	0.07236	1.0893
Bus8	Bus7	31	-12.228	-1.2886	0.01134	0.11666
Bus9	Bus8	32	-3.5855	7.2348	0.01847	0.24335
Bus9	Bus39	33	3.5855	-7.2348	0.0112	0.04756
Bus25	Bus37	34	-19.2734	-21.2873	0.09656	3.7338
Bus29	Bus38	35	-6.5422	-17.5104	.0.04785	0.93308
Bus12	Bus13	36	-0.71353	-1.4949	0.00081	0.02212
Bus12	Bus11	37	0.26053	-3.2041	0.00306	0.08331
Bus23	Bus36	38	-3.9839	-16.1509	0.02611	1.4203
Bus30	Bus2	39	76.13	9.9861	0	18.2878
Bus6	Bus31	40	-17.5391	-26.6958	0	4.6364
Bus10	Bus32	41	-56.88	-26.9739	0	14.1381
Bus20	Bus34	42	-65.8758	-21.6093	0.90425	18.0851
Bus19	Bus33	43	-55.2403	-46.2357	0.6497	13.1795
Bus19	Bus20	44	-32.1914	-13.1263	0.15132	2.9831
Bus22	Bus35	45	-4.65	-38.1525	0	3.814

LINE FLOWS

From Bus	To Bus	Line	P Flow [p.u.]	Q Flow [p.u.]	P Loss [p.u.]	Q Loss [p.u.]
Bus2	Bus1	1	20.2023	-8.709	0.12874	1.462
Bus1	Bus39	2	20.0736	-10.171	0.09161	2.1471
Bus10	Bus11	3	33.0887	4.6496	0.07964	0.84299
Bus13	Bus10	4	-23.7153	-21.521	0.07594	0.8034
Bus13	Bus14	5	23.001	20.0039	0.15501	1.7101
Bus15	Bus14	6	-6.7632	-17.4593	0.15169	1.7736
Bus16	Bus15	7	9.1912	-9.4626	0.03926	0.38705
Bus16	Bus17	8	5.1913	-12.3926	0.03168	0.38459
Bus16	Bus19	9	-79.1757	41.1349	8.2561	100.4969
Bus21	Bus16	10	-23.0394	10.6872	0.12269	2.0358
Bus24	Bus16	11	-25.8578	13.3757	0.06168	1.2049
Bus17	Bus18	12	5.1597	-12.7772	0.0316	0.35138
Bus25	Bus2	13	-29.8409	14.6656	1.1029	1.3367
Bus3	Bus2	14	-24.7829	-11.4431	0.20111	2.2932
Bus22	Bus21	15	-16.7656	18.0582	0.28522	4.8576
Bus23	Bus22	16	-1.2284	-12.2592	0.01714	0.2412
Bus24	Bus23	17	22.6602	-12.4205	0.41936	6.6055
Bus26	Bus25	18	-38.8131	6.1351	1.0804	10.8139
Bus27	Bus26	19	-11.9328	-3.2061	0.04477	0.43181
Bus28	Bus26	20	-11.1941	6.0061	0.16799	1.6785
Bus29	Bus26	21	-10.9081	8.2319	0.2262	2.2558
Bus29	Bus28	22	-4.1077	7.233	0.03519	0.28224
Bus18	Bus3	23	-3.2168	-14.713	0.05651	0.65065
Bus3	Bus4	24	4.3196	-4.049	0.00943	0.11865

Bus14	Bus4	25	15.9311	-0.93899	0.04099	0.63821
Bus4	Bus5	26	-6.4898	-15.57	0.04568	0.70784
Bus5	Bus8	27	19.3017	1.8725	0.05577	0.75456
Bus11	Bus6	28	33.2666	0.51919	0.13979	1.6121
Bus5	Bus6	29	-25.8372	-18.1503	0.03699	0.47255
Bus6	Bus7	30	24.7917	6.98	0.07236	1.0893
Bus7	Bus8	31	12.2393	1.4053	0.01134	0.11666
Bus8	Bus9	32	3.604	-6.9915	0.01847	0.24335
Bus39	Bus9	33	-3.5743	7.2824	0.0112	0.04756
Bus37	Bus25	34	19.37	25.0211	0.09656	3.7338
Bus38	Bus29	35	6.59	18.4435	0.04785	0.93308
Bus13	Bus12	36	0.71434	1.517	0.00081	0.02212
Bus11	Bus12	37	-0.25746	3.2874	0.00306	0.08331
Bus36	Bus23	38	4.01	17.5712	0.02611	1.4203
Bus2	Bus30	39	-76.13	8.3017	0	18.2878
Bus31	Bus6	40	17.5391	31.3322	0	4.6364
Bus32	Bus10	41	56.88	41.112	0	14.1381
Bus34	Bus20	42	66.78	39.6944	0.90425	18.0851
Bus33	Bus19	43	55.89	59.4152	0.6497	13.1795
Bus20	Bus19	44	32.3428	16.1093	0.15132	2.9831
Bus35	Bus22	45	4.65	41.9666	0	3.814

GLOBAL SUMMARY REPORT

TOTAL GENERATION

REAL POWER [p.u.]	342.7191
REACTIVE POWER [p.u.]	317.3751

TOTAL LOAD

REAL POWER [p.u.]	327.5351
REACTIVE POWER [p.u.]	85.211

TOTAL LOSSES

REAL POWER [p.u.]	15.184
REACTIVE POWER [p.u.]	232.1641

E.4. Load Flow Results for 50% Penetration in Summer

POWER FLOW REPORT

P S A T 2.0.0

Author: Federico Milano, (c) 2002-2007
e-mail: fmilano@thunderbox.uwaterloo.ca
website: http://thunderbox.uwaterloo.ca/~fmilano
File: C:\Program Files\MATLAB\R2006b\work\IEEE 39 Models\Geyser _S_50.mdl
Date: 23-Apr-2008 12:56:28

NETWORK STATISTICS

Buses:	39
Lines:	33
Transformers:	12
Generators:	10
Loads:	30

SOLUTION STATISTICS

Number of iterations:	7
Maximum P mismatch [p.u.]	0
Maximum Q mismatch [p.u.]	0
Power rate [MVA]	100

POWER FLOW RESULTS

Bus	V [p.u.]	phase [rad]	P gen [p.u.]	Q gen [p.u.]	P load [p.u.]	Q load [p.u.]
Bus1	1.0018	-0.03068	0	0	0	0
Bus10	1.0104	0.02464	0	0	0	0
Bus11	1.0048	-0.00124	0	0	0	0
Bus12	0.99145	0.00245	0	0	0.453	4.699
Bus13	0.99177	0.00841	0	0	0	0
Bus14	0.95205	-0.03089	0	0	0	0
Bus15	0.87086	-0.05176	0	0	15.9983	7.6494
Bus16	0.85385	-0.02622	0	0	15.8118	1.5524
Bus17	0.87623	-0.03932	0	0	0	0
Bus18	0.89688	-0.05096	0	0	8.3785	1.5908
Bus19	1.0093	1.0438	0	0	0	0
Bus2	0.97869	0.03215	0	0	0	0
Bus20	0.93326	1.1186	0	0	33.533	5.5
Bus21	0.87741	-0.10257	0	0	6.0251	2.5287
Bus22	1.0049	-0.26564	0	0	20.17	7.5939
Bus23	0.98351	-0.26575	0	0	26.4748	9.0497
Bus24	0.86825	-0.06383	0	0	3.2181	-0.9614
Bus25	0.96775	-0.01666	0	0	9.2208	1.9429
Bus26	0.94957	-0.28046	0	0	4.3392	0.5306

Bus27	0.93665	-0.31541	0	0	11.9328	3.2061
Bus28	0.99617	-0.41303	0	0	7.0512	0.9447
Bus29	1.033	-0.43642	0	0	20.2671	1.923
Bus3	0.93662	-0.04479	0	0	17.19	0.1284
Bus30	1.03	0.27098	76.13	9.6873	0	0
Bus31	0.982	0	12.8771	30.8221	0	0
Bus32	0.9831	0.20752	56.88	40.847	0	0
Bus33	0.9972	1.1627	55.89	58.9336	0	0
Bus34	1.0265	1.3378	66.78	39.4934	0	0
Bus35	1.0493	-0.25473	4.65	41.3739	0	0
Bus36	1.0635	-0.24828	4.01	17.1602	0	0
Bus37	1.0123	0.06022	19.37	24.374	0	0
Bus38	1.0278	-0.42195	6.59	17.5353	0	0
Bus39	1.0475	-0.11801	34.88	31.8358	56.1155	12.7069
Bus4	0.95249	-0.07205	0	0	26.69	9.8252
Bus5	0.99146	-0.06249	0	0	0	0
Bus6	1.001	-0.05203	0	0	0	0
Bus7	0.9876	-0.09126	0	0	12.48	4.4854
Bus8	0.98558	-0.10067	0	0	27.87	9.398
Bus9	1.0169	-0.11003	0	0	0	0

LINE FLOWS

From Bus	To Bus	Line	P Flow [p.u.]	Q Flow [p.u.]	P Loss [p.u.]	Q Loss [p.u.]
Bus1	Bus2	1	-19.7376	10.0497	0.12455	1.4128
Bus39	Bus1	2	-19.649	12.1221	0.08863	2.0724
Bus11	Bus10	3	-33.9408	-3.7164	0.08395	0.88933
Bus10	Bus13	4	22.8553	22.1656	0.0722	0.76317
Bus14	Bus13	5	-21.8305	-18.2647	0.14617	1.6108
Bus14	Bus15	6	5.9724	19.1112	0.14517	1.6948
Bus15	Bus16	7	-10.1711	9.7671	0.04295	0.42551
Bus17	Bus16	8	-5.0671	12.5445	0.03038	0.36801
Bus19	Bus16	9	87.4404	58.8548	8.1952	99.7543
Bus16	Bus21	10	22.7655	-8.6714	0.11834	1.9623
Bus16	Bus24	11	25.3565	-12.2624	0.05929	1.1579
Bus18	Bus17	12	-5.0368	12.8806	0.0303	0.33613
Bus2	Bus25	13	29.4283	-13.5951	1.0191	1.2337
Bus2	Bus3	14	26.8395	13.6498	0.22389	2.5577
Bus21	Bus22	15	16.6221	-13.1624	0.27405	4.6615
Bus22	Bus23	16	0.82802	12.2478	0.01632	0.22801
Bus23	Bus24	17	-21.678	18.7724	0.40103	6.3135
Bus25	Bus26	18	38.4649	3.9877	0.99606	9.9623
Bus26	Bus27	19	11.9771	3.6321	0.04426	0.42599
Bus26	Bus28	20	10.7609	-4.2626	0.15048	1.4839
Bus26	Bus29	21	10.3917	-5.8748	0.19944	1.9606
Bus28	Bus29	22	3.5593	-6.6911	0.0306	0.23217
Bus3	Bus18	23	3.3965	15.1005	0.05473	0.62909
Bus4	Bus3	24	-6.0148	4.3363	0.01437	0.19946
Bus4	Bus14	25	-15.8177	1.4762	0.04047	0.62977

Bus5	Bus4	26	4.9005	16.3017	0.04293	0.66389
Bus8	Bus5	27	-18.4034	-1.1916	0.05092	0.6867
Bus6	Bus11	28	-34.142	1.2736	0.14826	1.7114
Bus6	Bus5	29	23.3872	18.5934	0.03243	0.41336
Bus7	Bus6	30	-23.5659	-5.95	0.06606	0.99262
Bus8	Bus7	31	-11.0766	-1.3712	0.00932	0.09344
Bus9	Bus8	32	-1.5953	7.0185	0.01467	0.18333
Bus9	Bus39	33	1.5953	-7.0185	0.00883	-0.01169
Bus25	Bus37	34	-19.2765	-20.7594	0.09348	3.6146
Bus29	Bus38	35	-6.5462	-16.6817	0.04377	0.85359
Bus12	Bus13	36	-0.80558	-1.5036	0.00086	0.02341
Bus12	Bus11	37	0.35258	-3.1954	0.00306	0.08316
Bus23	Bus36	38	-3.985	-15.8023	0.02496	1.3579
Bus30	Bus2	39	76.13	9.6873	0	18.2696
Bus6	Bus31	40	-12.8771	-26.8096	0	4.0125
Bus10	Bus32	41	-56.88	-26.7713	0	14.0757
Bus20	Bus34	42	-65.8781	-21.4561	0.90187	18.0374
Bus19	Bus33	43	-55.2459	-45.867	0.64413	13.0666
Bus19	Bus20	44	-32.1946	-12.9878	0.15056	2.9683
Bus22	Bus35	45	-4.65	-37.6656	0	3.7084

LINE FLOWS

From Bus	To Bus	Line	P Flow [p.u.]	Q Flow [p.u.]	P Loss [p.u.]	Q Loss [p.u.]
Bus2	Bus1	1	19.8622	-8.6369	0.12455	1.4128
Bus1	Bus39	2	19.7376	-10.0497	0.08863	2.0724
Bus10	Bus11	3	34.0247	4.6057	0.08395	0.88933
Bus13	Bus10	4	-22.7831	-21.4025	0.0722	0.76317
Bus13	Bus14	5	21.9767	19.8755	0.14617	1.6108
Bus15	Bus14	6	-5.8272	-17.4164	0.14517	1.6948
Bus16	Bus15	7	10.2141	-9.3416	0.04295	0.42551
Bus16	Bus17	8	5.0974	-12.1765	0.03038	0.36801
Bus16	Bus19	9	-79.2452	40.8995	8.1952	99.7543
Bus21	Bus16	10	-22.6472	10.6337	0.11834	1.9623
Bus24	Bus16	11	-25.2972	13.4203	0.05929	1.1579
Bus17	Bus18	12	5.0671	-12.5445	0.0303	0.33613
Bus25	Bus2	13	-28.4092	14.8288	1.0191	1.2337
Bus3	Bus2	14	-26.6156	-11.0921	0.22389	2.5577
Bus22	Bus21	15	-16.348	17.8239	0.27405	4.6615
Bus23	Bus22	16	-0.8117	-12.0198	0.01632	0.22801
Bus24	Bus23	17	22.079	-12.4589	0.40103	6.3135
Bus26	Bus25	18	-37.4689	5.9746	0.99606	9.9623
Bus27	Bus26	19	-11.9328	-3.2061	0.04426	0.42599
Bus28	Bus26	20	-10.6105	5.7464	0.15048	1.4839
Bus29	Bus26	21	-10.1922	7.8354	0.19944	1.9606
Bus29	Bus28	22	-3.5287	6.9233	0.0306	0.23217
Bus18	Bus3	23	-3.3417	-14.4714	0.05473	0.62909
Bus3	Bus4	24	6.0292	-4.1369	0.01437	0.19946

Bus14	Bus4	25	15.8581	-0.84647	0.04047	0.62977
Bus4	Bus5	26	-4.8575	-15.6378	0.04293	0.66389
Bus5	Bus8	27	18.4543	1.8783	0.05092	0.6867
Bus11	Bus6	28	34.2903	0.43778	0.14826	1.7114
Bus5	Bus6	29	-23.3548	-18.18	0.03243	0.41336
Bus6	Bus7	30	23.632	6.9427	0.06606	0.99262
Bus7	Bus8	31	11.0859	1.4646	0.00932	0.09344
Bus8	Bus9	32	1.61	-6.8352	0.01467	0.18333
Bus39	Bus9	33	-1.5865	7.0068	0.00883	-0.01169
Bus37	Bus25	34	19.37	24.374	0.09348	3.6146
Bus38	Bus29	35	6.59	17.5353	0.04377	0.85359
Bus13	Bus12	36	0.80645	1.527	0.00086	0.02341
Bus11	Bus12	37	-0.34953	3.2786	0.00306	0.08316
Bus36	Bus23	38	4.01	17.1602	0.02496	1.3579
Bus2	Bus30	39	-76.13	8.5823	0	18.2696
Bus31	Bus6	40	12.8771	30.8221	0	4.0125
Bus32	Bus10	41	56.88	40.847	0	14.0757
Bus34	Bus20	42	66.78	39.4934	0.90187	18.0374
Bus33	Bus19	43	55.89	58.9336	0.64413	13.0666
Bus20	Bus19	44	32.3451	15.9561	0.15056	2.9683
Bus35	Bus22	45	4.65	41.3739	0	3.7084

GLOBAL SUMMARY REPORT

TOTAL GENERATION

REAL POWER [p.u.]	338.0571
REACTIVE POWER [p.u.]	312.0628

TOTAL LOAD

REAL POWER [p.u.]	323.2191
REACTIVE POWER [p.u.]	84.2937

TOTAL LOSSES

REAL POWER [p.u.]	14.8381
REACTIVE POWER [p.u.]	227.7691

E.5. Load Flow Results for 50% Penetration in Winter

POWER FLOW REPORT

P S A T 2.0.0

Author: Federico Milano, (c) 2002-2007
e-mail: fmilano@thunderbox.uwaterloo.ca
website: http://thunderbox.uwaterloo.ca/~fmilano
File: C:\Program Files\MATLAB\R2006b\work\IEEE 39 Models\Geyser_W_50.mdl
Date: 23-Apr-2008 13:44:55

NETWORK STATISTICS

Buses:	39
Lines:	33
Transformers:	12
Generators:	10
Loads:	30

SOLUTION STATISTICS

Number of iterations:	7
Maximum P mismatch [p.u.]	0
Maximum Q mismatch [p.u.]	0
Power rate [MVA]	100

POWER FLOW RESULTS

Bus	V [p.u.]	phase [rad]	P gen [p.u.]	Q gen [p.u.]	P load [p.u.]	Q load [p.u.]
Bus1	1.0017	-0.0411	0	0	0	0
Bus10	1.0103	0.01902	0	0	0	0
Bus11	1.0046	-0.00666	0	0	0	0
Bus12	0.9913	-0.00317	0	0	0.453	4.699
Bus13	0.99159	0.00259	0	0	0	0
Bus14	0.95181	-0.0373	0	0	0	0
Bus15	0.8705	-0.05931	0	0	15.9852	7.6431
Bus16	0.85343	-0.03432	0	0	15.7961	1.5508
Bus17	0.87587	-0.04768	0	0	0	0
Bus18	0.89659	-0.05956	0	0	8.373	1.5898
Bus19	1.0092	1.0367	0	0	0	0
Bus2	0.97839	0.02121	0	0	0	0
Bus20	0.93316	1.1115	0	0	33.533	5.5
Bus21	0.877	-0.11093	0	0	6.0194	2.5264
Bus22	1.0047	-0.27472	0	0	20.17	7.5939
Bus23	0.98322	-0.27493	0	0	26.618	9.0987
Bus24	0.86782	-0.07208	0	0	3.2149	-0.96045
Bus25	0.96646	-0.02855	0	0	9.2208	1.9429
Bus26	0.9467	-0.29906	0	0	4.3392	0.5306

Bus27	0.93374	-0.33423	0	0	11.9328	3.2061
Bus28	0.99408	-0.43649	0	0	7.0512	0.9447
Bus29	1.0317	-0.46192	0	0	21.0056	1.9931
Bus3	0.93643	-0.05373	0	0	17.19	0.1284
Bus30	1.03	0.26011	76.13	9.7883	0	0
Bus31	0.982	0	14.1114	30.9246	0	0
Bus32	0.9831	0.20193	56.88	40.8896	0	0
Bus33	0.9972	1.1557	55.89	59.0084	0	0
Bus34	1.0265	1.3308	66.78	39.5246	0	0
Bus35	1.0493	-0.2638	4.65	41.4633	0	0
Bus36	1.0635	-0.25746	4.01	17.2219	0	0
Bus37	1.0123	0.0484	19.37	24.7	0	0
Bus38	1.0278	-0.44749	6.59	18.0355	0	0
Bus39	1.0475	-0.12766	34.88	31.9511	56.3772	12.7662
Bus4	0.95229	-0.07861	0	0	26.69	9.8252
Bus5	0.99129	-0.06781	0	0	0	0
Bus6	1.0009	-0.05703	0	0	0	0
Bus7	0.98743	-0.09673	0	0	12.48	4.4854
Bus8	0.98541	-0.10638	0	0	27.87	9.398
Bus9	1.0168	-0.11778	0	0	0	0

LINE FLOWS

From Bus	To Bus	Line	P Flow [p.u.]	Q Flow [p.u.]	P Loss [p.u.]	Q Loss [p.u.]
Bus1	Bus2	1	-19.5558	10.0828	0.12294	1.3939
Bus39	Bus1	2	-19.4684	12.1264	0.08747	2.0436
Bus11	Bus10	3	-33.6766	-3.7373	0.08269	0.87585
Bus10	Bus13	4	23.1207	22.1907	0.07317	0.77358
Bus14	Bus13	5	-22.1187	-18.2557	0.14847	1.6366
Bus14	Bus15	6	6.2096	19.1205	0.14642	1.7098
Bus15	Bus16	7	-9.9221	9.7676	0.04191	0.41464
Bus17	Bus16	8	-5.1816	12.5857	0.03077	0.37301
Bus19	Bus16	9	87.4391	58.9336	8.2046	99.8692
Bus16	Bus21	10	22.8233	-8.67	0.11898	1.9731
Bus16	Bus24	11	25.4387	-12.2507	0.05964	1.1648
Bus18	Bus17	12	-5.1509	12.9264	0.0307	0.34073
Bus2	Bus25	13	30.291	-13.4119	1.0649	1.29
Bus2	Bus3	14	26.1603	13.6135	0.21489	2.4532
Bus21	Bus22	15	16.6849	-13.1695	0.2757	4.6904
Bus22	Bus23	16	0.88917	12.2853	0.01644	0.22991
Bus23	Bus24	17	-21.7604	18.8115	0.40372	6.3564
Bus25	Bus26	18	39.2802	4.3809	1.0433	10.4392
Bus26	Bus27	19	11.9773	3.6352	0.04454	0.42913
Bus26	Bus28	20	11.1046	-4.296	0.16025	1.5925
Bus26	Bus29	21	10.8159	-5.9281	0.21431	2.1247
Bus28	Bus29	22	3.8931	-6.8332	0.03311	0.25954
Bus3	Bus18	23	3.277	15.1473	0.0549	0.63108
Bus4	Bus3	24	-5.4658	4.2862	0.01262	0.1708
Bus4	Bus14	25	-15.8684	1.4992	0.04075	0.63439

Bus5	Bus4	26	5.3995	16.2857	0.04363	0.67506
Bus8	Bus5	27	-18.5782	-1.1779	0.0519	0.70045
Bus6	Bus11	28	-33.8542	1.2256	0.1458	1.6826
Bus6	Bus5	29	24.0631	18.5926	0.03361	0.4286
Bus7	Bus6	30	-23.835	-5.9368	0.06749	1.0146
Bus8	Bus7	31	-11.3452	-1.3528	0.00977	0.09863
Bus9	Bus8	32	-2.0381	7.0605	0.0153	0.19318
Bus9	Bus39	33	2.0381	-7.0605	0.00922	-0.00197
Bus25	Bus37	34	-19.275	-21.0257	0.09503	3.6743
Bus29	Bus38	35	-6.544	-17.1386	0.04599	0.89687
Bus12	Bus13	36	-0.77947	-1.5019	0.00085	0.02304
Bus12	Bus11	37	0.32647	-3.1972	0.00306	0.08313
Bus23	Bus36	38	-3.9849	-15.8547	0.02513	1.3672
Bus30	Bus2	39	76.13	9.7883	0	18.2757
Bus6	Bus31	40	-14.1114	-26.7696	0	4.155
Bus10	Bus32	41	-56.88	-26.8039	0	14.0857
Bus20	Bus34	42	-65.8778	-21.4799	0.90224	18.0448
Bus19	Bus33	43	-55.245	-45.9243	0.64499	13.0841
Bus19	Bus20	44	-32.1941	-13.0093	0.15068	2.9705
Bus22	Bus35	45	-4.65	-37.7391	0	3.7242

LINE FLOWS

From Bus	To Bus	Line	P Flow [p.u.]	Q Flow [p.u.]	P Loss [p.u.]	Q Loss [p.u.]
Bus2	Bus1	1	19.6788	-8.689	0.12294	1.3939
Bus1	Bus39	2	19.5558	-10.0828	0.08747	2.0436
Bus10	Bus11	3	33.7593	4.6132	0.08269	0.87585
Bus13	Bus10	4	-23.0475	-21.4172	0.07317	0.77358
Bus13	Bus14	5	22.2672	19.8923	0.14847	1.6366
Bus15	Bus14	6	-6.0631	-17.4107	0.14642	1.7098
Bus16	Bus15	7	9.964	-9.353	0.04191	0.41464
Bus16	Bus17	8	5.2124	-12.2127	0.03077	0.37301
Bus16	Bus19	9	-79.2345	40.9355	8.2046	99.8692
Bus21	Bus16	10	-22.7043	10.6431	0.11898	1.9731
Bus24	Bus16	11	-25.3791	13.4155	0.05964	1.1648
Bus17	Bus18	12	5.1816	-12.5857	0.0307	0.34073
Bus25	Bus2	13	-29.2261	14.7019	1.0649	1.29
Bus3	Bus2	14	-25.9454	-11.1603	0.21489	2.4532
Bus22	Bus21	15	-16.4092	17.8599	0.2757	4.6904
Bus23	Bus22	16	-0.87273	-12.0554	0.01644	0.22991
Bus24	Bus23	17	22.1642	-12.4551	0.40372	6.3564
Bus26	Bus25	18	-38.237	6.0583	1.0433	10.4392
Bus27	Bus26	19	-11.9328	-3.2061	0.04454	0.42913
Bus28	Bus26	20	-10.9443	5.8885	0.16025	1.5925
Bus29	Bus26	21	-10.6016	8.0528	0.21431	2.1247
Bus29	Bus28	22	-3.86	7.0927	0.03311	0.25954
Bus18	Bus3	23	-3.2221	-14.5162	0.0549	0.63108
Bus3	Bus4	24	5.4784	-4.1154	0.01262	0.1708

Bus14	Bus4	25	15.9092	-0.86482	0.04075	0.63439
Bus4	Bus5	26	-5.3558	-15.6106	0.04363	0.67506
Bus5	Bus8	27	18.6301	1.8783	0.0519	0.70045
Bus11	Bus6	28	34	0.45703	0.1458	1.6826
Bus5	Bus6	29	-24.0295	-18.164	0.03361	0.4286
Bus6	Bus7	30	23.9025	6.9514	0.06749	1.0146
Bus7	Bus8	31	11.355	1.4514	0.00977	0.09863
Bus8	Bus9	32	2.0534	-6.8673	0.0153	0.19318
Bus39	Bus9	33	-2.0288	7.0585	0.00922	-0.00197
Bus37	Bus25	34	19.37	24.7	0.09503	3.6743
Bus38	Bus29	35	6.59	18.0355	0.04599	0.89687
Bus13	Bus12	36	0.78032	1.5249	0.00085	0.02304
Bus11	Bus12	37	-0.32341	3.2803	0.00306	0.08313
Bus36	Bus23	38	4.01	17.2219	0.02513	1.3672
Bus2	Bus30	39	-76.13	8.4874	0	18.2757
Bus31	Bus6	40	14.1114	30.9246	0	4.155
Bus32	Bus10	41	56.88	40.8896	0	14.0857
Bus34	Bus20	42	66.78	39.5246	0.90224	18.0448
Bus33	Bus19	43	55.89	59.0084	0.64499	13.0841
Bus20	Bus19	44	32.3448	15.9799	0.15068	2.9705
Bus35	Bus22	45	4.65	41.4633	0	3.7242

GLOBAL SUMMARY REPORT

TOTAL GENERATION

REAL POWER [p.u.]	339.2914
REACTIVE POWER [p.u.]	313.5074

TOTAL LOAD

REAL POWER [p.u.]	324.3195
REACTIVE POWER [p.u.]	84.4618

TOTAL LOSSES

REAL POWER [p.u.]	14.9719
REACTIVE POWER [p.u.]	229.0457

E.6. Load Flow Results for 100% Penetration in Summer

POWER FLOW REPORT

P S A T 2.0.0

Author: Federico Milano, (c) 2002-2007
e-mail: fmilano@thunderbox.uwaterloo.ca
website: http://thunderbox.uwaterloo.ca/~fmilano
File: C:\Program Files\MATLAB\R2006b\work\IEEE 39 Models\Geyser _S_100.mdl
Date: 23-Apr-2008 11:58:06

NETWORK STATISTICS

Buses:	39
Lines:	33
Transformers:	12
Generators:	10
Loads:	30

SOLUTION STATISTICS

Number of iterations:	7
Maximum P mismatch [p.u.]	0
Maximum Q mismatch [p.u.]	0
Power rate [MVA]	100

POWER FLOW RESULTS

Bus	V [p.u.]	phase [rad]	P gen [p.u.]	Q gen [p.u.]	P load [p.u.]	Q load [p.u.]
Bus1	1.0025	0.01426	0	0	0	0
Bus10	1.0111	0.04957	0	0	0	0
Bus11	1.0053	0.02287	0	0	0	0
Bus12	0.99217	0.02741	0	0	0.453	4.699
Bus13	0.99259	0.03422	0	0	0	0
Bus14	0.95324	-0.00265	0	0	0	0
Bus15	0.873	-0.01809	0	0	16.0773	7.6871
Bus16	0.85651	0.01005	0	0	15.9103	1.5621
Bus17	0.87836	-0.00276	0	0	0	0
Bus18	0.89853	-0.01417	0	0	8.4093	1.5967
Bus19	1.0104	1.0736	0	0	0	0
Bus2	0.97948	0.07556	0	0	0	0
Bus20	0.93386	1.1483	0	0	33.533	5.5
Bus21	0.88009	-0.06424	0	0	6.0619	2.5442
Bus22	1.0064	-0.22169	0	0	20.17	7.5939
Bus23	0.98561	-0.22094	0	0	25.2875	8.6438
Bus24	0.87103	-0.02633	0	0	3.2388	-0.96758
Bus25	0.97035	0.02864	0	0	9.2208	1.9429
Bus26	0.95496	-0.22238	0	0	4.3392	0.5306

Bus27	0.94213	-0.25693	0	0	11.9328	3.2061
Bus28	1.0001	-0.34574	0	0	7.0512	0.9447
Bus29	1.0355	-0.36525	0	0	18.8382	1.7874
Bus3	0.93749	-0.00764	0	0	17.19	0.1284
Bus30	1.03	0.31418	76.13	9.4203	0	0
Bus31	0.982	0	7.3512	30.452	0	0
Bus32	0.9831	0.23234	56.88	40.6494	0	0
Bus33	0.9972	1.1925	55.89	58.4687	0	0
Bus34	1.0265	1.3674	66.78	39.2994	0	0
Bus35	1.0493	-0.21079	4.65	40.7339	0	0
Bus36	1.0635	-0.20347	4.01	16.709	0	0
Bus37	1.0123	0.10538	19.37	23.7171	0	0
Bus38	1.0278	-0.3507	6.59	16.5985	0	0
Bus39	1.0475	-0.07097	34.88	30.761	53.2799	12.0648
Bus4	0.95338	-0.04353	0	0	26.69	9.8252
Bus5	0.99215	-0.03872	0	0	0	0
Bus6	1.0016	-0.02968	0	0	0	0
Bus7	0.98831	-0.06653	0	0	12.48	4.4854
Bus8	0.98633	-0.07474	0	0	27.87	9.398
Bus9	1.0174	-0.07316	0	0	0	0

LINE FLOWS

From Bus	To Bus	Line	P Flow [p.u.]	Q Flow [p.u.]	P Loss [p.u.]	Q Loss [p.u.]
Bus1	Bus2	1	-19.2728	9.9365	0.11923	1.3501
Bus39	Bus1	2	-19.188	11.9138	0.08482	1.9773
Bus11	Bus10	3	-35.0478	-3.6586	0.08932	0.94704
Bus10	Bus13	4	21.7429	22.0143	0.06811	0.71913
Bus14	Bus13	5	-20.6224	-18.2532	0.13649	1.5021
Bus14	Bus15	6	4.8321	18.9786	0.13855	1.6147
Bus15	Bus16	7	-11.3838	9.6768	0.04798	0.47786
Bus17	Bus16	8	-4.9911	12.2828	0.02904	0.3508
Bus19	Bus16	9	87.4488	58.364	8.1369	99.0431
Bus16	Bus21	10	22.2801	-8.7169	0.11343	1.8792
Bus16	Bus24	11	24.6696	-12.3933	0.05661	1.1051
Bus18	Bus17	12	-4.9622	12.6031	0.02896	0.32031
Bus2	Bus25	13	27.7694	-13.8662	0.93275	1.1275
Bus2	Bus3	14	28.9686	13.6191	0.2526	2.8911
Bus21	Bus22	15	16.1048	-13.1403	0.26173	4.4454
Bus22	Bus23	16	0.32302	11.9584	0.01546	0.21402
Bus23	Bus24	17	-20.9937	18.5185	0.38057	5.9876
Bus25	Bus26	18	36.8954	3.2837	0.90896	9.0823
Bus26	Bus27	19	11.9766	3.6263	0.04375	0.42015
Bus26	Bus28	20	10.0976	-4.1914	0.13267	1.2859
Bus26	Bus29	21	9.5731	-5.7641	0.1726	1.6646
Bus28	Bus29	22	2.9138	-6.422	0.02626	0.18467
Bus3	Bus18	23	3.4999	14.8052	0.05278	0.60541
Bus4	Bus3	24	-8.0041	4.5307	0.02204	0.32515
Bus4	Bus14	25	-15.7503	1.3475	0.03999	0.62207

Bus5	Bus4	26	2.9764	16.3329	0.04079	0.62947
Bus8	Bus5	27	-17.3968	-1.2779	0.04549	0.6106
Bus6	Bus11	28	-35.3479	1.4435	0.15878	1.8346
Bus6	Bus5	29	20.4464	18.5731	0.02769	0.35176
Bus7	Bus6	30	-22.1937	-6.0213	0.05905	0.88506
Bus8	Bus7	31	-9.7065	-1.4669	0.0072	0.06901
Bus9	Bus8	32	0.78005	6.8151	0.01332	0.16191
Bus9	Bus39	33	-0.78005	-6.8151	0.008	-0.0327
Bus25	Bus37	34	-19.2796	-20.2203	0.09044	3.4968
Bus29	Bus38	35	-6.5502	-15.8227	0.03979	0.77581
Bus12	Bus13	36	-0.91495	-1.5147	0.00093	0.02516
Bus12	Bus11	37	0.46195	-3.1843	0.00306	0.08318
Bus23	Bus36	38	-3.9863	-15.418	0.02373	1.2911
Bus30	Bus2	39	76.13	9.4203	0	18.2538
Bus6	Bus31	40	-7.3512	-26.923	0	3.529
Bus10	Bus32	41	-56.88	-26.6199	0	14.0295
Bus20	Bus34	42	-65.8804	-21.3079	0.89958	17.9916
Bus19	Bus33	43	-55.2512	-45.5102	0.6388	12.9585
Bus19	Bus20	44	-32.1976	-12.8538	0.14984	2.9541
Bus22	Bus35	45	-4.65	-37.1379	0	3.596

LINE FLOWS

From Bus	To Bus	Line	P Flow [p.u.]	Q Flow [p.u.]	P Loss [p.u.]	Q Loss [p.u.]
Bus2	Bus1	1	19.392	-8.5864	0.11923	1.3501
Bus1	Bus39	2	19.2728	-9.9365	0.08482	1.9773
Bus10	Bus11	3	35.1371	4.6057	0.08932	0.94704
Bus13	Bus10	4	-21.6748	-21.2951	0.06811	0.71913
Bus13	Bus14	5	20.7589	19.7553	0.13649	1.5021
Bus15	Bus14	6	-4.6935	-17.3639	0.13855	1.6147
Bus16	Bus15	7	11.4318	-9.1989	0.04798	0.47786
Bus16	Bus17	8	5.0202	-11.932	0.02904	0.3508
Bus16	Bus19	9	-79.3119	40.6791	8.1369	99.0431
Bus21	Bus16	10	-22.1666	10.5961	0.11343	1.8792
Bus24	Bus16	11	-24.613	13.4985	0.05661	1.1051
Bus17	Bus18	12	4.9911	-12.2828	0.02896	0.32031
Bus25	Bus2	13	-26.8367	14.9937	0.93275	1.1275
Bus3	Bus2	14	-28.716	-10.7281	0.2526	2.8911
Bus22	Bus21	15	-15.843	17.5856	0.26173	4.4454
Bus23	Bus22	16	-0.30756	-11.7444	0.01546	0.21402
Bus24	Bus23	17	21.3742	-12.5309	0.38057	5.9876
Bus26	Bus25	18	-35.9865	5.7986	0.90896	9.0823
Bus27	Bus26	19	-11.9328	-3.2061	0.04375	0.42015
Bus28	Bus26	20	-9.965	5.4773	0.13267	1.2859
Bus29	Bus26	21	-9.4005	7.4286	0.1726	1.6646
Bus29	Bus28	22	-2.8875	6.6067	0.02626	0.18467
Bus18	Bus3	23	-3.4471	-14.1998	0.05278	0.60541
Bus3	Bus4	24	8.0261	-4.2056	0.02204	0.32515

Bus14	Bus4	25	15.7903	-0.72542	0.03999	0.62207
Bus4	Bus5	26	-2.9357	-15.7034	0.04079	0.62947
Bus5	Bus8	27	17.4423	1.8885	0.04549	0.6106
Bus11	Bus6	28	35.5067	0.39111	0.15878	1.8346
Bus5	Bus6	29	-20.4187	-18.2214	0.02769	0.35176
Bus6	Bus7	30	22.2527	6.9064	0.05905	0.88506
Bus7	Bus8	31	9.7137	1.5359	0.0072	0.06901
Bus8	Bus9	32	-0.76673	-6.6532	0.01332	0.16191
Bus39	Bus9	33	0.78805	6.7824	0.008	-0.0327
Bus37	Bus25	34	19.37	23.7171	0.09044	3.4968
Bus38	Bus29	35	6.59	16.5985	0.03979	0.77581
Bus13	Bus12	36	0.91588	1.5398	0.00093	0.02516
Bus11	Bus12	37	-0.45889	3.2675	0.00306	0.08318
Bus36	Bus23	38	4.01	16.709	0.02373	1.2911
Bus2	Bus30	39	-76.13	8.8334	0	18.2538
Bus31	Bus6	40	7.3512	30.452	0	3.529
Bus32	Bus10	41	56.88	40.6494	0	14.0295
Bus34	Bus20	42	66.78	39.2994	0.89958	17.9916
Bus33	Bus19	43	55.89	58.4687	0.6388	12.9585
Bus20	Bus19	44	32.3474	15.8079	0.14984	2.9541
Bus35	Bus22	45	4.65	40.7339	0	3.596

GLOBAL SUMMARY REPORT

TOTAL GENERATION

REAL POWER [p.u.]	332.5312
REACTIVE POWER [p.u.]	306.8094

TOTAL LOAD

REAL POWER [p.u.]	318.0332
REACTIVE POWER [p.u.]	83.1728

TOTAL LOSSES

REAL POWER [p.u.]	14.498
REACTIVE POWER [p.u.]	223.6367

E.7. Load Flow Results for 100% Penetration in Winter

POWER FLOW REPORT

P S A T 2.0.0

Author: Federico Milano, (c) 2002-2007
e-mail: fmilano@thunderbox.uwaterloo.ca
website: http://thunderbox.uwaterloo.ca/~fmilano
File: C:\Program Files\MATLAB\R2006b\work\IEEE 39 Models\Geyser_W_100.mdl
Date: 23-Apr-2008 13:48:23

NETWORK STATISTICS

Buses:	39
Lines:	33
Transformers:	12
Generators:	10
Loads:	30

SOLUTION STATISTICS

Number of iterations:	7
Maximum P mismatch [p.u.]	0
Maximum Q mismatch [p.u.]	0
Power rate [MVA]	100

POWER FLOW RESULTS

Bus	V [p.u.]	phase [rad]	P gen [p.u.]	Q gen [p.u.]	P load [p.u.]	Q load [p.u.]
Bus1	1.0023	-0.00646	0	0	0	0
Bus10	1.011	0.03834	0	0	0	0
Bus11	1.0053	0.01205	0	0	0	0
Bus12	0.99205	0.01618	0	0	0.453	4.699
Bus13	0.99242	0.02258	0	0	0	0
Bus14	0.95297	-0.01544	0	0	0	0
Bus15	0.87253	-0.03317	0	0	16.0598	7.6788
Bus16	0.85591	-0.00614	0	0	15.888	1.5599
Bus17	0.87788	-0.01946	0	0	0	0
Bus18	0.89817	-0.03131	0	0	8.4025	1.5954
Bus19	1.0101	1.0588	0	0	0	0
Bus2	0.979	0.05378	0	0	0	0
Bus20	0.93372	1.1336	0	0	33.533	5.5
Bus21	0.87948	-0.08092	0	0	6.0535	2.5406
Bus22	1.0061	-0.23971	0	0	20.17	7.5939
Bus23	0.98512	-0.23916	0	0	25.5741	8.7418
Bus24	0.8704	-0.04281	0	0	3.2341	-0.96617
Bus25	0.96793	0.005	0	0	9.2208	1.9429
Bus26	0.94958	-0.25909	0	0	4.3392	0.5306

Bus27	0.93667	-0.29404	0	0	11.9328	3.2061
Bus28	0.99614	-0.39192	0	0	7.0512	0.9447
Bus29	1.033	-0.41544	0	0	20.3153	1.9276
Bus3	0.93732	-0.02546	0	0	17.19	0.1284
Bus30	1.03	0.29252	76.13	9.5798	0	0
Bus31	0.982	0	9.8167	30.5555	0	0
Bus32	0.9831	0.22113	56.88	40.6834	0	0
Bus33	0.9972	1.1778	55.89	58.5733	0	0
Bus34	1.0265	1.3527	66.78	39.3431	0	0
Bus35	1.0493	-0.2288	4.65	40.8831	0	0
Bus36	1.0635	-0.22169	4.01	16.8148	0	0
Bus37	1.0123	0.08187	19.37	24.3271	0	0
Bus38	1.0278	-0.40097	6.59	17.5462	0	0
Bus39	1.0475	-0.09015	34.88	30.934	53.8034	12.1834
Bus4	0.95322	-0.0566	0	0	26.69	9.8252
Bus5	0.99203	-0.04933	0	0	0	0
Bus6	1.0015	-0.03964	0	0	0	0
Bus7	0.98819	-0.0774	0	0	12.48	4.4854
Bus8	0.98619	-0.08609	0	0	27.87	9.398
Bus9	1.0173	-0.08856	0	0	0	0

LINE FLOWS

From Bus	To Bus	Line	P Flow [p.u.]	Q Flow [p.u.]	P Loss [p.u.]	Q Loss [p.u.]
Bus1	Bus2	1	-18.9109	9.9866	0.11602	1.3125
Bus39	Bus1	2	-18.8284	11.9065	0.08253	1.9199
Bus11	Bus10	3	-34.5174	-3.6797	0.08669	0.91875
Bus10	Bus13	4	22.276	22.0475	0.0699	0.73836
Bus14	Bus13	5	-21.2019	-18.2241	0.14075	1.5498
Bus14	Bus15	6	5.3143	18.9925	0.14058	1.6393
Bus15	Bus16	7	-10.8861	9.6745	0.04564	0.45345
Bus17	Bus16	8	-5.2144	12.3615	0.02976	0.36009
Bus19	Bus16	9	87.4469	58.4745	8.15	99.2026
Bus16	Bus21	10	22.3975	-8.7048	0.11459	1.8988
Bus16	Bus24	11	24.8357	-12.3607	0.05725	1.1176
Bus18	Bus17	12	-5.1847	12.6903	0.02969	0.32886
Bus2	Bus25	13	29.4805	-13.5225	1.0195	1.2342
Bus2	Bus3	14	27.6226	13.5132	0.23335	2.6675
Bus21	Bus22	15	16.2294	-13.1442	0.26461	4.4959
Bus22	Bus23	16	0.44479	12.0271	0.01566	0.21722
Bus23	Bus24	17	-21.159	18.5762	0.38537	6.0641
Bus25	Bus26	18	38.5169	4.0215	0.99853	9.9872
Bus26	Bus27	19	11.9771	3.6321	0.04426	0.42597
Bus26	Bus28	20	10.7833	-4.2582	0.15098	1.4893
Bus26	Bus29	21	10.4189	-5.8702	0.20015	1.9685
Bus28	Bus29	22	3.5811	-6.6922	0.0307	0.23318
Bus3	Bus18	23	3.2708	14.8944	0.05305	0.6087
Bus4	Bus3	24	-6.9109	4.429	0.01757	0.25189
Bus4	Bus14	25	-15.8471	1.399	0.04052	0.63056

Bus5	Bus4	26	3.9737	16.2963	0.04164	0.64319
Bus8	Bus5	27	-17.7446	-1.2529	0.04732	0.63624
Bus6	Bus11	28	-34.7702	1.3657	0.15364	1.7743
Bus6	Bus5	29	21.7953	18.5639	0.02975	0.37851
Bus7	Bus6	30	-22.7298	-5.9959	0.06172	0.92603
Bus8	Bus7	31	-10.2418	-1.4324	0.00799	0.07813
Bus9	Bus8	32	-0.10303	6.8758	0.01339	0.16302
Bus9	Bus39	33	0.10303	-6.8758	0.00804	-0.03167
Bus25	Bus37	34	-19.2767	-20.721	0.09326	3.6061
Bus29	Bus38	35	-6.5462	-16.6917	0.04382	0.85452
Bus12	Bus13	36	-0.86251	-1.5109	0.00089	0.02432
Bus12	Bus11	37	0.40951	-3.1881	0.00305	0.08303
Bus23	Bus36	38	-3.986	-15.5082	0.02402	1.3066
Bus30	Bus2	39	76.13	9.5798	0	18.2632
Bus6	Bus31	40	-9.8167	-26.8516	0	3.7039
Bus10	Bus32	41	-56.88	-26.646	0	14.0374
Bus20	Bus34	42	-65.8799	-21.3412	0.90009	18.0018
Bus19	Bus33	43	-55.25	-45.5905	0.64	12.9828
Bus19	Bus20	44	-32.1969	-12.884	0.15	2.9572
Bus22	Bus35	45	-4.65	-37.2611	0	3.622

LINE FLOWS

From Bus	To Bus	Line	P Flow [p.u.]	Q Flow [p.u.]	P Loss [p.u.]	Q Loss [p.u.]
Bus2	Bus1	1	19.027	-8.6741	0.11602	1.3125
Bus1	Bus39	2	18.9109	-9.9866	0.08253	1.9199
Bus10	Bus11	3	34.604	4.5984	0.08669	0.91875
Bus13	Bus10	4	-22.2061	-21.3092	0.0699	0.73836
Bus13	Bus14	5	21.3427	19.7739	0.14075	1.5498
Bus15	Bus14	6	-5.1737	-17.3532	0.14058	1.6393
Bus16	Bus15	7	10.9317	-9.221	0.04564	0.45345
Bus16	Bus17	8	5.2441	-12.0014	0.02976	0.36009
Bus16	Bus19	9	-79.297	40.7281	8.15	99.2026
Bus21	Bus16	10	-22.2829	10.6036	0.11459	1.8988
Bus24	Bus16	11	-24.7784	13.4783	0.05725	1.1176
Bus17	Bus18	12	5.2144	-12.3615	0.02969	0.32886
Bus25	Bus2	13	-28.461	14.7566	1.0195	1.2342
Bus3	Bus2	14	-27.3892	-10.8458	0.23335	2.6675
Bus22	Bus21	15	-15.9648	17.6401	0.26461	4.4959
Bus23	Bus22	16	-0.42913	-11.8099	0.01566	0.21722
Bus24	Bus23	17	21.5443	-12.5121	0.38537	6.0641
Bus26	Bus25	18	-37.5184	5.9657	0.99853	9.9872
Bus27	Bus26	19	-11.9328	-3.2061	0.04426	0.42597
Bus28	Bus26	20	-10.6323	5.7475	0.15098	1.4893
Bus29	Bus26	21	-10.2187	7.8387	0.20015	1.9685
Bus29	Bus28	22	-3.5504	6.9254	0.0307	0.23318
Bus18	Bus3	23	-3.2178	-14.2857	0.05305	0.6087
Bus3	Bus4	24	6.9284	-4.1771	0.01757	0.25189

Bus14	Bus4	25	15.8876	-0.76839	0.04052	0.63056
Bus4	Bus5	26	-3.9321	-15.6531	0.04164	0.64319
Bus5	Bus8	27	17.7919	1.8891	0.04732	0.63624
Bus11	Bus6	28	34.9238	0.40856	0.15364	1.7743
Bus5	Bus6	29	-21.7656	-18.1854	0.02975	0.37851
Bus6	Bus7	30	22.7916	6.9219	0.06172	0.92603
Bus7	Bus8	31	10.2498	1.5105	0.00799	0.07813
Bus8	Bus9	32	0.11642	-6.7128	0.01339	0.16302
Bus39	Bus9	33	-0.09499	6.8441	0.00804	-0.03167
Bus37	Bus25	34	19.37	24.3271	0.09326	3.6061
Bus38	Bus29	35	6.59	17.5462	0.04382	0.85452
Bus13	Bus12	36	0.86341	1.5352	0.00089	0.02432
Bus11	Bus12	37	-0.40646	3.2711	0.00305	0.08303
Bus36	Bus23	38	4.01	16.8148	0.02402	1.3066
Bus2	Bus30	39	-76.13	8.6833	0	18.2632
Bus31	Bus6	40	9.8167	30.5555	0	3.7039
Bus32	Bus10	41	56.88	40.6834	0	14.0374
Bus34	Bus20	42	66.78	39.3431	0.90009	18.0018
Bus33	Bus19	43	55.89	58.5733	0.64	12.9828
Bus20	Bus19	44	32.3469	15.8412	0.15	2.9572
Bus35	Bus22	45	4.65	40.8831	0	3.622

GLOBAL SUMMARY REPORT

TOTAL GENERATION

REAL POWER [p.u.]	334.9967
REACTIVE POWER [p.u.]	309.2403

TOTAL LOAD

REAL POWER [p.u.]	320.2605
REACTIVE POWER [p.u.]	83.5154

TOTAL LOSSES

REAL POWER [p.u.]	14.7362
REACTIVE POWER [p.u.]	225.7248